# THE DETECTION OF GLYPHOSATE AND GLYPHOSATE-BASED HERBICIDES IN WATER, USING NANOTECHNOLOGY

Thesis submitted in fulfillment of the requirements of

**Doctor of Philosophy (Biochemistry)**

**Department of Biochemistry & Microbiology**

**Rhodes University**

**by**

**Louise Kashiyavala Sophia De Almeida**

**January 2015**

# Abstract

Glyphosate (N-phosphonomethylglycine) is an organophosphate compound which was developed by the Monsanto Company in 1971 and is the active ingredient found in several herbicide formulations. The use of glyphosate-based herbicides in South Africa for the control of alien invasive plants and weeds is well established, extensive and currently unregulated, which vastly increases the likelihood of glyphosate contamination in environmental water systems. Although the use of glyphosate-based herbicides is required for economic enhancement in industries such as agriculture, the presence of this compound in natural water systems presents a potential risk to human health. Glyphosate and glyphosate formulations were previously considered safe, however their toxicity has become a major focal point of research over recent years. The lack of monitoring protocols for pesticides in South Africa is primarily due to limited financial capacity and the lack of analytical techniques.

This study sought to determine the acute cytotoxic, genotoxic and pro-inflammatory potential of pure glyphosate and two glyphosate formulations (Roundup® and Wipeout®) at concentrations relevant to human exposure, using *in vitro* studies in a human white blood cell model (cytotoxicity and pro-inflammatory effects), human whole blood cell model (cytotoxicity and pro-inflammatory effects) and human cancer cell lines (cytotoxicity and genotoxicity). The human whole blood cell model proved a more sensitive and suitable model for glyphosate toxicological studies when compared to the human white blood cell model. Results of cytotoxic investigations using the MTT assay in human whole blood cells, indicated that pure glyphosate and Roundup® (Ro) demonstrated similar non-monotonic toxicological profiles, characterized by an inverted bell-shaped dose response curve at low dose exposure from 10 μg/ml. The Wipeout® (Wo) formulation demonstrated a monotonic (linear) dose response curve from a threshold concentration of 50 μg/ml. Preliminary evidence suggested the potential of glyphosate and glyphosate formulations to induce an acute inflammatory response when compared to the untreated control. Based on data obtained from ELISA assays, exposure of human whole blood cells to pure glyphosate (50 μg/ml), Ro (10 and 50 μg/ml) and Wo (50 μg/ml) resulted in significant elevations in the levels of the cytokine, TNF-α. In contrast, pure glyphosate (0.1

μg/ml), Ro (0.1, 0.7 and 10 μg/ml) and Wo (0.1, 0.7 and 50 μg/ml) caused a significant reduction in the plasma levels of the cytokine, IL-6.

Cytotoxicity (MTT assays) conducted in the cancer cell lines, HEC1A, MCF7 and MDA-MB-231 exposed to moderate doses (75-500 μg/ml) of glyphosate and glyphosate formulations, indicated varied toxicity depending on the cell type. The most significant results were observed in HEC1A cancer cells and toxicological profiles were characterized by a non-monotonic reduction in cell viability for pure glyphosate (75-500 μg/ml) and non-monotonic proliferative effects for Wo (75, 125 and 250 μg/ml). Genotoxicity investigations revealed the capacity of pure glyphosate and the glyphosate formulations to incur DNA damage in the HEC1A (ER positive) and MDA-MB-231 (ER negative) cells at the test concentration (500 μ/ml). The differential toxicities displayed by Ro and Wo in the HEC1A cancer cells and human whole blood cells, suggested the role of adjuvants as possible contributing factors to glyphosate toxicity.

Overall this study provided an important contribution to existing toxicological studies for glyphosate and glyphosate formulations in humans and validated the need to develop a rapid and reliable method for the detection of glyphosate in water.

This study presents the development of a novel first generation nanofiber-based colorimetric sensor for the detection of glyphosate in water, which has to the best of our knowledge not been reported in the literature for glyphosate. The glyphosate sensor development and assay principle were based on a previously reported spectrophotometric detection assay for glyphosate. Following the initial scale down (to improve the applicability of the assay towards sensor development) of the previously reported method (to a total assay volume of 1 ml), copper doped poly (vinyl) alcohol (cd-PVA) nanofiber sensors were produced using the electrospinning method under optimized process parameters (PVA polymer concentration: 7.5 %, flow rate: 0.5 ml/hour, voltage: 30 kV, needle tip to collector distance: 15 cm). A two step method was proposed for the detection of glyphosate using the cd-PVA sensor, which involved the reaction of glyphosate with carbon disulfide for the formation of a glyphosate dithiocarbamate intermediate and the application of the dithiocarbamate sample onto the cd-PVA nanofiber sensor, which would result in a visual color change from blue to yellow. Results in this study were quantified using the RGB color model, to determine effective intensity ($A_x$). The proof of

concept for the cd-PVA sensor system was validated for this study and the system was optimized with respect to carbon disulfide concentration (6 %) and pH (12). The cd-PVA sensor system was characterized by several beneficial characteristics which included, the rapid detection of glyphosate (~ 3 seconds), a low sample volume (30 µl), good short term storage stability under ambient conditions (~2.5 weeks), low-cross reactivity to the glyphosate structural analogs AMPA and glycine (16 % sensor reponse and no clear visual color change) and a satisfactory system precision (RSD value below 20 %). Calibration studies indicated a good sensitivity for the detection of pure glyphosate (practical LOD: 0.1 µg/ml) and satisfactory sensitivity for the detection glyphosate in Wo and Ro (practical LOD: 1.95 µg/ml), when compared to the only colorimetric chemical sensor (filter paper-based) reported for glyphosate to date.

The ability of the sensor system to quantify pure glyphosate and glyphosate in formulation in water was validated by good recovery data in distilled water samples (between 94.9 % ± 5.86 and 112.21 % ± 18.62), however recovery studies using environmental water samples (no pre-treatment) and interference studies demonstrated the susceptibility of this sensor system to compounds and ions commonly found in environmental waters. The pre-treatment/pre-concentration of water samples would therefore be a requirement when using this assay.

The data obtained in this study has demonstrated several aspects that make the cd-PVA sensor system a promising tool for application in the high-throughput screening of glyphosate in water. The cd-PVA sensor system did, however, demonstrate some limitations, such as low reproducibility (RSD values above 20 %) and poor long-term storage stability, therefore future investigations should focus on further optimizing the structure and integrity of the sensor nanostructure, towards further improving the applicability of this system.

**Keywords**

Herbicide, Glyphosate, Roundup®, Wipeout®, cytotoxicity, genotoxicity, immunotoxicity, colorimetric, nanofiber, poly (vinyl) alcohol, sensor

# Declaration

I declare that this thesis is my own, unaided work. It is being submitted for the degree of Doctor of Philosophy at Rhodes University. It has not been submitted before for any degree or examination at any other university.

…….....

Louise Kashiyavala Sophia De Almeida

On this ……..of…….20….

# Dedication

I dedicate this thesis to my parents, Toini and Filipe De Almeida, who have always supported and believed in me.

I also dedicate this thesis to my late friend Ilandra Meipii Markowitz (1986-2011). Everything you have taught me, I carry with me for life. You are dearly loved and missed.

# Acknowledgements

I would like to acknowledge my supervisor and co-supervisor, Prof. Brett Pletschke and Prof. Carminita Frost, for facilitating this research and for all their support throughout my PhD.

I further wish to thank the following persons in no particular order: Dr. Ron Fogel, Dr. Natasha Beukes, Dr. Susan Van Dyk, Dr. Samuel Chigome, Prof. Nelson Torto and members of lab 410, for all their valued advice.

I further wish to thank Jan Kruid for all the support and guidance.

I further wish to acknowledge the Water Research Commission (WRC) of South Africa for providing me with funding.

# List of outputs

## Publications

De Almeida L.K.S. Chigome S. Torto N. Frost C.L. Pletschke B.I. 2015. A novel colorimetric sensor strip for the detection of glyphosate. *Sensors and Actuators B: Chemical* 206: 357-363.

De Almeida LKS, Pletschke BI and Frost CL. 2014. Cytotoxic and genotoxic effects of low dose acute exposure to glyphosate and glyphosate formulations in human cell lines. (In preparation for *Pesticide Biochemistry and Physiology*)

## Conference Proceedings

De Almeida, L.K.S., Chigome, S., Torto, N., Frost, C. and Pletschke, B.I. A novel nanofiber-based colorimetric sensor for the detection of glyphosate in water. 24$^{th}$ South African Society for Biochemistry and Molecular Biology (SASBMB) Biennial Conference. Goudini Spa, Rawsonville, 6-9$^{th}$ July 2014. Poster presentation.

# Table of contents



## Chapter 1- General introduction

## Chapter 2- Problem statement, aims & objectives



## Chapter 3- The acute toxicity of glyphosate and glyphosate formulations in humans at low/moderate dose exposure (*In vitro* studies)

## Chapter 4- Optimization, scale down and partial validation of a glyphosate spectrophotometric assay (free system)

# List of figures

# List of tables

# List of Abbreviations

| | |
|---|---|
| 1-aminocyclopropane-1-carboxylic acid synthase | ACC |
| 2,4-Dichlorophenoxyacetic acid | 2,4-D |
| 2-Methyl-4,6-dinitrophenol | DNOC |
| 3-(4,5-dimethylthiazol-2-YI)-2,5-diphenyltetrazolium bromide | MTT |
| 4-Chloro-2-methylphenoxyacetic acid | MCPA |
| 5-Enolpyruvate-shikimate-3-phosphate | EPSP |
| 5-Ethyldipropyl-thiocarbamate | EPTC |
| Abscisic acid | ABA |
| Adenosine triphosphate | ATP |
| Agência Nacional de Vigilácia Sanitária | ANVISA |
| Aminomethylphosphonic acid | AMPA |
| Capillary electrophoresis | CE |
| Collectable nanofiber mat formation | NMF |
| Copper iodide | CuI |
| Department of Water Affairs and Forestry | DWAF |
| Dionised water | DI $H_2O$ |
| Dodecyltrimethylammonium bromide | DTAB |
| Drinking water quality guidelines | WQG |
| Droplet formation | DF |
| Electron capture detection | ECD |
| Electron paramagnetic resonance | EPR |
| Electron transport chain | ETC |
| Electrospinning/netting | ESN |

| | |
|---|---|
| Electrospray ionization mass spectrometry | ESIMS |
| Enzyme linked immunosorbent assays | ELISA |
| Estrogen receptor | ER |
| Ferrodoxin | FNR |
| Fetal bovine serum | FBS |
| Fiber formation | FB |
| Flame photometric detection | FPD |
| Fluorenylmethylchloroformate | FMOC-Cl |
| Fourier Transform Infrared spectroscopy | FTIR |
| Gas chromatography | GC |
| Genetically modified | GM |
| Genetically Modified-Glyphosate Resistant | GM-GR |
| Global Positioning System | GPS |
| Glyphosate oxidoreductase | GOX |
| Glyphosate resistant | GR |
| Hazard potential | HP |
| High performance liquid chromatography | HPLC |
| Human serum albumin | HSA |
| Indole-3-acetic acid | IAA |
| Inductively coupled plasma mass spectrometry | ICP-MS |
| Integrated weed management | IWM |
| Interleukin-1β | IL-1 β |
| Interleukin-6 | IL-6 |
| Ion chromatography | IC |
| Laser induced fluorescence | LIF |
| Lipopolysaccharide | LPS |

| | |
|---|---|
| Liquid chromatography | LC |
| Liquid-liquid extraction | LLE |
| Liquid-solid extraction | LSE |
| Mass tandem spectrometry | MS |
| Materials safety data sheets | MSDS |
| Maximum residue limits/levels | MRL |
| Metal ion affinity chromatography | IMAC |
| Mode of action | MOA |
| Multiplexed covalent microbead immunosorbent assay | FCMIA |
| Needle blockage | NB |
| Nicotine adenine dinucleotide phosphate | NADPH |
| Nitrogen phosphorous detection | NPD |
| No collectable nanofiber mat formation | NM |
| No fiber formation | NFF |
| Olive tail moment | OTM |
| *O*-phthalaldehyde | OPA |
| Partition coefficient | $K_{oc}$ |
| *p*-Dimethylaminocinnamaldehyde | *p*-DAC |
| Phosphoenol pyruvate | PEP |
| Photosystem I | PS I |
| Photosystem II | PS II |
| Plastoquinol | PQH |
| Plastoquinone | PQ |
| Poly (ethylene) oxide | PEO |
| Poly (ethylene) terephthalate | PET |

| | |
|---|---|
| Poly (vinyl) acetate/dimethyl formamide | $PVA_c$/DMF |
| Poly (vinyl) alcohol | PVA |
| Polyoxyethylene tallow amine | POEA |
| Polypyrrole | PPγ |
| Quantity index | QI |
| Reactive oxygen species | ROS |
| Red, green and blue color | RGB |
| Relative humidity | RH |
| Scanning electron microscopy | SEM |
| Shikimate-3-phosphate | S3P |
| Solid-phase extraction | SPE |
| Standard error of the mean | SEM |
| Supported liquid membrane extraction | SLM |
| Tail DNA | TDNA |
| Tail length | TL |
| Tetrabutylammonium chloride | TBAC |
| Tetramethylbenzidine | TMB |
| Theoretical maximum | H |
| Toxicological potential | TP |
| Trifluoroacetic anhydride | TFAA |
| Trifluoroethanol | TFE |
| Tris-EDTA | TE |
| Triton® X-100 | Triton-X |
| Tumour necrosis factor-α | TNF- α |
| Ultraviolet-visible spectrophotometry | UV-VIS |
| United States Environmental Protection Agency | USEPA |

| | |
|---|---|
| Voltage | kV |
| Weighted hazard potential | WHP |
| World Health Organization | WHO |

# CHAPTER 1- GENERAL INTRODUCTION

## 1.1 Weeds and weed control

### 1.1.1 The characteristics of weeds

There are several definitions used to describe the term "weed", but in weed science the most common definition is an undesired or unwanted plant (Holzner, 1982; Parashar *et al.*, 2009; Qureshi and Bhatti, 2001). Weeds display distinct characteristics which enable this group of plants to be ubiquitous, resilient and difficult to control. Firstly, weeds have the capacity to reproduce at a very early stage in their life cycle which is followed by rapid maturation. Muoghalu (2008) highlighted these characteristics in two highly invasive plants, namely *Tithonia diversifolia* and *Tithonia rotundifolia*, which are prevalent in several African countries, including South Africa. The results of this study confirmed rapid early growth, a short life cycle and high reproductive capacity in *T. diversifolia* and *T. rotundifolia* (reproductive maturity was reached in 2 and 4 months, respectively).

Secondly, the resilient nature of weeds shows the competitive advantage these plants have with respect to securing nutrients, light and water. This may be explained by some important characteristics, including the ability to display several patterns of seed dormancy (Gressel, 1999), large seed productions, specialized seed dispersal mechanisms (Gressel, 1999; Zimdahl, 2007) and the ability to grow in adverse conditions (e.g. drought) (Bogaard *et al.*, 1998; Javaid *et al.*, 2009).

Finally, several weed species have demonstrated the capacity to intrinsically adapt (at a genetic level) to their environment; this is possibly due to different selection pressures (Clements *et al.*, 2004). Although this theory was contested by Willis *et al.* (2000), there has been evidence to support this idea. Findings by Blair and Wolfe (2004) on the invasive plant species *Silene latifolia*, which was introduced to North America from Europe, support the idea of genetic adaptation. Investigations by Prati and Bossdorf (2004) showed evidence of genetic based allelopathic changes in the invasive plant species *Alliaria petiolata*.

### 1.1.2 Weed control methods

The importance of weed management, especially in the agricultural industry, has been well established, as weeds are one of the main causes of the reduction in the quality, growth and yield of produce (Datta and Knezevic, 2013; Holt, 1994; Khan *et al.*, 2003). This highlights the significant role of weeds from an economic perspective. Weeds also have had a variety of negative impacts worldwide, in other areas, such as biodiversity (Eiswerth *et al.*, 2000; Tilman, 1999; Zimmerman and Neser, 1999). There are several options available with respect to the removal and management of weeds and these are placed in different categories, mainly preventative measures (e.g. crop interference and crop rotation) (Jordan, 1993; Walker and Buchanan, 1982), cultural methods (e.g. the introduction of competitive varieties) (Melander *et al.*, 2012), physical control (e.g. mechanical methods such as hand pulling, hoeing and tillage) (Melander and Rasmussen, 2001; Rask and Kristoffersen, 2007), biological control (e.g. the use of plant pathogens) (Charudattan, 2001) and chemical control (e.g. the use of herbicides) (Snipes and Mueller, 1992). Most systems utilize integrated weed management (IWM) which is defined as the use of many weed control tools in an attempt to produce economically feasible crop yields while placing emphasis on environmental sustainability (Swanton and Weise, 1991). Due to the scope of this study, focus will be placed on the chemical control of weeds with respect to herbicides.

### 1.1.3 Herbicides

Herbicide is a term derived from the Latin, "*herba",* meaning plant and "*caedere",* meaning to kill (Bargagli, 1999). Herbicides are one of many sub-class groups of the broad class of substances known as pesticides (Budde, 2004). Herbicides are chemicals used to kill, control or reduce the growth and persistence of undesirable plants in the agricultural industry, forestry and in non-crop areas such as the gardening industry, industrial sites, lawns and roadsides (Dinelli *et al.*, 1996; Revitt *et al.*, 2002).

### 1.1.4 Brief history of herbicide development and use

The use of herbicides for weed control dates back to the Greek and Roman era. Although the most prevalent weed control method in this period was hand pulling, several metals and their salts (e.g. copper nitrate and sodium arsenate) were used to control broadleaf weeds in cereal crops (Bargagli, 1999). In 1874 sulphuric acid and salts were used as the first inorganic herbicides for controlling weeds by altering the pH of the soil. The first synthetic organic herbicide, 2-methyl-4, 6-dinitrophenol (DNOC) was developed in 1892 and was initially produced for use as an insecticide; it was then applied 1934 as a selective herbicide in cereals (Mothes-Wagner *et al.*, 1990). A large increase in the development and production of herbicides was observed only after the second world war (1945) with the production of (e.g. 2,4-dichlorophenoxyacetic acid (2,4-D)), the first herbicide to be distributed and used widely for the control of broadleaf plants (Kaupinnen *et al.*, 1993, McGuinness and Dowling, 2009) in wheat (Baghestani *et al.*, 2007), rice, oats, barley (Yadav and Jadhav, 2002) and maize production (Jofré *et al.*, 1996). Herbicides served as a chemical replacement to previous agronomic methods used in agriculture to limit weed populations due to characteristics such as increased efficiency and ease of application (Lodovichi *et al.*, 2013); previous techniques included crop rotation, tillage and mowing (Dinelli *et al.*, 1996). This change in weed control methods proved advantageous, with a reduction in overall costs and an increase in crop yield and quality being observed (Dinelli *et al.*, 1996; Kawahigashi *et al.*, 2007). The production and use of herbicides worldwide has increased significantly over the past 50 years and to date there are approximately 150 herbicide active ingredients which are formulated into commercial products (Aksakal *et al.*, 2013; Holt, 2013).

Herbicides are marketed and sold as formulations under trade names assigned by manufacturers. Herbicide formulations consist of the active ingredient and adjuvants/inert ingredients such as surfactants, wetting agents, penetrants, stabilizing agents, inorganic salts, buffering agents and emulsifiers (Tush *et al.*, 2013; Van Toor *et al.*, 1994, Wang and Liu, 2007). Adjuvants/inert ingredients are added to herbicides to increase the stability, solubility and efficacy of the herbicidal activity of the active agent, thereby reducing the volumes and application cycles required to achieve the desired herbicidal effect (Chahal *et al.*, 2012; Chan *et al.*, 2007; Garrido *et al.*, 2014; Hazen, 2000; Huston and Pignatello, 1999; Liu, 2004).

## Herbicide classification and properties

Herbicides are commonly classified according to chemical structure, the mode of action (MOA) and the site of action (Ohkawa *et al.*, 1999).

Although naturally occurring and inorganic substances have been used as herbicides, most herbicides are synthetic organic compounds (Budde, 2004). Herbicides that are grouped into classes according to chemical structure provide information on the activity of the herbicide in plants, animals, soil and water; however, it must be noted that herbicides from the same chemical families do not always display similar effects in plants (Holt, 2013). Some of the major herbicide chemical families/classes together with examples of herbicides belonging to the representative classes and examples of marketed trade names are shown in Table 1.1.

**Table 1.1:** Major classes of herbicides and examples of existent active ingredients and trade names.

| Chemical class/family | Active ingredient/s | [1a,b,c,d]Trade name/s | Reference |
|---|---|---|---|
| Benzoic acid | Dicamba[2] | Banvel, Clarity | González *et al.*, 2009 |
| Bipyridilium | Paraquat, diquat | Gramoxone Inteon, Reglone | Mulugeta & Megersa, 2004 |
| Carbamates | Propham, chlorpropham | Sprout Nip, Furloe | Crespo-Corral *et al.*, 2008 |
| Dinitroaniline | Trifluralin, pendimethalin | Treflan, Prowl | Wang & Arnold, 2003 |
| Phosphoorganics | Glyphosate | Roundup, Rodeo | Eash and Bushway, 2000 |
| Imidazolinone | Imazamox, imazaquin | Raptor, Scepter | Fragiorge *et al.*, 2008 |
| Phenoxycarboxylic acid | 2,4-D*, MCPA* | Butyrac, Weedone | Pereiro *et al.*, 2004 |
| Phenols | Dinoseb, bromoxynil | Potato Top Killer 300, Buctril | Argese *et al.*, 2005 |
| Pyridazinone | Norflurazon | Zorial Rapid 80 | Sandmann *et al.*, 1980 |
| Sulfonylurea | Mesosulfuron, triasulfuron | Osprey, Amber | Fenoll *et al.*, 2013 |
| Thiocarbamate | EPTC* | Eptam | Wilmesmeier & Wierman, 1995 |
| Triazine | Atrazine, simazine | Aatrex, Princep | Meakins *et al.*, 1994 |
| Triazinone | Metribuzin | Sencor | Buman *et al.*, 1992 |
| Urea (phenyl) | Linuron, diuron | Lorox, Karmex | Farré *et al.*, 2007 |
| Uracil | Terbacil | Sinbar | Tekel *et al.*, 1998 |

* Abbreviations: 2, 4-Dichlorophenoxyacetic acid (2,4-D), 4-Chloro-2-methylphenoxyacetic acid (MCPA), 5- Ethyl-dipropyl-thiocarbamate (EPTC). [1] Trade names for the representative herbicides were obtained from: [a] The Oklahoma co-operative extension fact sheet. Joe Armstrong (extension weed specialist). Understanding herbicide mode of action. Division of Agricultural Sciences and Natural Resources. Oklahoma State University. [b] Bayer Crop Science, chemical product and company information, materials safety data sheet (MSDS) no: 000000000029. [c] Mosanto Imagine, History of Monsanto´s glyphosate herbicides. June 2005. [d]Canadian water quality guidelines for the protection of aquatic life.

The MOA of herbicides refers to the adsorption, translocation and metabolism of the herbicide in the plant and is defined by the physical and/or behavioral alterations in plants linked to biological responses resulting from herbicide exposure (Spycher *et al.*, 2004). The mode of action of herbicides includes a sub-classification category which describes the pathway of herbicides in plants. Systemic herbicides are mobile in plants and entry can occur via the phloem

and/or the xylem (Foy, 1964; Bromilow *et al.,* 1990). Contact herbicides exert their herbicidal activity at the application site (Bussan and Dyer, 1999). The site of action or mechanism of action refers to the disruption of a specific biological process within the plant (Aliferis and Jabaji. 2011; Dayan and Watson, 2011). The MOA and site of action are often referred to interchangeably (Zimdahl, 2007). Modes of action include the inhibition of cell division, cell metabolism, cell growth and the inhibition light reactions in the plants (Jones, 2005).

Herbicides display three main mechanisms of action (Zimdahl, 2007). The first is the inhibition of respiration and photosynthesis in plants. Photosynthesis and respiration are interdependent physiological processes in plants that are essential to plant growth and maintenance (La Catoni and Gratani, 2014). Photosynthesis, which occurs in the chloroplasts, is generally described as the conversion of light to chemical energy utilizing atmospheric carbon dioxide and water for the production of adenosine triphosphate (ATP) and nicotine adenine dinucleotide phosphate (NADPH) for the reduction of carbon dioxide which allows the synthesis and formation of carbohydrates and other compounds crucial to plant growth. Respiration, which occurs in the mitochondria, involves the metabolism of carbon compounds for the production and of ATP (Checchetto *et al.,* 2013; Dayan and De Zaccaro, 2012; Noguchi and Yoshida, 2008; Raghavendra *et al.,* 1994). ATP plays a key role in energy dependent processes in plant cells (e.g. sucrose synthesis and repairing photosynthetic proteins) (La Catoni and Gratano, 2014; Roux and Steinebrunner, 2007). The respiration process in plants not only functions as a mechanism for the production of ATP, but amongst other functions provides the carbon structures required for biosynthetic processes and also plays a role in the regulation of reactive oxygen species (ROS) production during plant stress (e.g. abiotic stress factors) (Van Dongen *et al.,* 2011).

Two distinct forms of photosynthesis exist and are described as: 1) Oxygenic photosynthesis which occurs in higher plants, algae and cyanobacteria, utilizes water as a source of electrons and results in the formation of molecular oxygen and 2) Anoxygenic photosynthesis is a process that is executed by bacteria, whereby electrons are sourced from hydrogen gas, sulfur compounds and organic materials for carbon fixation and therefore does not result in the release of molecular oxygen (Broser *et al.,* 2011). Considering anoxygenic photosynthesis does not

occur in plants, further description of this process will not be detailed in this Chapter, as it falls outside the scope of this study.

Oxygenic photosynthesis in plants is characterized by two protein co-factor complexes known as photosystem I (PS I) and photosystem II (PS II) (Laisk *et al.*, 2014). These reaction systems are embedded in the thylakoid membrane and act as catalysts of the initial stages of photosynthesis (Figure 1.1).

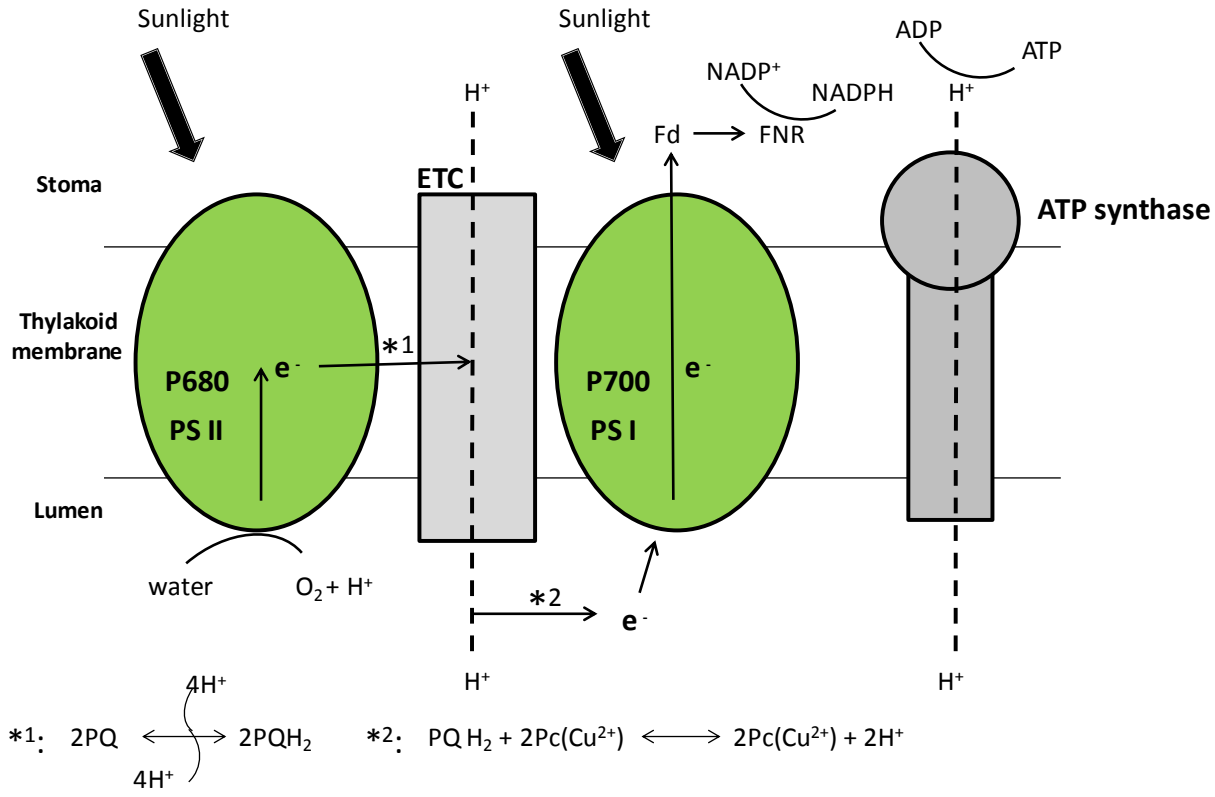


**Figure 1.1** : A schematic illustration of light reactions during oxygenic photosynthesis in plants. PSII: photosystem II, P680: primary electron donor in PSII, $e^-$: electrons, ETC: electron transport chain, PSI: photosystem I, P700: primary electron donor in PSI, Fd: ferredoxin, FNR: ferredoxin-$NADP^+$-oxidoreductase. *1: The chemical reaction representing the conversion of plastoquinone to plastoquinol, *2: The chemical reaction representing the $e^-$ transfer from plastoquinol to plastocyanin. (This image was adapted from Saenger *et al.*, 2012).

PSII utilizes energy from sunlight to oxidize water molecules releasing electrons ($e^-$) and forming the by-product oxygen (released into the atmosphere). PSII transfers $e^-$ from water to a mobile electron carrier known as plastoquinone (PQ) through the primary electron donor P680 (two chlorophyll *a* molecules), which causes the subsequent reduction of PQ to plastoquinol (PQH). The $e^-$ are then translocated through the electron transport chain (ETC) via the intermediate electron transfer complex, cytochrome *bf*, which passes the electrons to plastocyanin (Pc) (a water soluble carrier in the thylakoid lumen). The $e^-$ are then transferred to the stomal side of PS I, through the primary donor P700 (two chlorophyll *a* molecules) and donated to ferredoxin (Fd) (a water soluble mobile electron carrier) which is used in the reduction of nicotinamide adenine dinucleotide phosphate ($NADP^+$) (this reaction is catalyzed by ferredoxin-$NADP^+$-oxidoreductase (FNR)). This process produces reducing equivalents, required for the conversion of carbon dioxide to carbohydrates. The proton translocation across the thylakoid membrane (from the stroma to the lumen) results in a pH gradient and the resulting proton motive force drives the synthesis of ATP which is catalyzed by ATP synthase (Krauβ, 2003; Regner, 2012; Saenger, 2012; Shikanai, 2014; Yao *et al.*, 2012).

The majority of herbicide classes demonstrate herbicidal activity by the inhibition of photosynthesis (Bowes *et al.*, 1980; Duke, 1990) and most herbicides that display photosynthetic inhibition interfere with electron flow in PS II (Masojídek *et al.*, 2011). Herbicide classes that interfere with electron transport in the PS II reaction system include the triazines (e.g. atrazine and simazine) (Droppa *et al.*, 1981; Jursinic *et al.*, 1991), the trizinones (e.g. metribuzin and hexazinone) (Kennedy *et al.*, 2012; Schwenger-Erger and Barz, 2000) and the phenylureas (e.g. diuron and monuron) (Kennedy *et al.*, 2012; Malakondaiah and Fang, 1978). PS II inhibitors block electron transport by competitively binding to a PQ binding site on the D1 protein (functions in plastoquinone reduction by binding to quinone) in the PS II reaction center and thus halting electron transport beyond plastoquinone (Bowes *et al.*, 1980; Devine and Shukla, 2000; Ducruet and Ort, 1988, Newton and Tyler, 1989; Wilski *et al.*, 2006). The disruption of electron transport by PS II inhibitors results in two major effects, a deficiency in reduced $NADP^+$ which is required for carbon dioxide fixation and the production of free radicals which causes the photooxidation of important molecules such as the chlorophylls, carotenoids and unsaturated lipids in the chloroplasts (Devine and Shukla, 2000; Rutherford *et al.*, 1984; Yuan *et al.*, 2013).

Herbicides inhibit respiration by uncoupling mitochondrial oxidative phosphorylation (ATP synthase), photophosphorylation and/or obstructing electron transport (Moreland and Huber, 1979). These processes are necessary for the production of energy (ATP) which is required to drive several reactions, therefore, the interference of ATP production by these herbicides causes alterations in biological functions related to the growth and the metabolic processes of plants (Moreland *et al.,* 1972b). Herbicidal carbamates (e.g. chlorpropham and barban) (Macherel *et al.,* 1982; Rebeiz *et al.,* 1984), dinitroanilines (e.g. trifluralin) (Moreland *et al.,* 1972a; Sloan and Camper,1981) and phenols (e.g. dinoterb) (Belbachir *et al.,* 1980) are examples of herbicidal classes that inhibit the respiration process in the mitochondria of plants.

The second mechanism of action displayed by herbicides is the inhibition of plant growth. The growth and development of plants is regulated by plant hormones (Miransari and Smith, 2014) such as auxins (Finet and Jaillais, 2012), abscisic acid (ABA) (Li *et al.,* 2011), ethylene (Iqbal *et al.,* 2013), gibberellins (Swain and Singh, 2005), cytokinins (Choi *et al.,* 2011) and brassinosteroids (Bajguz and Tretyn, 2003). Herbicides act as synthetic mimics of the naturally occurring auxin indole-3-acetic acid (IAA). Auxins target IAA and at low auxinic herbicide concentrations a stimulation of growth (via cell division and elongation) is observed. The concentration and effect of naturally occurring auxins is tightly regulated in plants. Upon exposure to high concentrations of auxinic herbicides; auxin homeostasis is disrupted resulting in an uncontrolled auxin response. This causes a series of cascade reactions involving the induction of 1-aminocyclopropane-1-carboxylic acid synthase (ACC) (an enzyme involved in ethylene biosynthesis) resulting in increased levels of ethylene (involved in the stress response in plants and plays a key role in the regulation of plant growth and senescence) which stimulates the biosynthesis of ABA (mediates stomatal closure) (Grossmann *et al.,* 1996; Kelley and Riechers, 2007; Pirrung *et al.,* 1998). The biosynthesis of ethylene plays a very important role in the herbicidal effects observed in plants treated with auxinic herbicides, this is due to the release of the co-product cyanide during ethylene biosynthesis (Grossmann and Scheltrup, 1997; Sunohara and Matsumoto, 2008). Studies by Scheltrup and Grossmann (1995) concluded that increased levels of ABA was an additional contributing factor to herbicidal effects observed in plants, with a reduction in photosynthetic carbon dioxide and water consumption reported in the dicotyledonous weed, Cleaver (*Galuim aprine L*), upon exposure to the auxinic herbicide, Quinmerac. The treatment of susceptible plants with auxinic herbicides in plants results in

several growth and physiological abnormalities including leaf epinasty, the inhibition of root and shoot growth, stem curvature, chlorosis and ultimately, necrosis (Deshpande and Hall, 2002; Sunohara *et al.,* 2010). Herbicidal classes that act as auxinic herbicides include phenoxycarboxylic acids (e.g. 2,4-D and MCPA) and benzoic acids (e.g. dicamba) (Mithila and Hall, 2007; Ostrowski and Jakubowska, 2013).

The third mechanism of action displayed by herbicides is the inhibition of biosynthetic processes which includes, amongst others:

1) The inhibition of cell division and mitosis, which involves the disruption of mitotic cell division resulting in the depolymerization of tubulin subunits, causing the shortening or complete eradication of microtubules (regulate cell shape and mitosis), which ultimately results in severe defects in the elongation and development of roots (Anthony and Hussey, 1999; Lehnen and Vaughn, 1992; Vaughn, 2006). Dinitroanilines (e.g. trifluralin) is an example of a herbicide class that are commonly known as mitotic disrupters (Fernandes *et al.,* 2009).

2) The inhibition of carotenoid synthesis. Carotenoids are a group of pigments found in the thylakoid membrane and serve as protective agents against (e.g. chloroplast photo-oxidation) (Domonkos *et al.,* 2013). Carotenoid synthesis inhibiting or bleaching herbicides (e.g. norflurazon in the pyridazinone herbicide class), target the enzyme phytoene desaturase that catalyzes the desaturation of phytoene, which is required for carotenoid synthesis (Linden *et al.*, 1990; Millie *et al.,* 1990; Ruizzo *et al.,* 1992). The resultant effects of carotenoid deficiency include the destruction of photosynthetic membranes by reactive oxygen species and the degradation of chlorophyll, leading to plant discoloration and necrosis (Kim *et al.,* 2004).

3) The inhibition of amino acid synthesis. Amino acids have varied and diverse functions in plants (e.g. amino acids are the building blocks of enzymes and proteins) (Tegeder, 2012). Glyphosate (herbicide class: organophosphate), the main focal point of this study, exhibits this mechanism of action by targeting the enzyme 5-enolpyruvate-shikimate-3-phosphate synthase (EPSP) in the shikimate pathway, which is a pathway responsible for amino acid production (Gehin *et al.,* 2005). Greater detail on this mechanism of action by glyphosate will be provided in the sections to follow.

Although herbicides are commonly classified according to chemical structure and MOA, other criteria are also used in the classification of herbicides; these include the classification of a herbicide based on timing (post emergence or pre-emergence) and the classification of herbicides based on selectivity (selective and non-selective). Post-emergent is defined as the foliar application of a herbicide on target weeds that have germinated and emerged (Laganá *et al.*, 2000) and pre-emergent refers to the ground application of the herbicide preceding weed germination (Kilinc *et al.,* 2011; Nurse *et al.,* 2006). With respect to selectivity some herbicides are classified as selective, which means they show greater toxicity in some plants (e.g. broad-leafed plants) as compared to others (e.g. grasses) and the opposite holds true for non-selective herbicides, which are toxic to all plants (e.g. broad-leafed plants and grasses) (Holt, 2013).

## 1.2 Glyphosate (N-phosphonomethylglycine)

### 1.2.1 History and discovery of glyphosate, glyphosate structure and general properties of glyphosate based herbicides (additives and mixtures)

Glyphosate was developed by the Monsanto Company in the 1970´s (Pederson *et al.,* 2007; Woodburn 2000). The herbicidal potential of glyphosate was first demonstrated in 1971 (Carlisle and Trevors, 1987), during the study of the herbicidal effects of tertiary aminomethylphosphonic acids derived from primary and tertiary amines (Carlisle and Trevors, 1987). Glyphosate is a low molecular weight organophosphate compound, derived from glycine and contains three ionisable chemical groups (Figure 1.2) an amine (basic group), a carboxylate and the phosphonate group (acidic groups) with $pK_a$ values of 10.25, 2.27 and 5.57, respectively (Anadón *et al.,* 2009; Coutinho *et al.,* 2007; Schönherr, 2002).

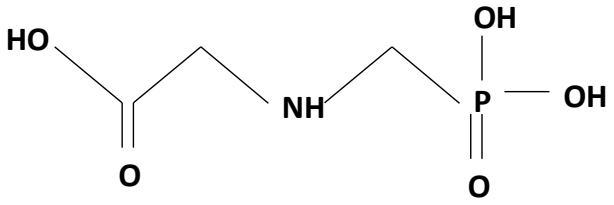


**Figure 1.2:** The chemical structure of glyphosate (This image was adapted from: Dzygiel & Wieczorek, 2000; Yue *et al.*, 2008).

This compound is characterized by a very stable carbon-phosphorous bond (Kools *et al.*, 2005) and crystalline structural studies have indicated that solid state glyphosate exists in a zwitterionic state with delocalization of the phosphonate proton onto the amine group (Sagatys *et al.*, 2000). Glyphosate is an amphoteric, non-volatile compound which demonstrates high polarity and water solubility, however glyphosate in the free acid form shows lower water solubility due to strong intramolecular hydrogen bonding (Schönherr; 2002; You and Koropchak, 2003). The general physiochemical properties of glyphosate acid are shown in Table 1.2.

**Table 1.2:** [1]A summary of the physiochemical properties of glyphosate acid

| Parameter | Glyphosate (acid) |
|---|---|
| Chemical name | *N*-(phosphonomethyl)-glycine |
| Formula | $C_3H_8NO_5P$ |
| Molecular mass | 169.1 |
| Melting point | 189.5 °C |
| Boiling Point | Decomposition |
| Solubility in water | 10.1 g/L (20 °C, pH 2, 995 g/Kg) |
| Relative density | 1.7 (995 g/Kg) |
| Dissociation constant | pKa 2.3 (20 °C), 5.73 (20 °C), 10.2 (25 °C) |
| Henrys law constant | $2.1 \times 10^{-7}$ Pa ($m^3$/mol) |
| Vapor pressure | $1.31 \times 10^{-5}$ Pa (25 °C) |
| Organic carbon partition coefficient ($K_{OC}$) | 9.0-60000 (L/Kg) |
| Soil half-life | 2-197 (days) |

[1] Battaglin *et al.,* 2005; European commission review report, 2002; Grunewald *et al.,* 2001

In 1974 glyphosate was registered with the U.S. Environmental Protection Agency (USEPA), thereafter the active ingredient was included into commercial herbicide formulation products under the trade name Roundup® and introduced into the global market. Glyphosate was marketed as a systematic, relatively non-selective, post-emergence herbicide (initially as a dessicant) for the control of several annual and perennial grasses, broad leaf weeds and sedges. The expiration of the patent held by the Monsanto Company in the year 2000 allowed a vast number of companies to begin formulating and selling glyphosate. To date, glyphosate commercial herbicide formulations are sold under a vast number of trade names by several companies including Monsanto (Al-Rajab and Schiavon, 2010; Johnson *et al.,* 2009; Linz and Homan, 2011; Mateos-Naranjo *et al.,* 2009; Mitsis *et al.,* 2011, Steinmann *et al.,* 2012).

Glyphosate has become the most important and most commonly used herbicide worldwide and predictions by the global market indicate that over a million metric tons of glyphosate will be used before the end of this decade (Ge *et al.,* 2012). The success and increased use of glyphosate is due to the many factors. Glyphosate has been described as a highly effective, economical (price reductions and increased supply due to patent expiry) broad spectrum herbicide which

demonstrates a shorter half-life than a majority of other herbicides and is believed to cause less ecotoxicological effects when compared to other herbicides (Binimelis *et al.,* 2009; Mamy and Barriuso, 2005; Shen *et al.,* 2013). The introduction, continuous development and adoption of genetically modified (GM) glyphosate resistant (GR) crops is an important contributor to the increase in the global glyphosate market and has provided an alternative approach with respect to constraints encountered in the control of weeds in various crops (Duke, 2003; Mamy and Barriuso, 2005; Woodburn, 2000; Yu *et al.,* 2007). Glyphosate resistant crops were introduced in 1996 and grown on 1.7 million hectares worldwide. By 2008 this number increased to 79 million hectares (Lane *et al.,* 2012). No tillage cropping (which entails growing crops without tilling, thereby reducing soil erosion and nutrient leaching) requires the use of herbicides to prevent the competitive growth of weeds and has also played an important role in the expanding use of glyphosate-based herbicides (Helander *et al.,* 2012).

In section 1.1.4 herbicide formulations were described as mixtures containing the active ingredient and adjuvants, which are used to improve the overall effectiveness of the herbicide. Commercial formulations of glyphosate are often aqueous mixtures containing between 40-79 % glyphosate in the form of glyphosate acid (pH below 2) or glyphosate salts such as monoammonium, diammonium, isopropylamine (most commonly used in glyphosate formulations), potassium, sodium and trimesium (trimethylsulfonium) salts (Johnson *et al.,* 2009; Saitúa *et al.,* 2012). Glyphosate salts are used in formulation due to high water solubility characteristics, however glyphosate salts demonstrate poor lipid solubility, which reduces the capacity for foliar penetration of glyphosate, and additional adjuvants are therefore required in commercial preparations (Schönherr, 2002).

Glyphosate formulations consist of a surfactant and other minor components, among which ammonium sulfate is frequently present (Green and Beestman, 2007; Kielak *et al.,* 2011, Mengistu *et al.,* 2013; Piola *et al.,* 2013, Saitúa *et al.,* 2012). Ammonium sulfate serves a dual function. First, ammonium ions competitively bind to glyphosate via carboxyl and phosphonate groups forming an ammonium-glyphosate complex that aids in the adsorption of glyphosate into plants. Secondly, ammonium sulfate demonstrates the capacity to overcome the effects on glyphosate efficacy presented by antagonistic compounds such as calcium, magnesium,

manganese and iron which may be present in the environment (e.g. hard water) (Cakmak *et al.*, 2009; Mueller *et al.*, 2006).

Surfactants make up the majority of adjuvants (26-74 %) used in herbicide formulations (together with solvents) with non-ionic surfactants like alcohol ethoxylates, alkylphenol ethoxylates and alkylamine ethoxylates (Figure 1.3) being primarily utilized in herbicide formulations (Chamel and Gambonnet, 1997; Krogh *et al.*, 2002).

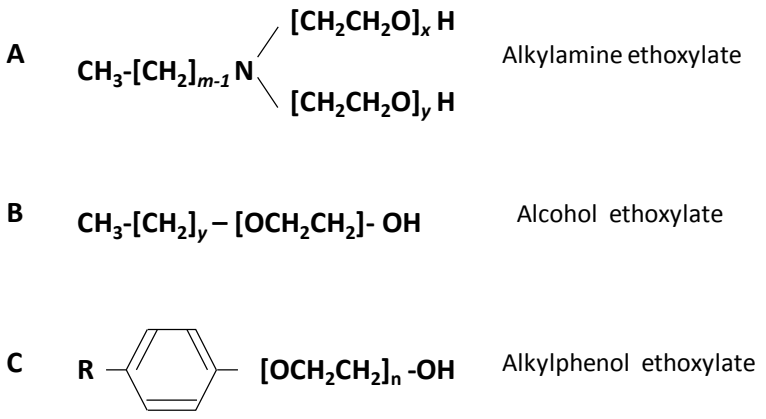


**Figure 1.3:** Chemical structures of non-ionic surfactants commonly used as adjuvants in herbicide formulations (Image was adapted from: Berryman *et al.*, 2004; DeArmond & DiGoregono, 2013; Krogh *et al.*, 2003.

Non-ionic surfactants are chemical compounds that are structurally defined by the presence of a hydrophobic moiety (often alkyl or alkylaryl in structure) and a hydrophilic moiety (most commonly a polyoxyethylene chain) (Schramm, 2000; Van Ginkel *et al.*, 1993). The most frequently used non-ionic surfactant in glyphosate commercial formulations is polyoxyethylene tallow amine (POEA), which belongs to the alkylamine ethoxylate family (Dinehart *et al.*, 2009; Tsui and Chu, 2003). Alkylamines are extracted from natural products (e.g. tallow oil, soya oil or coconut oil) and reacted with ethylene under high pressure and temperature, to form ethoxylated alkylamines (Figure 1.3) (Schreuder *et al.*, 1986; Tush *et al.*, 2013). Glyphosate alone does not demonstrate the capacity to penetrate through plant cuticles, and POEA is therefore a crucial

component in increasing the efficacy of glyphosate through the modification of physical and biological properties of the mixture to aid the entry of glyphosate into target weeds (Gimenes *et al.,* 2013; Mann *et al.,* 2009; Mbanaso *et al.,* 2013).

### 1.2.2 Glyphosate uptake, translocation, mechanism of action and metabolism in plants

The efficiency of herbicidal treatments is determined by the transport to and the amount (the concentration should be lethal dose) of the active ingredient that reaches the target site of action (Perkins *et al.,* 2008; Price and Anderson, 1985). In foliar applied herbicides like glyphosate, a successful herbicidal treatment is dependent on various interconnected factors such as the application of the herbicide, retention on the leaf surface, penetration into the tissue and translocation to the target site (Basi *et al.,* 2013; Knoche, 1994; Perkins *et al.,* 2008). Of these factors the most important are the retention of the herbicide on the leaf surface and penetration through the leaf surface via a lipid membrane known as the plant cuticle and translocation to the target site (Evelyne *et al.,* 1992; Perkins *et al.,* 2008; Stevens *et al.,* 1988; Yanase and Andoh, 1992). This cuticular membrane acts as the primary biological barrier which controls the penetration of xenobiotic compounds into the plant (Evelyne *et al.,* 1992). The structure of the cuticle and composition varies between plant species but most cuticles are 0.1-10 µm thick (Ramsey *et al.,* 2005). The cuticle is structurally characterized by two major lipid classes. The first is solid waxes (a mixture of long chain aliphatic compounds) and the transport limiting layer on the outer surface of the cuticle which is composed of cutin, and a matrix of polyhydroxylated $C_{16}/C_{18}$ fatty acids that are cross linked by ester bonds (Domínguez *et al.,* 2011; Evelyne *et al.,* 1992; Fagerström *et al.,* 2013; Santier and Chamel, 1998).

Surfactants in glyphosate formulations increase droplet retention by reducing the dynamic surface tension of the spray solutions, however mechanisms of surfactant assisted cuticular uptake of herbicides are not fully established (Liu, 2004; Mäkelä *et al.,* 1996; Stevens *et al.,* 1988; Wang and Liu, 2007). Studies have suggested that surfactants may possibly alter the permeability of the plant cuticle and researchers conducting studies on the mechanism of action of surfactant assisted herbicide uptake in plants have postulated a mechanism in which water soluble herbicides such as glyphosate penetrate the lipophilic cuticle via diffusion through a

hydrophilic pathway (Knoche and Bukovac, 1993; Ramsey *et al.*, 2005). This theory is however based on studies conducted on specific herbicide active ingredients, cuticle types and surfactants (Ramsey *et al.*, 2005). The uptake of herbicides in the presence of surfactants is dependent on the physiochemical properties of the active ingredient, structure and concentration of the surfactant and the characteristics of the leaf surface of different plant species (Liu, 2004; Liu *et al.*, 2004, Mercer, 2007; Paterson *et al.*, 1990; Stevens *et al.*, 1988; Wang and Liu, 2007). The postulated mechanism therefore provides generalized information with respect to the uptake of water soluble herbicides in plants.

Once absorbed into the plant, glyphosate is translocated in the plant through the symplastic pathway, primarily via phloem sieve tubes (Bromilow and Chamberlain, 2000; Geiger and Bestman; 1990), over long distances following a pattern of source to sink (with the same distribution pattern as photoassimilates) (Dewey and Appleby, 1983; Feng and Chiu, 2005). Glyphosate demonstrates good symplastic mobility and this is mostly due to the ionizable functionality of this herbicide (Bromilow and Chamberlain, 2000). Glyphosate is ultimately transported to the plastids, where its target enzyme, 5-enolpyruvyl-shikimate-3-phosphate synthase (EPSP synthase), an enzyme of the shikimate pathway, is located (Feng *et al.*, 2013; Gout *et al.*, 1992).

The shikimate pathway (not found in mammals) is an important pathway in plants, fungi, bacteria and algae required for the production of aromatic amino acids (phenylalanine, tyrosine and tryphtophan) and consists of seven enzymatic steps that lead to the conversion of *D*-erythrose-4-phosphate and phosphoenol pyruvate (PEP) to chorismate, a precursor to amino acids (Acuri *et al.*, 2004; Schmid and Amrhein, 1994) (Figure 1.4).

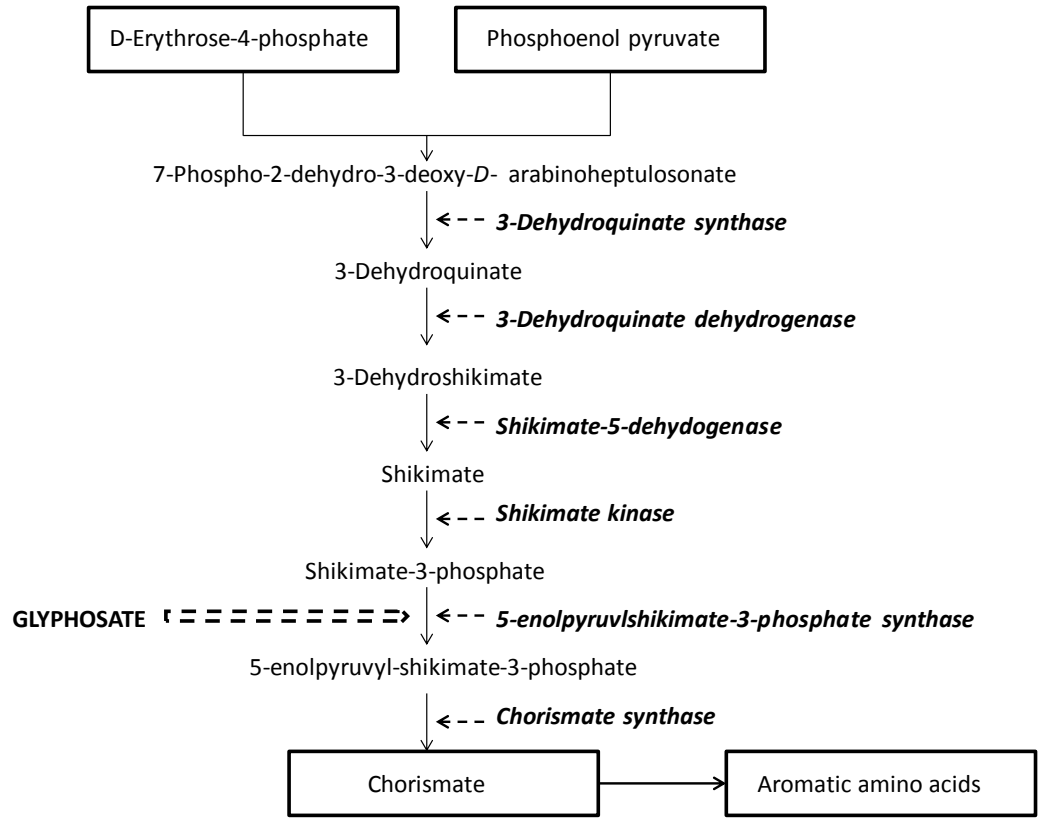


**Figure 1.4:** The biosynthetic shikimate pathway illustrating the conversion of *D*-erythrose-4-phosphate and phosphoenol pyruvate to chorismate (the precursor to aromatic amino acids) and the target site of glyphosate. (This image was adapted from: Elandalloussi *et al.*, 2005).

EPSP synthase is the sixth enzyme of the shikimate pathway and functions as a catalyst in the reaction involving the transfer of the enolpyruvyl group from PEP to shikimate-3-phosphate (S3P) forming the product 5-enolpyruvyl-shikimate-3-phosphate (EPSP) and inorganic phosphate (Figure 1.5). EPSP is an important intermediate of the shikimate pathway for the ultimate synthesis of aromatic amino acids. Glyphosate displays highly specific interactions with EPSP synthase and inhibits this enzyme by forming a ternary complex with EPSP synthase and S3P ((S3P)-EPSP synthase-(S3P)-glyphosate); this prevents the effective binding of PEP. The interaction between glyphosate and PEP is competitive; however the interaction between glyphosate and S3P is uncompetitive. Taking into consideration the competitive association between PEP and glyphosate, any conformational changes (even minor) in the glyphosate

structure significantly reduce the affinity of glyphosate for EPSP synthase. The inhibition of EPSP synthase by glyphosate halts the production of chorismate, resulting in the reduction of aromatic amino acid synthesis (resulting in a depletion of aromatic amino acids), reduced protein synthesis, reduced growth and premature cell death (Ahn *et al.,* 2004; Ali *et al.,* 2005; Boocock and Coggins, 1983; Caetano *et al.,* 2013; Eason *et al.,* 2000; Kaliannan *et al.,* 2002; Knowles *et al.,* 1993).

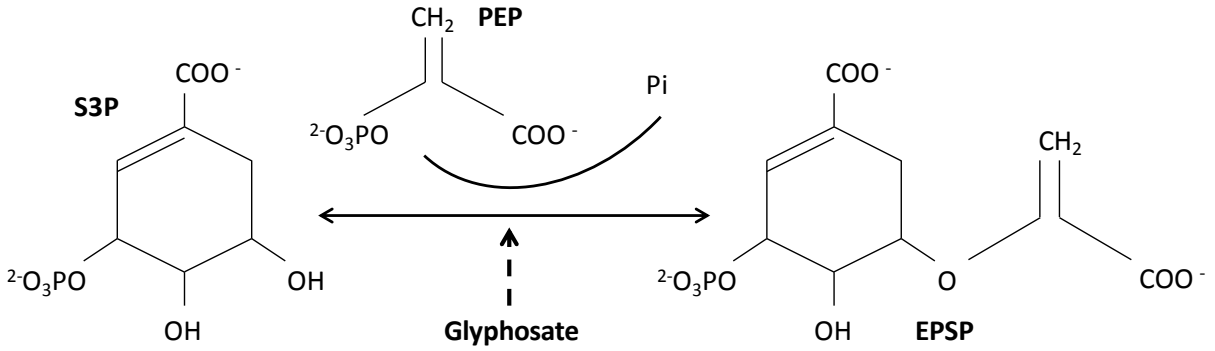


**Figure 1.5:** The chemical reaction catalyzed by EPSP synthase which involves the transfer of an enolpyruvyl group from PEP to S3P. Glyphosate competes with PEP to form a complex with EPSP synthase and S3P. (This image was adapted from Kaliannan *et al.,* 2002).

Glyphosate has been reported to inhibit other enzymes in this pathway due to its metal chelating properties (e.g. 3-deoxy-*D*-arabino-heptulosonate, 7-phosphate-synthase and dehydroquinate synthase). No other class of herbicide has been shown to inhibit EPSP synthase or any other enzymes in this pathway (Caetano *et al.,* 2013; Eason *et al.,* 2000).

The damaging effects in plants treated with lethal doses of glyphosate vary depending on the plant species, differences in physiological mechanisms and overall susceptibility to glyphosate (Eason *et al.,* 2000). Considering under normal growth conditions, 20 % of carbon fixed by plants flows through the shikimate pathway for the production of a large number of products (including vitamins, ligands and phenolic compounds such as the phyto hormone auxin), the indirect effects of this herbicide are widespread (Cedergreen and Olesen, 2010; Geiger *et al.,*

1999). Symptoms of glyphosate treatment include stunted growth, chlorosis and bleaching; these effects are mainly observed in metabolically active sink tissues like shoots, tips, buds, roots and immature leaves. Plants treated with glyphosate die one or two weeks after application of the herbicide (Eason *et al.,* 2000; Rojano-Delgado *et al.,* 2012).

The primary mechanism of action by glyphosate is the inhibition of EPSP synthase, but particular interest of the role of glyphosate in the disruption of photosynthesis has been the focal point of various studies. Geiger *et al.,* (1986) concluded that glyphosate inhibited photosynthesis in sugar beet leaves. Richard *et al.,* (1979) concluded that glyphosate showed no direct effects of on electron transport in PS I and PS II electron transport reaction centers in pea chloroplasts. However, more recent studies by Huang *et al.* (2012) have demonstrated the direct involvement of glyphosate in the reduction of electron transport through PS II and a reduction if chlorophyll *a* and *b* in cogongrass exposed to glyphosate concentrations between 0 and 2 %. More interestingly, Wong (2000) showed evidence of glyphosate stimulated growth, photosynthesis and chlorophyll *a* synthesis in fresh water green algae exposed to low doses of glyphosate (0.2 mg/L) and inhibition of these processes at higher glyphosate doses (2 mg/L). The potential role of glyphosate in the inhibition of photosynthesis has been demonstrated, however several studies show contrasting results and the mechanisms of action and the importance of these effects have not been well established (Geiger *et al.,* 1999; Yu *et al.,* 2007).

Knowledge on the metabolism of glyphosate in plants is limited. The first evidence of a possible glyphosate metabolic pathway was reported in soybean (*Glycine max L.*), corn (*Zea Mays L.*); tobacco (*Nicotiana tabacum L.*), wheat (*Triticum astivum L.*) and spruce (*Picea abie L.*), with evidence indicating the presence of aminomethylphosphonic acid (AMPA), a major metabolite of glyphosate degradation (Komoβa *et al.,* 1992; Sánchez-Bayo *et al.,* 2010). AMPA is structurally similar to glyphosate (Figure 1.6) and is a phosphoric acid analog of glycine (Fields, 1999).

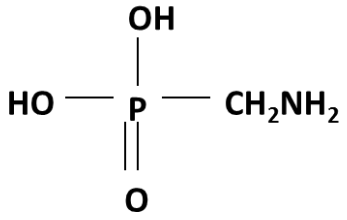


**Figure 1.6:** The chemical structure of aminomethyl phosphonic acid (AMPA) the primary metabolite of glyphosate metabolism. (This image was adapted from Motojyuku *et al.,* 2008).

Following this discovery several studies were conducted primarily in glyphosate resistant plants to determine whether the metabolism of glyphosate was a contributor to tolerance. Literature has proposed two possible mechanism of glyphosate metabolism in plants, the first is the cleavage of the oxidative bond by glyphosate oxidoreductase (GOX) resulting in the production of AMPA, and the second is the cleavage of the carbon (C)-phosphorous (P) bond by C-P lyase with AMPA and sarcosine as end products (Ding *et al.,* 2011a; Rojano-Delgado *et al.,* 2012). Some reports have stated that resistance in plants to glyphosate is aided by the presence of the GOX gene, for the metabolism of glyphosate (González-Torralva *et al.,* 2012a; Jiang *et al.,* 2013; Powles and Preston, 2006; Zhu *et al.,* 2013). Glyphosate metabolism in plants has been reported in some studies (Arregui *et al.,* 2003; Carlisle and Trevors, 1988; González-Torralva *et al.,* 2012b; Reddy *et al.,* 2004; Reddy *et al.,* 2008). In contrast to these studies some researchers have revealed little or no significant evidence of glyphosate plant metabolism (Dinelli *et al.,* 2006; Feng *et al.,* 2009; Lorraine-Colwill *et al.,* 2003; Zandstra and Nishimoto, 1977). This has led to the general idea that some plants are able to metabolize this compound at varying rates and others may simply form binding associations in different parts of the plant (Bradshaw *et al.,* 1997; Rojano-Delgado *et al.,* 2012; Sandberg *et al.,* 1980; Xiao-Ling *et al.,* 2011).

### 1.2.3 Glyphosate fate, behavior and chemistry in the environment (soil and water)

Significant amounts of glyphosate can enter the soil environment during pre-plant use, in the early stages of growth of glyphosate tolerant crops, after treatment due to direct application and

foliar wash-off from the target plant or during post harvest applications. The behavior of herbicides in soil is affected by different biological and physiochemical processes which directly affect their decomposition, accumulation, retention and their transport towards other environmental systems such as aquatic systems (Gevao *et al.,* 2000; Mamy and Barriuso, 2005; Mamy *et al.,* 2005; Zabaloy *et al.,* 2012).

The mobility and resultant leachability of a compound in soil is dependent on its sorption characteristics (size, shape, configuration, molecular structure, solubility, polarity and chemical functions) with strong sorption leading to immobilization and weak sorption causing the compound to be readily leachable (De Miranda Colombo and Masini, 2011; Gevao *et al.,* 2000). Overall, glyphosate in soil generally demonstrates a low volatilization potential (due to high water solubility and low vapor pressure) and fairly high sorption (>1.000 L $Kg^{-1}$) characterized by the immediate and high affinity binding/adsorption to soil constituents and demonstrates a moderate persistence in soil environments ranging from 1 to 174 days (average 47 days) (Candela *et al.,* 2007; Peruzzo *et al.,* 2008; Pessagno *et al.,* 2008; Sprankle *et al.,* 1975a; Torstensson and Aamisepp, 1977; Veiga *et al.* 2001). The sorption characteristics of glyphosate are affected by factors such as the chemical composition of soil, the competitive effects presented by the presence of phosphate in the soil and pH (Candela *et al.,* 2007; Candela *et al.,* 2010; Zhao *et al.,* 2009).

Glyphosate generally binds to soil constituents through the phosphoric acid group in a mechanism similar to that of phosphate and therefore often competes with phosphate (found in fertilizers) for sorption sites via the phosphoric acid moiety (De Santana *et al.,* 2006; Forlani *et al.,* 1999; Morillo *et al.,* 2000), however weak surface carboxyl binding with soil minerals has also been reported (Barja and Dos Santos Alfonso, 2005). The competitive effects of phosphates are important to consider as excessive application of phosphates (heavy application of fertilizers) may cause the accumulation of phosphate in soil and the occupation of available adsorption sites which would lead to a reduction in the capacity of the soil to retain glyphosate, thereby increasing the mobility and leaching properties of this herbicide (Khenifi *et al.,* 2010).

The effect of competitive binding to available adsorption sites demonstrated by glyphosate and phosphate on glyphosate sorption in various soil types has been well documented in literature. Dion *et al.* (2001) concluded that glyphosate sorption was highly dependent on phosphate

additions when assessing the competitive sorption of $^{32}$P-labeled phosphate and $^{14}$C-labeled glyphosate in low organic carbon systems (clay minerals dominated the available sorption sites). Findings by Gimsing and Borggaard (2002a) in goethite, gibbsite, illite, montmorillonite and two kaolinites with different specific surface areas, indicated that although competition was apparent, the degree of competition was primarily based on the type of adsorbent, (i.e. goethite and gibbsite) favored phosphate binding and in illite, montmorillonite and kaolinite competitive adsorption was equivalent in both glyphosate and phosphate. In batch adsorption experiments carried out on five different Danish surface soils, the adsorption of glyphosate and phosphate was observed to be both competitive and additive and the competition was less evident than in earlier studies in goethite and gibbsite (Gimseng and Borggaard, 2002b; Gimsing *et al.*, 2004). pH did not play a significant role in the competition between glyphosate and phosphate to the extent that phosphate additions did; however, an interesting finding in this study was the effect of pH on glyphosate adsorption, which concluded that a decrease in pH increased glyphosate adsorption with a minimal effect of pH being observed in phosphate adsorption (Gimsing *et al.*, 2004). The theory of additive and competitive adsorption was further confirmed in batch adsorption experiments conducted on four different Tanzanian soils namely; Andisol, Ultisol and two Oxisols (with variable charge clay minerals) (Gimseng *et al.*, 2007). Overall findings in this study suggested that phosphate showed stronger binding to soil constituents in comparison to glyphosate (determined by the Langmuir sorption isotherm). In sequential experiments phosphate was only able to displace small quantities of pre-sorbed glyphosate, suggesting that the amount of glyphosate and phosphate adsorbed was additive. However, when phosphate was adsorbed first, this binding suppressed glyphosate binding, possibly due to increased negative charges, which would repel negatively charged glyphosate (Gimseng *et al.*, 2007).

The importance and influence of pH on the adsorption of glyphosate presents conflicting theories in literature. Earlier studies by Glass (1987) found that the adsorption of glyphosate was not entirely dependent on pH in montmorillonite saturated with cations (sodium, calcium, magnesium, copper and iron) and proposed that the adsorption of glyphosate was based on the complexation of glyphosate with the cations through a cation exchange mechanism. In contrast, the importance of pH in glyphosate adsorption was demonstrated by McConnell and Hossner (1985) in kaolinite, hematite and goethite, with an increasing pH causing an increase in the negative charges on the mineral surfaces and glyphosate, resulting in a decrease in adsorption,

similar to the inverse relationship between pH and glyphosate observed by Gimseng *et al.* (2004). Findings by Morillo *et al.* (1997) in the clay mineral montmorillonite showed that glyphosate adsorption was greater at a lower pH of 4.2 and decreased at a higher pH of 6.8. Further studies by Morillo *et al.* (2000) validated earlier findings, with studies on the effect of copper addition to glyphosate adsorption in three different soils with different characteristics. This study concluded that the addition of copper caused a reduction in the pH of the soils, thereby increasing glyphosate adsorption and a lower pH resulted in a glyphosate species with a lower negative charge which would facilitate easier binding to negatively charged soil constituents.

Glyphosate can only co-ordinate (sorb) onto variable charge surfaces (mainly through hydrogen bonding and ion exchange) and not onto permanently negatively charged sites, as this herbicide is in an anionic state at the general pH range of soils (pH 4-8) (Borggaard and Gimsing, 2008; Vereecken, 2005). Therefore glyphosate co-ordinates strongly with metal ions (cations) and, upon contact with the soil, glyphosate is primarily immobilized by the formation of surface complexes with metal metal oxides such as iron and aliminium oxides and calcium (Khoury *et al.,* 2010). Other sorption sites for glyphosate include clay minerals, silica and soil organic matter (e.g. humic substances) (Candela *et al.,* 2010; Damonte *et al.,* 2007). Soil composition is an important factor in glyphosate adsorption and soils which contain a majority of permanently negatively charged minerals (e.g. illite, smectite) demonstrate poorer glyphosate sorption than soils containing a majority of variable charged minerals (Borggaard and Gimsing, 2008). Studies by Morillo *et al.* (2000) emphasized the effect of soil content on glyphosate adsorption and concluded that the most important contributing factors to soil adsorption were the amounts of iron and aluminum amorphous oxides and organic matter. Yu and Zhou (2005) stated soil organic matter as the greatest contributor to glyphosate adsorption. Studies by Albers *et al.* (2009) concur with previous studies and experiments conducted in different soils and humic substances led to the conclusion that soil organic matter was important in the adsorption of glyphosate. Glyphosate however demonstrated weaker sorption to humic substances (desorption occurred more readily) when compared to glyphosate sorption to amorphous aluminum and iron oxides.

The degradation and loss of activity of glyphosate in soil is primarily due to microbial activities, with photodecomposition and chemical decomposition playing a minor role, due to the presence of the carbon (C) - phosphorous (P) bond, which results in glyphosate being very chemically and thermally stable (Patsias *et al.,* 2001; Rueppel *et al.,* 1977; Singh and Walker, 2006; Veiga *et al.,* 2001). The microbial degradation of glyphosate is considered a co-metabolic process. This is because a majority of microorganisms, specifically bacteria, do not utilize glyphosate as a source of carbon or nitrogen (Forlani *et al.,* 1999; Sprankle *et al.,* 1975b; Zabaloy *et al.,* 2012). However there are some fungal species that have been reported to use glyphosate as a source of nitrogen (Singh and Walker, 2006). The degree of mineralization of glyphosate is strongly dependent on the microbial activities as well as the biomass of soil microorganisms and climatic conditions (e.g. temperature) (Araújo *et al.,* 2003; Laitinen *et al.,* 2009; Stenrød *et al.,* 2006) and microbial degradation is considered the most important glyphosate conversion process in soil that dictates the overall persistence and accumulation of glyphosate in soil (Singh and Walker, 2006). Generally, microbial degradation of glyphosate leads to the production of the primary metabolite AMPA and complete degradation ultimately results in the production of water and carbon dioxide (Araújo *et al.,* 2003; Forlani *et al.,* 1999). Several microorganisms (bacterial and fungal) have the capacity to degrade glyphosate and include *Pseudomonas species* (Kishore and Jacob, 1987), *Rhizobium species* (Liu *et al.,* 1991), *Anthrobacter species* (Pipke and Amrhein, 1988), *Penicillium species*, *Tricoderma viridae* and *Aspergillus niger* (Krzyśko-Lupicka and Orlik, 1997).

Glyphosate metabolism in soil occurs through the C-P lyase pathway (Ternan *et al.,* 1998) through two mechanisms outlined in Figure 1.7 (similar mechanisms have been proposed as a possible glyphosate degrading pathways in plants see section 1.2.2). The initial mechanism involves the cleavage of the C-P bond by C-P lyase, resulting in the production of sarcosine and the second mechanism involves, the conversion of glyphosate to AMPA, followed by the dephosphorylation of AMPA by C-P lyase, which is then further broken down to carbon dioxide and ammonium (Castro *et al.,* 2007; Dick and Quinn, 1995; Lerbs *et al.,* 1990; McAuliffe *et al.,* 1990). The kinetics of glyphosate degradation are affected by the sorption and desorption of glyphosate specifically in soils that show high mineralization capacity, as this directly influences the availability of glyphosate to microorganisms. Therefore, glyphosate degradation is often characterized by an initial rapid rate of degradation of available/unsorbed glyphosate, followed

by a slower rate of mineralization of glyphosate sorbed to soil (Gimsing *et al.*, 2004; Singh and Walker, 2006; Veiga *et al.*, 2001). The degradation time of glyphosate (due to microbial activity) varies from a few days to several months and in some instances years (Laitinen *et al.*, 2009).

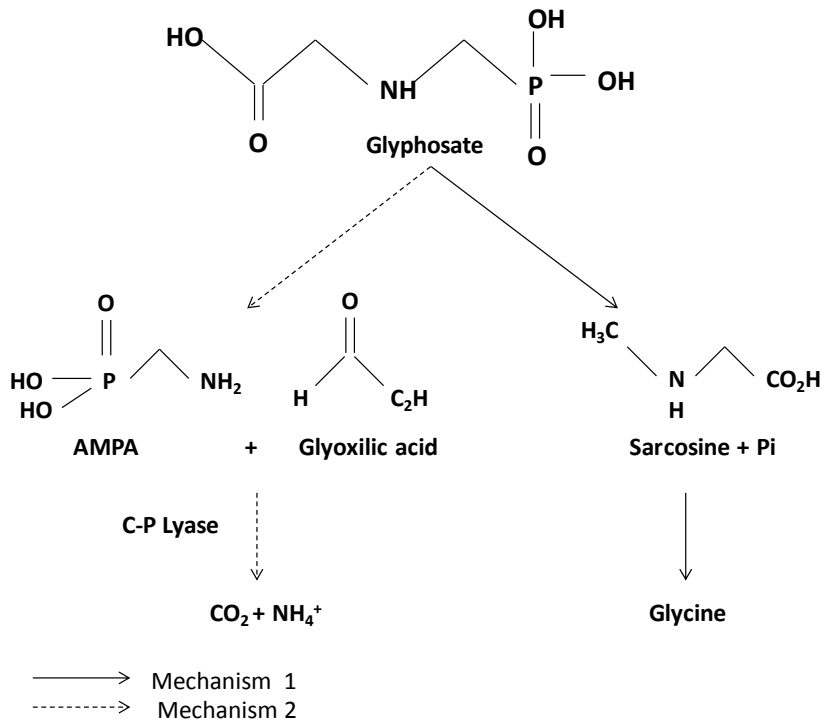


**Figure 1.7:** The metabolic degradation pathway of glyphosate by microorganisms in soil. (This image was adapted from Borggaard and Gimsing, 2008; Williams *et al.*, 2000)

Some researchers have suggested that the chemical and physical properties of glyphosate results in low mobility (due to its high adsorptive capacity), causing a minimal possibility for the compound entering water systems through leaching and surface runoff, with some studies reporting no detectable glyphosate or AMPA residues in surface and groundwater (Battaglin *et al.*, 2005; Comes *et al.*, 1976; Malaguerra *et al.*, 2013; Miller *et al.*, 1995; Ravanel *et al.*, 1999; Roy *et al.*, 1989; Tatum, 2004). It is however important to consider the type of soil in which glyphosate is applied, as evidenced by the literature presented in this section: glyphosate shows a variation of behavior depending on the soil system and the mobility of this compound is

extremely dependent on the extent of soil binding (e.g. soil half-life, the soil partition coefficient ($K_{oc}$)) and the level of microbial activity (Huang *et al.,* 1994).

The migration of herbicides (e.g. glyphosate from terrestrial to aquatic ecosystems) can occur through diffuse (indirect entry) sources from agricultural applications and involves the compound moving through soil layers in solution or sorbed to particles (glyphosate displays a similar mobility to phosphates when sorbed to soil particles) and entering water systems through surface (surface runoff) or sub-surface flow (leaching) (Borggaard and Gimsing, 2008; Carter, 2000; Hu *et al.,* 2011; Schwarzenbach *et al.,* 2006). Herbicides can also be transported to water systems through spraydrift from agricultural areas in relative close proximity (Huber *et al.,* 2000; Peterson and Batley, 1993). Leaching compounds may subsequently travel directly to groundwater, specifically in cases where the groundwater level is close to soil surfaces and rivers (Coleman *et al.,* 2002; Gregoire *et al.,* 2009). Together with soil properties surface runoff is dictated by climatic conditions (e.g. rainfall and land characteristics such as slope and distance from the point of application to the water body) and occurs when the rate of water application to the soil surface exceeds the storage capacity and infiltration rate of the soil (Bermúdez-Couso *et al.,* 2013; Holvoet *et al.,* 2007). Surface runoff is considered the major route of herbicide transfer from terrestrial to aquatic ecosystems (Rasmussen *et al.*, 2011) and herbicides transported via surface runoff are often transported to open water catchment areas including streams, rivers and lakes (Gregoire *et al.*, 2009).

Point source entry (direct entry) of herbicides into water systems occurs through either the direct application of the herbicide to the water system, improper management practices such as spillage and improper disposal of packaging material, and in urban areas by the application of herbicides to impervious surfaces like roads and sidewalks (Botta *et al.,* 2012; Gerecke *et al.,* 2002; Neumann *et al.,* 2003; Pitt *et al.,* 1999). These practices may directly deposit herbicides into sewage systems which commonly feed into surface water bodies (Gerecke *et al.,* 2002; Paul and Meyer, 2001; Ritter *et al.,* 2002).

Glyphosate is chemically stable in water systems with negligible susceptibility to photolysis. Studies by Antón *et al.* (1993) have indicated that glyphosate was stable in sunlight for 78 days (the entire duration of the study) with no statistically significant degradation occurring within the experimental period. Kylin (2013) suggested that the effects of light on glyphosate degradation

were most likely linked to increased metabolic activity. Similar to its behavior in soil, glyphosate displays sorption to sediments in water and is degraded primarily by microorganisms (the degradation pathway by microorganisms is illustrated in Figure 1.7), the extent to which is controlled by factors such as pH (an increase in acidic conditions increases glyphosate stability due to a reduction in microbial activity) and temperature (increased temperatures increase glyphosate degradation due to enhanced microbial activity) (Mallat and Barcelo, 1998; Petit *et al.*, 1995). The persistence of glyphosate in water is generally shorter than in soils and is considered to have a half-life ranging between 7-10 weeks in natural water systems (Struger *et al.*, 2008).

The propensity of glyphosate to contaminate ground water and open water systems through leaching and surface runoff has been evaluated and transport and mobility studies conducted by Landry *et al.* (2005) and Huang *et al.* (1994) in the soil types of chosen environments have demonstrated the potentially high leaching and surface runoff capacity of glyphosate. Desorption experiments by Alrajab and Schiavon (2010) showed the possibility of remobilization of herbicide residues (i.e. glyphosate does not remain permanently bound to soil constituents). Results in this study suggested that the possibility of contamination of groundwater by glyphosate was high over a long-term period, especially in soils with high adsorption capacity characteristics and low microbial activity. Hagner *et al.* (2013) hypothesized that glyphosate leaching was increased in the presence of plants, due to the transport of glyphosate from shoots to roots and ultimately to soil because of root exudates and plant decay. This study also demonstrated the role of climatic events such as rainfall on glyphosate mobility and concluded that heavy rainfall events increased glyphosate leaching in soil. A summary of studies that have indicated detectable glyphosate residues in both surface and groundwater are outlined in Table 1.3.

**Table 1.3:** A summary of selected studies showing glyphosate residue (µg/ml) detected in ground and surface waters in various countries.

| Country | Site | Glyphosate (µg/ml) | Study duration | Method detection limit (µg/ml) | Reference |
|---|---|---|---|---|---|
| Canada | Urban riparian groundwater | 1.4- 4.2 × $10^{-5}$ | NR | 1.0× $10^{-6}$-1.0× $10^{-5}$ | Van Stempvoort *et al.*, 2014 |
| Hungary | Danube river & Lake Velencei | 5.4- 7.6× $10^{-4}$ | 2 years | 5.0× $10^{-5}$- 1.2× $10^{-4}$ | Mörtl *et al.*, 2013 |
| Switzerland | Small catchment (25 $Km^2$) | 6.0 × $10^{-5}$- 4.2× $10^{-2}$ | 1 year | 2.0× $10^{-5}$ | Hanke *et al.*, 2010 |
| Germany | River Havel | 1.0× $10^{-4}$-2.0 × $10^{-3}$ | NR | 2.0-5.0× $10^{-5}$ | Litz *et al.*, 2011 |
| Germany | River Ruhr | 6.5 × $10^{-5}$- 5.9× $10^{-4}$ | 1 year | 2.5× $10^{-5}$ | Skark *et al.*, 1998 |
| Denmark | Esrtrup (drainage water) | Avg.[1] 3.5× $10^{-3}$ | 8 months | < 1.0× $10^{-5}$ | Kjaer *et al.*, 2011 |
| America | St. Joseph river watershed | Max.[2]1.8 ×$10^{-1}$ & 2.3 × $10^{-1}$ | 1 year | 2.0× $10^{-3}$ | Warnemuende *et al.*, 2007 |
| New Zealand | Estuaries | 5.8 ×$10^{-2}$- 9.5×$10^{-1}$ | NR | NR | Stewart *et al.*, 2014 |
| Spain | Surface water (Valenciana) | Max. 2.7× $10^{-3}$ | 1 year | 1.0× $10^{-3}$ | Hernández *et al.*, 1996 |
| Austria | River water | Max. 6.7× $10^{-4}$ | 10 months | 4.2 ×$10^{-2}$ | Popp *et al.*, 2008 |
| Canada | Rural Ponds | 4.2 ×$10^{-2}$- 1.1 ×$10^{-1}$ | 15 years | NR | Frank *et al.*, 1990 |

NR: not reported, [1]Avg: average glyphosate residue concentration, [2]Max: maximum glyphosate concentration

Herbicides are particularly important pollutants of water systems. Worldwide, several compounds are synthesized and manufactured yearly and a third of these compounds end up in the environment (Biziuk *et al.*, 1996). Based on the literature reviewed in this section the potential of glyphosate as an environmental contaminant has been confirmed; however, of greater relevance are the possible toxicological effects it may display upon exposure to non-target living organisms. The toxicological potential of glyphosate is discussed in the subsequent section.

### 1.2.4 Toxicological properties of glyphosate

Glyphosate is generally considered to be a relatively environmentally friendly herbicide because of its degradation capacity and its high affinity adsorption to soil particles (Brake and Evenson, 2004; Zhao *et al.*, 2009). Glyphosate targets the shikimate pathway (reviewed in section 1.2.2), a metabolic process which only occurs in plants, bacteria and fungi and the toxicological potential of glyphosate in humans and animals is therefore believed to be relatively low (Aparicio *et al.*, 2013). Environmental regulatory agencies such as United States Environmental Protection Agency (USEPA) and the World Health Organization (WHO) classify herbicides into categories based on acute toxicity studies carried out in various mammals (rats and mice are the more frequently used models) to determine the lethal median dose or LD50 which is representative of the quantity of compound required to cause the death of 50 % of a test population (Dost, 2003). These tests are often conducted as part of risk management and hazard identification protocols with respect to the production, use and handling of herbicides. Acute toxicity is defined as an immediate (often within 24 hours of exposure) adverse effect occurring after the exposure of a single dose or short term exposure to a compound and chronic exposure (adverse effects observed over long periods of time) studies usually begin as dose response studies under acute conditions (Walum, 1998).

Glyphosate has been classified as a category III herbicide by USEPA, with category I designated to herbicides that demonstrate high level of acute toxicity and category IV consisting of herbicides that demonstrate the lowest toxicity. Acute oral studies in various mammals indicated a glyphosate LD50 ranging between 3500-5000 µg/ml, primarily due to the low adsorption of glyphosate in the digestive tract. Dermal studies in rabbits (rabbits have the most permeable skin in comparison to other mammals) indicated concentrations of glyphosate as high as 5000 µg/ml only caused slight irritation and, with respect to carcinogenicity and reproductive toxicity, glyphosate has been classified as a category E (no evidence of carcinogenicity and reproductive toxicity risk in humans) (Dost, 2003; USEPA, 1993; WHO, 2004). LD50 is a common measure of acute toxicity, however it does not represent adverse effects (acute and chronic) that may occur at sub-lethal concentrations (Walum, 1998).

Several ecotoxicological studies have challenged the idea that glyphosate demonstrates low toxicity and have confirmed the deleterious effects of glyphosate and glyphosate based herbicides at sub-lethal concentrations in aquatic and terrestrial organisms. Examples include amphibian species such as *Xenopus laevis* (frog) (Güngördü, 2013; Hedberg and Wallin, 2010), fish species such as *Prochilodus lineatus* (neotropical fish) and *Caiman latirostris* (broad snouted caiman) (Langiano and Martinez, 2008; Poletta *et al.,* 2009), terrestrial organisms such as *Eisenia andrei* (earthworms), *Chordodes nobilii* (horsehair worms) and *Biomphalaria glabrata* (snails) (Achiorno *et al.,* 2008; Mona *et al.,* 2013; Piola *et al.,* 2013). Of particular interest in this study is the effect of this herbicide in humans at environmentally relevant concentrations and concentrations that humans are generally exposed to. Herbicides may target some organisms more specifically than others (however absolute selectivity is rare) and, due to their inherently toxic nature, herbicides pose a potential risk to human health (Bolognesi, 2003).

The extent of adverse health effects observed due to a specific herbicide is based on several factors such as the chemical class, exposure route, dose and exposure period (acute or chronic) (Hernández *et al.,* 2013). Human exposure to glyphosate residues may occur through various pathways including agricultural practices, contamination of surface and ground waters and entry into the food chain and routes (e.g. dermal oral and inhalation) (Hernández *et al.,* 2013; Richard *et al.,* 2005). The majority of herbicidal compounds have been reported to cause sub-lethal deleterious effects. Human health effects associated with acute and chronic exposure pesticide exposure include reproductive/teratogenic effects (Jacobsen *et al.,* 2012; Martenies and Perry, 2013), carcinogenic/oncogenic effects (Parrón *et al.,* 2013; Perez-Carreon *et al.,* 2009), genotoxic and neurotoxic effects (Dunkelberg *et al.,* 1994; Tuschl and Schwab, 2003) and immunotoxic effects (see review by Corsini *et al.,* 2013).

Human toxicity studies commonly use *in vivo* and *in vitro* assessments as measures of toxicity. *In vivo* experiments generally entail the use of whole, living organisms and data obtained on the acute toxicity effects of glyphosate is generally collected using animals models (e.g. rats) (Dalkvist *et al.,* 2009; Du *et al.,* 2013). The main disadvantages of *in vivo* testing relate to high costs associated with animal testing and a limited predictive power in context to extrapolating effects observed in whole animal models to human toxicity (Du *et al.,* 2013; Hartung, 2011; Olson *et al.,* 2000). *In vitro* the methods were selected for this study and involve the use of

components that have been isolated from an organism, (e.g. cells and cell lines, tissues and organs) which provide a more directed and convenient investigation (Du *et al.*, 2013). The advantages of *in vitro* analysis include the simplification of the system being studied and the avoidance of ethical issues presented when using animals (Scholz *et al.*, 2013). In the last decades *in vitro* toxicology has become increasingly used as an alternative to *in vivo* toxicology and has shown many practical applications, including being used as a screening tool and in the determination of effects of several different compounds (Bakand and Hayes, 2010; Scholz *et al.*, 2013).

A few studies have suggested that glyphosate displays low toxicity in humans. Vigfusson and Vyse (1980) demonstrated the low genotoxic potential by glyphosate in human lymphocytes and a more recent study by Mladinic *et al.* (2009) reported no apparent dose dependent effects in genotoxic and oxidative potential studies in human lymphocytes at glyphosate concentrations relevant to residential and occupational exposure. Pieniazek *et al.*, (2004) reported similar findings in human erythrocytes with the conclusions of the study suggesting glyphosate and its formulation Roundup® presented no potential toxic threat towards human erythrocytes. Several studies have, however, confirmed the toxic potential of glyphosate and glyphosate based herbicides in humans at sub-lethal concentrations. A summary of these studies is outlined in Table 1.4.

**Table 1.4:** A summary of *in vitro* and *in vivo* studies demonstrating the toxic potential of glyphosate and glyphosate based herbicides in human cell lines, human lymphocytes, human blood and rat models at concentrations (µg/ml) reported in the environment and concentrations generally exposed to humans.

**A. Human cell lines and organ tissues**

| Agent/Formulation | Cell line (type) | Glyphosate (µg/ml) | Exposure time (hours) | Toxicity | Reference/s |
|---|---|---|---|---|---|
| Glyphosate | MDA-MB-231 & T47D (breast cancer) | S[1] | 6 & 24 | Endocrine disruption | Thongprakaisang *et al.*, 2013 |
| Glyphosate | HaCaT & keratinocytes (human epidermal) | 0-11837 | 0.5 to 18 | Apoptosis, mitrochondrial membrane dysfunction | Heu *et al.*, 2012 |
| Glyphosate / 7 Roundup® formulations | MDA-MB453-kb2 (breast cancer) & HepG2 (liver) | 5-10 | 24 & 48 | Endocrine disruption | Gasnier *et al.*, 2009 |
| Glyphosate | HeLa (breast cancer) & HepG2 (liver) | 0.1-1.0 | 24 | Alteration in cysteine/glutathione metabolism | Hultberg *et al.*, 2007 |
| Glyphosate IPA formulation* | 3T3-L1 (fibroblast) | S[2] | 48 | Inhibition of proliferation, differentiation, apoptosis | Martini *et al.*, 2012 |
| Glyphosate/Roundup® | JEG3 (human placental) | S[3] | 18, 24, 48 | Disruption of aromatase activity and mRNA levels | Richard *et al.*, 2005 |
| Glyphosate | HepG2 (liver) | 507-2537 | 4 | Genotoxicity | Mañas *et al.*, 2009a |
| Glyphosate IPA* / Roundup (Bioforce®) | 293 (human placental kidney) & JEG3 (placental) | 36-7200 & 48-9600 | 1, 24, 48, 72 | Possible alterations in human reproduction & fetal development | Benachour *et al.*, 2007 |

**B. Human lymphocytes (HL) and human blood (HB)**

| Agent/Formulation | Sample number (n) | Glyphosate (µg/ml) | Exposure time | Toxicity | Reference/s |
|---|---|---|---|---|---|
| Glyphosate | n= 3 (HL) | 0.8-8.6 | 72 hours | Chromosome aberrations, oxidative stress | Lioi *et al.*, 1998 |
| Glyphosate & Roundup® | n= 2 (HL) | 30-6000 | 72 hours | Induction of sister chromatid exchanges | Bolognesi *et al.*, 1997 |
| Glyphosate | Serum pool (HB) | 5073-338200 | 1 | Inhibition of serum AchE, LDH, AST, ALT, AIP | El-demerdash *et al.*, 2001 |

**C. Mammalian toxicity (rat model)**

| Agent/Formulation | Study sample | Glyphosate (µg/ml) | Exposure time | Toxicity | Reference/s |
|---|---|---|---|---|---|
| Glyphosate | Wistar rats (oral dose) | 0.7 & 7 | 30-90 days | Biochemical alterations | Larsen *et al.*, 2012 |
| Glyphosate/ Roundup® | Leydig , Sertoli & germ cell (testes) | 1-10000 | 48 hours | Endocrine disruption | Clair *et al.*, 2012 |
| Glyphosate | Liver, serum | 20 | 21 days | Excessive lipid peroxidation | Beuret *et al.*, 2005 |
| Glyphosate/ Roundup® | Sertoli cells | 36 | 30 minutes | Oxidative stress, calcium overload, cell signaling misregulation | De Liz Oliveira Cavalli *et al.*, 2013 |
| Roundup® | Liver mitochondria | 0-3382 | NR | Uncoupling of oxidative phosphorylation | Peixoto, 2005 |
| Glyphosate/ Roundup® | Swiss albino mice (skin application) | 25 | 1-3 weeks | Tumor promoting activity | George *et al.*, 2010 |
| Glyphosate | Liver & brain | 10 | 5 weeks | Oxidative stress | Astiz *et al.*, 2009 |

**D. Human organs**

| Agent/Formulation | Organ /System | Case study | Exposure time | Toxicity | Reference/s |
|---|---|---|---|---|---|
| Glyphosate | Brain & nervous system | Healthy 54 year old man: accidental exposure while spraying glyphosate in his garden | 30 minutes | Parkinsonian syndrome, lesions on globus pallidus and substantia nigra | Barbosa *et al.,* 2001 |

S: Starter concentration not reported, concentrations reported as dilution factors only ($S^1$: $10^{-6}$-$10^{-12}$; $S^2$: 1:1000-1:10000; $S^3$: 0.05-2 %). *Glyphosate IPA formulation: glyphosate isopropylamine salt formulation, trade name not specified. *Glyphosate IPA: glyphosate isopropylamine salt. AchE: acetylcholineesterase, LDH: lacatate dehydrogenase, AST: aspartate amino transferase, ALT: alanine aminotransferase, AIP: alkaline phosphatases.

Herbicides are applied as formulations and the adjuvants present were generally considered "inert" but recently the role of adjuvants found in herbicide formulations in toxicity studies has been highlighted, as humans are exposed to these "inert" ingredients as well as the active compound (Hernández *et al.,* 2013; Mesnage *et al.,* 2013). Inert ingredients are known to increase the toxicity and exposure of pesticides (including herbicides) with severe and expansive implications to human health (see review by Cox and Surgan, 2006).

Current toxicological research has suggested that the presence of these adjuvants in glyphosate herbicidal formulations are important contributors to the enhancement of glyphosate toxicity. Benachour and Seralini (2009) implicated the surfactant POEA, a known adjuvant in glyphosate formulations such as Roundup®, in the alteration of human cell permeability and as an amplifier of glyphosate toxicity in human umbilical, embryonic and placental cells. Mesnage *et al.* (2013) concurred with the findings reported by Benachour and Seralini (2009) who proposed a possible mechanism for POEA toxicity in human liver, kidney and placental cells, which involves the disruption of cellular membranes during micellization, followed by the induction of extreme mitochondrial alterations. Evidence provided by many other researchers supports the

observations and conclusions reported by the aforementioned studies (Chan *et al.,* 2007; Hedberg and Wallin, 2010; Moreno *et al.,* 2014; Peixoto, 2005; Poletta *et al.,* 2009).

The ongoing debate surrounding the safety of glyphosate highlights the importance of glyphosate toxicology in humans. Considering this study was localized in South Africa the following section will address the issue of glyphosate and glyphosate based herbicides within a South African context.

### 1.2.5 Glyphosate and glyphosate based herbicides in a South African context

In sub-Saharan Africa, South Africa stands out as the leading country for pesticide use, primarily in the agricultural sector (Dalvie *et al.,* 2009; Rother *et al.,* 2008). Glyphosate-based herbicides are well established in the South African market with approximately 26 companies currently producing (e.g. Dow Agrosciences, Volcano Agroscience and Syngenta) glyphosate-based herbicide products, including the most popular formulation Roundup® (Mensah, 2013). Glyphosate based herbicides are used in South Africa primarily to control weeds and alien invasive plants and have become one of the principal products used in the country (Mensah, 2013). Monsanto has played a significant role in the South African agrochemicals (herbicides, fungicides and insecticides) industry since 1968 and entered the agricultural seed market in 1998 (Masifunde Education and Development Project Trust, 2010). In 1998, South Africa was the first country in the world to produce a genetically modified version of the country staple food, maize (African Centre for Biosafety, 2013). To date, Monsanto controls 50 % of the South African maize market (maize is the most important and most widely produced crop in South Africa). Sixty four % of all maize grown in South Africa is GM-GR (Genetically Modified-Glyphosate Resistant) and the continuous cultivation of GM- GR maize (GM-GR crops have been found to be heavily reliant on herbicide input despite contrasting reports) has subsequently resulted in the increased use of glyphosate based herbicides in the country. It has been reported that the overall use of glyphosate has increased from 12 million liters in 2005 to 20 million liters in 2012 (African Centre for Biosafety, 2012; African Centre for Biosafety, 2013). The only other commercialized South African GM-GR crop varieties are cotton and soybean (African Centre for Biosafety, 2012).

The success and ever increasing use of glyphosate herbicides in South Africa is also due in part to the promotion of glyphosate-based herbicide and GM-GR crop use by commercial farmers, public and private organizations and the government initiated Working for Water Programme, (founded in 1995) which promoted the use of glyphosate based herbicides in controlling alien invasive terrestrial and aquatic plant species (Binns *et al.,* 2001; Friends of the Earth International, 2008; Mensah, 2013). Project initiatives such as the Green Revolution programme/Massive Food Production Programme which was implemented in 2003 by Monsanto together with the South African government as a response to declining agricultural production in the Eastern Cape Province and involved the free distribution of GM-GR seeds to emerging farmers also ensures the continuous use of large quantities glyphosate based products (African Centre for Biosafety, 2008; Mtero, 2012).

South Africa is a semi-arid, water stressed country with scarce natural water resources (DWA, 2004). Surface and groundwater pollution are one of the most important problems facing South Africa to date and statistics indicate that before 1994 over 21 million people in South Africa were consuming and using poorly or unsanitized water (rural areas accounted for the greatest percentage of this total, resulting in 43,000 deaths per annum relating to contaminated water use). This alerted the South African government and even though significant changes have been made to improve water management and treatment; in 2004 five million South Africans were still using rivers and springs as a source of water (Momba *et al.,* 2006). The published South African Census report for 2011 indicates that currently a large majority of people living in rural areas still do not have access to treated water and are still heavily dependent on natural water resources including surface waters (e.g. river water and groundwater) (StatsSA, 2012).

Pesticide contamination of natural water sources poses a serious threat with respect to environmental and human health, however pesticide monitoring programs in South Africa are limited, primarily due a lack of analytical methods/techniques and limited finances (Dabrowski *et al.,* 2002; Dabrowski *et al.,* 2005; Dabrowski and Balderacchi, 2013; Dalvie *et al.,* 2006). Although South African data on pesticide contamination in aquatic environments is minimal in comparison to other developing countries (Ansara-Ross, 2012), there are some studies that have reported on the presence of pesticides in South African surface and groundwaters (Bollmohr *et al.,* 2007; Humphries, 2013; Schulz, 2001; Thiere and Schulz, 2004). Research on the

contamination of glyphosate in surface waters and groundwater in South Africa is therefore extremely limited. Studies conducted in the Hex River Valley (a grape farming area in the Western Cape Province of South Africa characterized by intensive agricultural practices) reported significantly high concentrations of glyphosate since the 1990s (Dalvie *et al.,* 2011; Maharaj, 2005; Meinhardt, 2009). The significance of pesticide pollution in water has not been prioritized by South African policy makers and regulatory bodies to the same extent as microbiological water contamination, as is evident in the South African water quality guidelines for drinking water (London *et al.,* 2005). Rigorous standards have been implemented for coliform concentrations and inorganic compounds for water systems (DWAF, 1996) but with only one standard existing for pesticides (atrazine) (DWAF, 1996; London *et al.,* 2005). The absence of drinking water quality guidelines for glyphosate (considering its extensive use) highlights the lack of regulation for glyphosate use in South Africa and the limited ability of South Africa to address issues of possible water contamination by this herbicide and potential public health issues (due to the high dependency on untreated water sources such as river water and groundwater, especially in poorer rural communities) which may arise due to human exposure. Dabrowski *et al.* (2014) prioritized and ranked pesticides in South Africa based on four indices. The first is the quantity index (QI) defined by the quantity of use. The second index was the toxicological potential (TP), which was defined by the potential pesticides to cause five main health effects (namely, endocrine disruption, carcinogenicity, tetragenecity, mutagenecity and neurotoxicity). The third index was the hazard potential (HP) defined by the exposure potential as an indication of an environmental hazard and the fourth index was defined as the weighted hazard potential (WHP) which multiplies the HP in context to the ratio of pesticide use to the total use of pesticides in the whole country. The top 25 pesticides in each category were defined as priority pesticides and, based on the findings in this study; glyphosate was ranked 1$^{st}$ and 6$^{th}$ in the QI and WHP category. Recently Mensah *et al.* (2013) derived South African water quality guidelines for the most popular formulation Roundup® in aquatic ecosystems, based on species sensitivity distribution in indigenous aquatic organisms. The short-term and long-term derived water standards for Roundup® were 0.250 and 0.002 µg/ml, respectively. The abovementioned studies highlight the importance of glyphosate-based herbicides in South Africa and provide a step forward towards including glyphosate-based herbicides into integrated water resource management.

In contrast to South Africa, international regulations for pesticides in drinking water are more stringently regulated. Drinking water quality guidelines (WQG) or maximum residues levels (MRL) for pesticides are set based on health risk assessments by agencies (e.g. WHO and USEPA; see section 1.2.4) (London *et al.*, 2005). The USEPA has set the MRL for glyphosate in drinking water at 0.7 µg/ml and MRLs for water in the European Union, Canada and Brazil are 0.1 $\mu g.l^{1}$, 0.28 µg/ml and 0.5 µg/ml, respectively (Coutinho *et al.*, 2008; Miro *et al.*, 2012).

The typical concentration range of glyphosate in natural water systems is still relatively unknown to a large extent (Miro *et al.*, 2012). The varied behavior of this herbicide in soil and water may likely be a causative factor (see section 1.2.3), however several methods have been developed for glyphosate detection and AMPA is often included in analytical methodologies because it is a major metabolite of glyphosate (Sadi *et al.*, 2004). Section 1.2.6 provides a general overview of the reported literature with regards to glyphosate detection methods.

### 1.2.6 Methods developed for glyphosate determination in water

Analytical methods used for the detection of glyphosate in water generally have to demonstrate high sensitivity due to the regulatory MRLs for glyphosate in drinking water (see section 1.2.5) (Ibáñez *et al.*, 2006; Lee *et al.*, 2013). Developing simple and rapid methods for the extraction and determination of glyphosate at the appropriate levels presents many challenges due to the complex behavior glyphosate displays (i.e. this compound is amphoteric and extremely soluble in water, demonstrates high polarity, insolubility in inorganic solvents and low volatility) (Corbera *et al.*, 2005; De Llasera *et al.*, 2005; Dimitrakopoulos *et al.*, 2010). To date, the literature available on glyphosate detection methods are well established and a variety of analytical techniques have been developed for glyphosate detection in water and other environmental matrices (Ghanem *et al.*, 2007). Stalikas and Konidavi (2001) provide a comprehensive review on the characteristics of available analytical methods used for the detection of glyphosate and related compounds in water and other matrices.

Initial methods developed for glyphosate detection involved thin liquid chromatography techniques (Rodrigues *et al.*, 1982; Sprankle *et al.*, 1978; Young *et al.*, 1977). More recently the majority of methods reported for glyphosate detection include gas chromatography (GC), liquid

chromatography (LC), capillary electrophoresis (CE) and immunoassays (Chen *et al.,* 2013a; Guo *et al.,* 2005; Khrolenko and Wieczorek, 2005). Table 1.5 summarizes the GC, LC and CE techniques used for the detection of glyphosate and AMPA in water. GC and LC methodologies offer high detection sensitivity (Table 1.5) and are often coupled to other detection systems for the improvement of detection sensitivity/specificity/selectivity with examples of the detection systems commonly including mass tandem spectrometry (MS) (Royer *et al.,* 2000), flame photometric detection (FPD) (Kataoka *et al.,* 1996), nitrogen phosphorous detection (NPD) (Hu *et al.,* 2008) and electron capture detection (ECD) (Eberbach and Douglas, 1991). Overall, however, these chromatographic methods are complex, costly and require large laboratory equipment with skilled technicians (Jenkins *et al.,* 2001).

**Table 1.5:** A brief summary of GC, LC and CE methods used for the detection of glyphosate /AMPA in water.

| Compound | Sample | Method | Detection | LOD (µg/ml) | Reference |
|---|---|---|---|---|---|
| Glyphosate & AMPA | Drinking water | GC | MS | $1.0 \times 10^{-2}$ | Alferness & Iwata, 1994 |
| Glyphosate & AMPA | Ultrapure water | GC | MS/MS[*1] | $5.0 \times 10^{-5}$ | Royer *et al.,* 2000 |
| Glyphosate & AMPA | River water | GC | FPD | ++ | Kataoka *et al.,* 1996 |
| Glyphosate & AMPA | Tap water | LC (HPLC) | FL[*2] | $2.0 \times 10^{-5}$ | Gauch *et al.,* 1989 |
| Glyphosate | Environmental water | LC (HPLC) | UV[*3] | $9.0 \times 10^{-4}$ | Qian *et al.,* 2009 |
| Glyphosate & AMPA | Drinking & surface water | LC (HPLC) | (EI)MS[*4] | $3.0 \times 10^{-5}$ | Vreeken *et al.,* 1998 |
| Glyphosate & AMPA | Surface & groundwater | LC | MS/MS | $2.0 \times 10^{-8}$ | Hanke *et al.,* 2008 |
| Glyphosate | River water | CE | LIF | $2.7 \times 10^{-4}$ | Jiang and Lucy, 2007 |
| Glyphosate & AMPA | Natural water | CE | NR | 8.5 & $6.0 \times 10^{-2}$ | Corbera *et al.,* 2005 |
| Glyphosate & AMPA | Water | CE | ECL | $3.0 \times 10^{-4}$ & $3.0 \times 10^{-2}$ | Hsu and Whang, 2009 |

++: limit of detection 8 & 12 pg [*1]MS/MS: tandem mass spectrometry , [*2]FL: fluorescence detection , [*3]UV: UV-VIS detection, [*4](EI)MS: electrospray ionization mass spectrometry, [*5]ECL: electrochemiluminescence NR: not reported

GC methods require extensive, time consuming and tedious chemical derivatization steps (all ionic groups require derivatization) with varying reagents such as trifluoroacetic anhydride (TFAA) and trifluoroethanol (TFE) for the formation of (e.g. *N*-trifluoroacetyltrifluoroalkyl ester derivatives) (Alferness and Iwata, 1994; Ibáñez *et al.,* 2006; Konar and Roy, 1990; Tsunoda, 1993; Wei *et al.,* 2013) which function in decreasing the polarity of the glyphosate compound, increasing volatility, thereby improving chromatographic separation and ultimately resulting in increased sensitivity during detection (Guo *et al.,* 2005; Motojyuku *et al.,* 2008).

LC methods, particularly high performance liquid chromatography (HPLC), for glyphosate detection are well established (Vreeken *et al.,* 1998) and are primarily based on cation and anion exchange separation which presents greater suitability with respect to the ionic properties of glyphosate and are often the preferred methods over GC (Hanke *et al.,* 2008). Glyphosate is however structurally similar to amino acids and lacks the appropriate chemical groups (e.g. chromophores and fluorophores) for detection using conventional systems (Qian *et al.,* 2009). Therefore, pre-column and post-column derivatizations are required in this methodology, to enable ease in the isolation, separation and detection of glyphosate which leads to the enhancement of detection sensitivity and selectivity (Botero-Coy *et al.,* 2013; Corbera *et al.,* 2005; Royer *et al.,* 2000). Fluorenylmethylchloroformate (FMOC-Cl) is the most commonly used pre-column derivatization reagent used in combination with LC techniques (e.g. HPLC) for the formation of a fluorescent derivative, which improves both detection and chromatographic retention (Hanke *et al.,* 2008, Kawai *et al.,* 1991, Patsias *et al.,* 2001). Post-column derivatization commonly uses reagents such as *o*-phthalaldehyde (OPA) and mercaptoethanol or OPA and *N,N*-dimethyl-2-mercaptoethylamine with fluorescence detection and ninhydrin with UV detection (Hogendoorn *et al.,* 1999; Ibáñez *et al.,* 2005).

Capillary electrophoresis (CE) has become a more frequently used method in recent years due to its high resolving power and speed (Chang and Liao, 2002; Khrolenko and Wieczorek, 2005), however the major drawback of CE analysis is its low detection sensitivity, primarily due to the limitations encountered with the injection volume (Sadi *et al.,* 2004). This method also requires the use of pre and post column derivatizations when coupled to UV and fluorescence detection (See *et al.,* 2010), however non derivatization procedures such as indirect absorptiometric detection (Cikalo *et al.,* 1996), indirect laser induced fluorescence (LIF) detection (Chang and

Liao, 2002) electrospray ionization mass spectrometry (ESIMS) (Safarpour and Asiaie, 2005), amperometric detection (Sato *et al.,* 2001), inductively coupled plasma mass spectrometry (ICP-MS) (Sadi *et al.,* 2004; Wuilloud *et al.,* 2005) and electrospray nucleation light scattering detection (You *et al.,* 2003) have been reported in literature for HPLC and CE methods. Literature has also reported on a few other methods which circumvent the need for derivatization and these include suppressed conductivity ion chromatography (IC) (Zhu *et al.,* 1999) and $^{1}H$ and $^{31}P$ NMR spectroscopy (Cartigny *et al.,* 2004). Amongst these methods indirect methods often suffer from low sensitivity, whereas the other methods are limited by expense and equipment availability. Some methods have not proven suitable in complex matrices (Chen et al 2013a; Chiu *et al.,* 2008, Coutinho *et al.,* 2008, Hao *et al.,* 2011; Hui-Min *et al.,* 2013,Yoshioka *et al.,* 2011).

Analysis of low concentrations of glyphosate is facilitated through extraction/pre-concentration procedures and these analytical tools play a pivotal role in the methodologies presented thus far (Hsu and Whang, 2009). Sample preparation techniques for the isolation/pre-concentration of glyphosate from different matrices include liquid-liquid extraction (LLE) (reviewed by Lambropoulou and Albanis, 2007), supported liquid membrane extraction (SLM) (Dżygiel and Wieczorek, 2000), liquid-solid extraction (LSE) (Andreu and Picó, 2004), solid-phase extraction (SPE) (reviewed by Hennion, 1999) and metal ion affinity chromatography (IMAC) (Rios *et al.,* 2004).

Currently, research into glyphosate detection has shifted focus, with greater attention being placed on detection systems that are dependent on basic biochemical principles such as selective immunoassays (Jenkins *et al.,* 2001). The development of enzyme linked immunosorbent assays (ELISA) for glyphosate detection has overcome the need for sample preparation, allowed for high detection sensitivity and specificity and was shown to be complimentary to and more cost-effective than available chromatographic techniques (Byer *et al.,* 2008; Mörtl *et al.,* 2013). Both direct (including a derivatization step with acetic anhydride for increased detection sensitivity) (Mörtl *et al.,* 2013) and indirect ELISA (not requiring derivatization) protocols (Clegg *et al.,* 1999) have been developed for glyphosate detection. Rubio *et al.* (2003) reported a detection limit as low as 0.6 $ng.ml^{-1}$ for glyphosate in nanopure, tap and river water samples with direct ELISA involving the use of antibody-coupled magnetic particles and acetic anhydride

derivatization. The reported LOD using this direct ELISA method was 500-fold lower than the LOD of the comparative HPLC method. A linker assisted-ELISA method developed by Lee *et al.* (2002) indicated a good correlation (r= 0.97) with the comparative HPLC-MS method studies conducted on surface and groundwaters and demonstrated a high sensitivity (0.084 $\mu g.L^{-1}$). A multiplexed covalent microbead immunosorbent assay (FCMIA) developed by Biagini *et al.* (2004), which includes a derivatization step for glyphosate and AMPA determination in water and urine, further demonstrated the potential of immunoassays, with no evidence of cross-reactivity being reported and a high glyphosate detection sensitivity being observed in water samples. There are several advantages to immunoassay methods; however these assays are often limited by the availability and cost of antibodies, stability and irreversible binding which prevents reusability (Jenkins *et al.*, 2001).

The direct ultraviolet-visible spectrophotometric (UV-VIS) detection of glyphosate has not yet been described in literature (Da Silva *et al.,* 2011), however indirect methods have been established involving initial derivatization procedures. An earlier report by Glass (1981) describing the colorimetric detection of glyphosate involved the formation of a phosphomolybdate heteropoly blue complex that could be detected at 830 nm after the oxidation reaction of glyphosate combined with hydrogen peroxide. More recently Jan *et al.* (2009) reported the detection of glyphosate at 435 nm after a derivatization step with carbon disulphide for the formation of a dithiocarbamic acid intermediate which was followed by a complexation reaction with copper to form a yellow colored complex. Glyphosate was determined with a limit of detection of 1.1 µg/ml and the method was validated for use in various environmental matrices including water. Bhaskara and Nagaraja (2006) developed a colorimetric detection system for glyphosate in environmental waters, which was based on the reaction of glyphosate with the chromogenic reagent ninhydrin in the presence of the catalyst sodium molybdate, which resulted in the formation of a purple product which could be detected at 570 nm. The *Sandells* sensitivity reported for this system was 5.2 $ng.cm^{-2}$. Spectrophotometric methods are simpler and more cost effective than chromatographic methods, however they demonstrate lower sensitivity and a narrower detection limit range (Zelaya *et al.*, 2011).

Although there are a vast number of different methodologies available for glyphosate detection, which have been outlined in this section, there is a continued need for the development of a

reliable, sensitive, rapid, portable and cost effective detection system for glyphosate in water, especially when placed in a South African context, where biomonitoring protocols for glyphosate in environmental waters are extremely limited. Advances in polymer sciences and nanotechnology have lead to investigations into (e.g. molecular imprinted polymers), which are synthetic materials which mimic biological receptors and polymer supported nanocomposites. Both systems are attractive alternatives to current methodologies and show great potential as sensing technologies in environmental applications such as remediation and the sensing of environmental pollutants such as glyphosate (Jenkins *et al.,* 2001, Lanza and Sellergren, 2001; review by Zhao *et al.,* 2011a, Zhao *et al.,* 2011b). For this study nanofiber technology was selected for the development of a chemosensor for glyphosate detection in water.

## 1.3 Nanofiber technology and chemical sensors

### 1.3.1 Chemical sensors based on nanofiber technology

Nanofibers are materials defined as one-dimensional nanosized aggregates that can be linear or helical in structure and can be produced from a wide variety of available polymers (Hui and MacLachlan, 2010; Jian *et al.,* 2008). Polymer nanofibers have been the focal interest of extensive research due to their distinctive properties and varied applications (Li and Xia, 2004) in areas such as biomaterial (Raveendran *et al.,* 2013; Toskas *et al.,* 2013), electronic and magnetic materials production (Park *et al.,* 2013; Yu *et al.,* 2014), chemical catalysis (Müller *et al.,* 2014) and enzyme immobilization (Lee *et al.,* 2008). Current research efforts have focused on the use of polymeric non-woven nanofibers in chemical sensor (also known as chemosensor) development (Kim *et al.,* 2006).

A good sensor is characterized by high sensitivity, selectivity, a rapid response time, small dimensions or potential for minaturization and low production costs (Jian *et al.,* 2008). This enables chemosensor technology to take advantage of the attractive features presented by polymeric non-woven nanofibers, including a large surface area to volume ratio, high porosity, small pore size and diverse physical and chemical properties (Frey and Li, 2007). These features could prove to be beneficial in the improvement of the sensing characteristics of a chemical sensor (e.g. an increased surface area to volume ratio allows for an increase in the contact ratio

between the sensing material and the analyte of interest), which would result in increased sensitivity and an improved response time (Hua *et al.,* 2013; Li *et al.,* 2008; Lv *et al.,* 2013). Polymer nanofibers can therefore serve as ideal supports or scaffolds for chemical sensing systems (Min *et al.,* 2013).

Several processing techniques have been developed for nanofiber preparation, such as molecular self assembly (Huang *et al.,* 2011), meltblown (Hassan *et al.,* 2013) and phase separation (Rajabzadeh *et al.,* 2012). Amongst the various processing techniques electrospinning is the most commonly employed method. Electrospinning is a simple and versatile process for small and large scale nanofiber fabrication and proves advantageous in comparison to other methods with respect to the cost and the time required for the production of nanofibers (Huang *et al.,* 2003; McCann *et al.,* 2004).

The basic apparatus required for the electrospinning process in shown in Figure 1.8 and is compromised of three main components namely: a high voltage power supply, a capillary feed tube containing the polymer solution with a metal needle/nozzle attachment and a grounded collection screen (Frenot and Chronakis, 2003). The presence of an electrical field causes the drop at the needle tip to distort into a conical shape known as the Taylor cone (Figure 1.8), due to repulsive forces resulting from the induced charge distribution on the drop surface and the surface tension of the polymer solution (Deitzel *et al.,* 2001). At a high voltage (critical voltage) electrostatic forces cause the ejection of a liquid jet from the Taylor cone. The liquid jet displays bending instabilities due to repulsive forces inside the jet and interactions with the external electrical field, causing it to elongate and become thinner followed by solvent evaporation which results in the formation of solid fibers (Chronakis, 2005; Kim and Reneker, 1999; Matthews *et al.,* 2002). The majority of electrospun nanofibers are deposited on the collection screen in a random fashion, forming a non-woven mat (Jian *et al.,* 2008). However, in some cases, controlled deposition techniques (e.g. atomic layer deposition are utilized for the formation of aligned fibers) (Donmez *et al.,* 2013; Hellmann *et al.,* 2009).

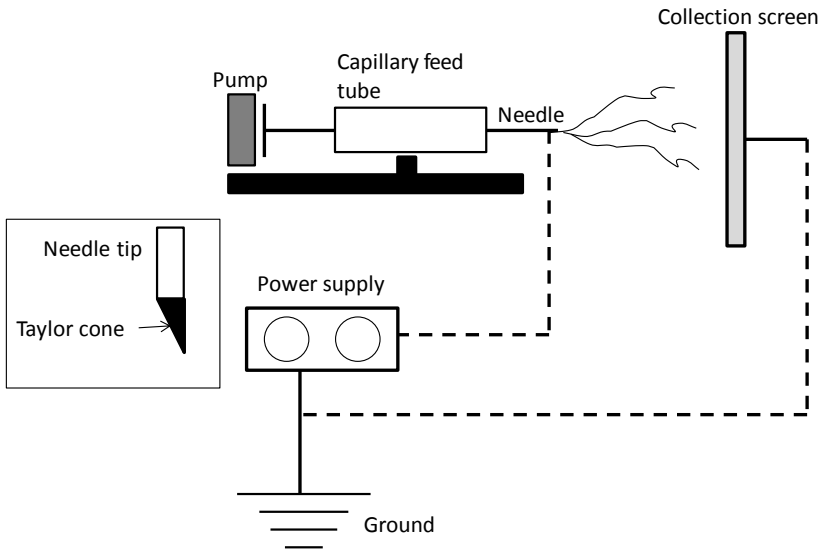


**Figure 1.8:** A schematic representation of electrospinning apparatus used during the electrospinning process. The key components of this system are: a high voltage power supply, a capillary feed tube with a metal needle attachment, and a grounded collection screen. (This image was adapted from Katepalli *et al.,* 2011).

To date more than 100 natural and synthetic polymers have been successfully electrospun (Feng *et al.,* 2013) and a few examples include poly (vinyl) alcohol (PVA) (Wu *et al.,* 2005), polystyrene (Casper *et al.,* 2004), poly (ethylene) oxide (PEO) (Wan *et al.,* 2006), nylon (Bergshoef and Vancso, 1999), chitosan (Bhattarai *et al.,* 2005) and poly (ethylene) terepthalate (PET) (Ma *et al.,* 2005) and the electrospinning process using available polymers can result in variety of different fiber morphologies (Ramakrishna *et al.,* 2006) (e.g. polymeric hollow (Li and Xia, 2004) and core-sheath (Wei *et al.,* 2005)). The ideal non-woven mat should however demonstrate particular characteristics, including a fiber surface with no defects (bead formation) and the resultant non-woven mat should be collectable (Fong *et al.,* 1999; Huang *et al.,* 2003). Obtaining a completely ideal nanofiber mat still remains a present challenge and this topical issue is outlined in greater detail in the review by Huang *et al.* (2003).

There have been several approaches used in the development of chemical sensors based on nanofibers, including the application of the sensing material on the nanofiber surface through

coating/grafting and the inclusion/incorporation of the sensing material into the polymer solution prior to electrospinning. Jian *et al.* (2008) and other reports in literature have demonstrated the use and potential of nanofiber-based chemosensors for the detection of various compounds. Wang *et al.* (2006) reported on the formation of composite nanofibers produced by the incorporation of tungsten isopropoxide sol-gel into poly (vinyl) acetate/dimethyl formamide ($PVA_c$/DMF) polymer solutions for the detection of ammonia. Liao *et al.* (2011) highlighted the potential use of polyaniline/single-walled carbon nanotube composite nanofibers as a gas chemosensor, with results demonstrating sensor reponses at hydrochloric acid and ammonia vapor at concentrations as low as 100 ppb. The practical utility of an electronic tongue developed by Oliveira *et al.* (2012) for the detection of the pesticide paraoxon in water has been demonstrated. This system was based on the use of electrospun nylon nanofibers modified with layer-by-layer polypyrrole (PPγ) and assembled onto graphite interdigitated PET substrates and connected to a flow analysis system.

Several analytical techniques have been developed for glyphosate detection in water, however nanofiber-based chemosensors may provide several advantages including portability, operational simplicity and cost effectiveness (Min *et al.,* 2013). The potential applications of solid state sensor materials are vast and include applications in basic laboratory assays, for field measurements and as commercial indicator kits in households (Min *et al.,* 2013).

# CHAPTER 2- PROBLEM STATEMENT, AIMS & OBJECTIVES

## 2.1 Problem statement

South Africa has limited natural water resources and, due to high evaporation rates, only 8% of overall rainfall is converted into usable water sources (Metcalf-Wallach, 2007). Surface and ground water pollution is one of the most serious environmental problems facing South Africa to date, more specifically for rural communities who remain heavily reliant on natural water resources such as surface and groundwaters (Nkwonta and Ochieng, 2009). These rural communities and settlements are spread over approximately 65% of South Africa (Momba and Mnqumevu, 2000). The potential human health and environmental impacts of glyphosate pollution in South African water resources are largely unknown and generally pesticide pollution has not been fully prioritized and integrated into water resource management strategies. Intensive monitoring and sampling for pesticide identification is limited by cost and the availability of analytical techniques.

Analytical techniques available for the detection of glyphosate are often complicated and require the use of expensive equipment. This highlights the need to develop a cost effective method that offers operational simplicity and reliability. The development of a nanofiber-based chemical sensor may prove to be a simpler strategy for glyphosate determination in water.

The ongoing debate on the potential hazardous effects of glyphosate on human health highlights the need to further assess the potential deleterious effects of glyphosate and glyphosate-herbicides in humans, more specifically at concentrations that represent concentrations likely to be encountered by humans.

## 2.2 Hypothesis

i. Glyphosate and glyphosate formulations are toxic to humans at low to moderate dose exposure.

ii. Nanofiber technology can be used to improve the detection of glyphosate (pure and in formulation) in water.

## 2.3 Aims and objectives

The overall aims and objectives of this study were as follows:

i. To determine the cytototoxic, genotoxic and pro-inflammatory response effects of low dose acute exposure to glyphosate and glyphosate-based herbicides in humans using well established techniques including the Comet assay and ELISA.
ii. To scale down, optimize and characterize a colorimetric spectrophotometric detection system documented in literature as the basis towards developing a nanofiber-based chemical sensor.
iii. To optimize and produce nanofibers (with the sensing material incorporated) using the electrospinning process.
iv. To develop and optimize a nanofiber-based chemical sensor for the detection of glyphosate and glyphosate-based herbicides in water and compare it to the scale-down system (micro-assay) and other colorimetric detection systems developed for glyphosate.
v. To characterize the sensing properties of the nanofiber-based chemical sensor with respect to sensitivity, reproducibility, stability, selectivity and application.

# CHAPTER 3- THE ACUTE TOXICITY OF GLYPHOSATE AND GLYPHOSATE FORMULATIONS IN HUMANS AT LOW/MODERATE DOSE EXPOSURE (*IN VITRO* STUDIES)

## 3.1 Introduction

Glyphosate and glyphosate formulations were previously regarded as safe and relatively non-toxic to humans and other organisms; however evidence continues to accumulate that glyphosate exposure is linked to impaired health. The toxicological properties of glyphosate were reviewed in Chapter 1 section 1.2.4. Considering the potential impact of glyphosate on human health and the continued debate around its safety, assessing the toxicity of glyphosate and glyphosate formulations has become a focal point of several research studies over recent years.

The first aim of this study was to present preliminary evidence of the cytotoxicity, genotoxicity and pro-inflammatory potential of glyphosate in humans as an important factor for the validation of developing a chemosensor for the rapid detection of glyphosate in water. In this study focus was placed on acute, low to moderate glyphosate exposure as these levels are more often within the range likely to be encountered by humans (Vom Saal and Welshons, 2006) and may provide critical information for future prolonged (sub-chronic or chronic) exposure (*in vivo* and *in* vitro) studies. No regulatory limits have been set for glyphosate in South African water systems, therefore concentrations selected were based (included, below or within the range) on the short term water standards (0.250 µg/ml) for Roundup® (Ro) in South African aquatic systems derived by Mensah *et al.* (2013), the maximum residue limits (MRL) for glyphosate in drinking water set by the USEPA (0.7 µg/ml), the health based values for glyphosate in drinking water set by the World Health Organization (0.9 µg/ml) and the MRL for glyphosate in drinking water established in Brazil (0.5 µg/ml) by the Agência Nacional de Vigilácia Sanitária (ANVISA) (Coutinho *et al.,* 2008; WHO 2004). In developing countries exposures to pesticides is generally higher (Ecobichon, 2001) and considering the extensive and poorly regulated use of glyphosate in South Africa, this study also undertook the evaluation of moderate exposure concentrations which were based on occupational and residential exposure levels (maximum 580 µg/ml) tested

by Mladinic *et al.* (2009) and exposure doses below the reported acute oral LD50 in *in vivo* rat (greater than 5000 μg/ml) toxicological studies (WHO, 1994).

The immune system acts as the defence system for the human body against pathogenic organisms, foreign chemicals and also functions in the repair of damaged tissue after injury (Watkins *et al.,* 1995). Upon direct contact of a foreign compound/antigen lymphocytes are activated, which is consequently followed by the production and release of several cytokines such as tumor necrosis factor alpha (TNF-α), interleukins 1 (IL-1), 6 (IL-6) and 8 (IL-8) (Watkins *et al.,* 2007). Cytokines act on, amongst other systems, the cell immune system, producing a large range of inflammatory effects which instigate several different processes (e.g. general tissue repair) (Watkins *et al.,* 1995). The pro-inflammatory cytokines TNF-α, IL-1β and IL-6 were evaluated in this study in human white blood cell and human whole blood as representative models of an immune response. These biological models were selected for this work as they have been utilized extensively in studies regarding chemical/compound/agent effects on the inflammatory response (commonly used as a measure of immunotoxicity) and both models contain the specific cells (e.g. macrophages) required for the production/ release of cytokines (Johnson *et al.,* 1996; Kawasaki *et al.,* 1999: Richardson *et al.,* 1989; Tracey 2002). TNF-α, IL-1β and IL-6 were selected for this study because they are hallmarks of acute inflammation responses. The acute inflammatory process occurs within seconds, hours or days and can therefore represent the short term effects of a toxin. TNFα and IL-1β (stimulated and released from macrophages) are highly important mediators of acute inflammation and are often the first cytokines to be upregulated in response to a toxin. The secondary inflammatory function displayed by these two cytokines involves the induction of IL-6 (produced by macrophages) synthesis, which regulates pro-inflammatory cytokines (Feghali *et al.,* 1997; Watkins *et al.,* 2007).

The human cell lines investigated in this study were the MCF-7, HEC1A estrogen receptor positive (ER positive) breast cancer and endometrial cancer cell lines and the MDA-MB-231 estrogen receptor negative (ER negative) breast cancer cell line. The MCF-7 and MDA-MB-231 breast cancer cell lines were selected because they have been shown to be suitable models for investigating the potential endocrine disruptive effects of xenobiotics in previous studies (Buteau-Lozano *et al.,* 2008; Markaverich *et al.,* 2002). The endocrine system is an intricate web

of cells, glands and tissues which produce/secrete several hormones which regulate several processes including metabolic activity, reproduction and growth and development (Maitra *et al.*, 2008; Solomon and Schettler, 2000). Endocrine disrupting compounds are described as exogenous compounds which can alter the normal functioning of the endocrine system at the level of the organism, progeny or sub-population which leads to several adverse effects (Birnbaum *et al.*, 2003).

The HEC1A cell line was selected for this study as it may prove a suitable model for glyphosate toxicological studies. Castro-Riveria and Safe (1998) indicated that the HEC1A cell line expressed the wild type form of the estrogen receptor and was estrogen (17β-estradiol) responsive, therefore this cell line may provide insight into ER associated glyphosate mechanisms of action. HEC1A is also linked to fertility and may in future provide additional insight into possible deleterious effects in human reproduction. Adverse effects on reproduction by glyphosate and glyphosate formulations have been reported in literature in placental derived JEG3 and human embryonic 293 cells (Benachour *et al.*, 2007).

Genotoxic studies were conducted as an assessment of DNA damage using the Comet assay/single cell gel electrophoresis assay which provides a powerful screening tool (Anwar, 1997). This method is an electrophoretic and fluorescence microscopy assay which provides several advantages including the simple, rapid and sensitive evaluation of DNA strand breaks at a single cell level (Fairbairn *et al.*, 1995). The main principle of the Comet assay is based on the migration of lysed, damaged or fragmented DNA strands (due to strand breaks) under electrophoresis, forming a migration pattern that assumes the shape of a comet, with the amount of DNA in the tail in comparison to the head and the length of the tail relating to the extent of DNA damage (Anderson *et al.*, 1998; Hovhannisyan, 2010; Moller *et al.*, 2000; Tice *et al.*, 2000; Yared *et al.*, 2002). Comet assay results can be analyzed using visual scoring, however image analysis systems are considered more consistent measures of DNA damage/migration (Faust *et al.*, 2004, Kumaravel and Jha, 2006). Parameters commonly used as a measure of DNA damage are the olive tail moment (OTM), which is a product of the tail DNA, the distance between the head and tail, the tail length (TL, μm), and the %tail DNA (TDNA), the proportion of DNA in the comet tail (Duez *et al*., 2003).

The second aim of the current study was to assess the contribution of adjuvants to glyphosate toxicity in humans and the glyphosate formulations Ro and Wipeout® (Wo) were included in this study.

## 3.2 Objectives

- To determine the cytotoxic and pro-inflammatory potential of glyphosate and glyphosate formulations in human white blood cells and human whole blood using the 3-(4,5-dimethylthiazol-2-YI)-2,5-diphenyltetrazolium bromide (MTT) assay and the enzyme-linked immunosorbent assay (ELISA).
- To determine the cytotoxic and genotoxic potential of glyphosate and glyphosate formulations in human breast and endometrial cancer cell lines using the MTT assay and the Comet assay.
- To evaluate the comparative toxicities of glyphosate and two glyphosate formulations using non-linear regression modeling and the standard statistical procedure, analysis-of-variance (ANOVA) in Microsoft® Excel® 2007.

## 3.3 Methods and materials

### 3.3.1. Materials

Please refer to the chemical list in Appendix I for all materials and chemical suppliers used in this study. Standard methods were used to prepare primary stock solutions of Ro (glyphosate concentration: 360 g/L), Wo (glyphosate concentration: 500 g/L) and pure glyphosate ($M_w$: 169.08, purity: 99.5 %) containing equivalent concentrations of glyphosate acid (1000 µg/ml). For all experiments, glyphosate and glyphosate formulation stocks were freshly prepared.

### 3.3.2 White blood cell isolation, cell culture and exposure

Blood was collected by venipuncture (ethical clearance was obtained for use of human blood samples) from healthy volunteers (n= 5, 16 ml/person) in ethylenediaminetetraacetic (EDTA) acid vacutainers. White blood cell isolation was carried out within 5 hours of collection. The blood samples were centrifuged twice at 500 × *g* and 2000 × *g* in an Eppendorf Centrifuge 5702 (Merck) for 10 minutes and the supernatants was retained (contained platelets, plasma and white blood cells/buffy coat). Lysis buffer (0.16 M $NH_4Cl$, 0.01 M $KHCO_3$, 0.006 M EDTA) was added to the supernatants in a 1:9 ratio (blood: lysis buffer) and the mixtures was vortexed for 10 seconds (Vortex V1 plus, BOECO) and incubated at 23 °C for 3 minutes. Mixtures were subsequently centrifuged at 2,000 × *g* for 10 minutes (Eppendorf Centrifuge 5702, Merck) and pellets containing white blood cells were retained. Pellets were washed twice with lysis buffer (3 ml) and each wash step was followed by centrifugation at 1,000 × *g* (Eppendorf Centrifuge 5702, Merck) for 5 minutes. The isolated white blood cells were diluted in RPMI 1640 medium (+ 25 mM hepes, + L-glutamine) supplemented with 5 % heat inactivated fetal bovine serum (FBS), 50 U/ml penicillin and 50 µg/ml streptomycin. White blood cells were stained with tryphan blue (0.4 %) and counted using a heamocytometer. Cells were seeded (180 µl/well, 250 000 cells/well) in 96 well cell culture plates (CELLSTAR®, greiner bio-one) and exposed to varying concentrations (20 µl, 0-1000 µg/ml) of pure glyphosate, Ro and Wo for 18 hours at 37 °C (standardized lab protocol). Samples were then centrifuged at 1000 × *g* (Eppendorf Centrifuge 5804 R, Merck) and the supernatants were retained and stored at -20 °C for cytokine analysis. The positive control for this study, lipopolysaccahride (5 µg/ml LPS) is an endotoxin found in gram negative bacteria and was selected for this study as it has been reported to induce inflammatory responses (Ertel *et al.,* 1995; Stoddard *et al.,* 2010). Pyrogen free water was used as the untreated control.

### 3.3.3 Whole blood cell culture and exposure

Blood was collected by venipuncture from healthy volunteers (n= 5, 16 ml/person) in heparin containing vacutainers. Samples were diluted in 1:10 in RPMI 1640 medium (+ 25 mM HEPES, + L-glutamine) supplemented with 5 % heat inactivated fetal bovine serum (FBS), 50 U/ml

penicillin and 50 μg/ml streptomycin, within 5 hours of collection. Blood (1 ml) samples were exposed to varying concentrations of pure glyphosate, Ro and Wo (100 μl, 0-500 μg/ml) for 18 hours at 37 °C (standardized lab protocol). Samples were then centrifuged at 900 × *g* for 5 minutes (Eppendorf Centrifuge 5804 R, Merck) and the supernatants were retained and stored at -20 °C for cytokine analysis. LPS and pyrogen free water were the positive and untreated controls used in this study respectively.

### 3.3.4 Breast cancer and endometrial cancer cell line culture

The MCF-7 and MDA-MB-231 breast cancer cell lines were obtained from the American Type Culture Collection (ATCC), USA. The HEC1A endometrial cancer cell line was kindly donated by Dr. H. Davis (Nelson Mandela Metropolitan University, Eastern Cape, South Africa). Cell lines were grown in Dulbeco´s Modified Eagle´s medium (DMEM) (+ 4.5 g/L glucose, + L-glutamine, phenol red) supplemented with 50 U/ml penicillin, 50 μg/ml streptomycin and 5 % heat inactivated fetal cal serum. Cell cultures were previously cultured in phenol containing DMEM medium, therefore for the present study cells were not cultured in phenol free medium to maintain a stable estrogen-sensitive phenotype, as the cells may still present steroid memory effects (Glover *et al.*, 1988). Cells were routinely maintained under standard culture conditions at 37 °C, 90 % humidity and 5 % $CO_2$. Confluent cells (70-80 %) were split and seeded at 100 000 cells/ well (1 ml) into 24-well plates (CELLSTAR®, greiner bio-one) and allowed to attach overnight at 37 °C. Once attached, the three cell lines were exposed to varying concentrations (0-500 μg/ml) of pure glyphosate, Ro and Wo (100 μl) for 24 hours at 37 °C (standardized lab protocol). The DNA topoisomerase inhibitor camptothecin (35 μg/ml) was used as a positive control (Hsiang *et al.*, 1985) in this study. All the data obtained was normalized relative to the untreated control (pyrogen free water).

### 3.3.5 Methylthiazol tetrazolium (MTT) assay (cytotoxicity assay)

The MTT cell viability assay is based on the cleavage of the MTT tetrazolium salt by metabolically active cells via the enzyme succinate dehydrogenase forming a purple formazan

product (Denizot and Lang, 1986). After the relevant exposure periods samples were incubated in MTT reagent (0.5 mg/ml, in the appropriate media) for 3 hours (white blood cells), 30 minutes (whole blood) or 3 hours (cancer cell lines) at 37 °C (standardized lab protocol). Color formation was analyzed spectrophotometrically at 560 nm in a Biotek Powerwave XS microplate reader.

### 3.3.6 Pro-inflammatory response study

Cytokine (TNF-α, IL-1β and IL-6) production and release was determined using commercial ELISA kits (eBioscience) and the assay was conducted according to the manufacturer's instructions. Briefly, 96-well microtitre plates were coated with TNF-α, IL-1β and IL-6 in coating buffer overnight at 4 °C. Following a wash step using wash buffer containing phosphate buffered saline (1 × PBS, ) and 0.05 % Tween-20, cells were blocked (eBioscience assay diluents) at 23 °C for 1 hour. Test samples, untreated controls, positive controls and cytokine standards (Appendix II) were incubated in the plates at 23 °C for 2 hours. After a wash step the biotin-conjugated detection antibody was added to the wells and incubated at 23 °C for 1 hour. Following another wash step Avidin-HRP was added and incubated at 23 °C for 30 minutes. The wells were washed the substrate solution tetramethylbenzidine (TMB) was added and allowed to develop for 15 minutes at 23 °C before the reaction was stopped with 1 M sulphuric acid solution. Absorbance values were determined spectrophotometrically at 450 nm (reference wavelength: 570 nm) using a Biotek Powerwave XS microplate reader. LPS (5μg/ml) was the positive control used in this study and pyrogen free water was used as the untreated control.

### 3.3.7 Cancer cell line exposure and the Comet assay (single cell gel electrophoresis)

The exposure concentrations chosen in this study were based on cell viability data and a positive control reference concentration was incorporated based on the glyphosate cytotoxicity results presented in literature in the HepG2 human liver cell line. The MCF-7, HEC1A and MDA-MB-231 cancer cell lines were exposed to pure glyphosate (500 μg/ml and 1000 μg/ml) Ro and Wo for (500 μg/ml and 800 μg/ml) for 4 hours at 37 °C. After exposure cells were prepared for the Comet assay, media was aspirated and cells were trypsinized with 2.5 % trypsin for 5 mins at 37 °C. All Comet assay procedures were conducted under dark conditions.

The Comet assay was conducted using the commercial kit, OxiSelect™ Comet Assay kit (Cell Biolabs, INC). Trypsinized cells were pooled (n= 3) and centrifuged at 700 × *g* for 2 minutes (Merck Minispin Eppendorf AG Centrifuge, Merck). The pelleted cells were retained and washed with ice-cold PBS (without $Mg^{2+}$ and $Ca^{2+}$) and centrifuged at 700 × *g* (Merck Minispin Eppendorf AG Centrifuge, Merck). Cells were resuspended at 100 000 cells/ml in ice cold PBS for the commencement of the assay.

Briefly 100 µl of molten agar (comet agarose was heated at 95 °C for 20 minutes and maintained at 37 °C until use) was added to together with 10 µl of resuspended cells. The mixture (75 µl/well) was immediately placed onto an OxiSelect™ comet slide. Slides were incubated at 4 °C for 15 minutes to allow the agarose to set. Once set slides were treated with lysis buffer (pre-chilled, pH 10) for 60 minutes at 4 °C and subsequently treated in alkaline solution (pH 13) for 30 minutes at 4 °C. Slides were subjected to alkaline electrophoresis for 18 minutes (300 mA) followed by neutralization in pre-chilled dionised water (DI $H_2O$), which was carried out twice for 2 minute intervals and washed with cold 70 % ethanol for 5 minutes. The slides were then air dried and once dried the slides were incubated with 100 µl of 1 × Vista Green dye prepared in TE buffer (10 mM Tris, pH 7.5, 1 mM EDTA) for 15 minutes at room temperature.

Comet assay slides were visualized with the Zeiss Axio Vert. A1 fluorescence microscope (5×) using a fluorescein isothiocyanate (FITC) filter (7 %). Images were obtained using an AxioCam MR3 Camera (stored in the Axio vision Rel.4.8 program). Image J Macro with a Comet assay plugin was used to calculate the tail length (µm), olive tail moment (arbitrary units) and tail DNA (%). Data analysis was conducted according to the Comet assay guidelines outlined by Tice *et al.* (2000) for *in vitro* genotoxicity testing. Briefly, 50 cells were analyzed from pooled cell cultures (n=3), per experimental treatment. Based on the fact that samples had been pooled, the 50 cells were analyzed on one slide.

### 3.3.8 Data analysis

All data were presented as means ± standard error of the means (SEM). ANOVA single factor analysis (Microsoft Excel) was used to determine significant differences between test sample groups relative to the untreated control, with 95 % ($P \leq 0.05$) or 99 % confidence ($P \leq 0.01$).

Where appropriate, the Shapiro-Wilk W test for data distributional assumptions and non-normality using the numerical analysis for Excel (numXL) add in, was applied. It is assumed that a P value below the alpha level (0.05) suggests that the data exhibits non-normal distribution (non-Gaussian) (Royston, 1992; Shapiro and Wilk, 1965).

Non-linear least square regression models were applied to cytotoxicity data in human whole blood exposed to varying concentrations of pure glyphosate, Ro and Wo, using the Graphpad Prism 6 software package (San Diego, CA). Goodness of fit was assessed using $R^2$, $R^2_{adjusted}$ values and by the assessment of upper and lower 95 % confidence limits associated with the model fit. The Wald-Wolfowitz (runs) test was used to establish the deviation of the non-linear regression model from the experimental data. The models were used to approximate the concentration of glyphosate and glyphosate formulations required to cause a half maximal response (half maximal effective concentration, EC50).

## 3.4 Results

### 3.4.1 Cytotoxic and pro-inflammatory response in isolated human white blood cells exposed to glyphosate and glyphosate formulations Ro and Wo

The acute cytotoxicity and pro-inflammatory effects in isolated human white blood cells exposed to pure glyphosate and the glyphosate formulations Ro and Wo for 24 hours were assessed using the MTT reduction assay and the ELISA method. The results of this study are presented in Figures 3.1 and 3.2. The concentrations chosen for this study were based on the regulatory drinking water standards for glyphosate (low dose), concentrations relevant to residential and occupational exposure (moderate dose) and the two highest concentrations tested for this study were approximately 5 and 6.6-fold lower than the reported LC50 reported for *in vivo* studies in rats (moderate to high dose exposure).

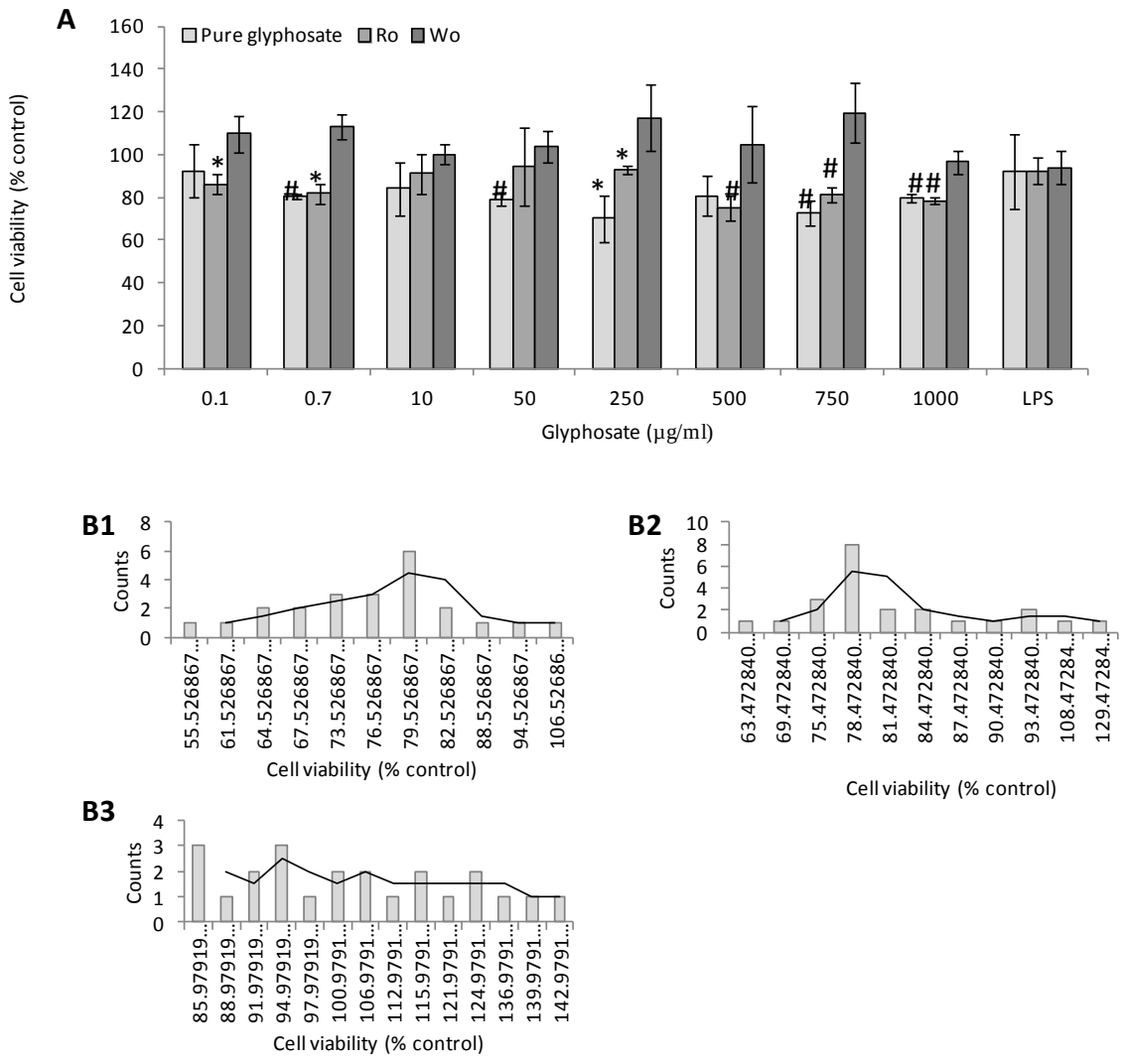


**Figure 3.1:** The effect of pure glyphosate (99.5 %) and glyphosate-based herbicides Ro and Wo on the cell viability of human white blood cells **(A)**. The cells were exposed at 37 °C over a 18 hour period (250 000 cells/well) at varying herbicide concentrations (0-1000 µg/ml). Lipopolysaccharide (LPS, 5 µg/ml) was used as a positive control in this study. Values are presented as mean values ± SEM (n=5). ANOVA single factor analysis was used to determine significant differences from the untreated control (not shown) $^{*}P \leq 0.05$, $^{\#}P \leq 0.01$. Frequency plots **(B)** showing the distribution of data for the different experimental treatments **B1:** pure glyphosate, **B2:** Ro and **B3:** Wo.

The Wo formulation showed no significant effects on the cell viability of human white blood cells as compared to the untreated control, however pure glyphosate and Ro treatments caused significant cell toxicity, with reductions ($^{*}P \leq 0.05$, $^{\#}P \leq 0.01$) in cell viability being observed at 0.7 (80.3 ±1.3), 50 (79.2 ± 3.1), 250 (70.1 ± 10.8), 750 (73.0 ± 5.6), 1000 (80.0 ± 1.8) µg/ml and 0.1, 0.7 (86.2 ± 4.9), 250 (82.0 ± 4.6), 250 (93.0 ± 4.9) , 500 (75.1 ± 5.8), 750 (81.3 ± 3.2), 1000 (78.4 ± 1.4) µg/ml pure glyphosate and Ro concentrations, respectively (Figure 3.1 A). No clear dose-dependent relationship was observed and the data obtained suggested a non-monotonic dose relationship.

Non-linear regression modeling applied to the present data (for pure glyphosate and Ro) did not lead to successful convergence and EC50 values were not determined for this experimental study. Regression analysis (linear and non-linear) is based on the assumption that the scatter of data follows a Gaussian/normal/ bell-shaped and although biological data often does not follow the ideal bell-shape the scatter should be close enough to Gaussian to satisfy the use of regression analysis (Motulsky and Christopoulos, 2003). Figure 3.1 B3 clearly indicates that the data distribution was non-Gaussian, however frequency plots obtained for pure glyphosate (Figure 3.1 B1) and the Ro formulation (Figure 3.1 B2) were less clear, therefore the Shapiro-Wilk normality test was applied to the data and this confirmed the non-Gaussian distribution of data obtained for the pure glyphosate treatment ($P = 0.02$) and the Ro formulation ($P = 0.0$). Results of the distribution plot and Shapiro-Wilk normality test for the pure glyphosate and Ro treatments suggests that the data obtained for human white blood cells may not have been suitable for non-linear regression modeling.

The positive control, LPS (5 µg/ml) demonstrated no significant cytotoxic effects in human lymphocyte cells for the exposed dose.

The dose-response curves obtained for pure glyphosate and Ro in human white blood cells indicated cytotoxic effects at concentrations falling within the USEPA MRL for glyphosate in drinking water, therefore this study selected concentrations between 0 and 50 µg/ml to assess the inflammatory response potential of pure glyphosate, Ro and Wo at these low levels of exposure.

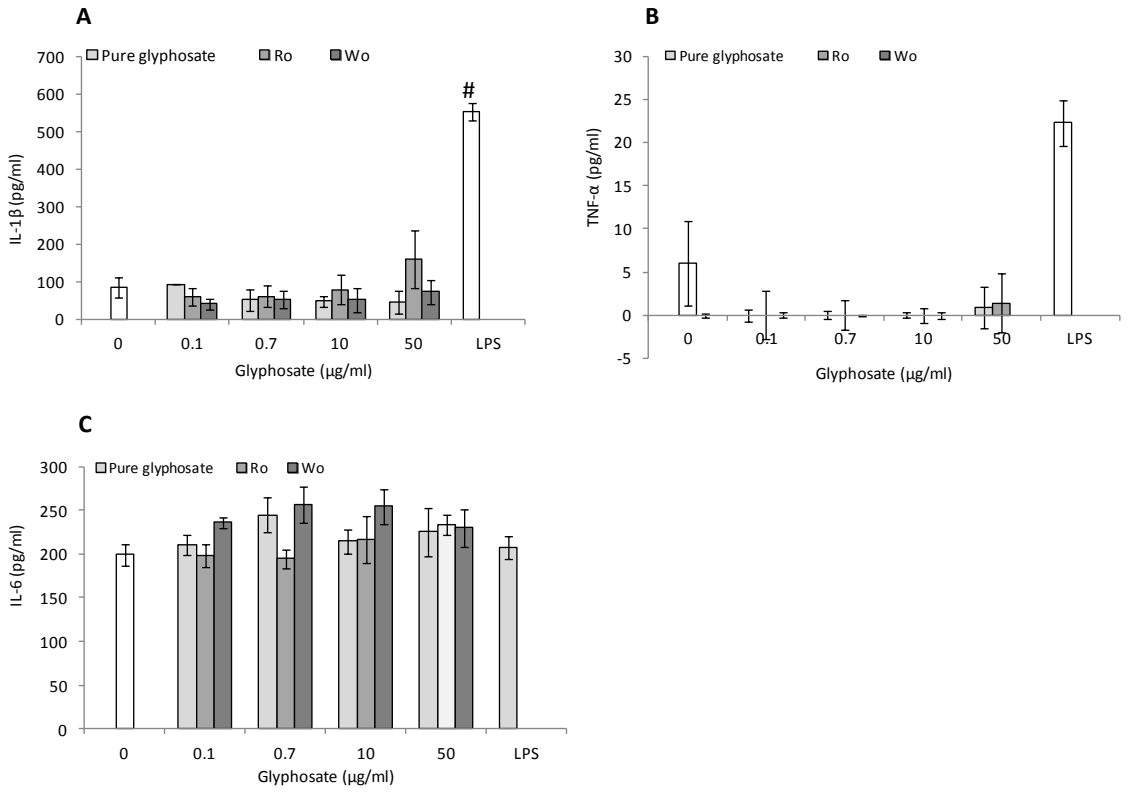


**Figure 3.2:** The pro-inflammatory effect of pure glyphosate and glyphosate based herbicides Ro and Wo on cytokine production/release in human white blood cells. **A:** IL-1β, **B:** TNF-α, **C:** IL-6. The white blood cells were exposed at 37 °C over a 24 hour period at varying herbicide concentrations (0-50 µg/ml). Lipopolysaccharide (LPS 5µg/ml) was used as a positive control in this study. Values are presented as mean values ± SEM (n= 3). ANOVA single factor analysis was used to determine significant differences from the untreated control $^{*}P \leq 0.05$, $^{\#}P \leq 0.01$.

The exposure of human white blood cells to varying herbicide concentrations (0-50 µg/ml) did not result in the significant induction in any of the three pro-inflammatory cytokines (IL-1β, TNF-α and IL-6) evaluated in this study (Figure 3.2). The positive control LPS (5µg/ml) only caused a significant induction in IL-1β (575 pg/ml ± 29) and, a non-significant induction was observed in TNF-α (22 pg/ml ± 2.6, P= 0.06). Interestingly, no TNF-α was detected at herbicide concentrations between 0.1 and 10 µg/ml and only a small amount (non-significant) was released at pure glyphosate (0.85 ± 2.4) and Ro (1.41 ± 3.4) concentrations of 50 µg/ml (Figure 3.2).

### 3.4.2 Cytotoxic and pro-inflammatory response in human whole blood cells exposed to glyphosate and glyphosate formulations Ro and Wo

The effects of pure glyphosate, Ro and Wo on cell toxicity in human whole blood after an 18 hour exposure period were assessed using the MTT reduction assay (Figure 3.3A, 3.3B, 3.3C) and the half maximal responses (EC50) (Table 3.1) for the different herbicidal treatments were determined using non-linear regression models (Figure 3.3a, 3.3b, 3.3c). This experimental study also investigated the effects of pure glyphosate, Ro and Wo on the production and release of the pro-inflammatory cytokines IL-1β, TNF-α and IL-6 using ELISA assays and these results are shown in Figure 3.4. The concentrations assessed in this study were representative of drinking water quality guidelines for glyphosate (low dose) as well as concentrations representative of occupational and residential exposure (moderate dose).

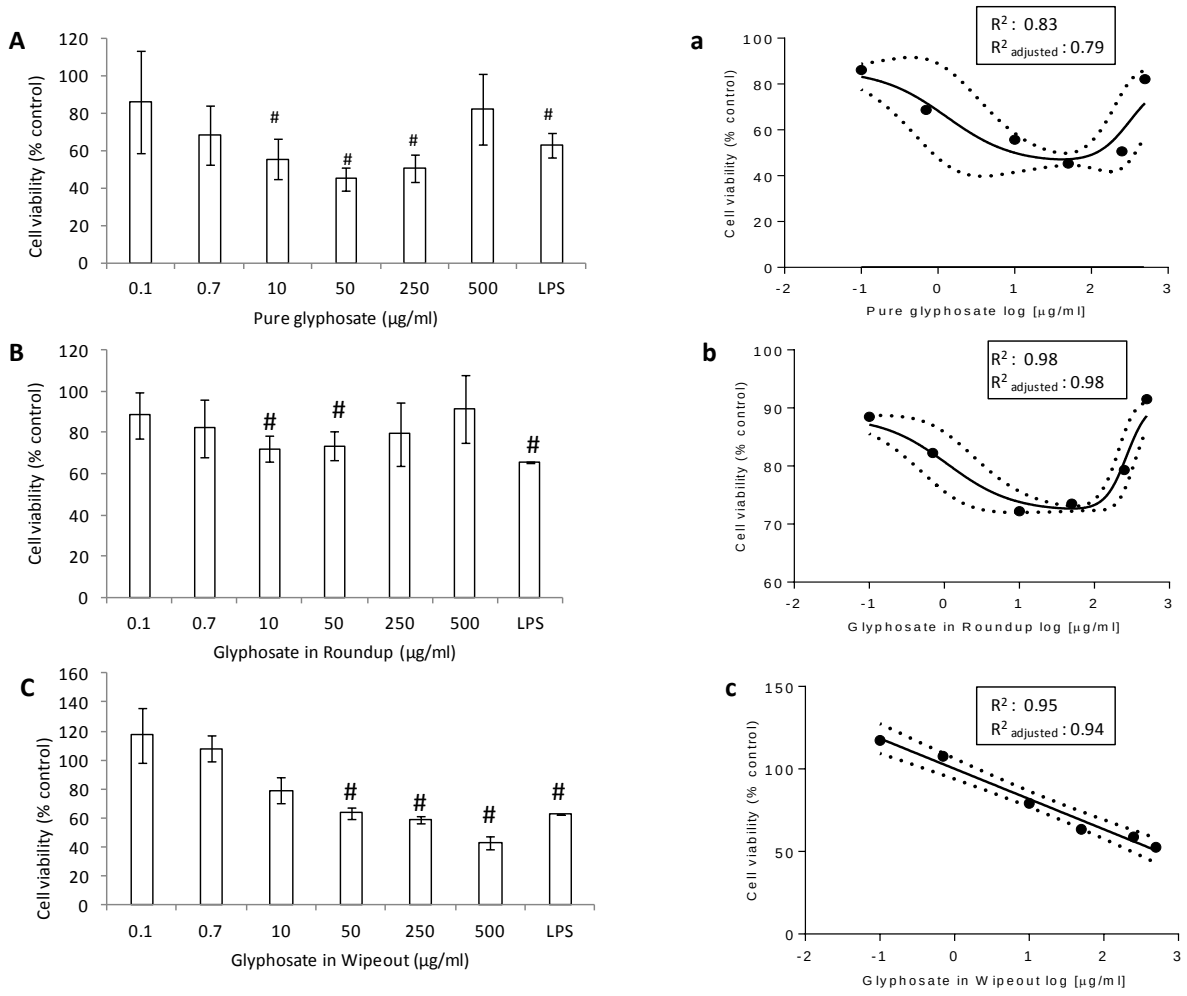


**Figure 3.3:** The effect of **A:** Pure glyphosate (99.5 %) and the glyphosate-based herbicides **B:** Ro and **C:**Wo on the cell viability in human whole blood. The cells were exposed at 37 °C over an 18 hour period (1 ml) at varying herbicide concentrations (0-500 µg/ml). Lipopolysaccharide (LPS, 5 µg/ml) was used as a positive control in this study. Values are presented as mean values ± SEM (n=5). ANOVA single factor analysis was used to determine significant differences from the untreated control (not shown) $^{*}P \leq 0.05$, $^{\#}P \leq 0.01$. The effect of A: pure glyphosate, C: Ro and E: Wo in human whole blood was described using non-linear regression analysis (Graphpad Prism 6). Goodness of fit was assessed by $R^2$, $R^2_{adjusted}$ values and upper and lower 95 % confidence intervals around the fit (dash lines). **a:** Bell shaped curve (biphasic curve): $Ymin + (Ymax\text{-}Ymin)/1+10^{(logEC50_1 - log\ [x])*nH1} + Ymax_2 - Ymin/1+10^{(log[x]-logEC50_2)*nH2}$ , **b:** Bell shaped curve (biphasic curve): $Ymin + (Ymax\text{-}Ymin)/1+10^{(logEC50_1 - log\ [x])*nH1} + Ymax_2 - Ymin/1+10^{(log[x]-logEC50_2)*nH2}$ **c:** linear curve: $Y = m*log(x) + c$.

Based on the observed biphasic nature of the curves obtained for pure glyphosate and Ro (Figure 3.3A and B) in human whole blood, a model describing a seven parameter bell shaped dose (combines two sigmoidal responses) response curve was selected. This model was previously described by Antachopoulos *et al.* (2007) and is based on equation (1):

$$Ymin + (Ymax\text{-}Ymin)/1+10^{(logEC50_1 - log\,[x])*n_H1} + Ymax_2 - Ymin/1+10^{(log[x]-logEC50_2)*n_H2} \quad (1)$$

Where *Y*, corresponds to the percentage cell viability. The *logEC50* values (1 and 2) describe the half maximal responses from the two different phases of the regression curve. $n_H1$ and $n_H2$ are the slope parameters for the different phases of the curve and *log [x]* correspond to the glyphosate concentrations.

Due to complexity of the bell-shaped dose response model (seven parameters) and the small number of data points (n= 6), the choice of initial parameter estimates was crucial (Motulsky and Christopoulos, 2003) and constraints were placed on the following parameters: *Ymin*, *Ymax*, $Ymax_2$, $n_H1$, $n_H2$ and *x* to allow the model to successfully converge.

The effects of Wo on whole blood showed a dose dependent relationship (Figure 3.3C), therefore non-linear least square regression was used to model linear data. Fitting linear data with non-linear regression utilizes a standard linear equation (refer to equation 2), however fitting linear data with non-linear regression in Graphpad Prism 6 is advantageous as it allows greater options with respect to data analysis (e.g. the ability to apply weighting to the data and the ability automatically exclude outliers) (Motulsky and Christopoulos, 2003).

Non-monotonic effects on cell viability were observed in whole blood cells exposed to pure glyphosate and the formulation Ro (Figure 3.3A and 3.3B). Both treatments caused negligible non-significant effects (relative to the untreated control) on cell viability at the lowest concentrations (0.1 and 0.7 µg/ml) investigated in this study, however a significant ($P \leq 0.01$) reduction in cell viability was observed at pure glyphosate and Ro concentrations of 10 and 50 µg/ml. In the pure glyphosate treatments the reduction in cell viability at lower concentrations was followed by a significant decrease in cell viability at a concentration of 250 µg/ml (51 % ± 7.2). A non-significant increase was observed in the Ro treatment at the same concentration ($P > 0.05$). The final phases of the dose-response curves were characterized by non-significant

increases in cell viability for both pure glyphosate (82 % ± 18.9) and Ro (91 % ± 16.4) at a treatment concentration of 500 µg/ml.

A significant ($P \leq 0.01$) monotonic dose response relationship was observed in whole blood cells treated with the formulation Wo (Figure 3.3C), with a reduction in cell viability observed from a threshold concentration of 50 µg/ml. The positive control (LPS, 5 µg/ml) used in this study proved a suitable control for this study and demonstrated overall significant cytotoxic effects on human whole blood cells.

The dose response profiles obtained for pure glyphosate and Ro were characterized by an inverted bell shaped curve. This non-linear regression model described the experimental accurately (Figure 3.3a and 3.3b) and the $R^2$ and $R^2_{adjusted}$ values obtained were 0.83, 0.79 for pure glyphosate and 0.98 for Ro. Further evaluation of goodness of fit indicated relatively narrow upper and lower 95 % confidence limits around the fit and the Wald-Wolfowitz test showed no significant deviation of the model in relation to the experimental data for both pure glyphosate (P= 0.9) and Ro (P=1.0).

The linear regression model applied to the Wo dose-response curve indicated a very good fit (Figure 3.3c) and the $R^2$ and $R^2_{adjusted}$ values obtained were 0.95 and 0.94 respectively. Narrow upper and lower 95 % confidence limits were observed around the fit and the Wald-Wolfowitz test demonstrated no significant deviation of the model (P= 0.1).

According to the half maximal inhibition (reduction) values ($EC50_1$) shown in Table 3.1 pure glyphosate and the formulation Ro induced similar inhibitory effects with $EC50_1$ output values showing a minimal difference of 15 % between Ro (1.1 µg/ml) and pure glyphosate (1.3 µg/ml) treatments. The $EC50_1$ values obtained for the formulation Wo (7.1 µg/ml) indicated a lower inhibitory effect on human whole blood when compared to the other herbicidal treatments.

**Table 3.1:** The half maximal response (EC50) values for pure glyphosate, Ro and Wo in human whole blood.

| Test | Model | Slope | Intercept | $EC50_1$ (µg/ml) | $EC50_2$ (µg/ml) |
|---|---|---|---|---|---|
| Pure glyphosate | NBSC[*1] | -1.0, -2.0[*] | - | 1.3 (0.2-10.1) | 317.7 (124.2-814.7) |
| Ro | NBSC | -1.0, -2.0[*] | - | 1.1 (0.3-3.9) | 269.8 (190.5-382.8) |
| Wo | LRC[*2] | -18.34 (-22-(-) 14.7)[*3] | 100.1 (94.0-106.4) | 7.1[*4] | - |

[*]: Constrained values representing the slope factors $n_H1$ and $n_H2$ respectively. [*1]: Non-linear bell shaped curve (NBSC).[*2] Linear regression curve (LRC).[*3]: Values in parenthesis indicate 95 % confidence limits for the corresponding parameter. [*4] The EC50 values was derived by the following equation: $EC50 = 10^{(\log [x]_{max} + \log [x]_{min})/2}$.

Based on the half maximal stimulation (induction) response values ($EC50_2$) shown in Table 3.1, pure glyphosate (317.7 µg/ml) and Ro (269.8 µg/ml) displayed a similar stimulatory effect with Ro producing only a slightly greater stimulatory effect (15 %) when compared to pure glyphosate.

Test concentrations chosen for pro-inflammatory studies were based on the results obtained in the cytotoxicity study. Concentrations of pure glyphosate Ro and Wo as low as 50 µg/ml indicated cytotoxic effects in human whole blood cells therefore this study investigated the effects of herbicide concentrations between 0 and 50 µg/ml on the production and release of the pro-inflammatory cytokines IL-1β, TNF-α and IL-6. The results obtained for the pro-inflammatory studies (Figure 3.4) suggested that exposure of whole blood to Ro and Wo showed no significant effects on the production release of the pro-inflammatory cytokines IL-1β a (Figure 3.4A). Pure glyphosate did, however, cause a significant induction of IL-1β at concentrations of 0.1 (36.2 ± 0.5 pg/ml), 0.7 (39.1 ± 0.6 pg/ml) and 50 µg/ml (33.3 ± 0.5 pg/ml) (Figure 3.4A).

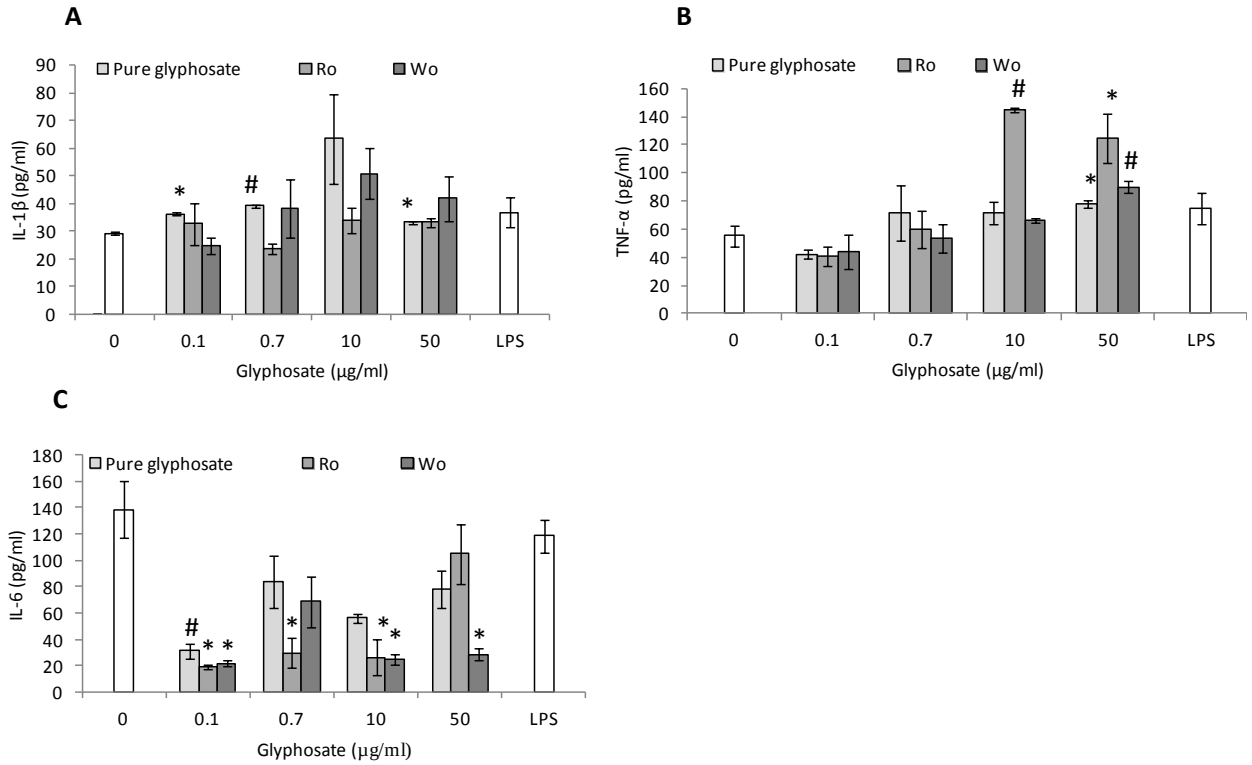


**Figure 3.4:** The pro-inflammatory effect of pure glyphosate and glyphosate based herbicides Ro and Wo on cytokine production/release in human whole blood cells. **A:** IL-1β, **B:** TNF-α, **C:** IL-6. The whole blood cells were exposed at 37 °C over an 18 hour period at varying herbicide concentrations (0-50 µg/ml). Lipopolysaccharide (LPS 5µg/ml) was used as a positive control in this study. Values are presented as mean values ± SEM (n= 3). ANOVA single factor analysis was used to determine significant differences from the untreated control $^{*}P \leq 0.05$, $^{\#}P \leq 0.01$.

Ro concentrations of 10 and 50 µg/ml caused a significant induction ( 145 ± 1.3 and 125 ± 17.8 pg/ml) of the pro-inflammatory cytokine TNF-α (Figure 3.4B) when compared to the untreated control. Pure glyphosate and Wo caused significantly elevated levels of TNF-α to a lesser extent than Ro, at 50 µg/ml (78 ± 2.4and 90 ± 3.8 pg/ml respectively).

A significant reduction in IL-6 plasma levels (Figure 3.4C) was observed at a pure glyphosate exposure concentration of 10 µg/ml (31.1 ± 6.0 pg/ml) when compared to the untreated control (138.4 ± 17.4 pg/ml), which was subsequently followed by non-significant increases at 0.7, 10

and 50 μg/ml. Similar results were obtained for Ro and Wo treatments. Ro caused a reduction in IL-6 levels at 0.1 (19.2 ± 2.0 pg/ml), 0.7 (29.7 ± 11.1 pg/ml), and 10 μg/ml (26.4 ± 13.3 pg/ml) and Wo treatments demonstrated significant reductions of this interleukin at 0.1 (31.1 ± 6.0 pg/ml), 10 (56.0 ± 3.2 pg/ml) and 50 μg/ml (78.0 ± 13.6 pg/ml).

Although LPS (5 μg/ml), the positive control in this study, demonstrated a significant reduction in the cell viability of whole blood cells (Figure 3.3) no significant release of IL-Iβ, TNF-α, and IL-6 was observed in this experimental study (Figure 3.4A, 3.4B and 3.4C).

### 3.4.3 Cytotoxic and genotoxic response in human cancer cell lines exposed to glyphosate

The cytotoxic and genotoxic effects of pure glyphosate Ro and Wo were investigated in three human cancer cell lines, namely MCF7, HEC1A and MDA-MB-231 after exposure to varying glyphosate concentrations (75-500 μg/ml) over a 24 hour period. Cytotoxic properties were evaluated using the MTT reduction assay (Figure 3.5) and the genotoxic potential of glyphosate, Ro and Wo (Figure 3.6, 3.7, 3.8 and 3.9) was assessed using the Comet assay. This study focused on moderate exposure at concentrations relevant to occupational and residential exposure.

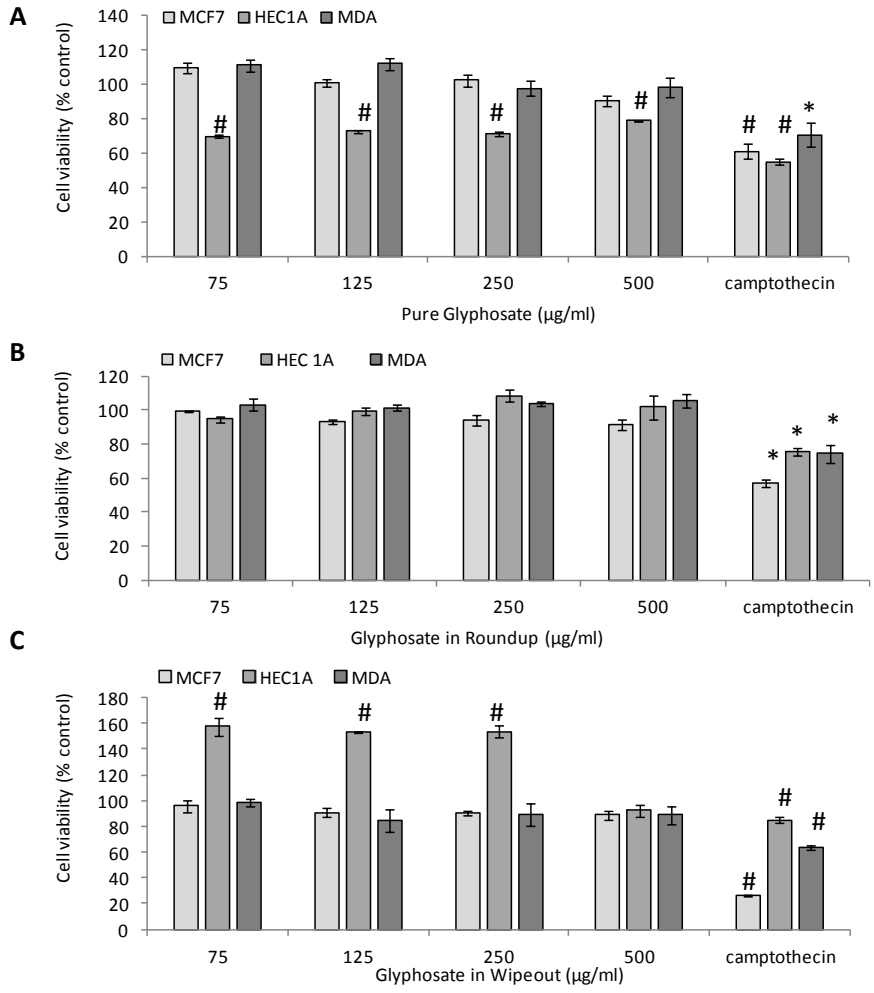


**Figure 3.5:** The cytotoxic effects of **A:** pure glyphosate **B:** Ro and **C:** Wo in the human cancer cell lines, MCF-7, HEC1A and MDA-MB-231. Cells were exposed at 37 °C over a 24 hour period (100 000 cells/well) at varying herbicide concentrations (0-500 µg/ml). Camptothecin (35µg/ml) was used as a positive control in this study. Values are presented as mean values ± SEM (n= 3). Anova single factor analysis was used to determine significant differences from the untreated control (not shown) $^{*}P \leq 0.05$, $^{\#}P \leq 0.01$.

Pure glyphosate caused an overall significant non-monotonic reduction ($P \leq 0.01$) (average inhibition 26.5 % ± 1.8) in the cell viability of the HEC1A endometrial cancer cell line at all the

concentrations tested (75-500 μg/ml) (Figure 3.5A), however no significant cell toxicity was observed in the MCF7 and MDA-MB-231 cell lines exposed to pure glyphosate.

The exposure of the three cancer cell lines to the Roundup formulation did not result in any significant cell toxicity at the concentrations tested (Figure 3.5B). The Wo formulation induced proliferation of the HEC1A cell line at 75, 125, 250 μg/ml (average stimulation 55 % ± 2.5) this was followed by a non-significant reduction in cell viability (92.2 % ± 4.6). Wo elicited no significant cytotoxic effects in the MCF7 and MDA-MB-231 cancer cell lines. Overall this data suggests that pure glyphosate and Wo show greater toxicity to HEC1A cells as compared to the Ro formulation.

Camptothecin (35 μg/ml) induced a significant reduction in cell viability relative to the untreated control in all three cancer cell lines and was therefore a suitable positive control for this study.

Cytotoxicity is not directly linked to genotoxic damage and the use of the Comet assay enables the determination of genetic damage at a single cell level widening the scope and preventing limitations with respect to the interpretation of cell toxicity data, more specifically at levels where significant cytotoxicity is not observed (Hartmann and Speit, 1997; Mañas *et al.,* 2009b; Vock *et al.,* 1998), therefore the main focus of this study was to evaluate whether significant DNA damage occurred at concentrations that did not generally demonstrate cytotoxicity in the cancer cell lines. The test concentration chosen for genotoxicity studies was selected based on the results observed in the cytotoxicity study and on glyphosate concentrations reported in literature to induce genotoxic damage in human cell lines. Pure glyphosate and the formulations Ro and Wo showed no significant toxicity effects in the MCF 7 and MDA-MB-231 breast cancer cell lines up to the maximum concentration (500 μg/ml) used in this study and Wo demonstrated non-significant reduction in cell viability at this concentration in the HEC1A cell line. A concentration of 500 μg/ml was therefore chosen for genotoxicity studies to determine whether any genetic damage was incurred by pure glyphosate and its formulations. Reference concentrations (positive control) were used in this study to ascertain whether herbicide concentrations above 500 μg/ml would cause significant comet formation. The cell viability study (MTT reduction assay) conducted by Gasnier *et al.* (2009) in human HepG2 liver cell lines established initial toxicity values for pure glyphosate at 1000 μg/ml and the maximum concentration reported for the initial toxicity for the Roundup formulation was 800 μg/ml. Based

on this work the reference concentrations chosen for the present study were 1000 μg/ml for pure glyphosate and 800 μg/ml for the Ro and Wo formulations.

As mentioned previously (Section 3.3.7), DNA damage in the HEC1A, MCF-7 and MDA-MB-231 cancer cell lines was determined using the Comet assay and after the exposure period (4 hours) florescent images (Vista Green dye) were developed in this assay for each herbicidal treatment. An example of typical images developed in the Comet assay is shown in Figure 3.6.

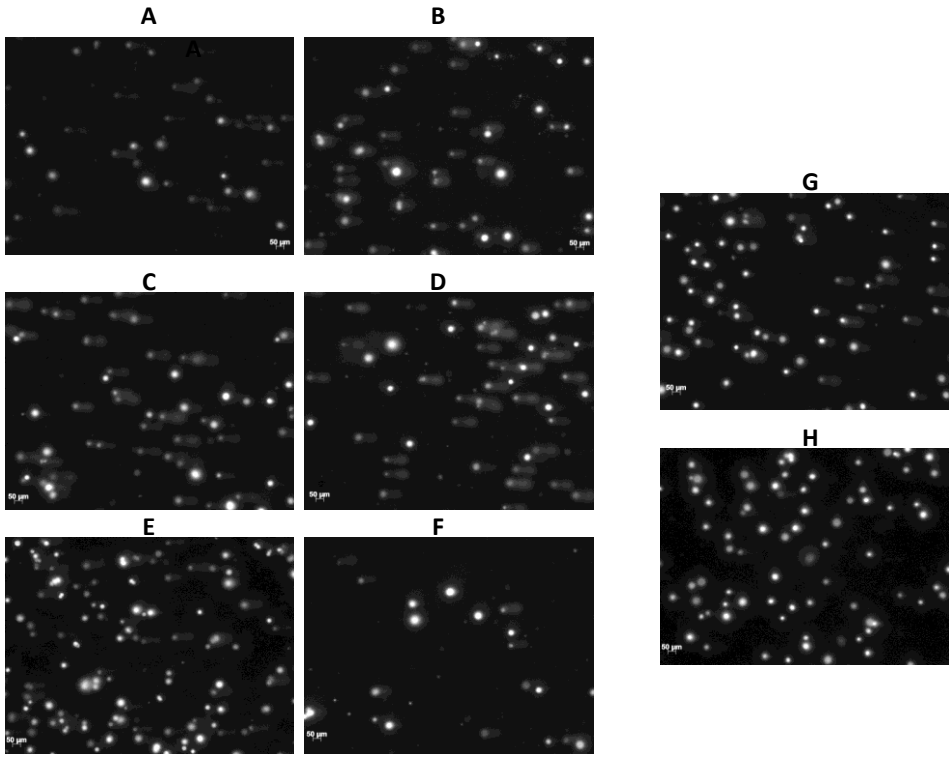


**Figure 3.6:** Typical images developed in Comet assay represented by the HEC1A endometrial cancer cell line. Cells were exposed for a period of 4 hours at 37 °C at the test and reference concentration of herbicide. **A:** 500 μg/ml pure glyphosate **B:** 1000 μg/ml pure glyphosate **C:** 500 μg/ml Ro **D:** 800 μg/ml Wo **E:** 500 μg/ml Wo **F:** 800 μg/ml Wo **G:** positive control (35 μg/ml camptothecin) **H:** untreated control (DMEM). FITC filter, magnification bar: 50 μm.

Image development was followed by analysis using Image J with a Comet assay plugin. Data was recorded and presented as: TL (tail length; μm) and OTM (olive tail moment) (Figure 3.7). The % TDNA (percentage tail DNA) (Appendix III) was also determined for this study, some discrepancies were however observed for % TDNA data when compared to TL and OTM. This occurrence has been previously documented in literature (Ündeğer and Başaran, 2005). The interpretation of Comet assay data interpretation is often limited and becomes difficult when different measurements show varied relationships with dose (Kumaravel and Jha, 2006), therefore a correlation study was conducted comparing the data obtained using the TL and OTM measurements (mean values as percentages against the untreated control). Positive correlations ($R^2$ value close to 1) with these two parameters were observed for pure glyphosate Ro and Wo treatments in the three cancer cells (Appendix II). The good correlation between the TM and OTM measurements suggested that these parameters would better reflect the Comet assay data.

The MCF-7 cancer cell line demonstrated the lowest sensitivity to glyphosate exposure and results indicated extremely low levels (non-significant) of DNA damage in all three herbicidal treatments at test (500 μg/ml) and reference concentrations (800 or 1000 μg/ml) (Figure 3.7).

Pure glyphosate induced significant (relative to the untreated control) DNA damage (Figure 3.7A and B) at the test concentration (500 μg/ml) in the HEC1A cells as demonstrated by the increase in TL (0.36) and OTM (26282) and at the reference concentration (1000 μg/ml) (TL: 0.24, OTM: 14519). Similar results were obtained in HEC1A cells exposed to the Ro (Figure 3.7 C and D) and Wo (Figure 3.7 E and F) formulations, with significant increases in tail length and olive tail moment being observed at both the test and reference concentrations.

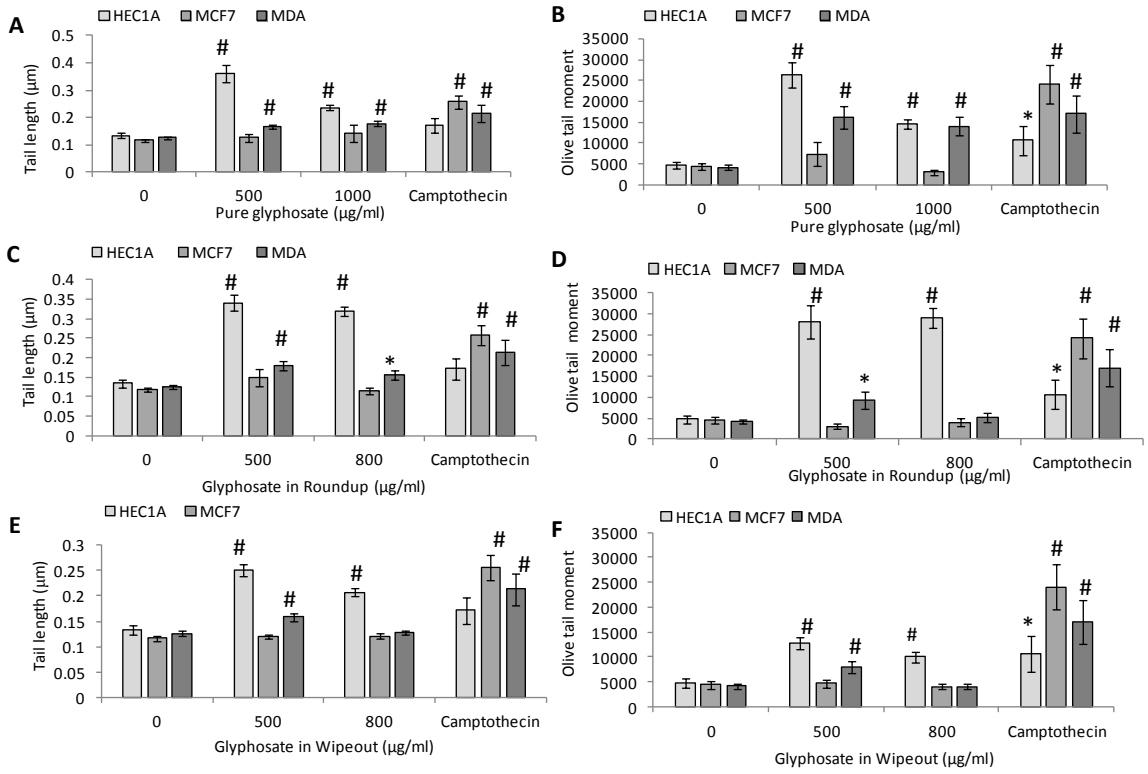


**Figure 3.7:** DNA damage in HEC1A, MCF-7 and MDA cell lines assessed by tail length (µm) (**A,C,E**) and olive tail moment (**B,D,F**). Cells were exposed at 37 °C over a 4 hour period to different concentrations (untreated, test concentration and reference concentration) of **A & B:** pure glyphosate **C&D:** Ro and **E&F:** Wo. Camptothecin (35 µg/ml) was used as a positive control in this study. Values are presented as mean values (± SEM) of 50 cells analyzed per experimental treatment. ANOVA single factor analysis was used to determine significant differences from the untreated control. $^{*}P \leq 0.05$, $^{\#}P \leq 0.01$.

The MDA-MB-231 cell line proved sensitive to glyphosate exposure when compared to untreated cells and pure glyphosate treatments demonstrated genotoxic activity at the test concentration (TL: 0.17, OTM: 16267) (Figure 3.7A and B) and reference concentration (TL: 0.18, OTM: 14027). Both Ro and Wo led to significant increases in TL (0.18, 0.16) and OTM (8004, 9313) at 500 µg/ml, however overall data at 800 µg/ml suggested low/non-significant levels of DNA damage by these two formulations (Figure 3.7 C, D, E and F).

Overall, the MCF-7 cell line showed the lowest sensitivity to pure glyphosate and its formulations when compared to the HEC1A and MDA-MB-231 cancer cell lines. Pure glyphosate, Ro and Wo showed greater ($P \leq 0.001$) DNA damage in the HEC1A cancer cell line when compared to the MDA-MB-231 cells. In the MDA-MB-231 cancer cell line there was no significant difference in the genotoxicity displayed by pure glyphosate in comparison to the Ro and Wo formulation, however pure glyphosate incurred DNA damage that was statistically similar to that observed for Ro ($P > 0.05$) but greater ($P \leq 0.001$) than that of the Wo formulation.

Camptothecin proved to be a suitable positive control in this study as it demonstrated significant genotoxic damage in the three cancer cell lines.

## 3.5 Discussion and future work

### 3.5.1 Cytotoxic and pro inflammatory properties of glyphosate, Ro and Wo in isolated human white blood cells and human whole blood

The cytotoxic and inflammatory potential of pure glyphosate and the glyphosate-based herbicide Ro and Wo was tested in two human *in vitro* models, namely isolated human white blood cells and human whole blood.

The cytotoxicity data for human white blood cells in Figure 3.1A demonstrated the toxic capacity (with significant reductions in cell viability) of pure glyphosate and Ro on human white blood cells at concentrations below and within the USEPA MRL range for glyphosate in drinking water. No cytotoxic effects were observed in white blood cells treated with the Wo formulation. The dose-relationship observed for this study was non-monotonic, however analysis of data distribution (Figure 3.1B) and the Shapiro-Wilk normality test confirmed non-Gaussian distribution in human white blood cells treated with the pure glyphosate and Ro (Figure 3.1B1 and 2). The data distribution may have been a contributing factor precluding the successful application of non-linear regression models to the experimental data and a dose relationship is required for the determination of EC50, therefore no EC50 values could be determined for this experimental study. Although we have demonstrated the cytotoxic capacity of pure glyphosate and the Ro formulation in human white blood cells at concentrations as low as 0.1 μg/ml (Ro

formulation) and 0.7 μg/ml (pure glyphosate and Ro formulation) none of the aforementioned herbicidal treatments (at the concentrations tested: 0-50 μg/ml) induced a significant (compared to the untreated control) production of the pro-inflammatory cytokines IL-1β, TNF-α and IL-6 (Figure 3.2). Pure glyphosate, Ro and Wo showed no inflammatory response effects in human white blood cells at the concentrations and exposure time tested in this study. LPS (5 μg/ml) was used as the positive control in this study and only caused significantly elevated levels of IL-1β. A study by Cassatella *et al.* (1993) concluded that IL-10 was a potent inhibitor of the LPS stimulated release of pro-inflammatory cytokines TNF-α, IL-1β and IL-8 in polymorphonuclear leukocytes. In order to gain further understanding into the potential effect of glyphosate and glyphosate formulations on acute inflammatory responses, future studies should consider the inclusion of the anti-inflammatory cytokine IL-10, as it plays a crucial role in limiting the time and degree of an acute inflammatory response.

Interestingly, to the best of our knowledge, no reports have documented the pro-inflammatory effects of glyphosate in human white blood cells and the mechanism/s of toxicity by glyphosate in human white blood cells have not been well established in literature; however there have been some reports on the toxic potential of this herbicide at concentrations which are within the range of this study. Most studies involving the effect of glyphosate on human lymphocytes focus on the possible genotoxic effects and reports have shown contrasting results. Results of vital staining using ethidium bromide and acridine orange by Mladinic *et al.* (2009) for cell viability assessment demonstrated the ability of technical grade glyphosate (98 % purity) to cause apoptosis and necrosis in metabolically activated human lymphocytes at concentrations of 2.9 and 580 μg/ml, respectively, after 4 hours of exposure at 37 °C. Bolognesi *et al.* (1997) showed the ability of glyphosate and its formulation Roundup to cause cytogenetic damage in human lymphocytes from concentrations of 100 and 1000 μg/ml, respectively. The cytogenetic damage observed was characterized by significant increases ($P < 0.05$) in sister chromatid exchanges in human lymphocytes after a 72 hour exposure period at 37 °C. Cytogenetic damage assessed using chromosome aberrations tests conducted by Mañas *et al.* (2009a) in human lymphocytes exposed to analytical grade glyphosate (96 %) for 48 hours demonstrated no significant effects at a concentrations ranging between 34 and 1015 μg/ml.

When comparing the white blood cell and whole blood model with respect to determining the toxic potential of pure glyphosate, Ro and Wo, the human whole blood model (Figure 3.3 and Figure 3.4) generally proved to be a more sensitive and a more suitable model for this study. Using whole blood is advantageous in comparison to white blood cells because it is more representative of an *in vivo* system and contains a greater variety of immune cells which are capable of contributing to a response (Duramad *et al.*, 2006). Inflammation reactions are complex and are multicellular, therefore the "cross-talk" and co-stimulation between different immune cells and other cell types in whole blood may also lead to an amplified immune response (Klinger and Jelkmann, 2002; Krakauer, 2002; Mesri and Altieri, 1999).

The toxicity of pure glyphosate, Ro and Wo in human whole blood cells was confirmed with results in Figure 3.3 demonstrating significant reductions in cell viability at varying concentrations. Non-linear regression analysis showed evidence of two different dose-response profiles i.e. an inverted bell shaped (U-shaped, non-monotonic) dose response curve for pure glyphosate and Ro (Figure 3.3 a and 3.3b) together with a linear (monotonic) regression curve for the Wo formulation from a threshold concentration of 50 μg/ml (Figure 3.3c).

Dose-response relationships based on the interaction of a chemical and a biological target are often monotonic and show an increase or decrease in response to the exposure (at increasing or decreasing concentrations) of the specific chemical (Deng *et al.*, 2000) as was the case for the Wo formulation in this study, however several toxicological studies have reported on non-monotonic dose-response relationships (particularly in low dose toxicity studies) which are commonly characterized by an a U, inverted U, J or β shape (Conolly and Lutz, 2004; Vandenberg *et al.*, 2012). Calabrese and Baldwin, (2001) have suggested that non-monotonic responses may be caused or linked by overcompensations in cell systems due to a disruption in homeostasis, which are dependent on the chemical concentrations and their affinity for stimulation or inhibition pathways. Although a promising theory and taking into consideration the scope of this study, this theory cannot be conclusively applied purely on the data obtained for the cytotoxicity of pure glyphosate and the Ro formulation in human whole blood. The results obtained in this study do, however, present a scope for future work in this specific area.

Minor differences (15 %) were observed for the EC50 values describing the inhibitory ($EC50_1$) and stimulation phases ($EC50_2$) of the dose response curves for pure glyphosate ($EC50_1$: 1.3

μg/ml, $EC50_2$: 317.7 μg/ml) and Ro ($EC50_1$: 1.1 μg/ml , $EC50_2$: 269.8 μg/ml) which suggested that both treatments displayed similar inhibitory and stimulatory effects. The calculated EC50 value for the Wo formulation was 7.1 μg/ml, which strongly suggests that Wo exhibited a lower inhibitory effect in human whole blood when compared to pure glyphosate and Ro. A study by Pieniążek *et al.* (2004) confirmed the toxicity of glyphosate and its technical formulation Roundup ULTRA 360 SL through the biochemical dysfunction of key biological parameters in human erythrocytes which corroborate the cell toxicity findings of the present study.These toxic effects were however observed at much higher threshold concentrations than reported in the present study and therefore the overall conclusions of that study was that glyphosate and the Roundup ULTRA 360 SL formulation displayed low toxicity in humans. In summary, after a 1 hour incubation of human erythrocytes with the Roundup formulation increased levels of methemoglobin (a product of hemoglobin oxidation) and lipid peroxidation were observed at 500 μg/ml and hemolysis occurred at 1500 μg/ml. Glyphosate (95 % purity) caused increases in levels of methemoglobin and lipid peroxidation at an exposure concentration of 1000 μg/ml and hemolysis occurred after a 24 hour incubation period at a glyphosate concentration of 1500 μg/ml. Both treatments caused significant increases in catalase activity and overall Roundup incurred slightly greater alterations in the functioning of erythrocytes than its active ingredient glyphosate and it was suggested that this was due to the presence of additives (Pieniążek *et al*., 2004).

With respect to the comparative toxicity of the different herbicidal treatments in the present study, results by Bolognesi *et al.* (1997) are in agreement, with no significant differences reported when comparing the relative toxicities of glyphosate and Roundup in human lymphocytes. However the majority of findings in literature present contrasting results to the present study. Many studies using a variety of different models have indicated that glyphosate formulations show greater toxicity than the active ingredient (Benedetti *et al.,* 2004; Duke *et al.,* 2003). Martinez *et al.* (2007) showed evidence of amplified toxicity of glyphosate in formulation in human peripheral blood mononuclear cells after exposure period of 96 hours. Koller *et al.* (2012) demonstrated that the Roundup formulation showed greater toxicity than glyphosate alone in human-derived buccal epithelial cells exposed to herbicide concentrations between 10 and 20 μg/ml. Findings by Richard *et al.* (2005) in human placental cells exposed to glyphosate and Roundup concentrations between 0.2 and 2% indicated a higher toxicity in formulation. Kim

*et al.* (2013) concluded that the amplification of toxicity was due to synergistic interactions of glyphosate and a common adjuvant found in glyphosate formulations, TN-20 (also known as POEA), after studies conducted in the rat H9C2 (heart cell line) cell line assessing the effects of glyphosate: TN-20 mixtures, as well as glyphosate and TN-20 separately for mitochondrial disruption, apoptosis and necrosis. Studies by Peixoto (2005) in Wistar rat mitochondria presented evidence that glyphosate had no significant effects on mitochondrial bioenergetics at concentrations as high as 2536 μg/ml, however the Roundup formulation indicated significant disruption in mitochondrial bioenergetics with a maximal effect on the mitochondrial transmembrane potential being observed at 1691 μg/ml, which led this study to infer that additives in formulation or synergistic effects between glyphosate and the additives caused the increased toxicity. Similar findings have been demonstrated in non-mammalian models, including Southwestern Australian frogs (Mann and Bidwell, 1999), fish and aquatic invertebrates (Folmar *et al.*, 1979).

Although pure glyphosate did not display a lower toxicity in comparison to the two formulations (Ro and Wo) at the concentrations tested in this study, adjuvants did play a role in cell toxicity in human whole blood as evidenced by the varying toxicities displayed by the two different formulations Ro and Wo. It must be taken into consideration that this was a short term study representing acute exposure (18 hours) and therefore sub-chronic and chronic exposure studies may reveal different comparative toxicological profiles than the initial profiles observed in this study, however this cannot be stated conclusively. The presence of human serum albumin (HSA) in human whole blood may be an important contributing factor to the different toxicities observed between glyphosate and glyphosate formulations. HSA is an important carrier of various substances in human blood including drugs and hormones and the binding of HSA to other molecules has been extensively studied (Nowak and Shaw, 1995). Evidence of the binding capacity of HSA to glyphosate has been confirmed by Yue *et al.* (2008), however no investigations were found at the time of this study relating to the binding of HSA and the additives commonly found in glyphosate based herbicides, primarily the non-ionic surfactant POEA, as it has been the most common adjuvant highlighted as an amplifier of glyphosate toxicity. Future studies in human whole blood should incorporate HSA binding studies with POEA and glyphosate, as it may allow insight into the bioavailability of both compounds to biological targets in human whole blood, more specifically at low dose exposure, and allow for a

greater understanding with respect to comparative toxicity assessments between the active ingredient and technical formulations.

In the pro-inflammatory studies in human whole blood LPS showed no significant induction (as compared to the untreated control) of the cytokines TNF-α, IL-1β and IL-6 (Figure 3.4), although a reduction in cell viability was observed in human whole blood cells (Figure 3.3). Comparisons for cytokine production therefore, were solely based on the untreated control. Reasons for this are unclear as LPS has been documented to stimulate cytokine production in human whole blood at concentrations as low as 50 ng/ml (Jagger *et al.,* 2002). A possible suggestion for future studies is to include varied concentrations above and below the concentration tested in this study, to determine the appropriate concentration of LPS that would induce significant secretions of the cytokines.

Levels of TNF-α, IL-1β and IL-6 were evaluated in human whole blood exposed to varying concentrations (0.1, 0.7, 10 and 50 µg/ml) of pure glyphosate, Ro and Wo as markers of an inflammatory response. Overall, the whole blood model showed greater sensitivity as compared to the white blood cells with respect to the release of pro-inflammatory cytokines. Results of this study (Figure 3.4B) indicated significant increases in the levels TNF-α in whole blood exposed to pure glyphosate (50 µg/ml), Wo (50 µg/ml) Ro (10 and 50 µg/ml). Ro induced TNF-α to a larger extent than pure glyphosate and Wo. Pure glyphosate caused increased levels of IL-1β at concentrations of 0.1, 0.7 and 50 µg/ml (Figure 3.4A). This effect was not demonstrated by Ro and Wo for IL-1β. All of the herbicidal treatments caused significant reductions in the levels of IL-6 at varying concentrations (Figure 3.4C). Studies on the effect of glyphosate and glyphosate formulation on cytokine levels in human whole blood are severely limited. Observations by Nakashima *et al.* (2002) indicated no significant changes in TNF-α and IL-1β production in human peripheral blood mononuclear cells at concentrations which caused significant inhibition of the cells. Gui *et al.* (2012) more recently however demonstrated the neurotoxic effects of glyphosate in rat pheochromocytoma cells (PC12 cells) and demonstrated that exposure to neurotoxic organophosphorous compounds (in rats) could directly cause an increase in the production of pro-inflammatory cytokines (such as TNF-α, IL-1β and IL-6) in the hippocampus, thalamus and piriform cortex (Astiz *et al.,* 2013; Kan *et al.,* 2007). A study by El-Shenawy (2009) concurs with the findings of the present study, with both glyphosate and its formulation

Roundup inducing significant increases in hepatic TNF-α levels (linked to the oxidative stress) in rats exposed to sub-lethal concentrations for 2 weeks. IL-6 showed a significant decrease in all of the herbicidal treatments. This cytokine plays a crucial anti-inflammatory role in acute inflammation and regulates the levels of circulating pro-inflammatory cytokines (in the case of this study, TNF-α and IL-1β) through a negative feedback mechanism (Xing *et al.*, 1998).

The main purpose of this study was to demonstrate the potential of glyphosate and glyphosate formulations to elicit an inflammatory response in humans, and preliminary evidence that pure glyphosate, Ro and Wo induce minor immunomodulatory effects was obtained. However, more substantial evidence would be required to fully understand the underlying role of glyphosate in immunotoxicity before this can be considered a definitive mechanism of toxicity by glyphosate and glyphosate formulations in humans.

### 3.5.2 Cytotoxic and genotoxic properties of glyphosate, Ro and Wo in human cancer cell lines

The effects of pure glyphosate, Ro and Wo on the cell viability in the HEC1A, MCF-7 and MDA-MB-231 cancer cell lines (after a 24 hour exposure period at varying herbicide concentrations (0-500 μg/ml) shown in Figure 3.5) indicate the differential toxicities obtained (depending on the cell type being tested) with the most significant results observed in the HEC1A endometrial cancer cell line, more specifically when this cell line was exposed to pure glyphosate and Wo.

Pure glyphosate caused a significant decrease in cell growth in the HEC1A cell line from 75 μg/ml in a dose-independent manner (Figure 3.5A). The mechanism of glyphosate toxicity in the HEC1A cells may have occurred due to the disruption of the normal functioning of mitochondria, as the effects of toxicity were measured by the MTT assay which uses succinate dehydrogenase found in the mitochondria as a measure of cell metabolism. Some investigators have shown evidence of the mitochondrial disruption capacity of glyphosate and glyphosate based herbicides. Olorunsogo (1979) studied the effects of glyphosate on the energy conservation in rat liver mitochondria (*in vivo*) at a concentration range of 60-120 μg/ml, the results of the study indicated that the uncoupling of mitochondrial oxidation was a major route of

glyphosate toxicity. More recent investigations by Benachour and Seralini (2009) conducted in human umbilical vein endothelial cells (primary neonatal umbilical cord veins), 293 embryonic kidney cell lines and JEG3 placental cell lines on the cell death mechanisms of glyphosate and glyphosate formulation exposure at concentrations from 1 μg/ml demonstrated the induction of apoptosis in these different cells when exposed to glyphosate alone. However, when in formulation, the initial toxicity of glyphosate was amplified, resulting in the inhibition of succinate dehydrogenase activity. The evidence presented by Benachour and Seralini (2009) is in contrast to the present findings of this study with respect to the Ro formulation. The three cancer cell lines chosen for the present study demonstrated extremely low sensitivity (no significant cytotoxic effects were observed) to the Ro formulation (Figure 3.5B) at the concentrations examined, however other studies have suggested a similar mechanism of cytotoxicity for Roundup to that observed by Benchour and Seralini (2009) in different cell models. *In vitro* studies by Gasnier *et al.* (2010) in human hepatic cell lines HepG2 and Hep3B exposed to 25 μg/ml of different Roundup formulations demonstrated the mechanism of cell toxicity via the inhibition of mitochondrial succinate dehydrogenase.

The Wo formulation caused dose-independent proliferative effects in the HEC1A (Figure 3.5C) cells at 75, 125 and 250 μg/ml. Similar findings were reported by Lin and Garry (2000) with proliferative effects observed in the MCF-7 cancer cell line following herbicidal treatments with glyphosate (2.28 μg/ml) and Roundup (10 μg/ml). The contrasting cytotoxic profiles observed for pure glyphosate and the Wo formulation strongly suggest that the proliferative effects observed were possibly due to the additives present in formulation. Cell cycle disruption and uncontrolled cell proliferation is an integral component of tumor formation and cancer (Sherr, 1996). Findings by Marc *et al.* (2004), using a sea urchin early developmental model, demonstrated the cell cycle disruptive capacity of five different glyphosate formulations at a threshold adverse concentration (glyphosate within the formulation) of 1.7 μg/ml.

The genotoxic potential of pure glyphosate, Ro and Wo was determined at a test concentration of 500 μg/ml and reference concentrations (based on the report by Gasnier *et al.*, 2009) of 800 and 1000 μg/ml in the HEC1A, MCF-7 and MDA-MB-231 cancer cell lines. DNA damage was evaluated by tail length (μm) and olive tail moment (arbitrary units) (Figure 3.7). Pure glyphosate, Ro and Wo induced significant comet formation in the HEC1A cells and similar

findings were observed for the MDA-MB-231 with significant DNA damage occurring at the test concentration in all herbicidal treatments. Comparatively, MDA-MB-231 showed a lower ($P \leq 0.001$) sensitivity to pure glyphosate, Ro and Wo than the HEC1A cells, based on extent of genotoxic damage observed. This may be explained by several factors such as the presence/absence of ER receptors and the presence and variety of co-factors/co-regulators which may directly or indirectly affect the binding capacity and bioavailability of a particular ligand (Vandenberg *et al.,* 2012).

Although significant DNA damage was observed in the MDA-MB-231 cell line no significant effects were observed in the Wo formulation at the reference concentration of 800 μg/ml (Figure 3.7C). The exact reason for this remains uncertain, but there has been some evidence of confounding results in the Comet assay caused by high cytotoxicity and this effect is cell type specific (Hartmann *et al.,* 2003). For example, Frei *et al.* (2001) indicated that a reduction in the cell viability of rat hepatocytes did not incur differences in tail length measurements.

To the best of our knowledge, no reports have examined the effects of pure glyphosate and its formulations in the HEC1A cell line, and based on the results of this study, this cell line has proven to be a sensitive model for investigating both cytotoxic and genotoxic potential of glyphosate and glyphosate-based herbicides. Although further studies are required to fully understand the underlying mechanism of toxicity of glyphosate in HEC1A cells, it may possibly be linked to the modulation of the ER receptors (ERα and ERβ) present in this cell line. The estrogen receptor belongs to the nuclear receptor superfamily and functions as a ligand-dependent transcriptional factor for the regulation of estrogen signaling (Lin *et al.,* 2009). Estrogens are important regulators of the growth and differentiation of several tissues, (e.g. the uterus, mammary glands and ovaries) (Rao *et al.,* 2011). The dysregulation of estrogen is the hallmark in breast and endometrium cancers, often causing uncontrollable cell proliferation (Rao *et al.,* 2011). Some pesticides have demonstrated endocrine disruptive capacities and act as xenoestrogens, which can bind to human ER α and ER β receptors (ER receptors mediate endogenous steroid hormones (e.g. 17-β estradiol is a regulator of the growth and development of female reproductive hormones) and exert estrogenic responses (Adams *et al.,* 2007; Lemaire *et al.,* 2006). Future studies should involve fully characterizing the interactions of glyphosate with the ER α and ER β receptors in HEC1A to determine their endocrine modulating potential.

Studies focusing on the endocrine disruption potential of glyphosate and glyphosate formulations have confirmed the ability of glyphosate and glyphosate formulations to exhibit xenoestrogenic behavior (George and Shukla, 2011). Gasnier *et al.* (2009) evidenced the endocrine disruptive capacity of glyphosate and four Roundup formulations in the HepG2 liver cell line and the androgen receptor positive MDA-MB-231-MB435-kb2 breast cancer cell line at low concentrations with endocrine effects being observed within a 24 exposure period. Thongprakaisang *et al.* (2013) reported the proliferative effects displayed by glyphosate at low dose exposure in the hormone dependent T47D breast cancer cell line.

The MDA-MB-231 breast cancer cell line is defined as a hormone independent cell line which expresses extremely low or no levels of ER α and ER β receptors and is characterized by estrogen-independent proliferation (Adams *et al.,* 2007; Wang and Kilgore, 2002). The genotoxic effects displayed by pure glyphosate, Ro and Wo on the MDA-MB-231 breast cancer cell line have not been demonstrated in this cell line, in glyphosate focused studies and, suggests that glyphosate and its formulations may incur cell damage through mechanisms that are non-estrogenic as well. Studies by Ventura *et al.* (2012) confirmed the non-estrogenic mechanisms (G2/M arrest) of the organophosphorous pesticide chlorpyrifos, which was commonly defined as an endocrine disruptor in the ER negative MDA-MB-231 breast cancer cell line. The mechanism proposed involved the binding of chlorpyrifos to tubulin sites, ultimately altering microtubule formation. Although most studies have not shown evidence of the significant effects of glyphosate in this cell line (Buteau-Lozano *et al.,* 2008; Thonprakaisang *et al.,* 2013) the primary research focus using this cell line is based on determining estrogenic effects and therefore experimental designs for these studies will generally not explore other mechanisms.

In the genotoxic study pure glyphosate and the Ro formulation showed greater genotoxicity ($P \leq 0.001$) than the Wo formulation in the HEC1A cell line. All herbicidal treatments did not display statistically different genotoxic effects in the MDA-MB-231 cell line. Relatively similar results were observed in the human whole blood study, with respect to the differential toxicities of pure glyphosate and glyphosate formulations. As stated previously, this was an acute study and longer exposure periods may result in larger differences in the toxicological profiles for pure glyphosate as compared to Ro and Wo.

Surprisingly, pure glyphosate and the two formulations Ro and Wo, did not exhibit significant genotoxic effects in the MCF-7 breast cancer cell line (which is also ER positive), based on the results observed under the experimental conditions selected for this study (Figure 3.7). Although previous studies have indicated the endocrine disruptive ability of glyphosate and glyphosate-based herbicides in this cell line (Hokanson *et al.*, 2007; Kojima *et al.*, 2004), the results of this study suggests that hormone regulation in breast cancer and endometrial cancer cells is far more complex and is highly dependent and strongly influenced by the cell type (Stoner *et al.*, 2004).

## 3.6 Conclusions

- The human whole blood system proved a more sensitive model in comparison to isolated human white blood cells for cytotoxicity and pro-inflammatory studies.
- Pure glyphosate, Ro and Wo demonstrated cytotoxic effects at low to moderate dose exposure in human blood cells, with two distinct toxicological profiles (inverted bell shape and linear) being observed.
- Adjuvants present in formulation played a role in glyphosate toxicity as evidenced by the different toxicologies observed in Ro and Wo, in human whole blood and the HEC1A cancer cells.
- Preliminary evidence suggested that pure glyphosate at its formulations (Ro and Wo) incured immunotoxicity effects, however further studies are required to confirm immunomodulation as a mechanism of toxicity.
- Cytotoxic effects of pure glyphosate, Ro and Wo vary depending on the cell type with the most significant results observed in the HEC1A cancer cell line exposed to pure glyphosate (reduction in cell viability) and Wo (proliferation of cancer cells).
- The carcinogenetic potential of glyphosate was confirmed at moderate dose exposure levels for pure glyphosate and its formulations in the ER-positive HEC1A cancer cell line and the ER-negative MDA-MB-231 cancer cell line.

In summary, this study confirmed the toxicity of glyphosate and glyphosate-based herbicides in humans, more specifically at levels representative of occupational and residential exposure. This is an important validation for the development of a chemical sensor for glyphosate detection. The

following Chapter looks at the scale-down, optimization and characterization of a glyphosate spectrophotometric detection system, which served as the basis for sensor development.

# CHAPTER 4- OPTIMIZATION, SCALE-DOWN, AND PARTIAL VALIDATION OF A GLYPHOSATE SPECTROPHOTOMETRIC ASSAY (FREE SYSTEM)

## 4.1 Introduction

A colorimetric spectrophotometric glyphosate detection assay was selected as the foundation for chemical sensor design and development, due to several advantageous characteristics (i.e. this method allows for the optical/naked eye detection of a specific analyte, is cost-effective and simpler than most analytical techniques reported for glyphosate detection) which when combined, allows for greater applicability towards the development of a solid state sensor. The colorimetric assay used in this study for the determination of glyphosate was based on the method reported by Jan *et al.* (2009). A schematic representation of the principle reaction is shown in Figure 4.1. A glyphosate dithiocarbamate intermediate is formed *in situ* by the substitution of the hydrogen atom on the secondary amide nitrogen of glyphosate with the electrophillic carbon atom of the carbon disulfide resulting in a glyphosate dithiocarbamate ligand, followed by the addition of copper for the formation of a yellow colored complex, which could be detected at 435 nm.

The critical step in this reaction was the derivatization of glyphosate for the formation of a dithiocarbamate intermediate. Derivatization is a modification procedure which provides suitable characteristics for an analyte of interest to improve its detectability (Zhang *et al.,* 2008). Considering that glyphosate is an amino compound (and therefore lacks a UV chromophore) the derivatization step was an important requirement to enable glyphosate metal complex formation and subsequent detection using UV-Vis spectrophotometry (Freuze *et al.,* 2007; Wycherley *et al.,* 1996). *In situ* derivatization is a simple process whereby an analyte of interest is incubated together with a derivatization reagent at sufficient quantities resulting in the formation of a derivatized product (Boyd-Boland *et al.,* 1994).

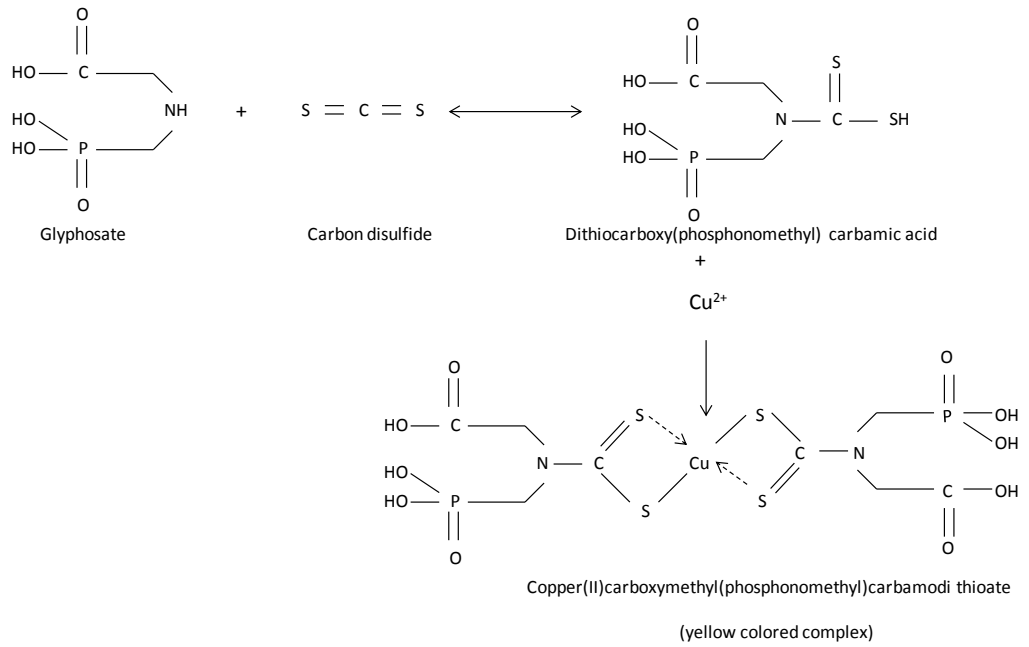


**Figure 4.1:** The principle reaction for the formation of the glyphosate dithiocarbamate-copper complex. (This image was adapted from Jan *et al.,* 2009).

Dithiocarbamates are sulfur containing ligands, the majority of which display a high affinity to transition metals (McClain and Hseih, 2004) and the use of carbon disulfide (solvent) for the production of various dithiocarbamates has been well established (Crnogorac and Schwack, 2009; Fogalia *et al.*, 1971; Grand and Tamres, 1968; Laintz *et al.*, 1992; Verma *et al.*, 1986). Dithiocarbamates have several applications in many different areas including trace metal detection in environmental samples (Elder *et al.*, 1975; Emteborg *et al.*, 1995; Yebra-Biurrun *et al.*, 1991), organic synthesis (Grainger and Innocenti, 2007), drug discovery (Anderson, 1999; Aryanpour *et al.*, 2012; Tandon *et al.*, 1996) and in the industrial production of synthetic materials (e.g. dithiocarbamates are used in the vulcanization of rubber) (Nieuwenhuizen *et al.*, 1999). The work conducted by Jan *et al.* (2009) demonstrated the ability of dithiocarbamates to form metal complexes for the determination of glyphosate soil, wheat and water samples.

The main aims of this study were to scale down, optimize and partially validate the spectrophotometric detection method reported by Jan *et al.* (2009), for the purposes of improving its applicability (the principle assay uses large sample volumes) towards the development of a

chemical sensor. The optimized conditions of the scale-down method would be used as a starting point for glyphosate sensor detection and data obtained in the partial validation of the system would allow for comparative analysis between the scale-down system and the chemical sensor.

## 4.2 Objectives

- To confirm the detection of glyphosate using the principle method reported by Jan *et al.* (2009) with a proof-of-concept study. The determination of glyphosate complex formation was carried out using spectrophotometric and visual analysis.
- To scale-down the principle method and optimize the scale-down system with respect to reagent concentration, pH and time.
- To determine the stoichiometric molar ratio of the glyphosate-copper complex and the optical characteristics (molar absorptivity and stability constant) of the system using Jobs Method of Continuous Variation.
- To determine the specificity, sensitivity (calibration characteristics) and precision (for pure glyphosate and glyphosate in formulation) of this system.
- A study was also conducted to determine the optimal storage conditions and storage time for glyphosate stock solutions.

## 4.3 Methods and materials

### 4.3.1 Materials

Please refer to the chemical list in Appendix I for all the materials and chemical suppliers used in this study. All glyphosate stocks were prepared freshly (refer to Chapter 3, Section 3.3.1) before any experimental studies and all experiments were conducted at room temperature (22 ± 2°C) unless stated otherwise.

### 4.3.2 Proof-of-concept study

All reactions were carried out in 100 ml separating funnels. Based on the method described by Jan *et al.* (2009), reactions containing 5 ml of carbon disulfide (1 % $CS_2$ in chloroform) and 2 ml of glyphosate solution (20 µg/ml in distilled water) were prepared and shaken for a few seconds to allow the formation of the dithiocarbamate ligand. This was followed by the addition of 1 ml ammonical copper (II) solution formed from copper nitrate salt (0.413 mM in 2 M ammonia solution), which was shaken for 3 minutes and allowed to stand at 24 °C. The resultant two layers were observed for color formation over a total period of 6 hours. The formation of a glyphosate dithiocarbamate-copper complex was assessed using spectral scan analysis (200-500 nm) in a $Powerwave_x$ spectrophotometer with KC junior software. Macroscopic images were obtained for visual analysis of glyphosate-complex formation using a SONY cyber-shot digital camera. This study was conducted in duplicate.

### 4.3.3 Scale-down assay for glyphosate determination

Scale-down experiments were conducted according the reaction principle outlined by Jan *et al.* (2009). However, modifications to the original protocol involved scaling down the total assay from 8 ml to 1 ml. The volume to volume ratio of glyphosate: carbon disulfide: copper was maintained at 2.5: 1: 5 and the concentration of glyphosate used was 1000 µg/ml (equivalent to a 50-fold increase when compared to the original concentration used in the proof of concept study). Six hundred and twenty five (625) µl of carbon disulfide (1 %) was added to 250 µl of glyphosate and shaken for a few seconds to allow the formation of the glyphosate dithiocarbamate intermediate. Ammonical copper (0.413 mM, 125 µl) was added and shaken for 3 minutes and allowed to stand at 24 °C. The resultant two layers were observed for color formation over a total period of 6 hours. The formation of a glyphosate dithiocarbamate-copper complex was assessed using spectral scan analysis (200-500 nm) in a $Powerwave_x$ spectrophotometer with KC junior software. Glyphosate, copper and carbon disulfide negative controls were included in this study. The negative controls used in this study were included in all subsequent experiments.

### 4.3.4 Optimization studies

The scale-down detection method was optimized with respect to reagent concentrations (copper and carbon disulfide), pH and assay time. The effect of copper and carbon disulfide concentrations on the detection of glyphosate was evaluated at concentrations ranging from 0-8 mM and 0-7 %, respectively. The effect of pH was determined at a range of 5-12 and the effect of reaction time was investigated over 540 minutes. Glyphosate complex formation was detected spectrophotometrically using a $Powerwave_x$ spectrophotometer with KC junior software. All future studies were conducted under the selected optimized conditions.

### 4.3.5 Jobs Method of Continuous Variation

Jobs Method of Continuous Variation was used to determine the stoichiometric molar ratio of the glyphosate dithiocarbamate intermediate and copper complex (Bosque-Sendra *et al.,* 2003). This method was based on the preparation of a series of solutions in which the total molar concentration was kept constant, while the volume fraction of the ligand (glyphosate dithiocarbamate) was varied from 0 to 1. A Jobs plot of maximum absorbance (corrected for uncomplexed copper and glyphosate) versus the volume fraction was constructed. The concentration ratios of glyphosate and copper used in the study were factored into the initial volume fraction obtained to determine the molar ratio. The maximum absorbance observed from the experimental data is indicative of the actual amount of equilibrated glyphosate-copper complex. Linear regression analysis was used to derive the theoretical maximum (H). The theoretical maximum is the point at which the two linear regression curves intersect and assumes 100 % complex formation.

The Jobs plot was used to determine equation (1): the molar absorptivity (ε, L/mol/cm) and equation (2): the stability constant ($K_f$) of the scale down glyphosate detection method.

$$\varepsilon l = H/[C] \quad (1)$$

where $\varepsilon$ is the molar absorptivity, $l$ is the path length, $H$ (derived as an average from the two linear regression equations) is the theoretical maximum absorbance and $C$ is the total concentration of copper (M)

$K_f = [complex]/ [Cu] [glyphosate]$ (2)

where $K_f$ is the stability constant, *[complex]* is the concentration (M) of the complex (derived from the Beer Lamberts law $H = \varepsilon[complex]l$, which assumes that the calculated molar absorptivity of the system is directly proportional to the concentration of the complex), *[Cu]* and *[glyphosate]* are the concentrations (in M) of the free species.

Results were determined at 435 nm using a Powerwave$_x$ spectrophotometer with KC junior software.

### 4.3.6 Scale-down detection system specificity

The specificity of the scale-down method was investigated by evaluating the detection of two glyphosate structural analogs, more specifically the primary metabolite of glyphosate degradation, aminomethylphosphonic acid (AMPA), and glycine, which is also a product of the glyphosate microbial degradation pathway. Equivalent concentrations were used in this study (1000 µg/ml) and glyphosate complex formation was assessed using spectral analysis (200-500 nm) and spectrophotometric determination at 435 nm using a Powerwave$_x$ spectrophotometer with KC junior software.

### 4.3.7 Glyphosate standard curve

Standard curves for pure glyphosate (0.1-1000 µg/ml), and glyphosate in the formulations Ro and Wo (50-760 000 µg/ml) were constructed and the calibration curves were used to determine system sensitivity: limit of detection (LOD, µg/ml), limit of quantification (LOQ, µg/ml) and precision (relative standard deviation, % RSD), together with other calibration characteristics of the system (correlation coefficient or $R^2$, intercept and slope).

The LOD and LOQ were determined (using the computer package Microsoft Excel) according to the following equations (Afkami *et al.*, 2006; Keyvanford and Karamian, 2009):

$y(\text{LOD}) = y\text{B} + 3\text{SB}$ (3)

$$LOD = (yLOD - yB)/m \quad (4)$$

where y(LOD) is signal for limit of detection, LOD is the limit of detection, *y*B is the intercept, 3SB is 3 times the standard error of the regression curve and *m* is the gradient of the regression curve.

$$y(LOQ) = yB + 10SB \quad (4)$$

$$LOQ = (yLOQ - yB)/m \quad (5)$$

where *y*LOQ is signal for limit of quantification, LOQ is the limit of quantification, *y*B is the intercept, 10SB is 10 times the standard error of the regression curve and *m* is the gradient of the regression curve.

The RSD was calculated according to the following equation:

$$\% RSD = (SD/m) \times 100 \quad (6)$$

where *RSD* is the relative standard deviation, *SD* is the standard deviation of the data set and *m* is the mean.

### 4.3.8 The stability of glyphosate stocks in water

The stability of glyphosate stock solutions under varying conditions was evaluated to determine the best storage conditions and maximum storage time allowed before experimental analysis, in an attempt to conserve reagent use in future studies. Mid-range glyphosate concentrations were selected for this study. Pure glyphosate (0.65 mg/ml), Ro (670 mg/ml) and Wo (610 mg/ml) stocks were prepared in distilled water and stored under light conditions at 23°C, and dark conditions at 23 °C and 4 °C. Samples (2 ml) were removed at regular time intervals over a period of 42 days and assayed for glyphosate. Glyphosate was detected spectrophotometrically at 435 nm using a Powerwave$_x$ spectrophotometer with KC junior software.

### 4.3.9 Data analysis

All data were presented as mean values ± SD (n=3) unless stated otherwise. Where appropriate, ANOVA single factor analysis (Microsoft Excel) was used to determine significant differences with 95 % ($P \leq 0.05$) or 99 % ($P \leq 0.01$) confidence. RSD (%) values below 20 % were considered acceptable (Dos Santos *et al.*, 2013).

## 4.4 Results

### 4.4.1 Proof-of-concept study

The detection of pure glyphosate (based on the spectrophotometric method described by Jan *et al.* (2009)) is shown in Figure 4.2.

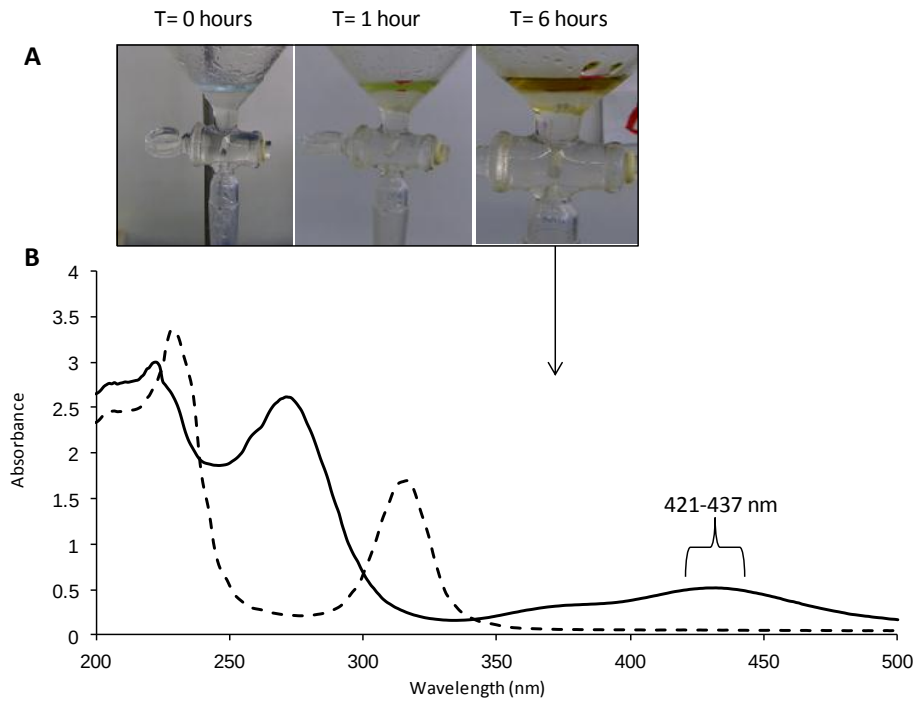


**Figure 4.2:** Macroscopic images of glyphosate complex formation and color development at time: 0, 1 and 6 hours **(A)** at a total assay volume of 8 ml and spectral scans (200-500 nm) of the two resultant layers **(B)** (at the 6 hour time point). The dash line represents the chloroform layer and the solid line represents the glyphosate complex layer. Macroscopic images were obtained using a SONY Cyber-shot digital camera. Although this study was conducted in duplicate, the macroscopic image shown is representative of a typical reaction.

The proof of concept study successfully confirmed the formation of a yellow colored glyphosate-complex with results showing the development of color (from blue to yellow) (Figure 4.2A) within 1 hour, after the incubation of the glyphosate dithiocarbamate intermediate (1000 µg/ml) with ammonical copper (0.413 mM). The color intensity increased over a 6 hour incubation period (from yellow to yellow-brown). Spectral scans (200-500 nm) of glyphosate complex layer (Figure 4.2B) indicated a peak between 421 and 437 nm and the chloroform layer showed two characteristic peaks at approximately 229 and 316 nm, with no interfering peaks observed within

the glyphosate complex detection range. A peak was also observed in the glyphosate complex sample between 250 and 300 nm.

### 4.4.2 Scale-down of the glyphosate spectrophotometric detection system

The results of the scale-down study for the detection of pure glyphosate are presented in Figure 4.3. The main reasons for scaling down this assay was to allow for the ease of assay preparations, particularly when sample sizes were large, to reduce the cost of reagents (less required) used and to reduce the waste generation. Ultimately these factors are important and would facilitate the applicability of this assay to the development of a chemical sensor.

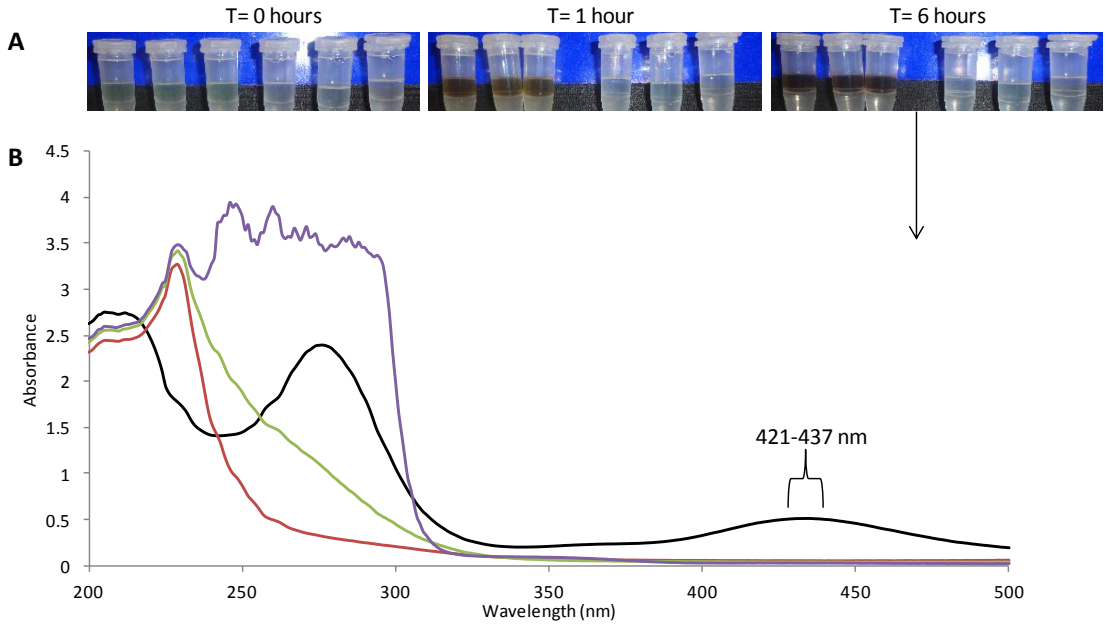


**Figure 4.3:** Macroscopic images of glyphosate complex formation and color development (n= 3) at time: 0, 1 and 6 hours with the corresponding negative controls **(A)** at a total assay volume of 1 ml and spectral scans (200-500 nm) of the glyphosate complex/ammonia layer and the appropriate controls **(B)**. Black line: glyphosate complex layer, red line: glyphosate control, green line: carbon disulfide control, purple line: copper nitrate control. Macroscopic images were obtained using a SONY Cyber-shot digital camera. All experiments were conducted at 22 ± 2 °C.

The scale-down of the glyphosate detection system was successful and comparable to the findings in the proof of concept study (Figure 4.2). Clear color development (from blue to yellow-brown) was observed in the glyphosate complex layer within 1 hour (Figure 4.3A) and spectral scans (200-500 nm) of the glyphosate complex layer indicated a peak between 421 and 437 nm (Figure 4.3B). The negative controls used in this study demonstrated no interfering peaks within the glyphosate detection range, therefore 435 nm was the wavelength selected for future studies.

### 4.4.3 Optimization study (reagent concentration and pH)

The effect of reagent concentrations (carbon disulfide and copper nitrate), pH and time on glyphosate determination were investigated (Figure 4.4), in order to determine the optimal parameters for the scale-down system.

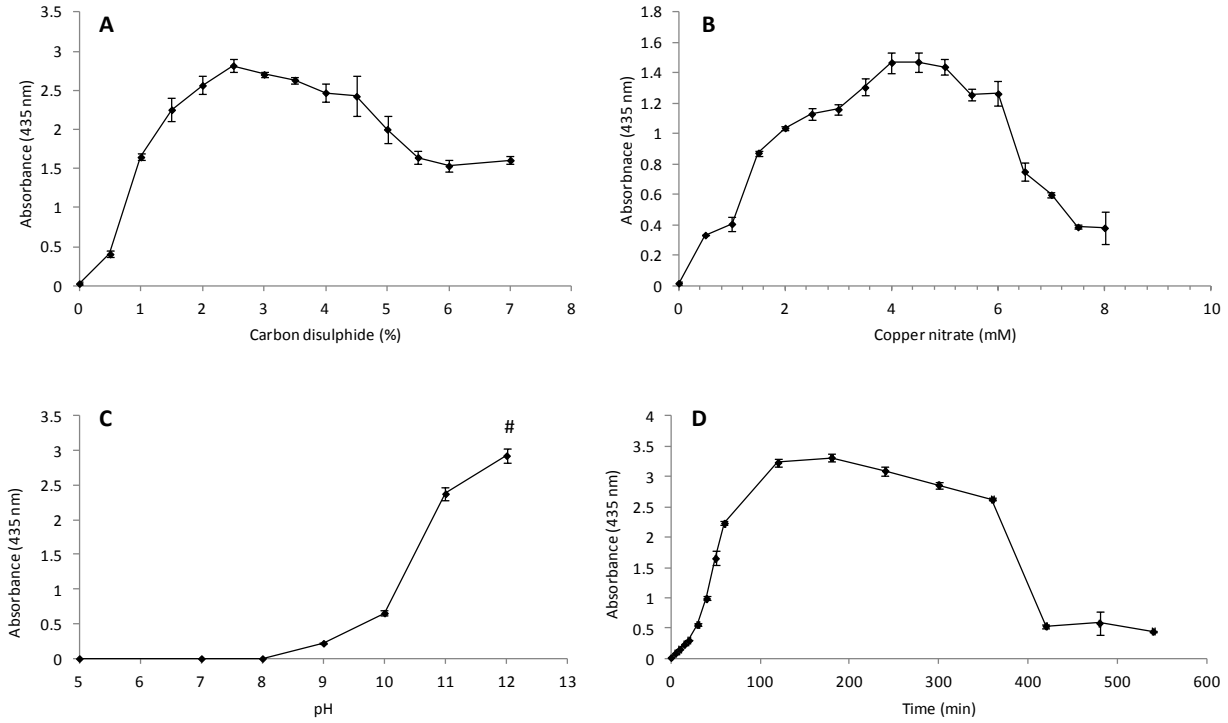


**Figure 4.4:** The optimization curves for the scaled-down glyphosate detection system (total assay volume: 1 ml) with respect to **A:** carbon disulfide (%), **B:** copper nitrate (mM), **C:** pH and **D:** time. Data points represent mean values ± SD (n= 3) and ANOVA single factor analysis was used to determine significance: $^{\#}P \leq 0.01$. Appropriate controls were included in this study. All experiments were conducted at 22 ± 2 °C (room temperature).

The effect of carbon disulfide (%) on glyphosate complex formation (Figure 4.4A) was characterized by an initial increase in absorbance values with increasing concentrations of carbon disulfide. The optimum was observed at carbon disulfide concentrations of 2% (2.6 ± 0.10), 2.5% (2.8 ± 0.08) and 3% (2.7 ± 0.03). The peak values obtained were statistically similar ($P > 0.05$), therefore the optimum carbon disulfide concentration selected was 2.5 %. Higher concentrations of carbon disulfide (from 4.5 %) resulted in a gradual decrease in absorbance. The effect of copper on glyphosate complex formation (Figure 4.4B) resulted in a relatively similar profile, whereby an increase in the initial concentrations of copper led to increased absorbance

values. The optimal values obtained were at copper nitrate concentrations of 4 (1.5 ± 0.07), 4.5 (1.53 ± 0.06) and 5 mM (1.48 ± 0.05). Considering these values demonstrated no statistical difference ($P > 0.05$), the middle concentration of 4.5 mM was selected as the optimum. A decreasing trend was observed above copper nitrate concentrations of 6 mM.

The pH profile (Figure 4.4C) obtained indicated the highest absorbance value at pH 12 (2.96 ± 0.11) suggesting that glyphosate complex formation occurred optimally under highly alkaline conditions, with pH values ranging from 5-8 showing negligible glyphosate detection. pH values above 12 were not investigated in this study. pH conditions beyond 12 were considered too extreme and may limit the practical applicability of the assay towards the development of a chemical sensor.

The effect of reaction time (t) on glyphosate complex formation (Figure 4.4D) was evaluated from t= 0 to 540 minutes (9 hours). A gradual increase was observed from t= 5 minutes (0.09 ± 0.01) to 60 minutes (2.23 ± 0.03), with maximum absorbance values at t= 120 minutes (3.23 ± 0.06) and 180 minutes (3.31 ± 0.06). An 80 % reduction in absorbance values was observed between t= 360 and 420 minutes. Although the optimal times for the detection system were 120 minutes (2 hours) and 180 minutes (3 hours), the values obtained showed statistical similarity ($P> 0.05$) and therefore the shorter time period of 2 hours was selected for future experiments.

### 4.4.4 Jobs Method of Continuous Variation

Jobs method of continuous variation was used to determine the stoichiometric ratio of binding between glyphosate and copper (Figure 4.5). The molar absorptivity (ε) and stability constant ($K_f$) of the glyphosate detection system was calculated using the Jobs plot and the values are presented in Table 4.2.

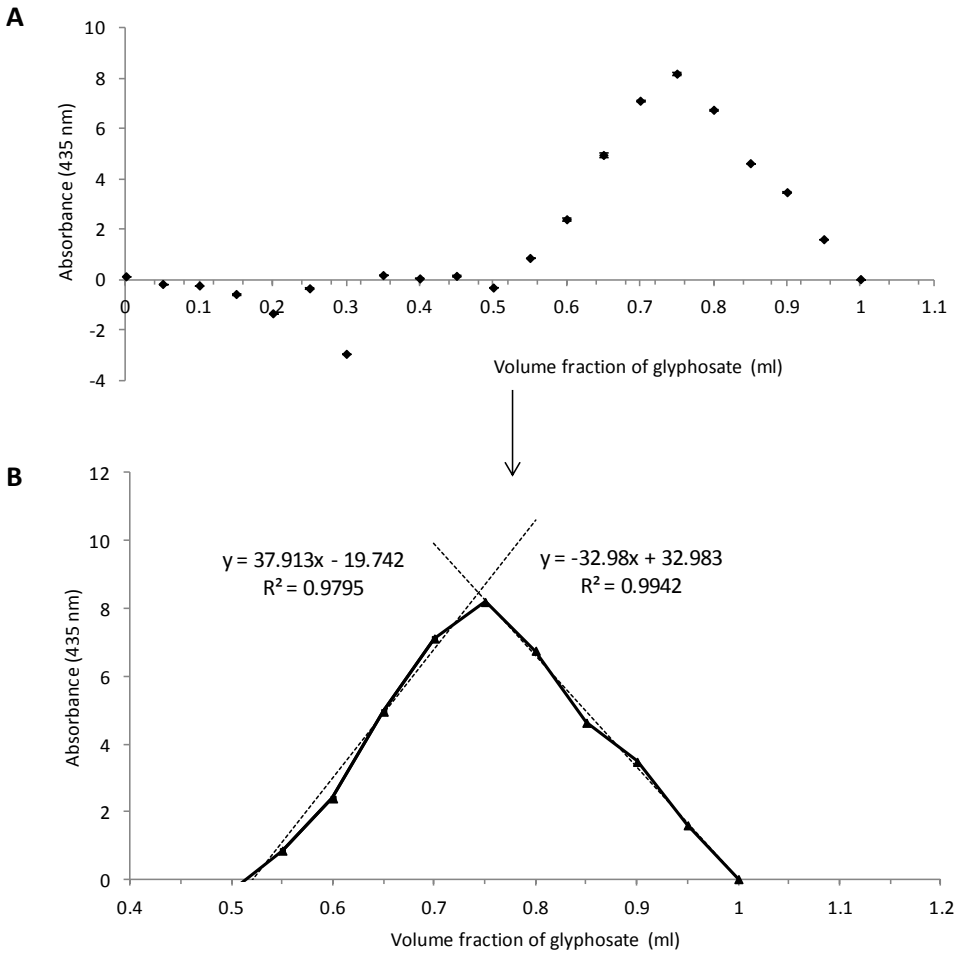


**Figure 4.5:** The stoichiometry of glyphosate complex formation with copper assessed by Jobs Method of Continuous Variation. The data indicates volume fraction values of glyphosate from **A:** 0-1 and from **B:** 0.5-1. Data points represent mean values ± SD (n= 3). Solid line: experimental data, Dash lines: Theoretical extrapolation of the experimental data using linear regression analysis. Appropriate controls were used in this study.

The bell-shaped curve representative of the Jobs plot was only observed from a glyphosate: copper volume fraction of 0.5 (Figure 4.5A). Results from Figure 4.5B indicate an experimental volume fraction of 0.75 and therefore a glyphosate: copper volume ratio of 4:3 or 1.3:1. The stoichiometric molar ratio was determined by factoring in the concentrations of glyphosate (5.9 mM equivalent to 1000 µg/ml) and copper (4.5 mM) used in this study, i.e. the glyphosate

concentration used was 1.31 times greater than the copper concentration and thus the results demonstrated a glyphosate: copper complex molar ratio of approximately 2:1 (calculated value 1.7:1). The theoretical volume fraction of 0.74 (calculated using the linear regression equations) and a molar ratio of approximately 2:1 (calculated value 1.8:1) for the glyphosate-copper complex validated the accuracy of the experimental results obtained.

**Table 4.1:** The optical characteristics molar absorptivity ($Lmol^{-1}.cm^{-1}$) and stability constant ($K_f$) determined for the scaled-down spectrophotometric glyphosate detection system.

| Optical characteristics | Value | Reported value Jan *et al.* (2009) |
|---|---|---|
| E | $1.866 \times 10^3$ | $1.864 \times 10^3$ |
| $K_f$ | $1.69 \times 10^2$ | $1.06 \times 10^5$ |

ε: Molar absorptivity ($Lmol^{-1}.cm^{-1}$), $K_f$: Stability constant

The molar absorptivity ($1.866 \times 10^3$ L/mol/cm) obtained for the scale down system was found to be comparable to the value reported ($1.864 \times 10^3$ $Lmol^{-1}.cm^{-1}$) by Jan *et al.* (2009). The stability constant determined for the scale-down system was approximately 600-fold lower ($1.69 \times 10^2$) than the value ($1.06 \times 10^5$) reported by Jan *et al.* (2009).

### 4.4.5 Glyphosate detection system specificity

The specificity of the glyphosate detection system was investigated by determining the detection of the glyphosate structural analogs AMPA (1000 µg/ml) and glycine (1000 µg/ml) (Figure 4.6).

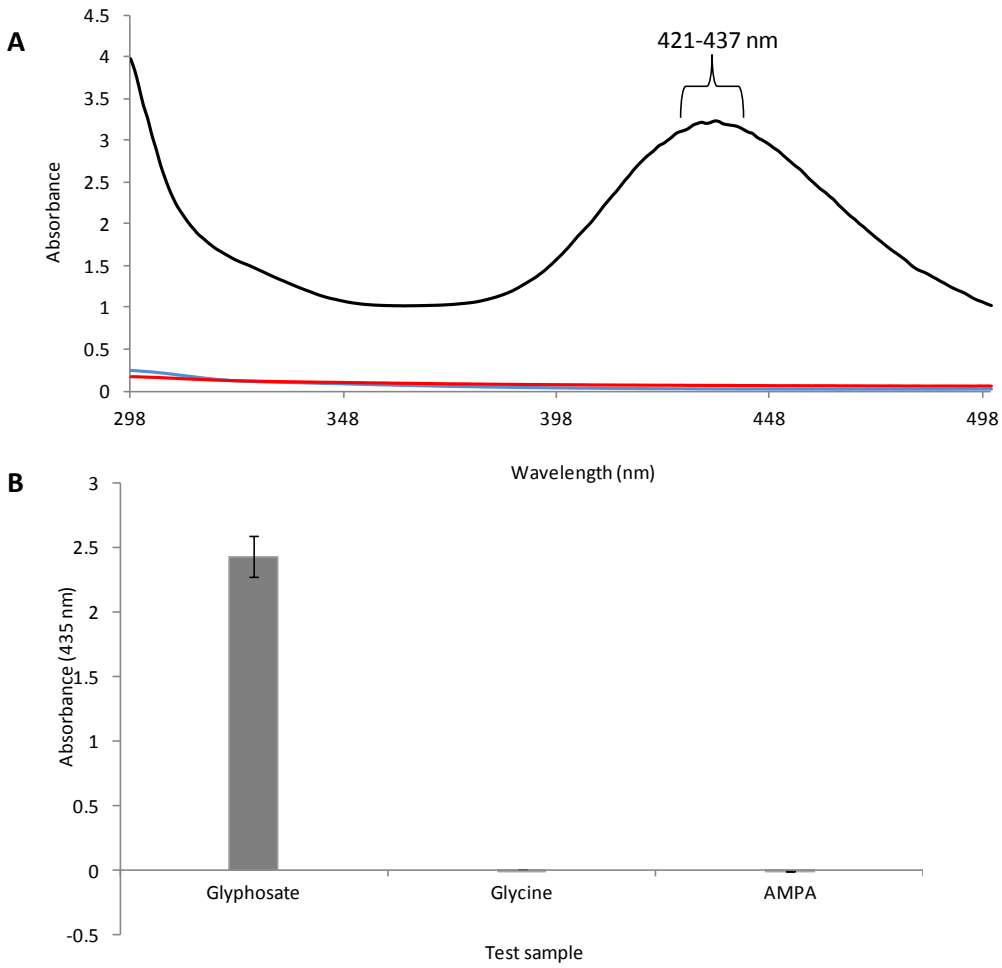


**Figure 4.6:** Glyphosate detection system specificity evaluated by the detection of glyphosate structural analogs glycine and AMPA. **A:** Spectral (298-500 nm) analysis of glyphosate (black ), glycine (blue) and AMPA (red). **B:** Spectrophotometric detection (435 nm). Data points represent mean values ± SD (n= 3). Appropriate controls were used in this study.

Results shown in Figure 4.6 suggest that this detection system was very specific for the detection of glyphosate (2.45 ± 1.6) with a reduction of 98.8 and 97.5 % in absorbance being observed for glycine (0.031 ± 0.001) and AMPA (0.06 ± 0.0003), respectively (Figure 4.6B). Spectral scans (298-500 nm) analysis showed no evident peaks (for AMPA and glycine) in the detection range for the glyphosate complex (421-437 nm) (Figure 4.6A). Overall, the detection system displayed

very good specificity for glyphosate with negligible detection of the two glyphosate structural analogs being observed.

### 4.4.6 Glyphosate calibration curve and the application of the scale-down method to glyphosate formulations Wo and Ro

The calibration curve (0.1-1000 μg/ml) obtained for pure glyphosate is shown in Figure 4.7. The scale down system was applied to the two glyphosate formulations selected for this study, Wo and Ro and calibration curves were also constructed. Results are shown in Figure 4.8. Table 4.2 summarizes the calibration characteristics of the scale down method for pure glyphosate and the glyphosate formulations.

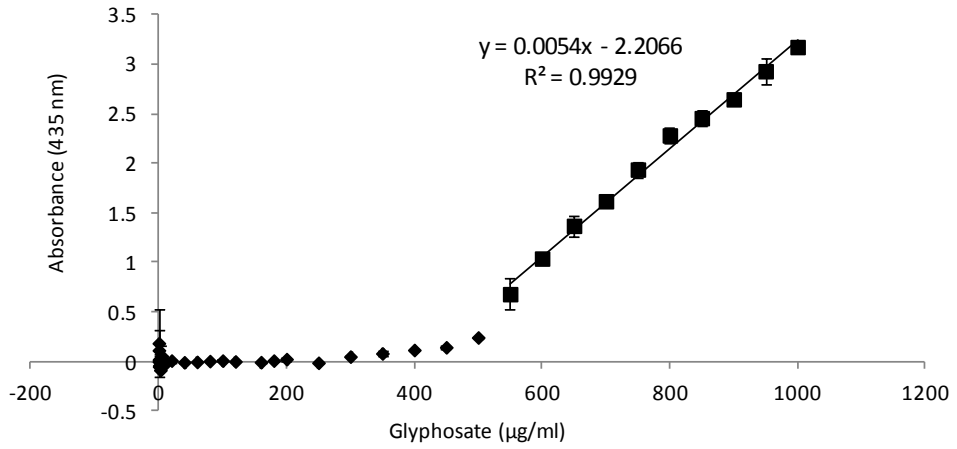


**Figure 4.7:** Standard curve for glyphosate (0-1000 μg/ml). Data points represent mean values ± SD (n= 3). Appropriate controls were included in this study.

The pure glyphosate calibration curve obtained was not rectilinear but demonstrated a slight sigmoidal profile (Figure 4.7). No detectable levels of the glyphosate complex were observed at lower concentrations ranging between 0.1 and 350 μg/ml. The linear range of this curve was observed between 550-1000 μg/ml ($R^2$= 0.9929).

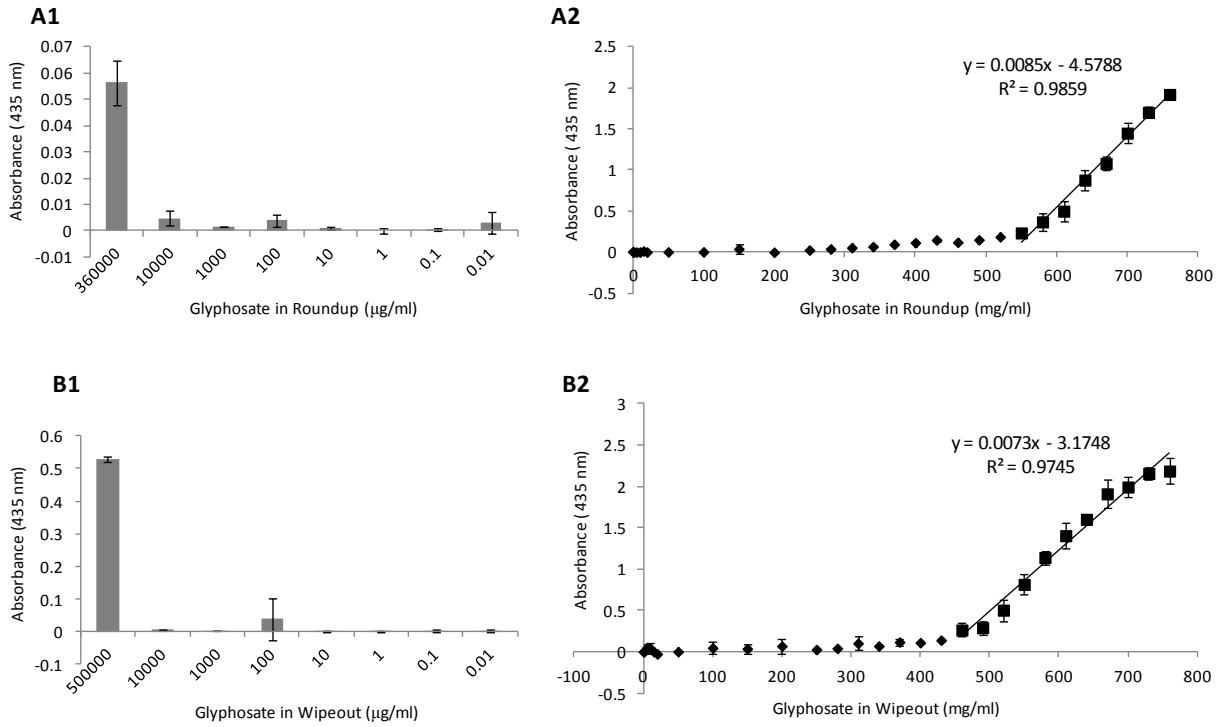


**Figure 4.8:** The detection range for glyphosate formulations **A1:** Ro and **B1:** Wipeout using the scale-down glyphosate detection method and the standard curves produced for glyphosate in the formulations **A2:** Ro (0-760 mg/ml) and **B2:** Wo (0-760 mg/ml). Data points represent mean values ± SD (n= 3). The appropriate controls were used in this study.

The detection method demonstrated lower sensitivity to the glyphosate formulation Ro and Wo (Figure 4.8A1 and 4.8B1) when compared to the detection of pure glyphosate (Figure 4.7), with very low levels of glyphosate in Wo and Ro being detected at concentrations as high as 360000 and 10000 µg/ml respectively, therefore the calibration curves for glyphosate formulations were constructed at starting concentrations higher than those selected for pure glyphosate. Concentrations were generally expressed as µg/ml in this study; however the unit mg/ml was used in this study in for the purposes of simplifying the graphical presentation of data.

Ro and Wo calibration curves (50-760 × $10^3$ µg/ml) are shown in Figure 4.8A2 and 4.8B2 and no or very low detectable glyphosate levels were observed between a concentration range of 50-400 × $10^3$ µg/ml in Ro and 50-430 × $10^3$ µg/ml in Wo. The linear range for glyphosate in Ro was

550-760 × $10^3$ µg/ml ($R^2$= 0.985) and 460-760 × $10^3$ µg/ml ($R^2$= 0.974) for Wo. Both calibration curves displayed a similar sigmoidal pattern to that observed for pure glyphosate.

**Table 4.2:** The calibration characteristics (over the entire range of the regression curve) determined for pure glyphosate and glyphosate in Ro and Wo, using the scale-down detection method. To accurately determine the LOD and LOQ values of the scale down system, the regression equations used represented the entire range of the regression curves for pure glyphosate, Ro and Wo.

| **Parameter** | **Pure glyphosate** | **Ro** | **Wo** | **Reported value Jan *et al.* (2009)** |
|---|---|---|---|---|
| Linear range (µg/ml) | 550-1000 | 550-760× $10^3$ | 460-760 × $10^3$ | NR |
| LOD (µg/ml) | 402.1 | 670.1 × $10^3$ | 503.4 × $10^3$ | 1.1 |
| LOQ (µg/ml) | 1340.2 | 2234.0× $10^3$ | 1678.1× $10^3$ | 3.7 |
| Intercept | 0.14 | 0.21 | 0.29 | 0.01 |
| Slope | 0.0026 | 0.0016 | 0.0025 | 0.014 |
| *RSD (%) | 5.5 | 11.8 | 13.4 | 2.37 |
| $R^2$ | 0.84 | 0.58 | 0.71 | 0.99 |

NR= Not reported, *RSD values obtained over the linear range of the standard curves

When comparing the calibration characteristics obtained for pure glyphosate and glyphosate in Ro and Wo in the scale down system, the data in Table 4.2 strongly suggests that the detection of pure glyphosate was more sensitive as evidenced by lower LOD and LOQ values in comparison to glyphosate detection in Ro and Wo formulations. The scale-down system also demonstrated a fairly good system precision in the detection of pure glyphosate, Ro and Wo (RSD values below 20 %). Greater system precision (lower RSD value) however was observed in pure glyphosate detection in comparison to Ro and Wo. Overall, the scale down system demonstrated poorer sensitivity and precision when compared to the results reported by Jan *et al.* (2009).

### 4.4.7 The stability of glyphosate and glyphosate formulation stock solutions in water

A study was conducted to determine the stability of pure glyphosate and glyphosate formulation stocks over time (42 days) in distilled water at 23 °C (light and dark conditions) and 4 °C (dark conditions) (Figure 4.9). Considering stock solutions were prepared freshly before experiments in all the studies conducted, this experiment was used to determine the best storage conditions and the maximum storage time for glyphosate stocks for future studies.

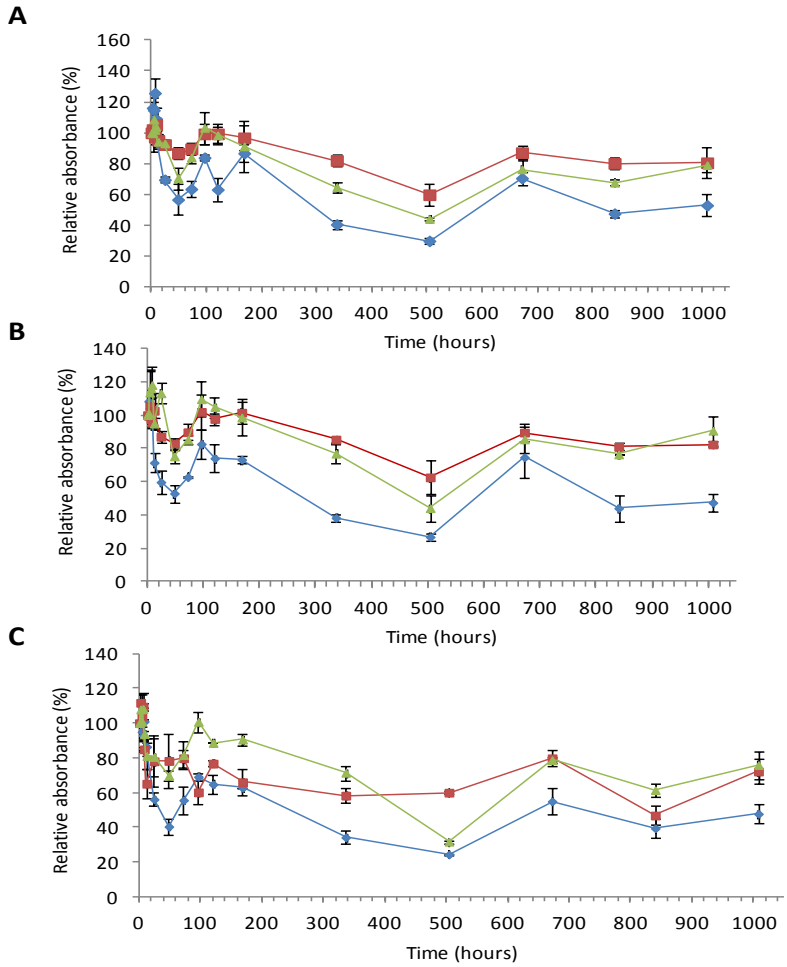


**Figure 4.9:** The stability of pure glyphosate (blue), Ro (green) and Wo (red) in water was investigated over 42 days under varying conditions. **A:** 23°C (light conditions) **B:** 23 °C (dark conditions) and **C:** 4 °C (dark conditions). Data points represent mean values ± SD (n= 3). Appropriate controls were used in this study and the spectrophotometric analysis was conducted at 435 nm.

Pure glyphosate and glyphosate in the Ro and Wo formulations was detected over the entire duration of the study (42 days) under all the conditions tested, (i.e. light conditions at 23 °C) (Figure 4.9A) and dark conditions at 23°C (Figure 4.9B) and 4 °C (Figure 4.9C), with similar stability profiles being observed for pure glyphosate and the glyphosate-based herbicides. Although pure glyphosate and the glyphosate formulations were detected over the 42 day period under all experimental conditions tested, variations were observed within different time intervals at 23 °C and 4 °C, characterized by increases (peaks) and decreases (troughs) in relative absorbance.

## 4.5 Discussion and future work

### 4.5.1 Proof of concept, scale-down, optimization and glyphosate complex stoichiometric evaluation

A proof of concept study, based on the method reported by Jan *et al.* (2009), was carried out to test whether the conditions for the principle reaction reported would result in successful glyphosate (in its dithiocarbamate intermediate form) copper complexation, which could be detected spectrophotometrically. The results obtained (Figure 4.2) from macroscopic images and spectroscopic studies indicated that this method was successful with a change in color (from blue to yellow) in the ammonia layer and a characteristic glyphosate-copper complex peak being observed between 421 and 435 nm. These results are in agreement with the findings of Jan *et al.* (2009) which demonstrated the formation of a yellow colored complex which was detected at the selected wavelength of 435 nm. The proof of concept study confirmed the ability of the copper ions to co-ordinate with the bidentate glyphosate dithiocarbamate ligand. The reaction conversion of glyphosate to a dithiocarbamate is reversible, and an incomplete conversion is a common occurrence when producing dithiocarbamates, and thus the second peak observed in the glyphosate complex sample could be attributed to the uncomplexed glyphosate dithiocarbamate. This observation is in agreement with previously reported data which state that dithiocarbamates generally demonstrate UV absorption between 250 and 280 nm, a peak range which is commonly associated with the S-C=S group (Halls, 1969; Lee *et al.*, 1989; Murthy and Ryan, 1982; Zhu *et al.*, 2002). Spectral scans of the chloroform layer showed no interfering peaks at the

detection range (421-435 nm) for the glyphosate complex. The chloroform layer was characterized by two peaks at 229 and 316 nm, which corresponded closely to values reported in literature with respect to the UV absorption range for chloroform (below 250 nm) and carbon disulfide (271-374 nm), respectively (Hearn and Joens, 1991; Upstone, 2000).

The use of this assay as the basis for chemical sensor development offers many advantages, including the ease of synthesis and preparation of the glyphosate dithiocarbamate derivative and the color change that occurs upon complex formation with the copper ions, which can be visualized by the naked eye. However, this assay was limited by the large assay volumes required (total assay volume: 8 ml), therefore to improve the applicability of this assay towards chemical sensor development, the scale-down of this method was an important requirement. The scale-down of the principle assay method from a total assay volume of 8 ml to 1 ml was successful (Figure 4.3). Control reactions were not detailed by Jan *et al.* (2009), therefore this study selected three negative controls (glyphosate, carbon disulfide and copper control) and spectral scan analysis demonstrated the absence of interfering peaks within the detection range of the glyphosate complex. Thus, the selected wavelength for future studies was 435 nm.

The analytical conditions of the scale down method were optimized with respect to reagent concentrations (carbon disulfide and copper), pH and assay time. Optimal carbon disulfide (Figure 4.4A) and copper nitrate (Figure 4.4B) concentrations were 2.5 % and 4.5 mM, respectively. Both profiles demonstrated a similar trend characterized by an initial increase in absorbance values with increasing reagent concentrations; interestingly, this was followed by a decrease in signal from carbon disulfide and copper concentrations above 4.5 % and 6 mM, respectively. Similar reagent versus absorbance profiles (for carbon disulfide and copper) were obtained by Jan *et al.* (2009), although the optimization experiments reported in the Jan *et al.* (2009) study used reagent volume for the determination of optimal values. The present study selected the use of reagent concentrations for the determination of optimal conditions to maintain the total assay volume at 1 ml. The data suggests that excessive amounts of carbon disulfide and copper nitrate limit the detection of glyphosate. The reason for the observed trends are not entirely clear, however literature has stated that excess dithiocarbamate ligand (which in this case of this study may be formed in the presence of greater carbon disulphide concentrations beyond the optimum) severely interferes with direct detection methods such as spectrophotometry (Bond

and Wallace, 1984; Mueller and Lovett, 1987). Similar results were published by Shar and Banger (2002) in a study involving the spectrophotometric determination of copper (II) complexed with a dithiocarbamate (diethyldithiocarbamate). In the Shar and Banger (2002) study an initial increase in absorbance was observed with increasing dithiocarbmate ligand concentrations of up to $5 \times 10^4$ mol.dm$^{-3}$; however concentrations higher than this caused dissolution problems, which resulted in erroneous absorbance correction due to a higher ratio of ligand to complex absorptivity. Although no dissolution problems were observed in the current study, the decreasing trend observed with copper concentrations greater than 6 mM may have occurred, due to a shift in the detection spectrum, once all the co-ordination sites for copper were occupied, resulting in an increase in the amount of free ammonical copper (increased blue color) in solution (Fritz and Sutton, 1956).

The effect of pH on glyphosate detection was investigated and the results (Figure 4.4C) indicated a strong association between pH and glyphosate detection. Glyphosate detection was optimal under high alkaline conditions (pH 12) and similar findings were reported by Jan *et al.* (2009). The $pK_a$ value determined by potentiometric titration studies for the secondary amine group on the glyphosate structure was 10.3 (Ridlen *et al.,* 1997), therefore increasingly alkaline conditions favor the deprotonation of this amine group forming an amide anion which facilitates the formation of the glyphosate dithiocarbamate ligand via nucleophilic attack towards carbon disulfide (Halls *et al.,* 1968; Oliver *et al.,* 2011; Sanchéz *et al.,* 1999; Toumi *et al.,* 2008). Dithiocarbamate ligands demonstrate greater susceptibility to decomposition (resulting in the release of carbon disulfide due the breakdown of the C-N bond) under neutral and acidic conditions when compared to alkaline conditions; therefore high alkaline conditions also provide increased ligand stability (Benedini *et al.,* 2006; Leyden and Cuttrell, 1975; Rogachev *et al.,* 1999).

Glyphosate detection was evaluated as a function of time (Figure 4.4D). The optimal assay time chosen for future studies was 2 hours (120 minutes). A gradual decline in glyphosate detection was observed after 3 hours (180 minutes) and within 7 hours (420 minutes) an 80 % reduction in the detection signal was observed. The decline in glyphosate detection after 3 hours may be due to the general instability exhibited by dithiocarbamates in solution, which decompose over time, either photochemically or thermally, into the corresponding amine derivative and carbon

disulfide (Hayashi *et al.*, 1987; Hirai *et al.*, 1977). Electron paramagnetic resonance studies by Jeliazkova *et al.* (1996) on dithiocarbamate-copper mixed ligand complexes demonstrated the susceptibility of these complexes to photodecomposition through the homolytic cleavage of the copper-sulfur bond, resulting in the release of a copper ion and a dithiocarbamate radical. Although the Jan *et al.* (2009) study did not investigate the effect of time on the glyphosate complex detection, a glyphosate spectrophotometric study conducted by Sharma *et al.* (2012) involving the formation of a glyphosate dithiocarbamate ligand using acetonitrile, followed by the production of a yellow-green complex after the addition of copper, indicated that the kinetic stability of the colored complex as a function of time was approximately 90 minutes. This was lower than the complex stability observed in our current study. This does, however, support the theory that dithiocarbamate ligands are susceptible to destabilization effects in solution. Future studies could validate this theory, by measuring the disappearance of glyphosate in solution over time, using techniques such as UV-Vis spectral analysis and/or Fourier Transform Infrared spectroscopy (FTIR).

The stoichiometric molar ratio determined (Figure 4.5) for glyphosate (dithiocarbamate intermediate) and copper complexation using the Jobs Method of Continuous Variation, was 2:1. Theoretical values extrapolated from linear regression analysis in this study validated the accuracy of the results obtained from the experimental data. The reaction reported by Jan *et al.* (2009) followed a glyphosate-copper molar ratio of 2:1, which confirms the findings of our present study. The molecular structure illustrated by Jan *et al.* (2009) (Figure 4.1) suggests that the copper (II) ions complex with two glyphosate dithiocarbamate ligands through co-ordination of the copper molecule with four sulfur groups. Cu (II) ions commonly form square planar complexes (Cao *et al.*, 2000, De Lima *et al.*, 2011) with dithiocarbamates. Electron paramagnetic resonance (EPR) studies by Cobianco *et al.* (2000) are in agreement with the molecular structure proposed by Jan *et al.* (2009), with the findings of the study showing that copper (Cu II)-dithiocarbamate complexes generally demonstrate a square planar co-ordination with two dithiocarbamate groups co-ordinating to the copper ion via four sulfur groups.

The molar absorptivity (L/mol/cm) and the stability constant ($K_f$) (Table 4.2) of the scale-down method was determined using the Jobs plot. The calculated molar absorptivity of the scale down glyphosate detection system ($1.866 \times 10^3$ L/mol/cm) was found to be very similar to the reported

value ($1.864 \times 10^3$ L/mol/cm) by Jan *et al.* (2009), however the stability constant obtained for the scale-down method ($1.69 \times 10^2$) was 600-fold lower when compared to the reported value ($1.06 \times 10^5$). This strongly suggests that glyphosate and copper ions in the scale down system demonstrates a lower tendency for complex formation and displayed lower complex stability when compared to the detection system described by Jan *et al.* (2009). To the best of our knowledge, other spectrophotometric techniques used for glyphosate detection have not been reported on glyphosate complex stability constants and therefore could not be used as a basis for comparison. The scaling down process may be a contributing factor to the lowered stability of the glyphosate-copper complex, primarily if the reactions are volume limited. However this cannot be conclusively stated and further research in this area would be required. Due to the scope of this study, however, the effect of assay volume on complex stability was not investigated.

### 4.5.2. Scale-down glyphosate detection system specificity, sensitivity and precision

The specificity, sensitivity and precision of the scale-down method was investigated to allow for future comparative analysis between the scale-down method and the chemical sensor developed for glyphosate detection in water.

The scale down glyphosate detection system demonstrated a very high specificity towards glyphosate, with extremely minimal detection of the structural analogs glycine and AMPA being observed (Figure 4.6). Carbon disulfide displays the capacity to react with both primary (glycine and AMPA) and secondary amines (glyphosate) to form dithiocarbamates (Niu *et al.,* 2012); however, dithiocarbamates derived from secondary amines demonstrate greater chemical stability than those derived from primary amines (Fuentez-Martinez *et al.,* 2009; Mclain and Hseih, 2004). Studies by Zhu *et al.* (2008), based on the production of dithiocarbamates derived from primary and secondary amines, demonstrated that these two different types of amines show significant differences in reactivity and product stability. Generally, dithiocarbamates derived from secondary amines showed good reactivity and stability and, although some primary amines in the study fared relatively well, the study concluded that secondary amines were more reliable for dithiocarbamate production. With specific reference to our current study, the specificity

observed for glyphosate strongly suggests that this may have been due to the poorer reactivity of carbon disulfide with the primary amines of glycine and AMPA when compared to the secondary amine of glyphosate.

The method described by Jan *et al.* (2009) only reported on the detection of glyphosate alone, however the detection of glyphosate in formulation was an important consideration, not only because it is commercially available in this form, but another important factor to consider was that compounds present in formulation may alter the initial system characteristics observed, (e.g. sensitivity (LOD and LOQ)). The scale down method was successfully applied to the detection of glyphosate in formulation under optimized conditions, however greater sensitivity (Table 4.2) was observed in the detection of pure glyphosate (LOD: 402.1 μg/ml) when compared to the detection of glyphosate in the Ro (LOD: $670 \times 10^3$) and Wo (LOD: $503.4 \times 10^3$). These differences may have been due to the presence of adjuvants in the glyphosate formulations which may have led to a reduced sensitivity at lower glyphosate concentrations. Overall, the scale down method demonstrated lower sensitivity and precision in comparison to the method reported by Jan *et al.* (2009), however considering the lower affinity of the system for glyphosate complex formation as determined by $K_f$, this observation was not entirely unexpected.

### 4.5.3 Glyphosate stock solution stability and storage

Pure glyphosate, Ro and Wo demonstrated similar stability profiles under all the conditions tested (Figure 4.9). Glyphosate was detected in all three samples over the duration of the study and did not demonstrate susceptibility to photolysis as the stability profiles observed for all three samples under dark and light conditions were relatively similar. However, large variations were observed between different time points characterized by increases and decreases in the relative absorbance (%) over the 42 day period. This trend has been documented in literature and reports by Antón *et al.* (1993) on the degradation of glyphosate in water report no significant degradation of glyphosate over a total time period of 78 days, but found that the levels of herbicide were erratic and concluded that this may be due the linkage/adsorption of glyphosate to glassware surfaces. Considering the large variations in the detection levels of glyphosate over

time, future studies should involve the continued use of freshly prepared glyphosate stocks, or polyethylene and/or polypropylene storage containers (Huguenot *et al.*, 2010; Kylin, 2013).

## 4.6 Conclusions

- The proof of concept study confirmed the successful formation of a yellow colored glyphosate dithiocarbamate copper complex. This method was successfully scaled-down to a total assay volume of 1 ml and the detection wavelength selected for glyphosate complex determination was 435 nm.
- The scaled-down method was optimized with respect to carbon disulfide (2.5 %) and copper (4.5 mM) concentrations. The optimal pH (12) and assay time (2 hours) were also established for this method. These conditions were the initial parameters used for the proof of concept study in the detection of glyphosate using chemical sensor technology.
- The scale-down method was successfully applied for the detection of glyphosate in the formulations Ro and Wo, however the system demonstrated greater sensitivity and precision towards pure glyphosate in comparison to glyphosate in the formulations Ro and Wo.
- Future studies should employ the use of freshly prepared glyphosate stocks or polyethylene and/or polypropylene storage containers, to prevent any confounding results, due to variations in the relative absorbance (under all storage conditions) observed in the glyphosate stability studies.

The following Chapter (Chapter 5) presents the development of a nanofiber based chemical sensor for glyphosate detection, the proof of concept study (using the optimized conditions from the scale-down method) and the determination of optimal conditions for the detection of glyphosate.

# CHAPTER 5- GLYPHOSATE NANOFIBER BASED CHEMICAL SENSOR DEVELOPMENT, PROOF OF CONCEPT AND OPTIMIZATION

## 5.1 Introduction

The electrospinning process is a straightforward and practical approach towards the production of nanofibers and is based on the release of an electrically charged jet of a polymer solution upon the application of an electrical field which subsequently results in the formation of solid nanofibers (the electrospinning process was reviewed in greater detail in Chapter 1 section 1.3) (Gunn and Zhang, 2010; Murugan and Ramakrishna, 2007). The electrospinning set-up is very simple and economically feasible (Sell *et al.*, 2009) (Figure 5.1), however the process itself is more complex and depends on several factors including physical, technical and molecular parameters (Lukás *et al.*, 2009).

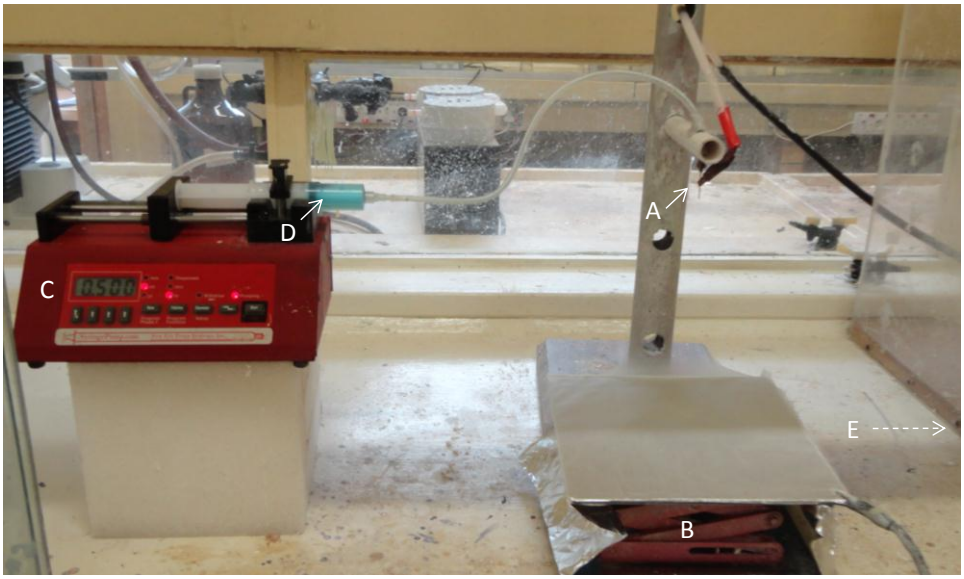


**Figure 5.1:** The electrospinning setup used in the present study. **A:** metal needle (inner diameter: 0.3 mm) connected to the positive voltage supply, **B:** collector (covered with aluminum foil), **C:** pump, **D:** Syringe (containing polymer solution), **E:** voltage supply. This image was obtained using a SONY Cyber shot digital camera.

The electrospinning process can be applied to a large variety of different polymers (synthetic and natural) which can be spun into nanofibers with varied sizes (average fiber diameters can range from 100 nm to 5 μm) and shapes, with a wide range of advantageous properties which can be applied in industrial and biomedical applications (Frenot and Chronakis, 2003; Gupta and Wilkes, 2003; Subbiah *et al.,* 2005). The first aim of this study was the production of a colorimetric nanofiber based sensing strip (chemical sensor) for the detection of glyphosate in water. The approach used for this study involved the use of the nanofibers as scaffolding material with the incorporation of the sensing material within the nanofiber structure. The use of nanofibers would provide advantageous characteristics such as a large specific area to volume ratio which would theoretically increase the contact ratio between glyphosate and the incorporated sensing material, thereby improving the overall detection of glyphosate (Frey and Li, 2007).

A chemosensor or chemical sensor is defined as small device which translates a chemical or biochemical alteration (quantitative, semi-quantitative or qualitative), based on the chemical reaction between analyte of interest and sensing device (Buttner *et al.,* 2011). The development of a colorimetric chemical sensor was of great interest in this study due to the potential advantages compared to other reported methods for glyphosate detection such as simplicity, practicality and the potential for visual quantification (Albert *et al.,* 2000). Other sensor methods developed for glyphosate detection include a fully automated immunosensor (immunocomplex capture) (Gonzalez-Martinez *et al.,* 2005) and a colorimetric chemical sensor based on the reaction of glyphosate and *p*-dimethylaminocinnamaldehyde (*p*-DAC) on filter paper (solid support) (Da Silva *et al.,* 2011). However, to the best of our knowledge, during the time of this study, there have been no reports based on nanofiber-based colorimetric chemical sensors for glyphosate detection.

The surface matrix selected for this study was poly(vinyl)alcohol (PVA). PVA is a semi-crystalline (Figure 5.2) water soluble polymer which is produced (commercially) from the polymerization and hydrolysis of poly(vinyl)acetate (PVAc) (Hassan and Peppas, 2000). The extent of hydrolysis (related to the content of acetate groups) determines the physical and chemical properties of PVA (Hassan and Peppas, 2000).

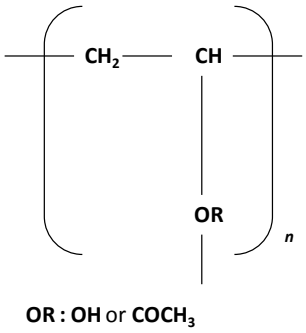


**Figure 5.2:** The chemical structure of PVA. (This image was adapted from Kadajji & Betageri, 2011).

PVA polymers demonstrate several attractive features (i.e. it is non-toxic/bio-compatible, demonstrates good chemical and thermal stability, high permeability and is easily processed) (Bolto *et al.,* 2009; Mudigoudra *et al.,* 2012), which has led to the use of this polymer in a wide range of industrial applications including the biomedical and sensor fields (Adhikari and Majumdar, 2004; Kadajji and Betageri, 2011; Kim *et al.,* 2008). The properties displayed by PVA make this polymer an excellent candidate as a solid support structure in the development of a chemical sensor.

The sensor method developed was based on the principle reaction reported by Jan *et al.* (2009). A two step method was proposed involving the reaction of glyphosate and carbon disulfide for the formation of a dithiocarbamate intermediate, which was followed by the addition of the dithiocarbamate sample onto copper (sensing material) doped PVA nanofibers (Figure 5.3).

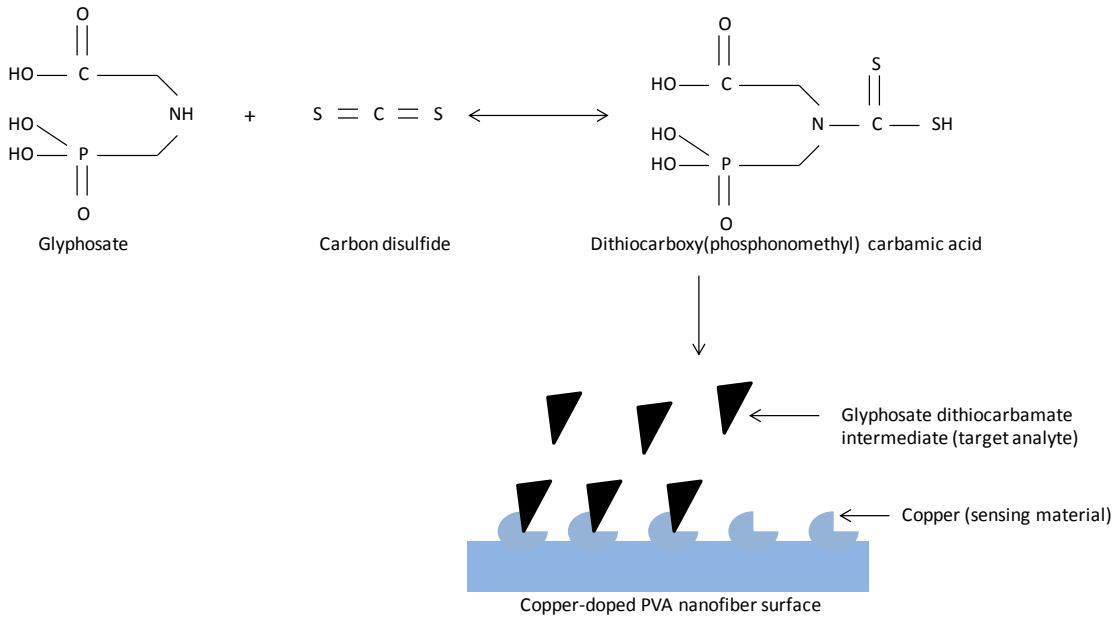


**Figure 5.3:** A schematic illustration of the proposed two step process for the detection of glyphosate. The initial step involves the formation of the glyphosate dithiocarbamate intermediate, followed by the application of this sample onto the solid state nanofiber based chemical sensor.

The second aim of this study was to determine whether the proposed method would lead to successful glyphosate-copper complex formation evaluated visually by a color alteration (from blue to yellow) in the nanofiber based sensor strip.

This study employed both visual (naked eye) and quantitative assessments to determine the sensor response signal. Visual evaluations of colorimetric sensors simplifies data analysis as the use of instruments is not required; however this approach is limited by the resolving power of the naked eye and is subjective, therefore this approach can only be used for qualitative and semi-quantitative analysis (Balaji *et al.*, 2006; Cho *et al.*, 2005; Zhang *et al.*, 2006). Quantitative determinations in colorimetric sensor systems in literature are based on the measurement of color in the sensor using a variety of imaging devices which include digital color analyzers (Ellerbee *et al.*, 2009 Hirayama *et al.*, 2000), digital cameras (Zhang and Suslick, 2005) and desktop scanners (Birch and Stickle, 2003). The approach of this study was based on the use of the RGB (tristimulus) color model after the extraction of digital images using a digital camera. The RGB

color model is an additive color model in which red, green and blue colors are added in various ratios to produce a large variation of colors and RGB values can be extrapolated for any color. The determination of RGB intensity is the most commonly used color space for single and multianalyte quantitative detection analysis (Cantrell *et al.,* 2010). With specific reference to the current study RGB values were extrapolated using a well known computer software program, namely, Adobe Photoshop CS5.1 and the effective intensity of the RGB values was calculated as a linearized function (Abbaspour *et al.,* 2008; Abbaspour *et al.,* 2010; Sharma and Amlathe, 2012a; Sharma and Amlathe 2012b, Suzuki *et al.,* 2006).

The final aim of this study was to determine the optimal conditions for glyphosate detection for the chemical sensor system.

## 5.2 Objectives

- To produce bead free copper-doped PVA nanofibers using the electrospinning process. Nanofiber morphology characterization was carried out using scanning electron microscopy (SEM) analysis and Fourier Transform Infrared spectroscopy (FTIR).
- To conduct a proof of concept study for glyphosate detection using the developed chemical sensor based on visual observations and the quantitative determination of glyphosate.
- To optimize the chemical sensor system with respect to pH and carbon disulfide concentration, based on visual observations and the quantitative determination of glyphosate.

## 5.3 Methods and materials

### 5.3.1 Materials

Please refer to the chemical list in Appendix I for all the materials and chemical suppliers used in this study. All glyphosate stocks were prepared freshly (refer to Chapter 3, Section 3.3.1) before any experimental studies.

### 5.3.2 Synthesis of copper-doped PVA nanofiber chemical sensor strips and the optimization of nanofiber parameters for PVA nanofiber and nanofiber mat formation

Fully hydrolyzed PVA polymer (> 99%, average molecular weight: 146 000-186 000 g/mol) was added to distilled water (the solvent used in this study) and the solution was subjected to reflux heating at 90-95 °C for 5 hours, to allow the polymer to completely dissolve in the solvent. PVA polymers with a higher degree of hydrolysis (greater than 80 %) generally demonstrate poorer water solubility and require temperatures above 80°C to disrupt the strong intra- and inter-molecular bonds, thereby improving the water solubility characteristics of the polymer (Hassan and Peppas, 2000; Koski and Shivkumar, 2004). The polymer solution was allowed to cool to room temperature (23°C). The PVA polymer solution was then added into a 15 ml syringe with a metal needle attachment (inner diameter: 0.3 mm) and polymer solution was subjected to the electrospinning process. PVA nanofiber and nanofiber mat formation was optimized by varying the following parameters: PVA polymer concentration (%, w/v), flow rate (ml/hour), voltage (kV) and needle tip to collector distance (15 nm). The evaluated parameters are shown in Table 5.1.

**Table 5.1:** The parameters tested for PVA nanofiber and nanofiber mat formation and the corresponding visual observations.

| PVA polymer concentration (%) | Flow rate (ml/hour) | Voltage (kV) | Needle tip to collector distance (cm) | Visual observation |
|---|---|---|---|---|
| 5.5 | 0.2 | 25 | 10 | NFF, DF |
| 5.5 | 0.3 | 25 | 10 | NFF, DF |
| 5.5 | 0.8 | 25 | 10 | NFF, DF |
| 6 | 0.2 | 25 | 10 | NFF, DF |
| 6 | 0.4 | 25 | 10 | NFF, DF |
| 6 | 0.2 | 25 | 9 | NFF, DF |
| 6 | 0.4 | 25 | 9 | NFF, DF |
| 6 | 0.5 | 20 | 15 | NFF, DF |
| 6 | 0.5 | 25 | 15 | NFF, DF |
| 6 | 0.8 | 25 | 15 | NFF, DF |
| 6.5 | 0.4 | 20 | 15 | NFF, DF |
| 6.5 | 0.4 | 25 | 15 | NFF, DF |
| 6.5 | 0.3 | 25 | 15 | NFF, DF |
| 6.5 | 0.2 | 25 | 15 | NFF, DF |
| 6.5 | 0.5 | 27 | 15 | NFF, DF |
| 6.5 | 0.5 | 28 | 15 | NFF, DF |
| 6.5 | 0.2 | 30 | 15 | NFF, DF |
| 7.5 | 0.3 | 30 | 15 | FB, NB, NM |
| 7.5 | 0.4 | 30 | 15 | FB, NB, NM |
| 7.5 | 0.5 | 30 | 15 | FB, NMF |
| 8 | 0.4 | 30 | 13 | FB, NB, NM |
| 8 | 0.5 | 20 | 13 | FB, NB, NM |
| 8 | 0.8 | 15 | 13 | FB, NB, NM |
| 9 | 0.4 | 20 | 13 | FB, NB, NM |
| 9 | 0.8 | 20 | 13 | FB, NB, NM |
| 10 | 0.4 | 20 | 13 | FB, NB, NM |
| 10 | 0.8 | 20 | 13 | FB, NB, NM |
| 12 | 0.4 | 15 | 10 | FB, NB, NM |
| 12 | 0.8 | 15 | 10 | FB, NB, NM |

NFF (no fiber formation), DF (droplet formation), FB (fiber formation), NB (needle blockage), NMF (collectable nanofiber mat formation), NM (no collectable nanofiber mat formation)

Based on the visual observations, the electrospinning parameters selected for future studies were at a PVA polymer concentration of 7.5 % (w/v), 0.5 ml/hour flow rate, a voltage of 30 kV and a needle to collector tip distance of 15 cm. Nanofiber mats were collectable after 5 ml of the

polymer solution had been electrospun, therefore the time selected for the electrospinning process was 10 hours. Copper (in the form of copper (II) nitrate hydrate) was added to pure PVA polymer solution at a maximum concentration of 180 mM, equivalent to 3.35 % w/v (this concentration was selected for future studies based on visual observations. Copper nitrate concentrations above 180 mM limited nanofiber mat formation (i.e. nanofibers were suspended around the electrospinning apparatus and did not settle onto the collection screen). The selected copper nitrate concentration was 40 fold higher than the optimum copper concentration used in the scale-down method. The resultant copper-doped PVA solution was electrospun under the optimized conditions.

The addition of surfactant, such as the non-ionic surfactant Triton® X-100 (Triton-X), to highly hydrolyzed PVA polymer solutions before electospinning is generally required for the successful production of PVA electrospun nanofbers. Several studies have shown the benefits of using Triton-X (at varying concentrations) in the production of PVA nanofibers. Yao *et al.* (2003) demonstrated the reproducible electrospinnability of fully hydrolyzed PVA nanofibers (10 % wt in distilled water) and complete non-beaded fiber formation only upon the addition of Triton-X at a concentration of 0.3 % (w/v) (critical micellar concentration). Studies by Kenawy *et al.* (2007) and Wang *et al.* (2006) utilized the surfacatant Triton-X at concentrations of 2.5 % (w/v) and 0.6 % (w/v), respectively, to successfully electrospin PVA (10 % w/v) polymer solutions. Although nanofiber mat formation was achieved in the absence of Triton-X in our study, the effect (on the resultant nanofiber morphology) of adding Triton-X (1 % v/v) to PVA polymer solutions (for both pure PVA and copper-doped PVA) before the electrospinning process was investigated.

Once the electrospinning process was complete, nanofiber mats were collected, separated from the aluminum foil and cut into 10 mm × 10 mm nanofiber squares.

### 5.3.3 Nanofiber partial characterization (SEM and FTIR analysis)

SEM analysis using a Zeiss Evo MA 15 scanning electron microscope was conducted to evaluate nanofiber morphology and the resultant fiber diameters (μm). Samples were sputter coated with gold in a JEOL JFC-1200 fine coater (spray time: 30 minutes). Images were obtained using

Tescan digital microscopy imaging software (Vega TC) at an accelerating voltage of 20 kV. Fiber diameters were determined using the Scandium programme (SEM image platform) and size-distribution (frequency) plots were constructed in Microsoft Excel.

### 5.3.4 Proof-of-concept study

The conditions selected for the proof of concept study were based on the optimal conditions obtained for the scale down method (a pH of 12 and a carbon disulfide concentration of 2.5 % v/v). The pH of this system was adjusted using 0.1M sodium hydroxide. Pure glyphosate (1000 µg/ml) was combined with carbon disulfide (2.5 % v/v) in a 1:2.5 ratio; for the formation of the glyphosate dithiocarbamate intermediate. A sample volume of 30 µl (selected based on the maximum chemical sensor surface coverage) was subsequently injected onto the glyphosate chemical sensor. The concentration of pure glyphosate used in this study was based on the upper limit of the standard curve produced for the scale-down method. Color progression was captured using a digital camera and the effective intensity of the extrapolated RGB values was calculated. Three negative controls were used in this study (glyphosate, carbon disulfide and a blank strip).

### 5.3.5 Optimization studies (glyphosate chemical sensor)

The effect of varying pH conditions (5-12) and carbon disulfide concentration (0-7 %) on glyphosate detection were determined. Color progression was captured using a digital camera and the effective intensity of the RGB values was calculated. Three negative controls were used in this study (glyphosate, carbon disulfide and a blank strip).

### 5.3.6 Data analysis

Unless stated otherwise, all data was presented as mean values ± SD (n=3) and all experiments were conducted at room temperature (23 ºC).

Macroscopic images were obtained using a SONY Cyber shot digital camera. Images were captured at a consistent height of 25 cm in a laminar flow hood (to maintain a fairly consistent light source). The image characteristics were as follows: bit depth (24 bit), compressed bit/pixel (4 bit), width (1920 pixels), height (1080 pixels), horizontal and vertical resolution (72 dpi). Digital images were imported into Adobe Photoshop CS5.1 software and 4 representative areas on each strip were analyzed (sample size 101 × 101 average for each representative area). The tristimulus RGB values were determined and the effective intensity ($A_x$) was calculated in Microsoft Excel based on the equations (shown below) reported by Abbaspour *et al.*, (2008).

$$A_r = -\log (R_s/R_b) \quad (1)$$

$$A_g = -\log (G_s/G_b) \quad (2)$$

$$A_b = -\log (B_s/B_b) \quad (3)$$

where $A_{(x= r,g,b)}$ is the effective intensity for the red, green and blue value. $R_s$, $G_s$, $B_s$ are the tristimulus color values obtained for the test reaction sample. $R_b$, $G_b$, $B_b$ are the average tristimulus color values obtained from the negative controls.

## 5.4 Results

### 5.4.1 PVA nanofiber morphology and partial characterization

The PVA and copper doped PVA nanofibers produced under optimized synthesis and electrospinning conditions are shown in Figure 5.4. The morphology of the resultant nanofibers was assessed in the presence and absence of the surfactant Triton-X (1%) using SEM analysis. Macroscopic images of the nanofiber mats were also taken to evaluate optical differences between PVA only and copper doped PVA nanofiber mats.

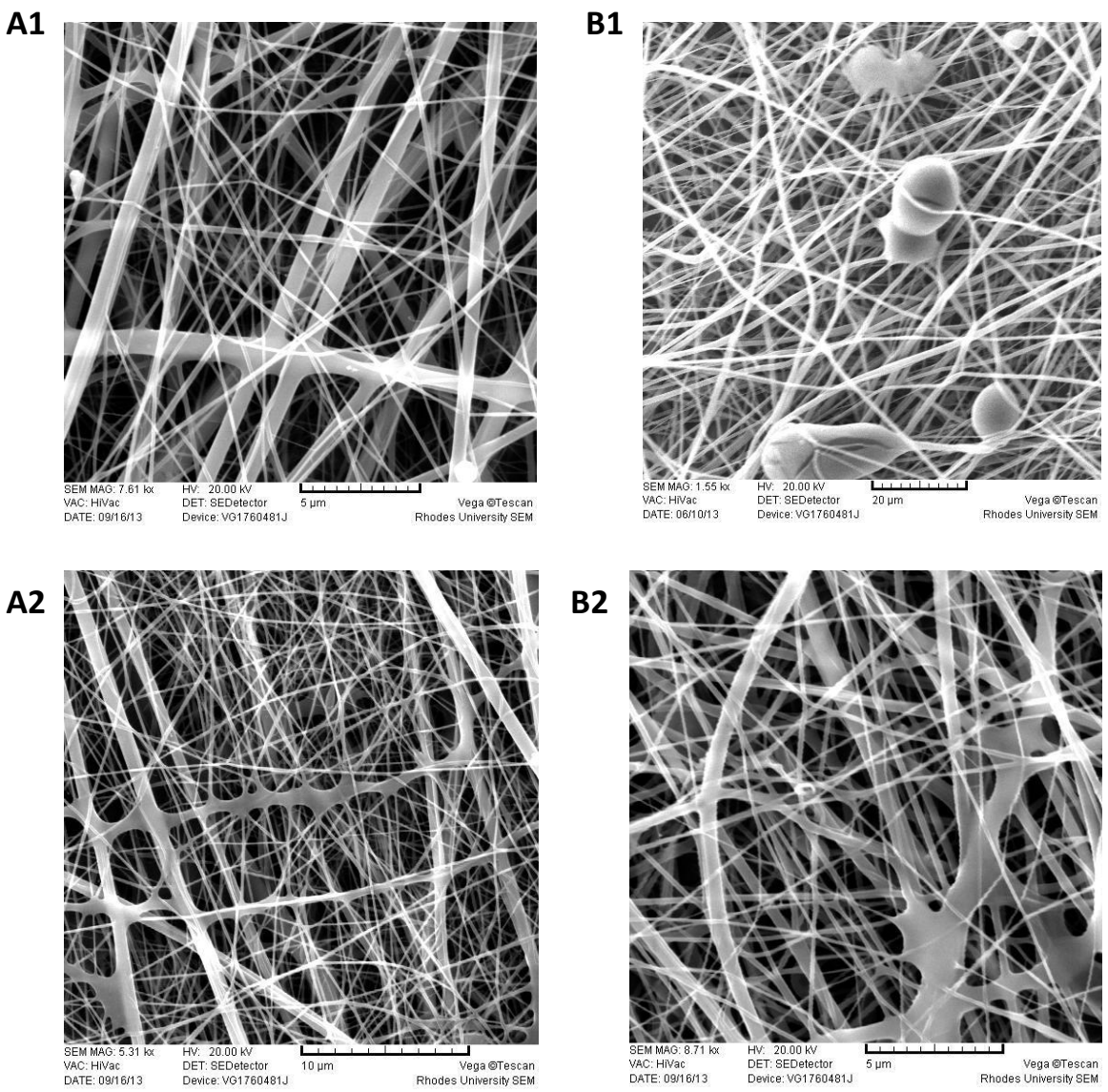


**Figure 5.4:** Representative SEM micrographs shown for pure PVA (7.5 % w/v) nanofibers and copper doped PVA (7.5 w/v PVA and 180 mM copper equivalent to 3.35 % w/v) nanofibers without **(A1,B1)** (SEM magnifications: 7.61 and 1.55 kx) and with **(A2, B2)** (SEM maginifications: 5.31 and 8.71 kx ) the addition of 1% Triton X-100, respectively. SEM micrographs were obtained at an accelerating voltage of 20 kV. The nanofiber mats were electrospun under the optimized parameters: needle to tip distance, 15 cm ; voltage, 30 kV and flow rate, 0.5 ml/h.

Nanofiber mats were successfully produced under the optimized electrospinning conditions, however bead formation was observed to a small extent in nanofiber mats spun with PVA only (Figure 5.4A1) and to a larger degree in mats spun with PVA together with copper (Figure 5.4B1). The addition of copper to PVA electrospinning solutions resulted in a change in fiber morphology.

The addition of Triton-X significantly improved the nanofiber mats produced with both pure PVA and copper doped PVA mats indicating no bead formation (Figure 5.4A2 and B2). Triton-X (1%) was therefore added to all subsequent electrospinning solutions for nanofiber mat production. The addition of Triton-X did change the morphologies of the resultant nanofiber mats when compared to nanofibers electrospun in the absence of the surfactant; however the representative nanofiber mats in Figure 5.4A2 and 5.4B2 demonstrated similar morphologies characterized predominantly by long, smooth nanofibers dispersed in a random orientation. The nanofibers produced displayed heterogeneous morphologies as evidenced by the appearance of flat branched fibers as well as smaller fibers that split in a vertical direction from the larger fibers.

PVA only and copper doped PVA mats showed a clear color alteration from grey/white to blue, which was brought on from the incorporation of copper into the PVA electrospinning solution.

Size distribution plots were constructed to determine the fiber diameters of PVA only and copper doped PVA electrospun mats (Figure 5.5)

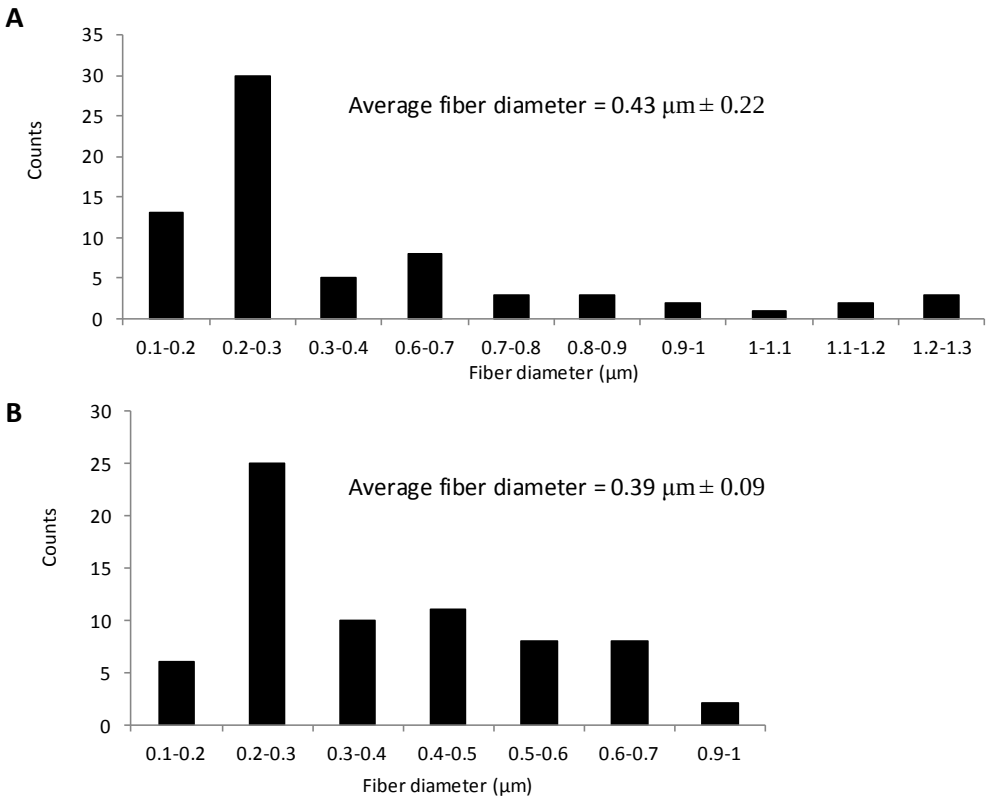


**Figure 5.5:** Size (μm) distribution graphs shown for Pure PVA (7.5 % w/v) nanofibers **(A)** and copper doped PVA (7.5 w/v PVA and 180 mM copper equivalent to 3.35 % w/v) nanofibers **(B)**. Each distribution graph was constructed using n = 70 fiber diameter values. Nanofiber diameters were obtained using the SEM imaging platform Scandium and distribution plots were constructed in Microsoft Excel using the Pivot table function.

Size distribution plots obtained from 70 fibers from different SEM micrographs indicated a wider fiber size distribution for PVA only (Figure 5.5A) when compared to copper doped PVA nanofiber mats (Figure 5.5B). The mean calculated fiber diameters for pure PVA and copper-doped PVA nanofiber mats were 0.43 ± 0.22 and 0.39 ± 0.09 μm respectively (Appendix IV). Fibers with diameters ≥ 0.8 μm were also observed in both mats.

FTIR analysis was used to evaluate the interactions between PVA and copper and the results are shown in (Figure 5.6). The IR band positions and their assignments for PVA only and copper doped PVA nanofibers are shown in Table 5.2.

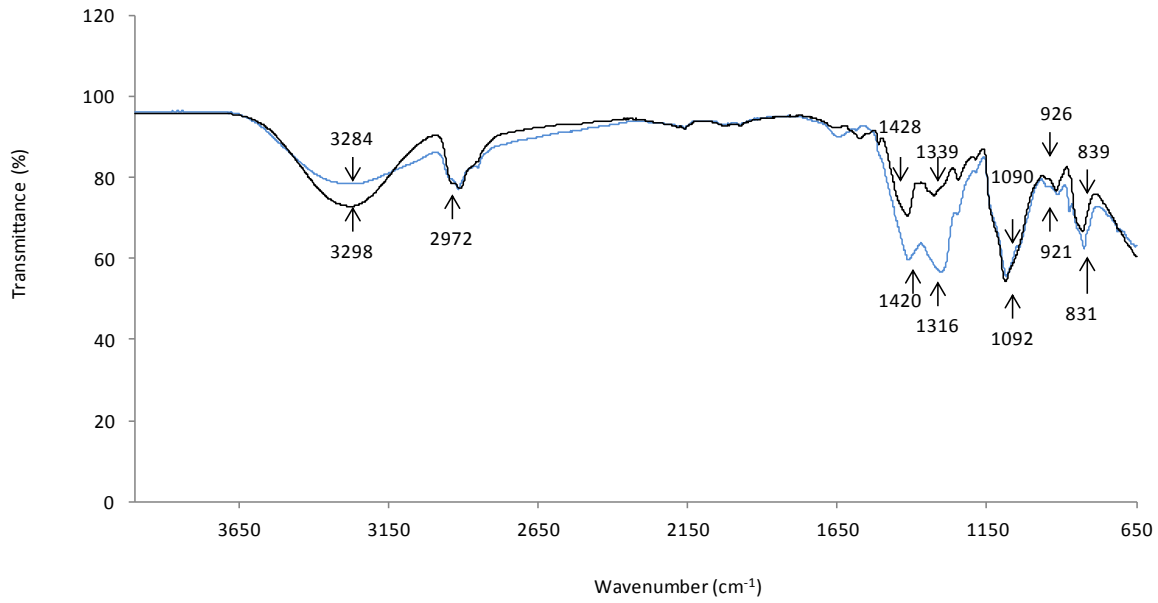


**Figure 5.6:** The FTIR spectra of PVA only (7.5 % w/v) (black) nanofibers and copper doped PVA (7.5 w/v PVA and 180 mM copper equivalent to 3.35 % w/v) (blue) nanofibers. The spectra were recorded at room temperature (22 ± 2°C) in the frequency range: 4000-650 $cm^{-1}$.

The FTIR spectrum (Figure 5.6) demonstrated some absorption bands, which are characteristic to the stretching and bending vibrations of O-H, C-H and C-O groups for pure PVA. The absorption peaks for pure PVA were assigned as follows: The relatively broad absorption peak at 3298 $cm^{-1}$ corresponds to the stretching vibration of hydroxyl (O-H) groups. The medium band corresponding to the asymmetric stretching of C-H was observed at 2972 $cm^{-1}$. Absorption peaks at 1428 and 839 $cm^{-1}$ were assigned to the bending and stretching of the $CH_2$ group, respectively. Bands corresponding to C-O (strong and sharp band) and C-C stretching (weak band) vibrations

were observed at 1092 and 926 $cm^{-1}$ respectively. The weak band at 1339 $cm^{-1}$ was assigned to the combined frequency of OH and $CH_2$ groups (Raju *et al.*, 2007).

**Table 5.2:** The IR band assignments and their corresponding vibration frequencies for PVA only and copper doped PVA nanofibers.

| **Band assignment** (Raju *et al.*, 2007; Coates, 2000) | **Wavenumber ($cm^{-1}$)** | |
|---|---|---|
| | **PVA only** | **PVA/copper** |
| OH (stretching) | 3298 | 3284 |
| CH (asymmetric stretching) | 2972 | 2972 |
| $CH_2$ (bending) | 1428 | 1420 |
| $CH_2$ (stretching) | 839 | 831 |
| CO (stretching) | 1092 | 1090 |
| CC (stretching) | 926 | 921 |
| $CH_2$ and OH | 1339 | 1316 |

No new peaks were apparent in the copper doped PVA IR spectrum (Figure 5.6). The addition of copper into the PVA polymer demonstrated alterations in the PVA structure as evidenced by varying signal intensities and the differences in vibration frequency (shifts) observed for some chemical groups (Table 5.2), which suggests that copper does interact with PVA and displays effects on inter and intra molecular hydrogen bonds in the polymer. Peak broadening and a decrease in vibration frequency (3298-3284 $cm^{-1}$) was observed for the band corresponding to hydroxyl group stretching and the addition of copper caused a relatively large shift to a lower wavenumber (1339-1316 $cm^{-1}$) in the band concerned with $CH_2$ and OH groups. The results obtained strongly suggest the co-ordination of copper ions with hydroxyl groups in the PVA structure.

### 5.4.2 Proof-of-concept study

The proof of concept study was based on the initial formation of a glyphosate dithiocarbamate intermediate using carbon disulfide as the derivatization reagent, followed by the application of this sample to copper doped PVA nanofibers. The results of this study are shown in Figure 5.7.

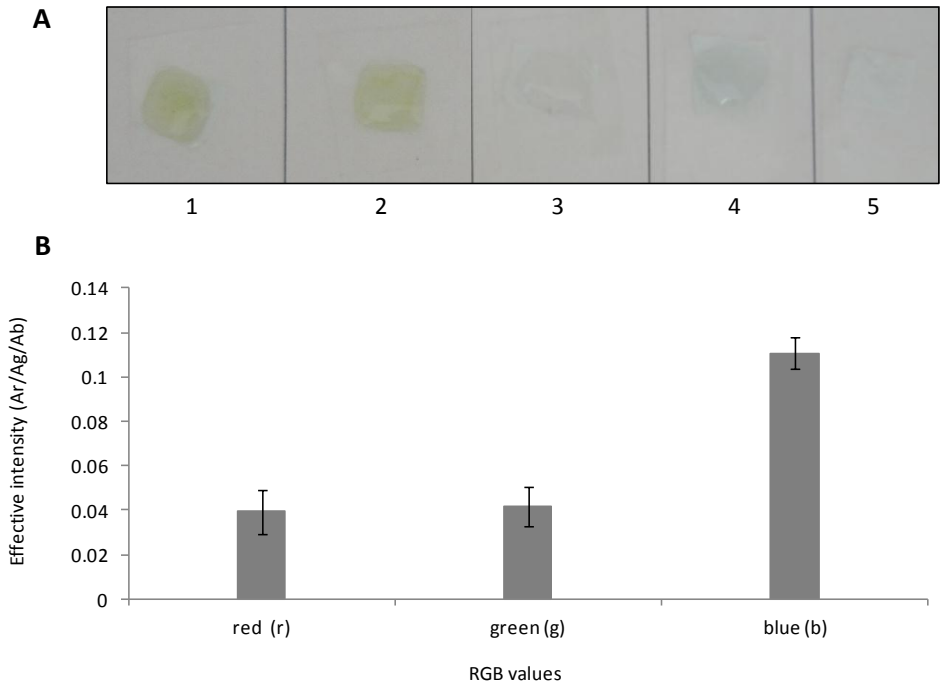


**Figure 5.7:** Macroscopic images showing the visual colorimetric response for glyphosate-complex formation on copper doped PVA nanofibers **(A1 and A2)** together with glyphosate **(A3)**, carbon disulfide **(A4)** and blank strip/no test **(A5)** controls. The effective color intensity values for the sensor strip were calculated following the extrapolation of RGB values using Adobe Photoshop CS5.1. Images were taken immediately after the addition of the glyphosate (1000 µg/ml) sample (Volume: 30 µl) using a SONY Cybershot digital camera. Values are presented as mean values ±SD (n=2).

The proof of concept study for the determination of glyphosate using a copper doped nanofiber based chemical sensor was successful. A color change from blue to yellow was observed (Figure 5.7A) immediately (approximately 3 seconds) upon the application of the glyphosate

dithiocarbamate sample to the copper doped PVA chemical sensor. No color change was observed in the negative controls used in this study (glyphosate and carbon disulfide) and therefore it can be concluded that the color reaction observed in the test samples was due to glyphosate-copper complex formation. The effective intensity of the RGB values was calculated for the duplicate test samples and results (Figure 5.7B) indicated that the R (0.04 ± 0.009) and G (0.04 ± 0.009) values demonstrated lower sensitivity when compared to the B value (0.11 ± 0.007).

### 5.4.3 Optimization studies

The effect of pH (5-12) and carbon disulfide concentration (0-7 %) on glyphosate determination was evaluated (Figure 5.8) to determine the optimal conditions required for glyphosate detection.

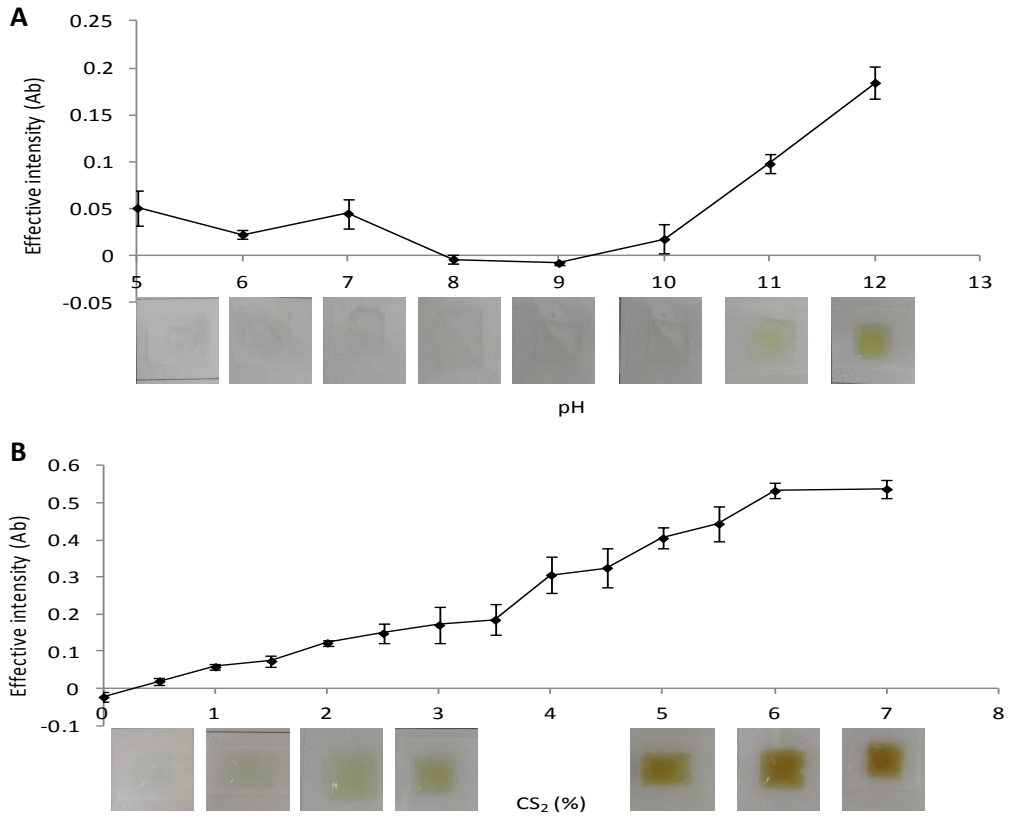


**Figure 5.8:** The optimization curves for the glyphosate nanofiber-based chemical sensor with respect to **A:** pH and **B:** carbon disulfide concentration (%). Corresponding macroscopic images demonstrating color progression on the sensor strip at varying pH values and carbon sulfide concentrations are shown below the relevant curve. Data points represent mean values ± SD (n=3) and appropriate controls were used in this study.

Glyphosate sensor detection demonstrated a strong dependence towards the pH (Figure 5.8A). The results were comparable to those obtained for the scale-down method. Optical (visual color change) and quantitative assessments indicated that glyphosate determination was optimal under highly alkaline conditions (pH 11 and 12) and the optimal pH value selected for future studies was pH 12.

The effect of carbon disulfide concentrations on glyphosate detection was characterized by an increase in effective intensity with increasing concentrations of carbon disulfide up to 6 % at which point no further increase was observed (Figure 5.8B). Upon evaluation of the macroscopic

images, color intensity increase was observed up to 5 % after which it was difficult to determine the differences in color change, this is due to the poor resolving power of the naked eye (Ding *et al.*, 2011b) and demonstrates the importance of using both optical and quantitative analysis in sensor studies based colorimetric detection. The results of this study were not similar to those obtained for the scale-down method (i.e. no decreasing trends were observed) and a higher optimal carbon disulfide concentration (6 %) was selected for future studies.

## 5.5 Discussion and future work

### 5.5.1 Nanofiber morphology and partial characterization

Several factors are known to affect the electrospinnability of a polymer solution and the resultant nanofiber morphology, and these include polymer concentration, the polymer molecular weight, solution viscosity, solution surface tension, applied voltage, electrical field, flow rate, solution volatility and environmental conditions such as humidity and temperature (Thompson *et al.*, 2007; Shenoy *et al.*, 2005). At the time of this study environmental conditions could not be kept consistent as the required facilities were unavailable, however governing parameters such as flow rate, polymer concentration, needle tip to collector distance and voltage were selected for manipulation to determine the appropriate conditions required for nanofiber and nanofiber mat formation (Table 5.1). Electrospinning parameters which resulted in successful nanofiber formation and nanofiber mat formation were observed under the following conditions: a PVA (> 99 % hydrolyzed, average molecular weight: 146,000-186,000 g/mol) concentration of 7.5 % (w/v), a needle tip to collector distance of 15 cm, a flow rate of 0.5 ml/hour and a voltage of 30 kV. Electrospinning parameters assessed in this study are generally interconnected and the resulting nanofiber produced is primarily due to the synergistic effects of the differing parameters; however to date the exact mechanisms of fiber formation are not entirely understood (Rošic *et al.*, 2012).

Overall a polymer solution can be electrospun if during the application of an electrical field electrostatic forces overcome the surface tension of the polymer solution causing the formation of a Taylor cone and the subsequent release of the solution jet which remains undisrupted (not broken) until the solid fibers are formed (Garg and Bowlin, 2011, Reneker and Chun, 1996).

Considering this criteria, polymer solution characteristics (e.g. polymer concentration, polymer molecular, polymer solution viscosity weight, conductivity and surface tension), have been highlighted in literature as one of the most critical parameters in nanofiber production (Deitzel *et al.,* 2001; Rošic *et al.,* 2012). Studies by Tan *et al.* (2005) evaluated the effect of solution properties, processing conditions and ambient conditions on nanofibers spun from poly ($_L$-lactid-*co*-caprolactone) and poly ($_L$-lactid acid) polymer solutions and the results observed reflected the importance of polymer solution characteristics on nanofiber production, with the study concluding that polymer solution characteristics which included polymer concentration and molecular weight were dominant parameters for fiber formation and the resulting nanofiber morphology. Tao and Shivkumar (2007) demonstrated the dependence of PVA nanofiber morphology on the molecular weight of PVA. The scope of this study was to produce defect free (non-beaded) nanofibers as scaffolds for chemical sensor development, therefore underlying mechanisms for resultant nanofibers produced were not fully explored, however conclusions could be drawn based on valid assumptions of the viscosity of the polymer solution at varying concentrations and surface tension effects based on the degree of hydrolysis of the PVA polymer.

Polymer solution concentration and molecular weight, which undoubtedly determine the viscosity of the solution, are extremely important factors, which play a key role in the stabilization and formation of nanofibers and the resultant nanofiber morphology (Koski and Shivkumar, 2004; Tan *et al.,* 2005). Generally, the viscosity of a polymer solution should be high enough in conjunction with electrostatic repulsion in order to overcome forces due to surface tension and, depending on the solution concentration, molecular weight and degree of hydrolysis of PVA, a minimum concentration of the polymer is necessary for fiber formation and maximum concentrations exist where the solution can no longer be electrospun (Koski and Shivkumar, 2004; Tiwari and Venkatraman, 2012). The surface tension of PVA polymers is extremely dependent on the degree of hydrolysis of PVA and a degree of hydrolysis near 100 % is characterized by high surface tension (Yao *et al.,* 2003).

Results of the present study indicated that the minimum PVA concentration required for successful nanofiber mat formation was 7.5 % with a few beads being observed (Figure 5.4A1). Based on visual observations the application of an electrical field to polymer solutions below this

concentration (Table 5.1) resulted in the formation of droplets (electrospray) and splatter effects on the collection screen, which may have been predominantly due to the low polymer viscosity which, together with the electrostatic forces, may have not been sufficient enough to overcome forces due to high surface tension, which resulted in the breakage of the solution jet and droplet formation (Huang *et al.*, 2003; Lee *et al.*, 2003). Some authors have documented similar effects to those observed in this study in different polymers. Results reported by Gupta *et al.* (2005), based on using the electrospinning process for the production of poly(methylmethacrylate) nanofibers, indicated that dilute polymer solutions caused droplet formation, which was reportedly due to insufficient chain entanglement and, as polymer solution concentrations were increased, the appearance of uniform fibers and beads were observed. Ki *et al.* (2005) indicated combined bead and fiber formation in the production of gelatin nanofibers at a 7 % wt concentration.

The formation of beads in the PVA nanofiber was attributed to jet instabilities (solution jet deformation) and studies by Fong *et al.* (1999) confirmed that this was an effect of the inverse relationship between surface tension and viscosity. At low polymer solution concentrations the surface tension is higher. High surface tension would cause jet instabilities (Raleigh instability), (i.e. the capacity of the jet to retain its shape is lowered at the capillary tip, causing the formation of bead structures within nanofibers). The theory that bead formation could be reduced with increased polymer concentration (solution viscosity) and subsequent decrease in surface tension is well established and has successfully yielded uniform fibers in literature (Huang *et al.*, 2001; Safi *et al.*, 2007; Yu *et al.*, 2004). In the current study, polymer solution concentrations above 7.5 % (8-12 %) may have produced (visual observation) minimal fibers on the collection screen (Table 5.1), however increasing polymer concentrations (above 7.5 %) failed to result in collectable nanofiber mats, with severe needle blockage occurring during electrospinning. This strongly suggests that a continued increase in the viscosity (higher polymer concentrations) of the PVA polymer solutions inhibited nanofiber mat formation. The lack of nanofiber mat production and needle blockage may be explained by the limited continuous flow of the polymer solution to the capillary tip and the drying of polymer droplets at the needle tip preventing continued jet release and suppressing electrospinning (Lee *et al.*, 2003; Pham *et al.*, 2006). Although the working range for electrospinning PVA nanofibers was extremely narrow, collectable fiber mat formation was achieved. A more recent study by Zuo *et al.* (2005)

suggested that bead formation may not only be affected by surface tension effects but by other parameters as well including the solution flow rate and conductivity. Similar findings were observed by Uyar and Besenbacher (2008) which highlighted the continued challenge in yielding non-beaded nanofibers and concluded that solution conductivity played a critical role in producing bead free nanofibers at low polymer solution concentrations. Zong *et al.* (2002) yielded uniform non-beaded nanofibers from poly ($_L$-lactid-*co*-caprolactone) and poly ($_L$-lactid acid) polymer solutions by increasing the polymer solution concentration and incorporating salt (NaCl) thereby increasing the charge density of the solution.

The addition of copper (3.35 % w/v) to the PVA electrospinning solution under the optimized parameters also resulted in successful nanofiber and nanofiber mat production and caused an alteration in the nanofiber morphology. The production of bead free copper doped PVA acetate nanofibers, using much higher copper concentrations (14 % wt), has been described in literature (Abu-Saied *et al.,* 2012), however results of the present study indicated that the addition of copper (3.35 % w/v) did not result in the production of non-beaded fibers. Interestingly, larger beads were observed in the copper doped PVA nanofibers when compared to pure PVA (Figure 5.4B1).

The incorporation of 1 % Triton-X successfully prevented bead formation during the electrospinning process for both pure PVA and copper doped PVA nanofibers (Figure 5.4A2 and B2). The improvement in nanofiber morphology may be explained by a decrease in the surface tension in the PVA polymer solution due to the inclusion of the non-ionic surfactant. Studies by Yao *et al.* (2003) are in agreement with the present findings. Fiber formation via electrospinning using fully hydrolyzed PVA (> 99 %, molecular weight: 115 000, 10 % wt) was only possible with the addition of Triton-X 100 (0.3 % wt) due to the lowered surface tension of the PVA polymer solution determined by contact angle measurements. Surfactants including Triton-X have been regularly used for the prevention/reduction of bead structures and for the improvement of uniformity in electrospun nanofibers and other authors have reported on the beneficial effects of surfactant inclusion into polymer solutions for fiber formation using the electrospinning process. The addition of Triton-X 100 (0.5 % wt) improved the uniformity of the co-axial fibers PLGA 80/20 (a copolymer of polylactic acid and polyglycolide)-PVA, due to a reduction in interfacial tension and the production of a stable Taylor cone (Tiwari and Venkatraman, 2012).

Similar findings were reported by Chronakis *et al.* (2006), with the addition of Triton-X 100 resulting in thinner and smoother polypyrrole (PPy)-PEO nanofibers, which was attributed to a decrease in surface tension. Although bead structures were still apparent, Bhattarai *et al.* (2005) reported that the addition of Triton-X 100 significantly improved Chitosan-PEO (polyethyleneoxide) nanofiber formation with the appearance of fibrous structures upon the inclusion of the surfactant. Lin *et al.* (2004) concluded that the addition of the cationic surfactants dodecyltrimethylammonium bromide (DTAB) and tetrabutylammonium chloride (TBAC) stopped the formation of beaded fibers during electrospinning of polystyrene due to increases in net charge density. The addition of Triton X®-405 reduced the number of beads formed in the polystyrene nanofiber.

The addition of Triton-X resulted in an alteration in the morphology of the pure PVA and copper-doped PVA nanofibers when compared to the nanofibers with no surfactant addition, however the resultant nanofibers presented similar morphologies. The addition of Triton-X 100 resulted in the formation of heterogeneous nanofibers characterized by long smooth fibers, flat branched fibers as well as smaller fibers which spilt from larger fibers (Figure 5.4A2 and B2). The appearance of varied fiber morphologies, (e.g. flat ribbons and flat branched nanofibers), have been well established in literature (Huang *et al.*, 2003; McCann *et al.*, 2006; Yuan and Su, 2004) with the morphologies being attributed to different factors including fluid mechanical effects and electrical charges during electrospinning (Frenot and Chronakis, 2003). Due to the observed heterogeneity of the nanofiber mats, future studies would employ the use of one copper-doped PVA mat per experiment to reduce experimental variation. Although this would suffice at the scale of this study, the heterogeneity of the nanofiber mats produced may cause a greater impact when applying this technology at an industrial scale where the homogeneity of nanofibers may become more crucial. This is due to the fact that homogenous fibers provide better color homogeneity and purity which is an important factor to consider for the production of colorimetric chemical sensors in future scaling-up studies (Ding *et al.*, 2011b).

The frequency plots for pure PVA and copper-doped PVA nanofiber mats suggest that the addition of the copper PVA polymer solutions slightly improved the overall quality of the nanofiber mats produced. Copper inclusion resulted in a relatively narrower size distribution and a reduction in the average fiber diameter (1.1 fold reduction), (i.e. the average fiber diameters for

pure PVA and copper-doped PVA mats were 0.43 ± 0.22 and 0.39 ± 0.09 μm, respectively) (Figure 5.5). The reasons for the wide nanofiber diameter distribution observed for the pure PVA mat are not entirely clear. The presence of varied nanofiber diameters in an electrospun mat is a regular occurrence in literature, however there is no common theory (Malašauskiené and Milašius, 2010) to explain these observations. This is largely due to the intrinsic complexity of the electrospinning process (Lukás *et al.*, 2009). Resultant nanofiber diameter sizes are governed by several factors, including polymer type, molecular weight, concentration and applied voltage (Malašauskiené and Milašius, 2010). Therefore, the combination of these factors most likely explain the wide nanofiber diameter distribution observed in pure PVA.

Larger fiber diameters observed for both mats (≥ 0.8 μm) were attributed to the large flat branched fibers. The average fiber diameters for pure PVA are in agreement with reports in literature (Lee *et al.*, 2004). Tao and Shivkumar (2007) reported fiber diameter sizes ranging from 0.2 to 0.4 μm in electrospun PVA nanofiber mats obtained at varying concentrations (0-40 %) as well as varying molecular weights (9,500-155,000 g/mol). Su *et al*. (2011) demonstrated the beneficial properties of metal ion incorporation into polymer solutions while investigating the doping effects of chloride salts on monovalent ($Na^+$, $K^+$), bivalent ($Ca^{2+}$, $Sr^{2+}$, $Zn^{2+}$, $Mg^{2+}$, $Fe^{2+}$) and trivalent ($Fe^{3+}$) metal ions on the spinnability of chitosan-PEO blended nanofibers, with results indicating a reduction in fiber diameter together with the removal of bead structures upon the inclusion of calcium and iron ions.

The results of the IR spectrum (Figure 5.6 and Table 5.2) obtained for pure PVA and copper-doped PVA nanofibers demonstrated evidence for the interaction of copper and PVA, with the band weakening observed in the band corresponding to hydroxyl groups on the PVA and the relatively large peak shift (to a lower wavenumber) in the band assigned to $CH_2$ and OH groups, suggesting the possible co-ordination of copper with the hydroxyl groups on the PVA structure. The co-ordination of copper and the hydroxyl groups found on PVA has been supported in literature. Relatively similar results were observed by Li *et al*. (2009) in the FTIR spectral analysis of PVA-silica hybrid polymers doped with copper (as a copper chloride salt), with lowered peak intensities being observed (with increasing concentrations of copper) (2, 4 and 20 %) in the bands assigned to hydroxyl groups (3248 $cm^{-1}$) and deformation vibrations of hydroxyl groups (1562 $cm^{-1}$). This study hypothesized that copper co-ordinated with the hydroxyl groups

on PVA through a deprotonation reaction, whereby the lone electrons on the hydroxyl groups of PVA entered into the empty orbits of copper, resulting in a decrease in hydroxyl groups. In contrast, Makled *et al.* (2013) suggested the presence of increasing concentrations of copper iodide (5, 7.5, 10 and 15 %) in PVA-copper iodide (CuI) composite fibers did not reflect large changes in vibration bond positions of PVA, however there was evidence that copper addition affected the strength of the hydrogen bonding on hydroxyl groups. Other authors have presented theories on the co-ordination of copper and hydroxyl groups on PVA. Earlier findings by Yokoi *et al.* (1986) proposed that this interaction was hydrophobic and characterized by the solubilization, stabilization and encapsulation of copper by the PVA chains, resulting in the hydrophilic hydroxyl groups facing outwards and the hydrophobic backbones facing inwards. A more recent study by Tomita *et al.* (1996) however suggested that this interaction is due to the direct complexation/chelation of copper ions with two adjacent hydroxyl groups on the PVA structure.

### 5.5.2 Proof of concept study and optimization studies

The nanofiber based chemical sensor (copper-doped PVA) developed in this study successfully detected the presence of glyphosate at 1000 μg/ml as demonstrated by the results in Figure 5.7A. Color change from blue to yellow was observed immediately upon the injection of the glyphosate dithiocarbamate intermediate (volume: 30 μl) at a volume 4 fold lower than was required in the scale down method. The immediate reaction observed upon the application of the glyphosate dithiocarbamate sample at a low sample volume, appears to be due to the increased availability of metal ions for the ligand which may be due to the increased contact ratio as a consequence of the large surface area to volume ratio provided by the PVA nanofibers (Chigome and Torto, 2011; Huang *et al.*, 2002). No color alteration was observed in the negative controls which further validated the proof of concept. Although FTIR analysis evidenced the possible coordination of copper with the hydroxyl groups on the PVA structure, the positive signal observed suggests that sufficient copper ions were still accessible for complex formation with the glyphosate dithiocarbamate intermediate. Although the effective intensity of the representative R, G, B colors provided a signal in the detection of glyphosate, the effective intensity of the blue color value was selected as the reference for future studies as it demonstrated the greatest

sensitivity when compared to the R and G values (Figure 5.7B). Similar results were reported by Dakashev *et al.* (2013) using the tristimulus (RGB) values in the evaluation of a yellow colored complex ferric sulphosalicyclic acid for the determination of iron. The B value demonstrated significant changes in comparison to the R and G values and the authors emphasized the use of the most sensitive tristimulus value (B value) with respect to improving the analysis of the colorimetric data.

The effect of pH and carbon disulfide concentration on the detection of glyphosate was evaluated. Similar results were obtained with respect to pH conditions when compared to the scale-down method (please refer to Chapter 4, section 4.4.3, Figure 4.4). Highly alkaline conditions favored the formation of the glyphosate dithiocarbamate-copper complexation due to the deprotonation of the amine group in the glyphosate structure (Maqueda *et al.*, 1998; McConnell and Hossner, 1985; Morillo *et al.*, 2000, Sheals *et al.*, 2002), therefore pH 12 was selected as the optimal pH for future studies. The optimal carbon disulfide concentration was observed at 6 %, above which no further increases in signal response were observed and the system reached saturation possibly due to the available binding sites on glyphosate being fully occupied.

## 5.6 Conclusions

- The production of defect free (non-beaded) copper-doped PVA nanofiber mats as colorimetric chemical sensors for glyphosate detection was successful.
- A copper-doped PVA (cd-PVA) sensor successfully detected glyphosate in water. The addition of small sample volume (30 μl) of glyphosate dithiocarbamate (1000 μg/ml) resulted in a rapid positive detection signal for glyphosate.
- The optimal conditions for the sensor system were observed at a pH of 12 and a carbon disulfide concentration of 6 %.

In Chapter 6 the method validation for the sensor system is investigated and compared to the scale-down system, other existing spectrophotometric detection systems, and colorimetric chemical sensor systems currently available for glyphosate detection.

# CHAPTER 6- NANOFIBER-BASED COLORIMETRIC SENSOR FOR GLYPHOSATE (CD-PVA SENSOR): METHOD VALIDATION

## 6.1 Introduction

Colorimetric chemical sensors are attractive tools for the determination of various environmental pollutants, as these systems provide visual (naked eye), on-site, real time qualitative or semi-qualitative detection, which is easily quantifiable through the use of (e.g. digital cameras or scanners) (Cate *et al.,* 2014; El-Safty and Shenashen, 2012; Kreno *et al.,* 2011). This is particularly important for developing countries, such as South Africa, where the use of expensive equipment and skilled technicians for the analysis of compounds is often a financial limitation (Zhao *et al.,* 2008). Analytical method validation (also known as suitability testing) is defined as the investigation of various analytical parameters of a proposed method, towards proving the suitability of the method for its intended purpose and involves obtaining results within satisfactory uncertainty levels (González and Herrador, 2007; Green, 1996; Taverniers *et al.,* 2004). The quality of an analytical system is evaluated based on several criteria, which include cost, simplicity of operation/analysis, sensitivity, specificity, selectivity, accuracy (reproducibility and precision), applicability and stability (Araujo, 2009; El-Safty and Shenashen, 2012, Shrivastava and Gupta, 2011).

Initial studies (refer to Chapter 5) involved the development and optimization of the copper doped-PVA (cd-PVA) nanofiber sensing system. These studies revealed the successful validation of the proof of concept and the sensor system parameters were optimized with respect to pH and carbon disulfide concentration. The main aim of this Chapter was to determine the analytical quality of the cd-PVA sensor system, to obtain useful and valuable insights into the benefits and possible limitations of this system. The analytical information obtained in this study would also determine the practicality of the cd-PVA with regards to its use.

## 6.2 Objectives

- To evaluate the color development time and color stability of the cd-PVA sensor system.
- To determine the storage stability of the cd-PVA sensors under two different storage conditions (4 ºC and 23 ºC, i.e. room temperature).
- To investigate the accuracy of the cd-PVA sensor system. The accuracy of the system was determined by assessing the intra-assay (precision) and inter-assay variability (reproducibility).
- To determine the sensitivity (calibration studies), specificity (structural analogs), selectivity (interfering species) and applicability (recovery) of the cd-PVA sensor system.

## 6.3 Methods and materials

### 6.3.1 Materials

Please refer to the chemical list in Appendix I for all the materials and chemical suppliers used in this study. All glyphosate stocks were prepared freshly (refer to Chapter 3, Section 3.3.1) before any experimental studies.

### 6.3.2 Color development time and color stability of cd-PVA sensor system

To investigate the color development time and color stability of the cd-PVA sensor system, 30 µl of the glyphosate dithiocarbamate intermediate (1000 µg/ml) sample was injected onto the cd-PVA sensor strips and the effective intensity ($A_b$) was measured at varying time intervals, over a period of 5 hours. Three negative controls were used in this study (glyphosate, carbon disulfide and a blank strip).

### 6.3.3 Cd-PVA sensor system storage stability

The storage stability of the cd-PVA sensor was evaluated under two different storage conditions, at 4 ºC (in the refrigerator) and 23 ºC, over a period of 24 days. A volume of 30 µl of the glyphosate dithiocarbamate intermediate sample was injected onto the cd-PVA sensor strips and the effective intensity ($A_b$) measurements were determined at 3 day intervals. The cd-PVA sensor strips were stored in foil wrapped containers (in the dark) for the entire duration of this experiment. Three negative controls were used in this study (glyphosate, carbon disulfide and a blank no test strip).

### 6.3.4 Cd-PVA sensor system precision and reproducibility

The reproducibility and precision of the cd-PVA sensor system was investigated by determining the inter-assay variation (consisted of 8 replicates) and the intra-assay variability (consisted of 40 replicates). The reproducibility and precision of the system was determined at two different glyphosate concentrations, at 1000 and 400 µg/ml, respectively. These concentrations were selected to represent the highest maximum concentration of glyphosate used in the current study and a concentration representing an upper limit concentration of the standard curve produced for pure glyphosate. Three negative controls were used in this study (glyphosate, carbon disulfide and a blank no test strip).

Data was presented as % RSD (calculated according to the equation in Chapter 4, section 4.3.7) and mean % RSD. The average relative sensor response (RSR) within the cd-PVA nanofiber mats was also determined based on the fraction of the response values obtained at 400 µg/ml against the response values obtained at 1000 µg/ml. The RSR was used a measure of internal consistency for the cd-PVA sensor system and was calculated according to equation 1.

$$RSR\ (\%) = \text{Average}\ (R_{v\ (400\ \mu g/ml)}/R_{v\ (1000\ \mu g/ml)})*100 \qquad (1)$$

where RSR is the average relative sensor response, $R_{v\ (400\ \mu g/ml)}$ are the response values obtained at 400 µg/ml of pure glyphosate and $R_{v\ (1000\ \mu g/ml)}$ are the response values obtained at 1000 µg/ml of pure glyphosate. The ideal RSR was theoretically assumed to be 40%.

### 6.3.5 Glyphosate standard curve (cd-PVA system sensitivity)

Calibration curves were constructed for pure glyphosate (0.01-500 μg/ml) and glyphosate in Ro (1.95-500 000 μg/ml) and Wo (1.95-500 000 μg/ml). The system sensitivity was evaluated based on the practical limit of detection (practical LOD) (μg/ml) and the precision (% RSD). Other calibration characteristics determined for the cd-PVA system included the linear range, $R^2$, intercept and slope. The practical LOD, included in this study, represented the lowest glyphosate concentration that caused a visual color alteration in the cd-PVA sensor, which could be differentiated from the controls (Abbaspour *et al.,* 2010; Wang *et al.,* 2011). Three negative controls were used in this study (glyphosate, carbon disulfide and a blank no test strip).

### 6.3.6 Application of cd-PVA sensor system (recovery)

Glyphosate concentrations selected for the recovery study were based on the mid-range concentration and lower range concentration of the calibrations curves (linear range) constructed for pure glyphosate (200 μg/ml and 60 μg/ml) and glyphosate in the formulations Wo ($250 \times 10^3$ μg/ml and $65 \times 10^3$ μg/ml) and Ro ($250 \times 10^3$ μg/ml and $65 \times 10^3$ μg/ml). Environmental water samples were collected from two environmental water systems namely, Grey Dam (Grahamstown, Eastern Cape, South Africa) and Swartkops estuary (Port Elizabeth, Eastern Cape, South Africa) (Figure 6.1).

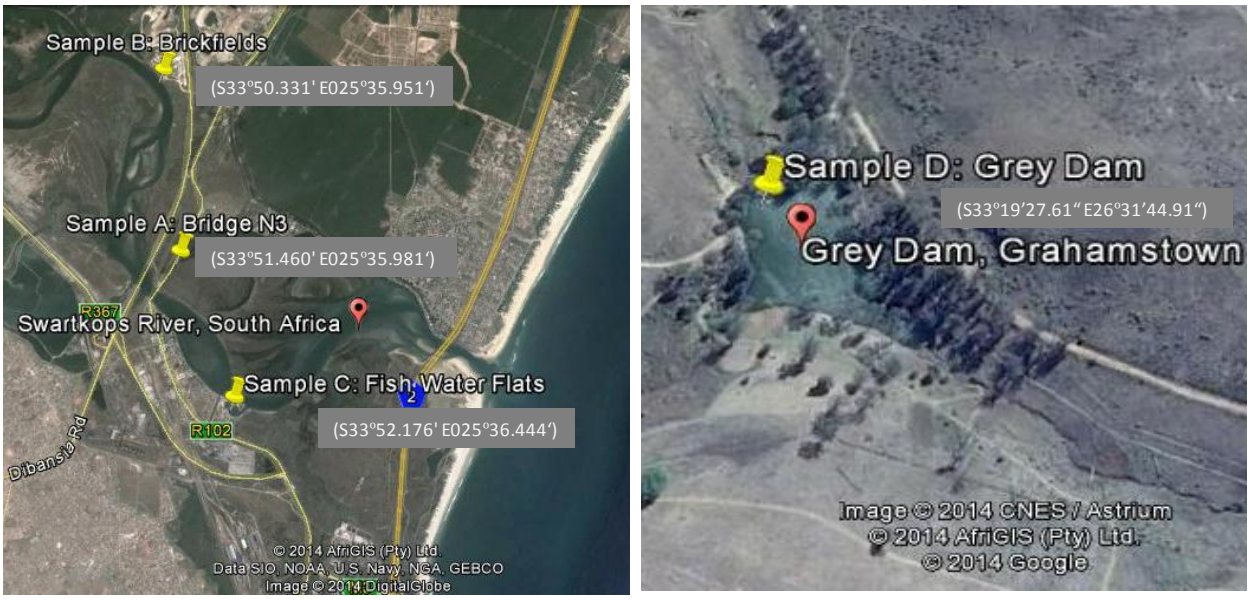


**Figure 6.1:** Map of the Swartkops estuary in Port Elizabeth, Eastern Cape, South Africa **(1)** and Grey Dam **(2)** showing the sampling sites. Three representative samples collected from the Swartkops estuary, sample A: Bridge N3, sample B: Brickfields and sample C: Fishwater flats. One representative sample was collected from Grey Dam, sample D: Grey Dam. Images were obtained using Google Earth and the Global Positioning System (GPS) coordinates for each sampling site is indicated in brackets.

A control water sample (distilled water) representative of pristine water was included in this study. Environmental water samples were collected in glass Schott bottles and stored at 4º C until further analysis (analysis was carried out within 24 hours of water sample collection). Water samples were filtered (Munktell filter paper, 3 HW 125 mm) to remove large sediments and no other pre-treatment strategies or pre-concentration methods were employed in this study. Water samples were spiked with the afore mentioned concentrations of pure glyphosate and glyphosate in formulation (Wo and Ro) and the recovery (%) of the cd-PVA sensor system was investigated. The concentration of glyphosate recovered from the water samples was calculated based on the regression equation for the linear range of the calibration curve ($y = mx + c$). Three negative controls were used in this study (glyphosate, carbon disulfide and a blank no test strip).

Recovery (%) was determined based on the following equation:

$$\text{Recovery (\%)} = [\text{Glyph}_{\text{recovered}}]/ [\text{Glyph}_{\text{spiked}}] \times 100 \quad (1)$$

where $[\text{Glyph}_{\text{recovered}}]$ is the recovered concentration of glyphosate determined using the regression equations and $[\text{Glyph}_{\text{spiked}}]$ is the spiked glyphosate concentration.

Recovery values between 70 % (minimum) and 120 % (maximum) were considered acceptable (Vogelgesang and Hädrich, 1998) in this study.

### 6.3.7 Cd-PVA sensor system specificity (structural analogs)

The specificity of the cd-PVA sensor system for glyphosate was investigated by determining the sensor response of the system towards the glyphosate structural analogs, aminomethyl phosphonic acid (AMPA) and glycine. Three different solutions containing equivalent concentrations of glyphosate, glycine and AMPA (1000 μg/ml) were prepared and combined with carbon disulfide (6 %) for the formation of the dithiocarbamate intermediates. Thirty μl of the dithiocarbamate samples were then injected onto the cd-PVA sensor strips and analyzed. Three negative controls were used in this study (glyphosate, carbon disulfide and a blank no test strip).

### 6.3.8 Cd-PVA sensor system selectivity (interference study)

The effects of varying concentrations of metal ions (magnesium, calcium, iron, potassium, manganese and zinc), anions (chloride, sulfate) and other chemical compounds (citric acid and ethylenediaminetetraacetic acid/EDTA) commonly found in aquatic systems on the detection of pure glyphosate and glyphosate in formulation (Ro and Wo) were investigated. Concentrations selected for this study were based on the regulatory standards for these ions in South African environmental water systems (DWAF, 1996). Table 6.1 indicates the regulatory limits for glyphosate in South African environmental waters and concentrations above and below these limits were also included in this study.

**Table 6.1:** The South African regulatory standards for different metal ions and anions in environmental water systems, together with the representative salts used in the interference study.

| Compound | Metal ion/ anion | Compliance limit (µg/ml) |
|---|---|---|
| Magnesium chloride | Magnesium ($Mg^{2+}$) | 50 |
| Calcium chloride | Calcium ($Ca^{2+}$) | 1000 |
| Ferrous sulfate | Iron ($Fe^{2+}$) | 10 |
| Potassium chloride | Potassium ($K^{+}$) | 10 |
| Manganese sulfate | Manganese ($Mn^{+}$) | 10 |
| Zinc sulfate | Zinc ($Zn^{2+}$) | 20 |
| Sodium chloride | Chloride ($Cl^{-}$) | 2000 |
| Sodium sulfate | Sulfate ($SO_4^{2-}$) | 500 |

No regulatory limits were available for the compounds EDTA and citric acid; therefore the concentrations selected for these compounds were based on previous work (evaluation of interfering effects of compounds commonly found in South African water systems on the enzyme β-D-galactosidase) which was conducted by Wutor *et al.* (2007) and ranged from 50 to 200 µg/ml. Mid-range glyphosate concentration values (obtained from the standard curves) were selected for this study. Pure glyphosate (200 µg/ml), Ro ($250 \times 10^3$ µg/ml) and Wo ($250 \times 10^3$ µg/ml) were incubated with the relevant compounds and ions for 15 minutes at 24 °C before the samples were assayed for glyphosate. Three negative controls were used in this study (glyphosate, carbon disulfide and a blank strip).

### 6.3.9 Data analysis

All data were presented as mean values ± SD (n=3) unless stated otherwise. Where appropriate, ANOVA single factor analysis (Microsoft Excel) was used to determine significant differences with 95 % ($P \leq 0.05$) or 99 % ($P \leq 0.01$) confidence. RSD (%) values below 20 % were considered acceptable (Dos Santos *et al.*, 2013).

## 6.4 Results

### 6.4.1 Color development time and color stability of the cd-PVA sensor system

The color development time and the stability of color on the cd-PVA sensing area were monitored over a period of 5 hours following the injection of the glyphosate dithiocarbamate sample onto the cd-PVA sensor strips. The results are shown in Figure 6.2.

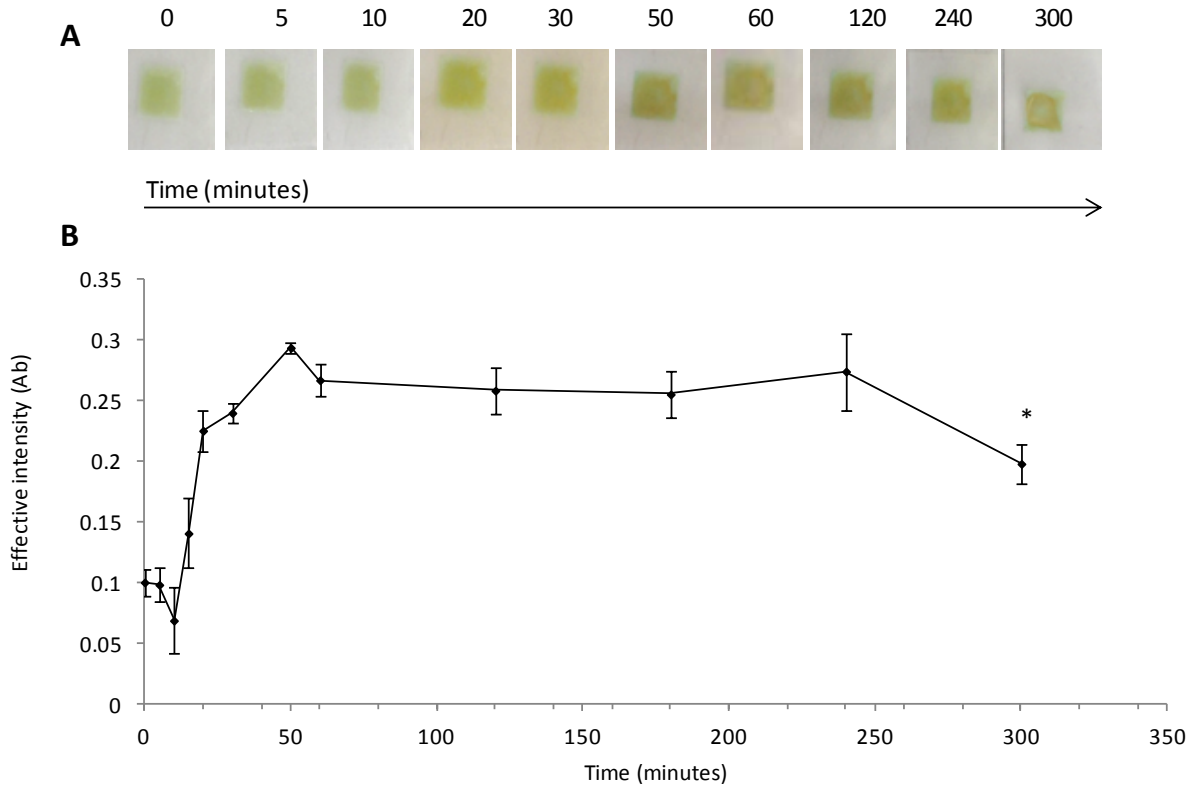


**Figure 6.2:** Macroscopic images **(A)** and the effective intensity **(B)** of color on the cd-PVA sensor strips after the injection of the glyphosate dithiocarbamate sample (30 µl) as a function of time. Values are presented as mean values ± SD (n=3). ANOVA single factor analysis was used to determine statistical significance: $^{*}$ $P \leq 0.05$. Appropriate controls were used in this study.

The optical (Figure 6.2A) and quantified (Figure 6.2B) results indicate that a yellow coloration was detectable immediately upon the injection of the glyphosate dithiocarbamate sample (t= 0 minutes). The initial trend observed was characterized by an increase in color intensity with an increase in time, over a total period of 50 minutes (0.29 ± 0.004). The initial increase was followed by a non-significant reduction in color at 60 minutes (P = 0.11) and no significant ( P > 0.05) changes in color were observed thereafter for up to 240 minutes (4 hours), which suggests that the color reaction of the cd-PVA sensor system was stable for up to 4 hours. A significant reduction in color intensity was observed at 5 hours (0.20 ± 0.02, 31.03% reduction when compared to the peak effective intensity). Although the greatest color intensity was observed after 50 minutes, based on the visual data, an increase in time resulted in greater color non-uniformity within the sensing area (from t= 30 minutes), therefore for future experiments, images captured for quantification were obtained at 5 minutes, to eliminate possible artifacts caused by heterogeneous coloration over the sensing area (Suslick *et al.*, 2004).

### 6.4.2 The storage stability of the cd-PVA sensor system

The shelf-life of the cd-PVA sensor strips was investigated and cd-PVA sensor strips were stored at 4 and 23 (room temperature) °C in the dark for 24 days. The results observed over the storage period are indicated in Figure 6.3.

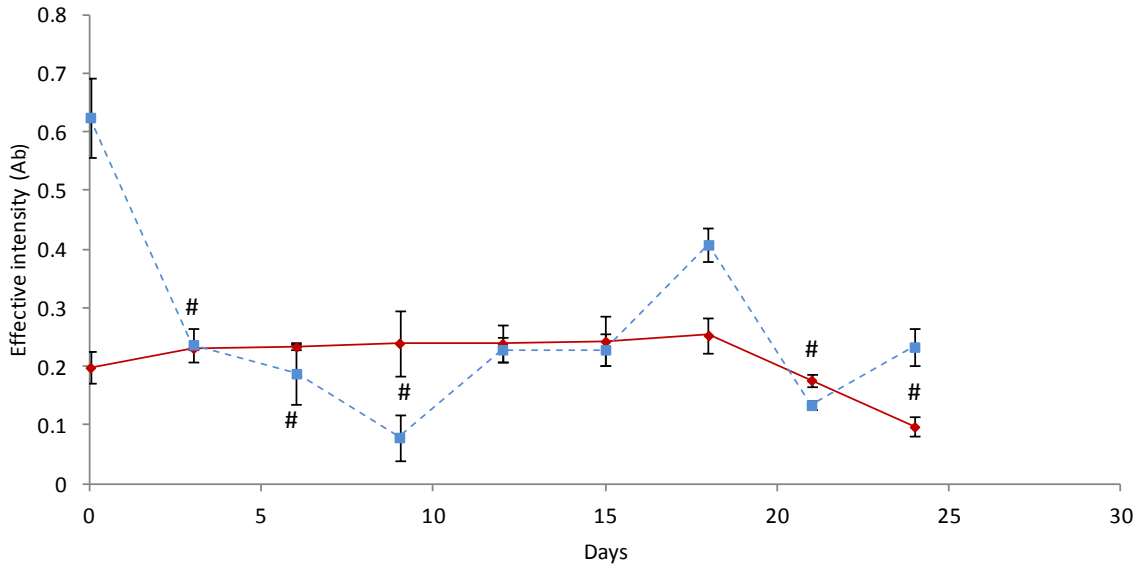


**Figure 6.3:** The effect of storage time on the cd-PVA sensor system at 23 (room temperature) °C (red solid line) and 4 °C (blue dash line) over a period of 24 days. The cd-PVA sensor strips were stored in the dark during the duration of this study. Values are presented as mean values ± SD (n=3). ANOVA single factor analysis was used to determine statistical significance: $^{*}P \leq 0.05$, $^{\#}P \leq 0.01$. Appropriate controls were used in this study.

Based on the overall results observed in Figure 6.3, the cd-PVA sensor strips demonstrated greater stability at 23°C when compared to 4 °C. The sensor strips displayed an erratic trend over the 24 day period at 4 °C, characterized by a significant decrease in the sensor response from day 0 (0.63 ± 0.07) to day 9 (0.07 ± 0.04, an 89 % reduction in sensor response was observed at day 9 when compared to day 0), which was followed by a fluctuation (decreasing and increasing trends) in glyphosate detection signals for the remainder of the study duration. The cd-PVA sensor strips were stable for 18 days at 23°C, with no significant changes in the detection of glyphosate ($P > 0.05$) being observed over this time period. The detection of glyphosate decreased significantly after a storage period of 21 (0.17 ± 0.01, 30 % reduction in sensor signal when compared to day 18) and 24 (0.09 ± 0.02, 64 % reduction in sensor signal when compared to day 18) days, respectively. The average signal RSD for glyphosate on cd-PVA sensors stored at 23 and 4 °C was 11.7 and 16.34 %, respectively, which further indicated the greater stability of this sensor system at 23 °C.

### 6.4.3 Cd-PVA sensor system precision (intra-assay variability) and reproducibility (inter-assay variability)

The reproducibility and precision of the cd-PVA sensing system was determined based on the analysis of inter (8 replicates, assay variation between mats) and intra (40 replicates, assay variation within the mat) assay variability obtained at 400 and 1000 μg/ml of pure glyphosate. Results are shown in Table 6.2.

**Table 6.2:** The reproducibility and precision of the cd-PVA sensor system evaluated at two different glyphosate concentrations (1000 and 400 μg/ml).

| **Parameter** | **[Glyphosate]**[a] | **Average**[b] | **SD**[c] | **RSD**[d] **(%)** | |
|---|---|---|---|---|---|
| Inter-assay variability | 1000 | 0.58 | 0.22 | **37.14** | |
| Inter-assay variability | 400 | 0.23 | 0.11 | **45.83** | |
| **Parameter** | **[Glyphosate]**[a] | **Mat No.**[e] | **Average**[f] | **SD**[c] | **RSD**[d] **(%)** |
| Intra assay-variability | 1000 | 1 | 0.34 | 0.12 | 5.84 |
| | | 2 | 0.33 | 0.06 | 17.19 |
| | | 3 | 0.47 | 0.10 | 21.22 |
| | | 4 | 0.54 | 0.05 | 8.67 |
| | | 5 | 0.61 | 0.10 | 16.46 |
| | | 6 | 0.68 | 0.07 | 10.89 |
| | | 7 | 0.71 | 0.11 | 14.77 |
| | | 8 | 0.98 | 0.09 | 9.36 |
| **Mean RSD (%)**[g] | | | | | **13.05 ± 0.08** |
| Intra assay variability | 400 | 1 | 0.11 | 0.02 | 20.67 |
| | | 2 | 0.12 | 0.02 | 14.90 |
| | | 3 | 0.17 | 0.01 | 7.01 |
| | | 4 | 0.22 | 0.03 | 14.16 |
| | | 5 | 0.24 | 0.06 | 23.80 |
| | | 6 | 0.26 | 0.07 | 25.06 |
| | | 7 | 0.32 | 0.02 | 5.39 |
| | | 8 | 0.43 | 0.07 | 16.48 |
| **Mean RSD (%)**[g] | | | | | **15.93 ± 0.04** |

[a:] Pure glyphosate concentration (μg/ml), [b:] Average effective intensity (n= 8) on cd-PVA sensor strips obtained from different mats, [c:] Standard deviation, [d:] Relative standard deviation, [e:] Electrospun mat number, [f:] Average effective intensity (n=5) of cd-PVA sensor strips obtained from the same mat, [g:] Mean relative standard deviation.

The results in Table 6.2 show higher RSD values (above 20 %) between electrospun mats (inter assay variation) when compared to the RSD values (below 20 %) obtained within electrospun mats (intra assay variation). Although the glyphosate sensor system reproducibility between mats was relatively low, the observed data suggests that better results would be obtained when using sensing strips from the same electrospun mat, as the system displayed good internal precision.

The relative response of the cd-PVA sensor system was calculated to determine the internal consistency of this system. The results are shown in Table 6.3.

**Table 6.3:** The relative response of the cd-PVA sensor system calculated as the percentage signal response produced at pure glyphosate concentrations of 400 μg/ml against 1000 μg/ml.

| **Mat No.**[a] | **Average Fraction**[b] | **RSR (%)**[c] |
|---|---|---|
| 1 | 0.31 ± 0.07 | 31.51 ± 6.38 |
| 2 | 0.37 ± 0.05 | 37.45 ± 4.85 |
| 3 | 0.38 ± 0.08 | 38.18 ± 10.03 |
| 4 | 0.41 ± 0.02 | 40.60 ± 2.66 |
| 5 | 0.39 ± 0.07 | 38.98 ± 6.47 |
| 6 | 0.039 ± 0.10 | 38.51 ± 8.84 |
| 7 | 0.46 ± 0.10 | 45.70 ± 12.29 |
| 8 | 0.44 ± 0.09 | 44.42 ± 10.02 |
| **Mean fraction** | **0.39 ± 0.08** | |
| **Mean RSR (%)**[d] | | **39.4 ± 3.16** |

[a:] Electrospun mat number, [b:] Average fraction (n=5) determined by equation: effective intensity$_{400\ \mu g/ml}$/effective intensity$_{1000\ \mu g/ml}$, [c:]Relative sensor response, [d:]Mean Relative sensor response.

The theoretical relative response (40 %) was comparable to the calculated relative sensor response of the cd-PVA system (39.4 ± 3.16 %) (Table 6.3), with a minor difference of ~ 0.6 %, which further validated the internal consistency of the sensing system when detecting glyphosate.

### 6.4.4 Calibration parameters

To investigate whether the cd-PVA sensor system could provide the qualitative and/or quantitative detection of glyphosate, the relationship of effective intensity over a wide range of concentrations of pure glyphosate (0.1- 500 μg/ml) and glyphosate in Ro ( $1.95 – 500 \times 10^3$) and Wo ($1.95 – 500 \times 10^3$) was established. Macroscopic images (Figures 6.4 and 6.6) were used to

demonstrate the optical colorimetric response on the cd-PVA sensor system and the graphical representation (quantified data) of calibration curves are shown in Figures 6.5 and 6.7.

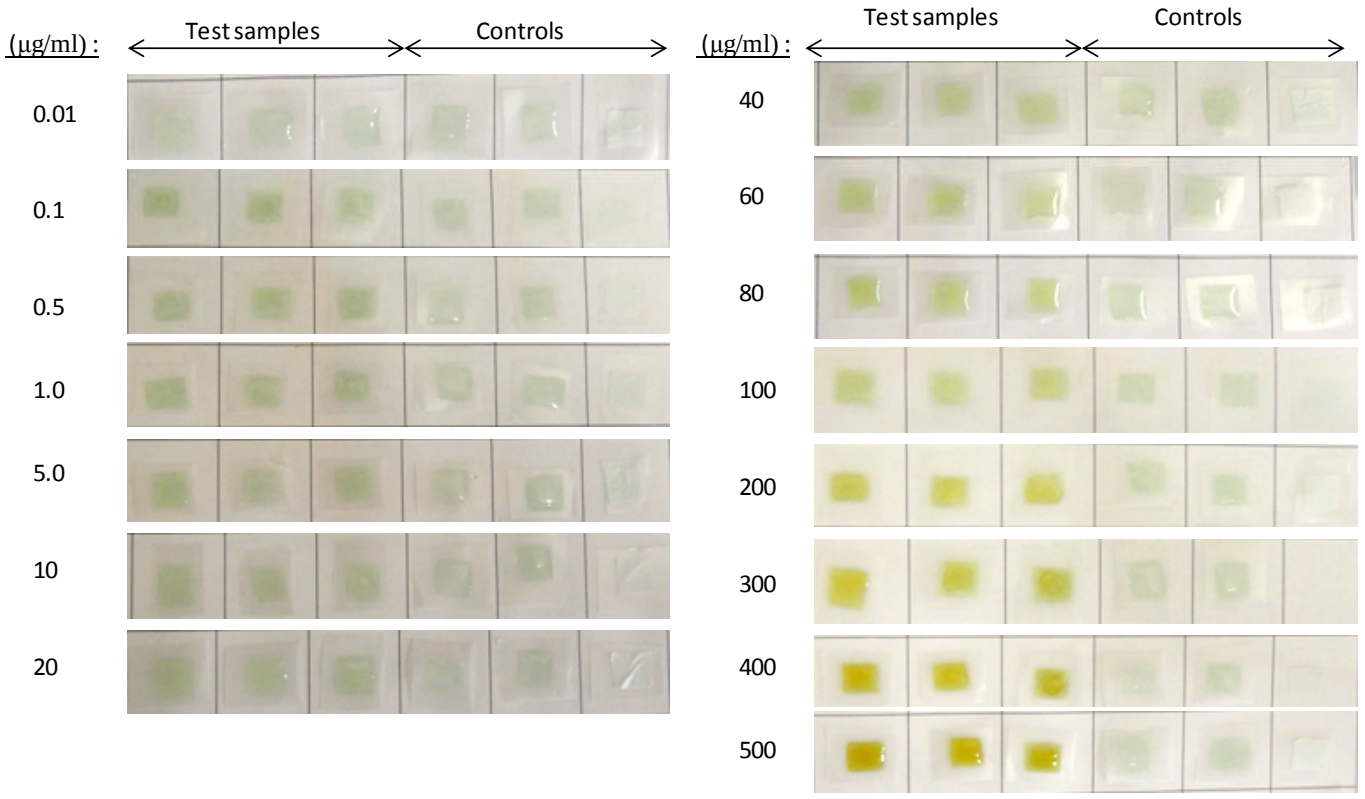


**Figure 6.4:** Macroscopic images demonstrating the optical colorimetric response of the cd-PVA sensor strips upon the injection of pure glyphosate (dithiocarbamate intermediate, sample volume: 30 µl) with a concentration range of 0.01-500 µg/ml.

Based on the qualitative analysis of optical results shown in Figure 6.4 the minimum target concentration of glyphosate that produced a change in color on the cd-PVA sensor strip, which was visually different from that of the controls, was 0.1 µg/ml (green-yellow coloration). This concentration was therefore considered the practical detection limit for the cd-PVA sensing system. Semi-qualitative analysis of the sensing system indicated that increasing concentrations of glyphosate from 0.1-20 µg/ml resulted in a relatively similar color alteration (no

differentiation in color between the different concentrations was optically observed), however further increasing glyphosate concentrations from 40- 500 µg/ml caused a gradual visual increase in the yellow color intensity on the cd-PVA sensing strips.

Figure 6.5 shows the calibration curve of pure glyphosate using the cd-PVA sensor system. Although glyphosate was detectable at levels as low as 0.1 µg/ml, concentrations of glyphosate between 0.1-40 µg/ml demonstrated non-linearity ($R^2$= 0.43) as shown in the inset figure. The linear response ($R^2$= 0.96) of the cd-PVA sensing system was observed at a glyphosate concentration range of 60-500 µg/ml.

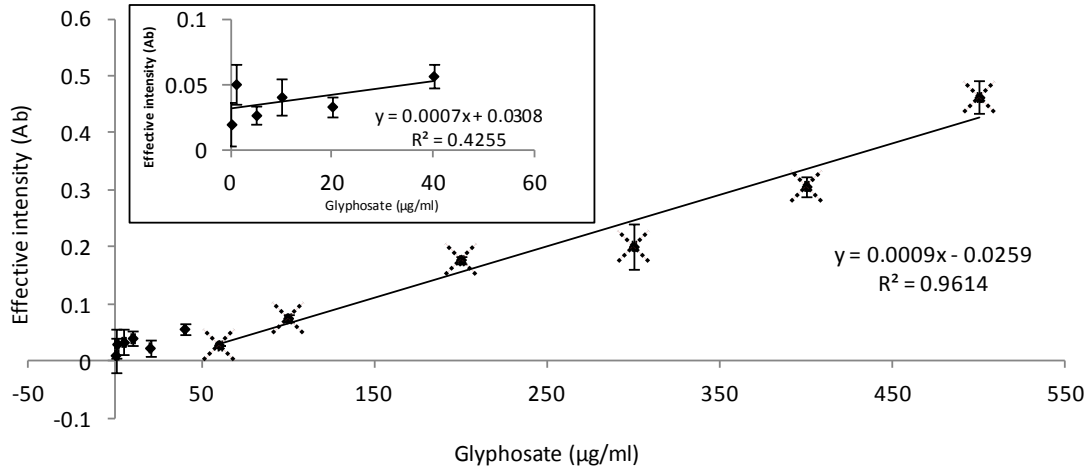


**Figure 6.5:** The effective intensity of cd-PVA sensor strips as a function of pure glyphosate (dithiocarbamate intermediate) concentrations. The linear regression equation and $R^2$ was extrapolated from the linear range of the calibration curve (60-500 µg/ml). The inset graph shows the linear regression equation and $R^2$ of pure glyphosate concentrations below the linear range of the calibration curve (0.1-40 µg/ml). Values are presented as mean values ± SD (n=3). Appropriate controls were used in this study.

The cd-PVA system was applied to glyphosate in the two formulations Ro and Wo. The macroscopic images, used to demonstrate the optical colorimetric response on the cd-PVA sensor system, and the calibration curves constructed for glyphosate in the formulations Ro and, Wo are shown in Figures 6.6 and 6.7 respectively.

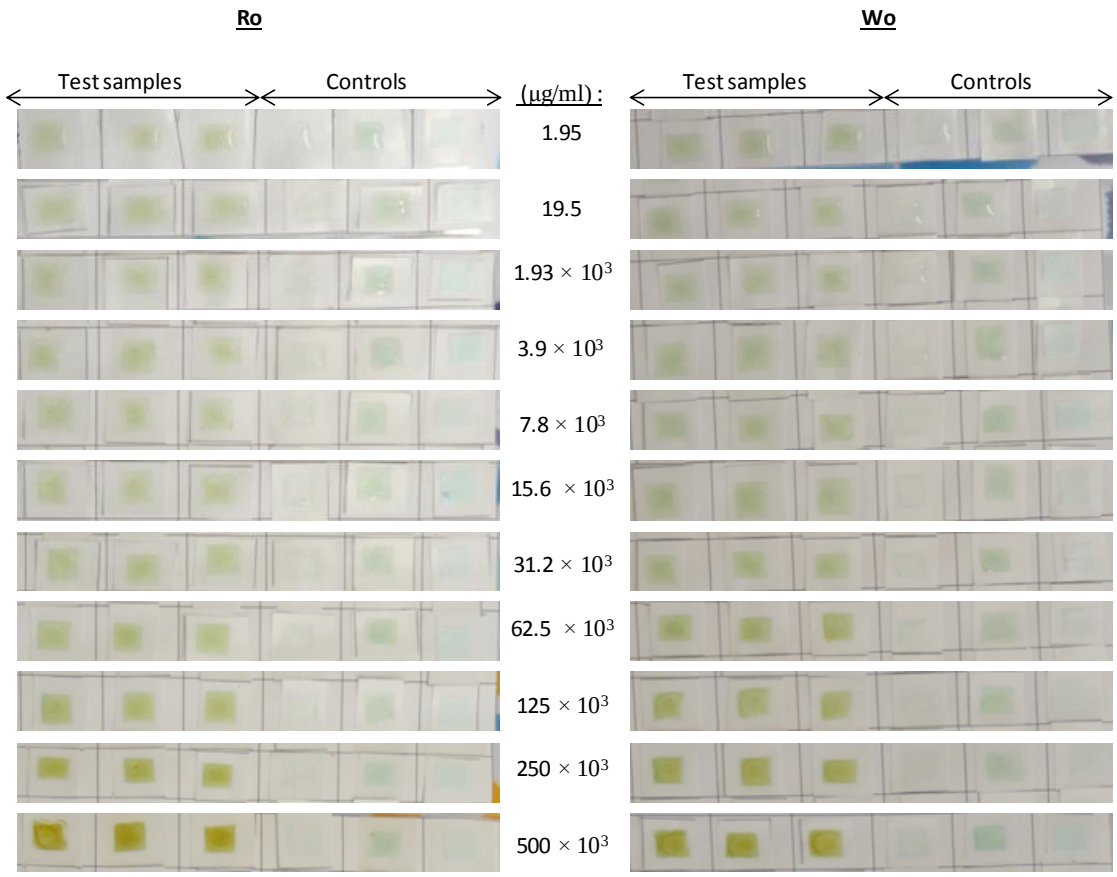


**Figure 6.6:** Macroscopic images demonstrating the optical colorimetric response of the cd-PVA sensor strips upon the injection of the glyphosate in the formulations Ro and Wo (glyphosate dithiocarbamate intermediate, sample volume: 30 µl) with a concentration range of 1.95- 500 × $10^3$ µg/ml.

The qualitative analysis of the colorimetric response of the cd-PVA sensor strips (upon the injection of glyphosate in the formulations Ro and Wo) at varying concentrations indicated that the practical detection limit for glyphosate was 1.95 µg/ml for both formulations (Figure 6.6). The practical detection limit for glyphosate in formulation was higher than that observed for pure glyphosate (0.1 µg/ml) (Figure 6.4). Semi-qualitative analysis of the cd-PVA sensor response to increasing concentrations of glyphosate revealed no clear differences in color intensity at glyphosate concentrations ranging between 1.95-15.6 × $10^3$ µg/ml and 1.95-7.8 × $10^3$ µg/ml for Ro and Wo, respectively. Glyphosate concentrations ranging from 15.6 × $10^3$- 500 × $10^3$ µg/ml

and $7.8 \times 10^3$- $500 \times 10^3$ μg/ml resulted in increasing yellow color intensities for glyphosate in Ro and Wo respectively.

Calibration curves were constructed for glyphosate in Ro (Figure 6.7A) and Wo (Figure 6.7B) and the linear range was observed at a glyphosate concentration range of $15.6 \times 10^3$- $500 \times 10^3$ μg/ml for Ro ($R^2$= 0.98) and $7.8 \times 10^3$- $500 \times 10^3$ μg/ml for Wo ($R^2$= 0.98). Glyphosate concentrations below the above mentioned linear range demonstrated non-linearity (inset figures), however based on the data obtained the cd-PVA system demonstrated the capacity to detect glyphosate at levels below the linear region.

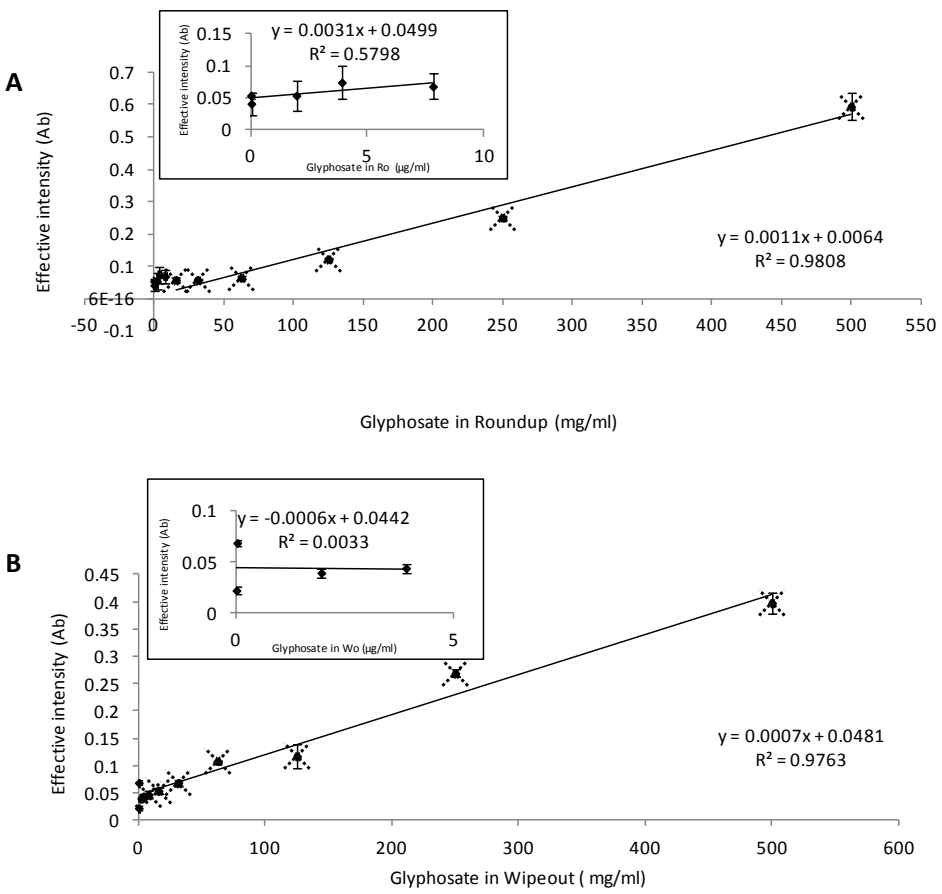


**Figure 6.7:** The effective intensity of cd-PVA sensor strips as a function of glyphosate (dithiocarbamate intermediate) concentrations in the formulations Ro **(A)** and Wo **(B)**. The linear regression equations and $R^2$ values were extrapolated from the linear range of the calibration curves (15.62-500 mg/ml for Ro and 7.81-500 mg/ml for Wo). The inset graphs show the linear regression equations and $R^2$ values of glyphosate concentrations below the linear range of the calibration curve (0.00195-7.81 mg/ml for Ro and 0.00195-3.9 mg/ml for Wo). Values are presented as mean values ± SD (n=3). Appropriate controls were used in this study.

A summary of the analytical performance of the cd-PVA sensor system in the detection of pure glyphosate and glyphosate in the formulations Ro and Wo is shown in Table 6.4.

**Table 6.4:** The calibration characteristics (over the entire range of the regression curve) determined for pure glyphosate and, glyphosate in Ro and Wo using the cd-PVA sensor system.

| Parameter | Pure glyphosate | Ro | Wo |
|---|---|---|---|
| Practical LOD (μg/ml) | 0.10 | 1.95 | 1.95 |
| Linear range (μg/ml) | 60-500 | 15.62-500 × $10^3$ | 7.81-500 × $10^3$ |
| Intercept | 0.016 | 0.037 | 0.045 |
| Slope | 0.0008 | 0.001 | 0.0007 |
| RSD (%) | 12.1 | 17.9 | 9.41 |
| $R^2$ | 0.96 | 0.97 | 0.97 |

Glyphosate in Ro and Wo formulations demonstrated lower sensitivity, as evidenced by higher practical LOD (1.95 μg/ml) values when compared to pure glyphosate (0.1 μg/ml). The calculated relative standard deviation of the calibration curves for pure glyphosate and, glyphosate in Ro and Wo was less than 20 % (n=3) demonstrating the acceptable internal precision of cd-PVA sensing system for pure glyphosate and glyphosate in formulation.

### 6.4.5 Application of the cd-PVA sensor system in real environmental water samples

The influence of matrix effects from real environmental water samples on the accuracy and practical use of the cd-PVA sensor response system was investigated by measuring the recovery of glyphosate in different water samples spiked at two different glyphosate concentrations based on medium and low level concentrations of the linear range of the standard curves (pure and in formulation). The macroscopic images shown in Figure 6.8 demonstrate the optical response of the sensor in different water samples spiked with glyphosate, Ro and Wo.

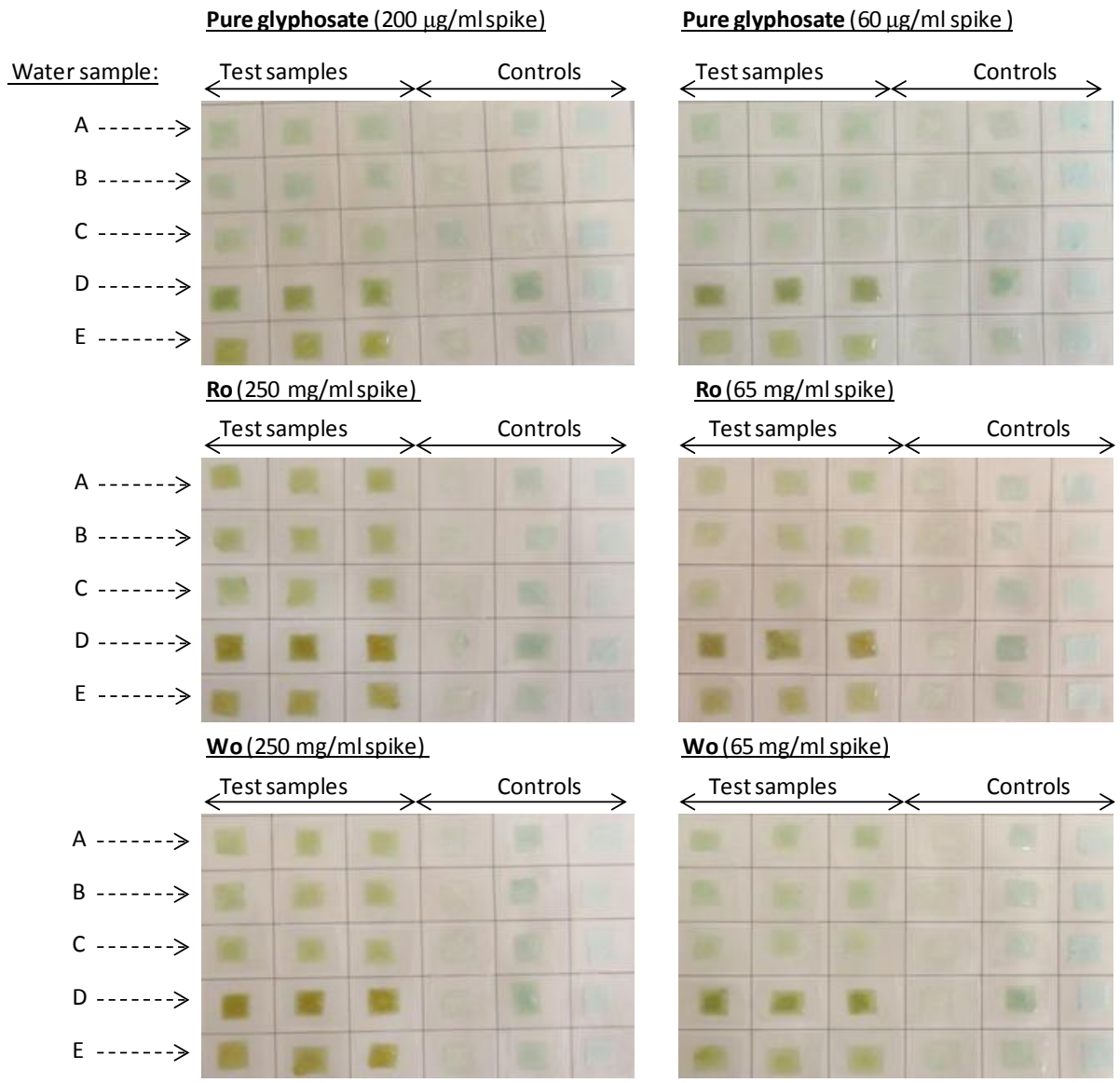


**Figure 6.8:** Macroscopic images demonstrating the colorimetric response of the cd-PVA sensor strips to glyphosate (pure glyphosate and glyphosate in the formulations Ro and Wo) spiked environmental water samples **(A, B, C and D)**. Control water sample (distilled water) **(E)**.

The results in Figure 6.8 showed a positive response signal for pure glyphosate at both concentrations (200 and 60 µg/ml) in the environmental water sample D and the control water sample E (distilled water), however slight to negligible sensor responses were observed in the

environmental samples A, B and C. The sensor system demonstrated visually observable positive signals towards all environmental water samples and the control water sample spiked with the glyphosate formulations Ro and Wo, which were characterized by variations in color intensity. The environmental water sample D and the control water sample demonstrated the greatest overall color intensity for both formulations at the concentrations tested when compared to the environmental water samples A, B and C.

The recovery of glyphosate in the water samples was determined using the regression equations obtained from the calibration curves (linear range) for pure glyphosate (Figure 6.9A2), Ro (Figure 6.9B2) and Wo (Figure 6.9C2) (Hamzah *et al.*, 2011). The recovery of glyphosate and glyphosate in formulation (Ro and Wo) was quantified and the results are shown in Figures 6.9A1, B1 and C1.

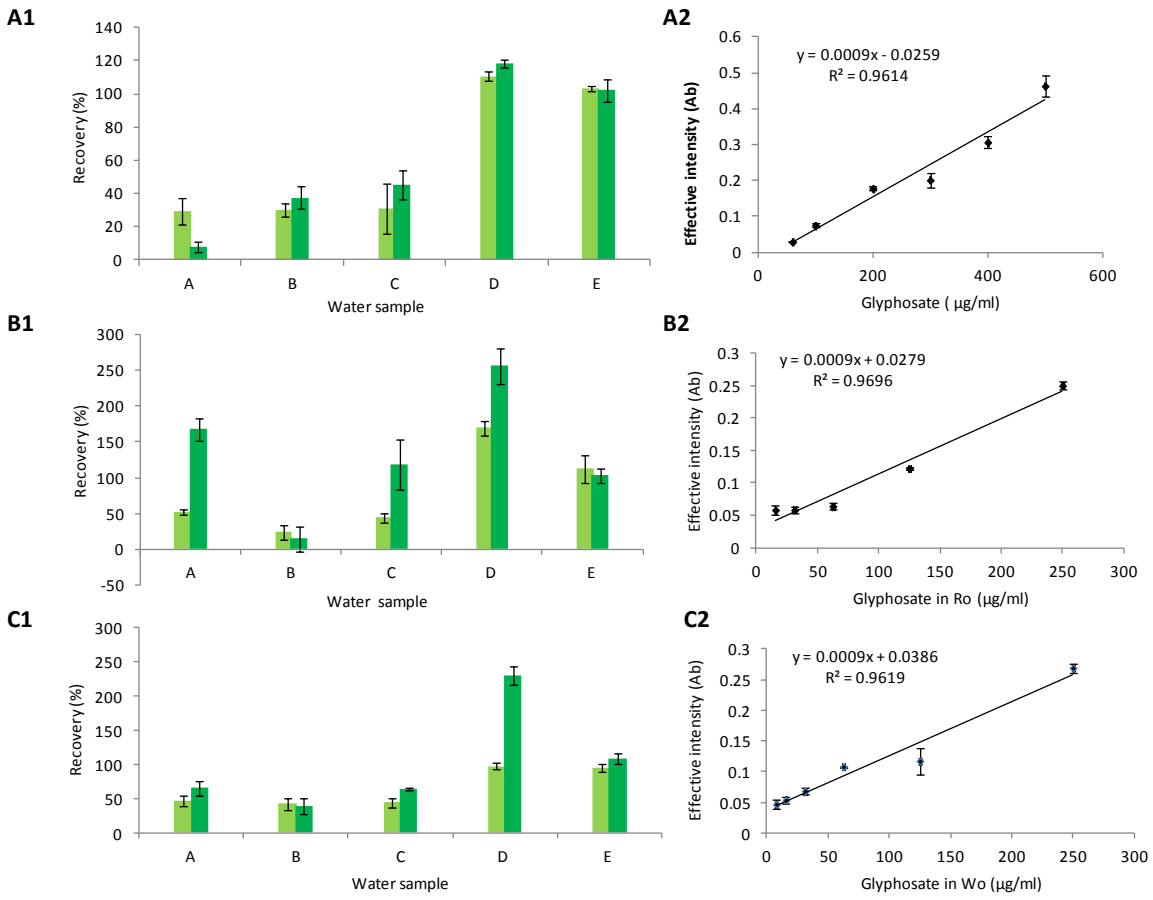


**Figure 6.9:** The percentage recovery of pure glyphosate **(A1, light green bars = 200 µg/ml spike and dark green bars = 60 µg/ml spike)**, glyphosate in the Ro formulation **(B1, light green bars = 250 mg/ml spike and dark green bars = 65 mg/ml spike)** and in the Wo formulation **(C1, light green bars = 250 mg/ml spike and dark green bars = 65 mg/ml spike)** from environmental samples **(A, B, C, D)**. Control water sample (distilled water) **(E)**. The regression equations used to quantify the recovery of pure glyphosate **(A2)**, glyphosate in the Ro formulation **(B2)** and glyphosate in the Wo formulation **(C2)** are shown. Values represent mean values ± SD (n=3). Appropriate controls were used in this study.

The poorest recoveries (below 70 % or above 120 %) were observed for pure glyphosate, Ro and Wo in the environmental water samples A (Bridge N3), B (Brickfields) and C (Fishwater Flats) at the concentrations tested (Figure 6.9). Good recoveries were obtained for pure glyphosate (Figure 6.9A1) in the environmental sample D (Grey Dam), with a recovery of 110.42 % ± 2.8

and 118.02 % ± 2.3 being observed at the 200 µg/ml and 60 µg/ml spike, respectively. The recovery of glyphosate in the Wo formulation in sample D demonstrated good recovery at the higher spiked concentration of 250 mg/ml (94.9 % ± 5.86), however possible interfering effects were observed at the lower concentration (65 mg/ml) with a recovery of 229.7 % ± 13.06 being observed. A poor recovery was observed for glyphosate in Ro for environmental sample D at both the 250 mg/ml (169.2 %± 9.41) and 65 mg/ml spike (256.4 % ± 24.71).

Very good recoveries (between 94.9 % ± 5.86 and 112.21 % ± 18.62) were obtained for the control water sample E (distilled water).

### 6.4.6 Cd-PVA sensor system specificity

The specificity of the cd-PVA sensor strips for glyphosate detection was investigated (Figure 6.10) by determining the sensor response of the cd-PVA sensor system for the glyphosate structural analogs glycine and AMPA.

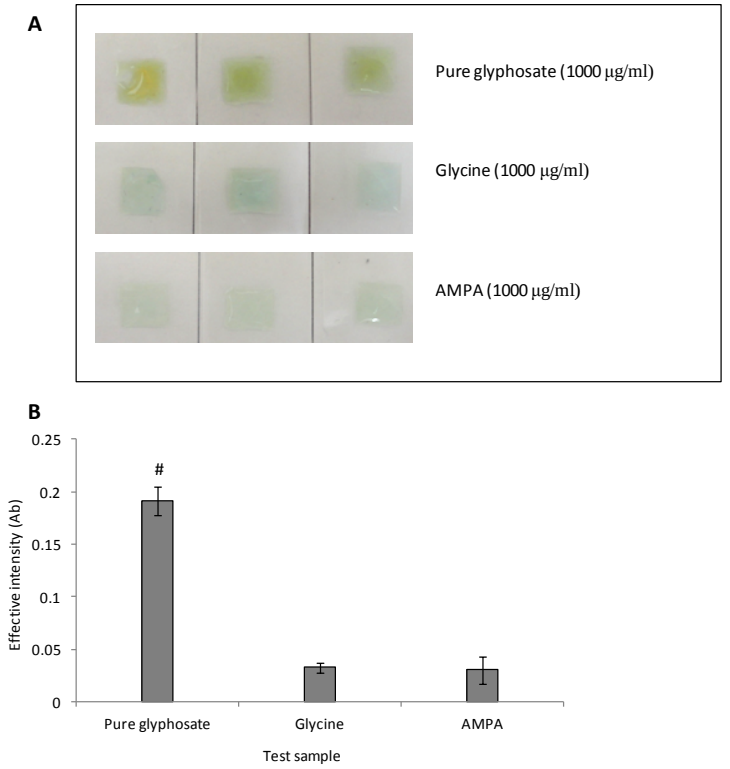


**Figure 6.10:** Cd-PVA sensor system specificity was investigated by evaluating the detection of glyphosate structural analogs glycine and AMPA. Macroscopic images **(A)** and the effective intensity **(B)** of cd-PVA sensor strips. Values are presented as mean values ± SD (n=3). ANOVA single factor analysis was used to determine statistical significance: $^{\#}$ $P \leq 0.01$. Appropriate controls were used in this study.

The visual data obtained (Figure 6.10A) indicated no clear color change (based on naked eye assessments) in the cd-PVA sensor strips after the addition of glycine (1000 µg/ml) and AMPA (1000 µg/ml), in contrast to pure glyphosate (1000 µg/ml), which produced a distinct color change from blue to yellow upon the injection of the sample to the cd-PVA sensor strips. Quantitative assessments (Figure 6.10B) showed that the response observed for pure glyphosate was significantly ($P \leq 0.01$) higher ($0.192 \pm 0.013$) than AMPA ($0.030 \pm 0.013$) and glycine ($0.032 \pm 0.004$) and AMPA and glycine only produced 16 % of the sensor response observed for pure glyphosate.

### 6.4.7 Cd-PVA sensor system selectivity

The effect of ions and compounds commonly found in environmental water systems was investigated by determining the response of the cd-PVA sensor system in the presence of these compounds and ions. The concentration range selected for this study included the regulatory standards (with the exception of EDTA and citric acid) for these compounds and ions in South African aquatic systems (DWAF, 1996) and concentrations above and below this compliance limit. The results in Figure 6.11 and Figure 6.12 demonstrate the susceptibility of the cd-PVA sensor system to varying compounds and ions.

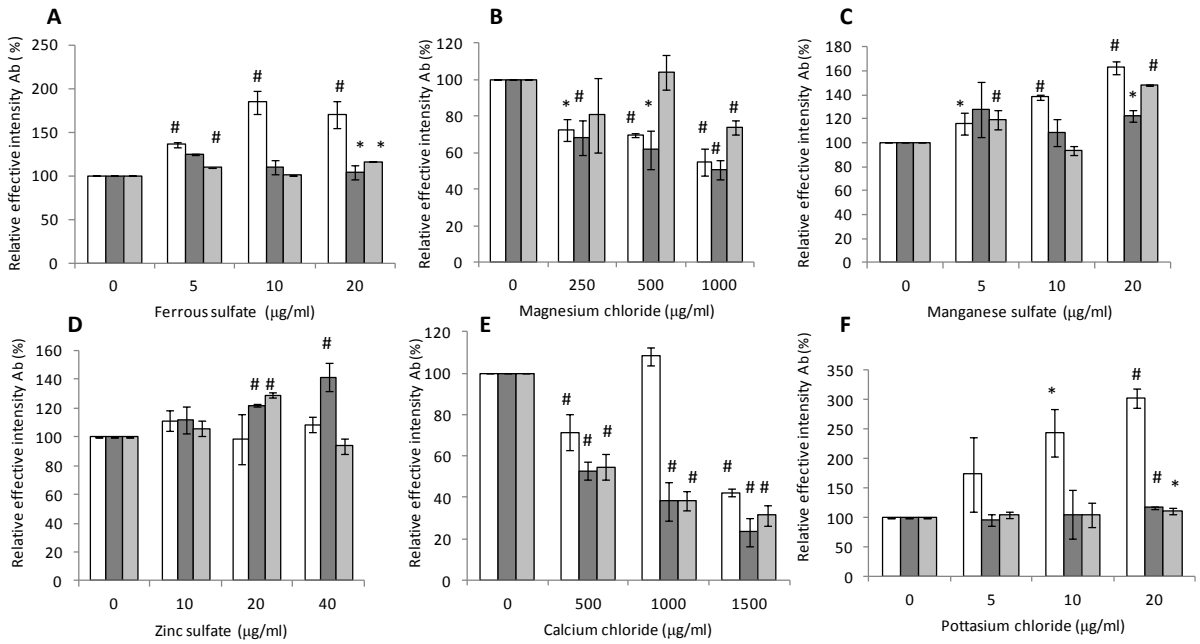


**Figure 6.11:** The interference of metal ions commonly found in environmental waters systems in the detection of pure glyphosate (white) and glyphosate in the formulations Wo (dark grey) and Ro (light grey) using the cd-PVA sensing system. Values are presented as mean values ± SD (n=3). Appropriate controls were used in this study. This experiment was conducted at 23 °C. ANOVA single factor analysis was used to determine significance relative to samples with no added compounds. $^{*}P \leq 0.05$, $^{\#}P \leq 0.01$.

The effect of the presence of metal ions on the detection of pure glyphosate, Ro and Wo was investigated and the results are shown in Figure 6.11. Different metal ions caused varied interfering effects on the detection of pure glyphosate, Ro and Wo. The extent of interference by the metal ions was ranked based on the overall (for pure glyphosate, Ro and Wo) significant interference observed for the system. $Ca^{2+}$ ions displayed the greatest interference overall (Figure 6.11F) on the sensor system, with a significant reduction ($P \leq 0.01$) in signal response being observed for pure glyphosate at concentrations below (500 µg/ml) and above the compliance limit (1500 µg/ml). Surprisingly, no significant interfering effects were observed at the compliance limit (1000 µg/ml). Similar results were obtained for the glyphosate formulations (Ro and Wo), with a decrease in signal response being observed with increasing concentrations of $Ca^{2+}$ ions. The other metal ions were ranked from greatest to lowest interferent as follows: $Mg^{2+} > Fe^{2+} > Mn^{+} > K^{+} > Zn^{2+}$. $Fe^{2+}$, $Mn^{+}$ and $K^{+}$ ions significantly enhanced the signal response for pure glyphosate, Ro and Wo at varied concentrations, while $Mg^{2+}$ demonstrated a negative interference (inhibition) for the detection of pure glyphosate and its formulations at different concentrations. Interestingly, $Zn^{2+}$ ions exhibited no interfering effects on the detection of pure glyphosate; however an increase in sensor response was observed for the formulation Wo at both the compliance (20 µg/ml) limit and the highest concentration tested (40 µg/ml). The interference of $Zn^{2+}$ ions on the detection of the Ro formulation was characterized by an increase in signal response at the compliance limit (20 µg/ml) followed by a non-significant reduction in signal at the highest concentration tested (40 µg/ml).

The effect of varying compounds and ions on the detection of pure glyphosate, Ro and Wo is also shown in Figure 6.12. The different compounds and ions demonstrated a similar result to the findings observed for the metal ions (Figure 6.11), with respect to the varying interfering effects exhibited in the presence of these ions on the detection of pure glyphosate and the glyphosate formulations. $Cl^{-}$ ions and EDTA demonstrated no significant interfering effects on the detection of pure glyphosate at all the concentrations tested ($P > 0.05$). In comparison, $Cl^{-}$ ions demonstrated a significant reduction in signal response for the Wo formulation at 1000 µg/ml (81 % ± 1.9) and an increase in signal response at 3000 µg/ml (117 % ± 8.8). The detection of Ro was significantly enhanced by the presence of $Cl^{-}$ ions at the highest concentration tested (3000 µg/ml). EDTA demonstrated a significant decrease in signal for Wo at a concentration of 50 (90 % ± 5.2) and 100 µg/ml (87 % ± 4.2), however the presence of this compound significantly

enhanced the signal response for Ro at 50 (114 % ± 8.7) and 200 µg/ml (128 % ± 6.8). $SO_4^{2-}$ ions demonstrated no significant effects on Ro, however a significant reduction in the signal was observed for pure glyphosate at 500 µg/ml (79 % ± 1.3) and Wo at 250 µg/ml (66 % ± 3.5), which was followed by an increase in signal for Wo at the highest concentration tested (1000 µg/ml). Citric acid demonstrated a significant reduction in signal for pure glyphosate at concentrations of 50 and 200 µg/ml and a significant increase in the detection signal for Wo (100 µg/ml) and Ro (50 µg/ml).

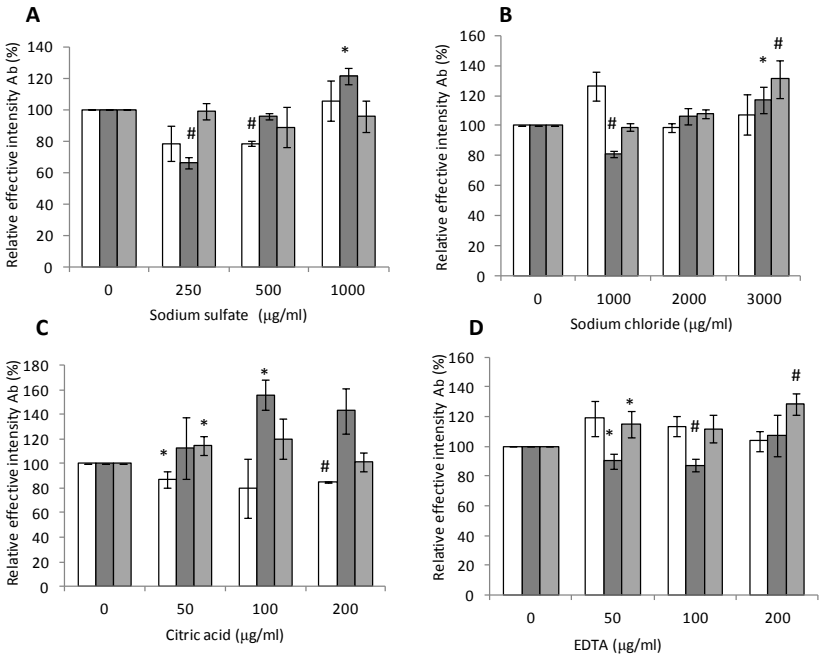


**Figure 6.12:** The interference of compounds and ions commonly found in environmental water systems in the detection of pure glyphosate (white) and glyphosate in the formulations Wo (dark grey) and Ro (light grey) using the cd-PVA sensing system. Values are presented as mean values ± SD (n=3). Appropriate controls were used in this study. This experiment was conducted at 23 °C. ANOVA single factor analysis was used to determine significance relative to samples with no added compounds. $^{*}P \leq 0.05$, $^{\#}P \leq 0.01$.

## 6.5 Discussion and future work

### 6.5.1 Color development time and color stability of the cd-PVA sensor system

The color development time and color stability was established for the cd-PVA sensor system (Figure 6.2). Following the application of the glyphosate dithiocarbamate intermediate sample (30 µl) onto the cd-PVA sensor strips an immediate color change was observed (color change from blue to yellow occurred within approximately 3 seconds), this was followed by a continued increase in effective intensity over a 50 minute period. After 50 minutes the cd-PVA sensor system reached equilibrium and a stable color response was observed for up to 4 hours. The increasing effective intensity over time was not an unexpected result. As the glyphosate dithiocarbamate permeated into the cd-PVA matrix, additional yellow colored complexes were formed with accessible copper ions in the nanofiber scaffold over time resulting in increased color intensity (yellow to dark yellow). Similar trends for color development reactions in colorimetric chemical sensors have been described in literature. A chemical sensor based on functionalized mesoporous silica for the detection of mercury ions was developed by Balaji *et al.* (2005) and results indicated an increase in color development (from orange to green) over the sensing area for 4 minutes before the saturation of the system was achieved. Studies by Jayawardane *et al.* (2013) evaluated the effect of color development time on the sensitivity of a disposable paper-based sensor developed for the determination of copper in natural and waste waters. Results from this study demonstrated an increase in color (from yellow to red/purple after the application of two copper standard solutions at 0.5 and 2.0 µg/ml) over the sensor area for 10 minutes and the sensor was stable for up-to 45 minutes, therefore a color development time of 15 minutes was selected for future analysis. Based on the results in Figure 6.2 the maximum color intensity was obtained after 50 minutes of the colorimetric reaction and this would theoretically be the ideal color development time for the qualitative/quantitative analysis of glyphosate. However in the present study, the color observed over the sensing strip from t= 30 minutes demonstrated color non-uniformity.

There are several techniques available for the immobilization of sensing materials into a chosen polymer matrix for the development of a chemical sensor (reviewed by Lange *et al.*, 2008). This study selected a physical doping strategy (in this context physical doping refers to the incorporation of the sensor reagent into the polymer solution before electrospinning) for the

production of the cd-PVA chemical sensor. This strategy was selected due to its simplicity, low production cost and the ability to maintain the original properties of the sensing reagent within a matrix (Akamatsu *et al.,* 2004; Shi and Seliskar, 1997). Although the doping strategy provides various attractive characteristics and is commonly used in chemical sensor development, the major limitation presented by this strategy is the migration or leaching of matrix reagents (Lobnik *et al.,* 1998). Several studies have reported on the migration/leaching of sensing reagents within a specific polymer matrix when employing this strategy (Lee and Okura, 1997; Likhar *et al.,* 2009; O´Riordan *et al.,* 2005; Werner *et al.,* 1995). The addition of the aqueous glyphosate dithiocarbamate sample to the cd-PVA sensor strips resulted in the partial migration of matrix components, through the pores of the PVA matrix into different sites of the polymer, leading to an uneven distribution of the resultant yellow colored complex (copper (II) carboxymethyl (phosphonomethyl) carbamodi thioate) as the aqueous solvent dried over time. The significant ($P \leq 0.05$) decrease in the effective intensity after 5 hours occurred due to the migration of matrix components towards the outer boundary of the polymer, resulting in spot spreading and a reduction in the overall measured effective intensity (Abbaspour *et al.,* 2010). Reagent mobility commonly occurs when the physical dimensions of the entrapped compounds are smaller than the average pore diameter of the polymer matrix, which upon the addition of an aqueous sample would cause some proportion of the compounds to leach into solution and readily migrate through the pores of the matrix network (Butler *et al.,* 1998; Shi and Seliskar, 1997). The weak hydrophobic interactions between entrapped copper ions and the PVA matrix (Muradov *et al.,* 2009; Matsuo *et al.,* 1998) may have also been a contributing factor to resultant migration observed.

Generally to circumvent possible artifacts caused by color non-uniformity in sensor areas (due to reagent migration), quantitative assessments are often determined over more than one area of the sensor and an average is obtained (Chen *et al.,* 2013b; Shi and Seliskar, 1997). However in the present study, the analysis of sensor strips at 50 minutes may limit the practical use of the cd-PVA sensor because color non-uniformity may lead to the poor repeatability of effective intensity measurements and may cause increased difficulty in evaluating the final color during qualitative (naked eye) assessments (Abe *et al.,* 2008; Jayawardane *et al.,* 2013). The color development over the sensing area of the cd-PVA sensor strips demonstrated the greatest color homogeneity from t= 0-20 minutes and the sensor reached a quantifiable response immediately

upon the application of the glyphosate dithiocarbamate sample (t= 0 minutes). Based on these observations, a color development time of 5 minutes was selected and would be suitable for future qualitative and quantitative assessments.

The color uniformity of the cd-PVA sensor system could be improved by employing a different immobilization strategy. Future studies could investigate the possibility of covalently grafting copper ions onto the PVA matrix. Covalent bonding techniques have been shown to reduce or eliminate the migration and leaching of matrix reagents, due to the formation of strong bond interactions between the sensing reagent and the matrix backbone (Kim *et al.,* 2011; Lindner *et al.,* 1993; Zhang *et al.,* 2007), which would result in a more even distribution of color across the sensing area. Covalent linkage may provide an efficient and alternative route for the reduction of the migration or leaching of analytes in a polymer matrix, however this may be accompanied by increased production costs and increased process complexity (functionalization of the polymer and coupling reactions) (Koren *et al.,* 2012). Although covalent attachment reduces/eliminates the migration or leaching of reagents from a solid matrix, it must be considered that this method may also present limitations such as increased sensor response times and demonstrate reduced signal alterations (Basabe-Desments *et al.,* 2007). A study by Lobnik *et al.* (1998) compared the effect of utilizing chemical doping and covalent immobilization in sol-gel based pH optical sensors on several parameters including reagent leaching and response time. Although leaching was observed with the doping strategy and was successfully eliminated using covalent bonding methods, the conclusions of this study indicated that the chemical doping method was the better strategy (due to a rapid response time and greater signal changes), as covalent attachment led to increased response times and smaller signal changes in the sensor. An alternative method which would control and reduce the pore diameter of the PVA matrix for the efficient entrapment of copper ions could be developed in future studies, to avoid or minimize problems associated with migration of matrix components in the cd-PVA sensor system. A reduction in polymer nanofiber pore diameters generally occurs when the average size of the nanofibers is reduced (Dotti *et al.,* 2007). For future studies this could be achieved by further manipulation and optimization of electrospinning parameters.

Generally, the cd-PVA sensor system demonstrated an improved color response time when compared to the scale-down method (refer to Chapter 4, section 4.4.3). The cd-PVA sensor

system color response time was characterized by a rapid (immediate) naked eye color development, which was quantifiable at t= 0 minutes, this was observed to be faster than the initial quantifiable response (5 minutes) observed for the scale-down method (refer to Chapter 4, section 4.4.3). In addition, the peak reaction time was observed after 2 hours in the scale/down method as compared to a peak reaction time of 50 minutes when using the cd-PVA sensor. The colorimetric response to a specific analyte in polymer-based sensors is dependent on several factors, including the nature of the polymer, the porosity of the polymer, the thickness of the polymer matrix and the concentration of the analyte being tested (Arshak *et al.*, 2004). The improved response time observed in this study (when compared to the scale down system) can be attributed to the increased and rapid accessibility of the glyphosate dithiocarbamate molecules to copper ions, due to the large surface area to volume ratio, porous structure and small nanofiber diameters provided by the PVA nanofiber network. These properties would facilitate the rapid mass-transfer (low mass-transfer limitation) of the glyphosate dithiocarbamate intermediate molecules to the copper ions in the PVA matrix (Huang and Choi, 2007; Viriji *et al.*, 2004).

Studies in literature reporting on chemical sensors for glyphosate are extremely limited. To the best of our knowledge, only one glyphosate chemical sensor system has been reported to date. A study by Da Silva *et al.* (2011) was conducted on a filter paper based colorimetric chemical sensor for the detection of glyphosate and its commercial formulations in water. This assay was based on the reaction between glyphosate and p-dimethylaminocinnamaldehyde (*p*-Dac) and the results indicated that a total reaction time of 8 minutes was required for the development on a colorimetric response, during which a heating step (45ºC) was necessary. Based on the findings in literature it can be concluded that the cd-PVA sensor provides an advantage over the current colorimetric chemical sensor reported for glyphosate, due to the very rapid colorimetric response observed in the presence of glyphosate under ambient (23ºC) conditions. The colorimetric response observed for the cd-PVA sensor system could not be compared to the principle method proposed by Jan *et al.*(2009), as the study did not investigate the effects of reaction time on the detection of glyphosate and the total reaction time required for the formation of the yellow colored glyphosate complex was not reported.

### 6.5.2 The storage stability of the cd-PVA sensor system

The storage stability of the cd-PVA sensor system was evaluated under two different storage conditions (23 and 4ºC) over 24 days. Generally, the results in Figure 6.3 indicated that the different storage conditions demonstrated a significant influence on the stability of the cd-PVA sensor system and the resultant functionality of the system with respect to glyphosate detection, as evidenced by the varied sensor responses observed at 4ºC and under ambient conditions (23ºC).

The sensor system displayed the poorest stability at a storage temperature of 4ºC. The trend observed under low temperature conditions was characterized by a significant decrease in the sensor response over 9 days, followed by large fluctuations (increasing and decreasing trends) in sensor signals over the duration of the study. The appearance of condensation (suggesting the presence of moisture within the container) was visually observed (from day 3 to day 24) inside the storage container (images not shown), during the storage of cd-PVA sensor strips at low temperatures (4 ºC in the refrigerator). The relative humidity (RH) of the storage unit (refrigerator) was not controlled or determined in our study. Although the effect of RH on the cd-PVA sensor system was not investigated in the current study, the appearance of condensation under low temperature storage conditions is known to occur, due to the combined effect of high RH and small temperature fluctuations (less than 0.5ºC) within a storage unit (Paull, 1999). The results observed in our study strongly suggest that the mechanical properties of PVA nanofibers are susceptible to moisture (Peijs *et al.*, 1995) and the RH in the storage unit may have had a direct influence on the resultant poor storage stability of the cd-PVA sensor system. Studies by Peresin *et al.* (2014) have highlighted the effects of RH on the PVA nanofiber mat structure, with conclusions from these studies demonstrating the plasticizing effect of moderate to high RH on PVA nanofibers, which was caused by the adsorption of water molecules by PVA (weak binding of water molecules and the hydroxyl groups in the PVA structure), resulting in the softening of the PVA matrix and a reduction in the mechanical strength of the polymer. The study mentioned above proposed the inclusion of cellulose nanocrystals into the PVA nanofiber structure to increase the mechanical and tensile strength of the matrix under humid conditions. The incorporation of cellulose nanocrystals increased the resistance of the PVA nanofiber mats to the plasticizing effect, due to the strong hydrogen bond formed between the cellulose nanocrystals

and the hydroxyl groups on the PVA structure (Ago *et al.,* 2012), which limited the capacity of water molecule binding and increased the overall rigidity of the PVA nanofiber network (Peresin *et al.,* 2010a; Peresin *et al.,* 2014). This may be an important factor to consider for future studies using the cd-PVA sensor system, as this would significantly improve the applicability of this sensor, more specifically when the sensor is utilized in high RH environments.

The cd-PVA sensor system demonstrated the highest stability under ambient (23 ºC) storage conditions. The sensor system was stable for up-to 18 days (Figure) and demonstrated greater internal precision (RSD: 11.7 %) when compared to low temperature storage (RSD: 16.3 %). The storage of cd-PVA sensors under ambient temperatures provides an advantage with respect to lowering operational costs (i.e. power consumption is not required) (Arya *et al.,* 2012). The storage stability of the glyphosate colorimetric chemical sensor developed by Da Silva *et al.* (2011) was not reported and therefore could not be compared to the cd-PVA sensor system.

The short-term (2-3 weeks) shelf life (under ambient conditions) of the cd-PVA sensor system was satisfactory (the cd-PVA sensor was stable for ~2.5 weeks), however the significant decrease in the sensor response observed after 21 (30 % reduction in the sensor response) and 24 (64 % reduction in the sensor response) days, indicated the limitation of this system, with respect to long-term storage (several months to years). The tensile strength and Youngs modulus (tensile modulus) are key factors which are commonly used to characterize the mechanical properties (high tensile strength and tensile modulus generally lead to increased mechanical integrity) of polymer nanofibers (Buell *et al.,* 2009; Camposeo *et al.,* 2013; Chew *et al.,* 2006; Frone *et al.,* 2011; Yao *et al.,* 2014). A common limitation encountered with using PVA nanofibers is their poor mechanical strength and low integrity, which has been characterized by low tensile strength and modulus, primarily due to the formation of hydrogen bonds with oriented crystalline regions during nanofiber processing and production, which subsequently limit the maximum attainable mechanical properties (Govaert and Peijs, 1995; Peresin *et al.,* 2010b). Studies by Stachewicz *et al.* (2012) investigated the mechanical properties of electrospun PVA nanofibers utilizing fiber bending tests and atomic force microscopy. The study demonstrated the inverse relationship between tensile modulus and fiber diameter, characterized by an increase in tensile modulus with a decrease in nanofiber diameter and significant improvements in tensile modulus observed in nanofibers with diameters below 300 nm. In the current study, the average nanofiber diameter of

the cd-PVA nanofibers was 320 nm (refer to Chapter 5, Figure 5.5B), therefore the poor long-term storage stability may be conferred poor mechanical integrity due to low tensile strength and modulus. Several techniques have been reported in literature as ways to reinforce the physical and mechanical properties of PVA. These include cross-linking methods using dyhydrothermal treatment (Scothford *et al.,* 1998), glutaric dialdehyde (Naebe *et al.,* 2008), gluteraldehyde (Kim *et al.,* 1992) and glyoxal (Ding *et al.,* 2002). Blending methods for structural reinforcement by the production of composite fibers have also been attempted and examples involve the incorporation of chitosan (Sajeev *et al.,* 2008), cellulose (Kubo and Kadla, 2003), cellulose fibrils and aggregates (Cheng *et al.,* 2009) and the addition of the clay compound hydrotalcite (Zhou *et al.,* 2011). Future studies could investigate the use of these methods towards the improvement of the mechanical integrity of the cd-PVA sensor system.

The instability of the copper nitrate (sensing material) within the PVA polymer matrix may also be a contributing factor to the poor long-term storage stability of the cd-PVA sensor (under both storage conditions). Physical entrapment (physical doping) of the copper nitrate into the PVA matrix may limit the long term shelf life of the cd-PVA sensor, due to copper nitrate aggregation and migration over time, as this is a common storage stability limitation encountered with the physical doping method (Balaji *et al.,* 2005, Koren *et al.,* 2012; Lev *et al.,*1995). The previously mentioned cross-linking and reinforcement methods have demonstrated a secondary role, primarily with respect to the prevention of enzyme leakage and the increase in enzyme mechanical strength (Datta *et al.,* 2013). We propose that these cross-linking and reinforcement methods may also improve the stability and limit the migration of the copper salt entrapped within the PVA matrix. This would be advantageous not only for long-term storage stability, but may also be beneficial with respect to limiting color non-uniformity due to matrix reagent migration (discussed in section 6.5.1).

### 6.5.3 Cd-PVA system precision (intra-assay variation) and reproducibility (inter-assay variation)

The reproducibility of the cd-PVA sensor system was evaluated by determining the intra-assay variability and inter-assay variability at two different pure glyphosate concentrations (400 µg/ml

and 1000 μg/ml). Based on the results observed in Table 6.2 the cd-PVA sensor system demonstrated poor reproducibility, which was characterized by RSD values above 20 % at glyphosate concentrations of 400 μg/ml (45.8 % ± 0.11) and 1000 μg/ml (37.1 % ± 0.22). This result was not entirely unexpected and could be explained by the heterogeneity observed in cd-PVA nanofibers produced after the electrospinning process, as previously mentioned (refer to Chapter 5, section 5.5.1).

The cd-PVA sensor system demonstrated very good system precision with RSD values below 20 % being observed at glyphosate concentrations of 400 μg/ml (15.9 % ± 0.04) and 1000 μg/ml (13.1 % ± 0.08). The internal consistency of this sensor system was further validated by the calculated RSR (%) which was 39.4 % ± 1.6. Generally, the results of this study suggest that better results would be obtained when utilizing sensor strips from the same mat as compared to sensor strips from various mats. As previously mentioned in Chapter 5, section 5.5.1, all sensor studies employed the use of one cd-PVA mat per experiment to reduce experimental variation, which was satisfactory at the scale of this study. However, the heterogeneity observed in the nanofiber mats may have greater implications during industrial scale production, therefore future studies should involve further optimization of the electrospinning process under controlled environmental conditions (in our study electrospinning was not conducted under controlled environmental conditions as the relevant equipment was not available), as electrospinning conditions play a crucial role in the production of homogenous fibers (Ertas and Uyar, 2014).

### 6.5.4 The sensitivity of the cd-PVA sensor system

The sensitivity of the cd-PVA sensor system was investigated by evaluating the calibration characteristics of the system. Based on naked eye assessments from the macroscopic images obtained in Figures 6.4 and 6.6 at varying concentrations of glyphosate, a positive sensor response was achieved at low concentrations of pure glyphosate (0.1- 40 μg/ml) and glyphosate in the formulations Wo (1.95 – 3.9 × $10^3$ μg/ml) and Ro (1.95 – 7.8× $10^3$ μg/ml), however the calibration curves constructed demonstrated poor linearity at the these concentrations in pure glyphosate ($R^2$= 0.43) and glyphosate in the formulations Wo ($R^2$= 0.003) and Ro ($R^2$= 0.58) (Figures 6.5 and 6.7). Good correlation coefficients (Table 6.4) were observed in the linear range

for pure glyphosate (60- 500 μg/ml, $R^2$= 0.96) and glyphosate in Wo ($7.8 \times 10^3$ – $500 \times 10^3$ μg/ml, $R^2$= 0.97) and Ro ($15.6 \times 10^3$ – $500 \times 10^3$ μg/ml, $R^2$= 0.97). The results observed therefore indicate that the cd-PVA sensor system could be utilized for semi-qualitative/qualitative determinations at lower glyphosate concentrations, with quantitative determinations being achievable at higher concentrations.

The practical LOD was selected as an accurate representation of the cd-PVA sensor system sensitivity and was used for comparative analysis. The use of the practical limit of detection (based on naked eye assessments or the lowest analyte concentration which resulted in a sensor signal response) for the measurement of system sensitivity in sensors has been reported by several authors (Abbaspour *et al.,* 2010; Guo *et al.,* 2010; Kim *et al.,* 2001; Nath and Chilkoti, 2002; Wang *et al.,* 2008; Wang *et al.,* 2011; Yang and Tae, 2006; Yao *et al.,* 2010).

The cd-PVA sensor system displayed a significant increase in system sensitivity and precision when compared to the scale-down glyphosate method (refer to Chapter 4, Table 4.3). The practical LOD values for pure glyphosate (0.1 μg/ml) and glyphosate in the Ro (1.95 μg/ml) and Wo (1.95 μg/ml) formulations (Table 6.4) were $4.0 \times 10^3$, $3.4 \times 10^5$ and $2.8 \times 10^5$ times lower, respectively, than the reported LOD values for the scale-down method. RSD values obtained for the calibration curves for pure glyphosate and glyphosate in Ro and Wo were all below 20 % indicating greater system precision, when compared to the scale-down system. The sensitivity of a sensor is directly associated with the availability of detection sites for molecular binding interactions (Matlock-Coangelo and Baeumner, 2014). Electrospun nanofibers are inherently characterized by a high surface area to volume ratio and a porous non-woven structure (Chigome and Torto, 2011; Huang *et al.,* 2003; Long *et al.,* 2009; Ramakrishna *et al.,* 2006). The drastic increase in sensitivity observed in the cd-PVA sensor system, when compared to the scale-down method, was attributed to these characteristic features (Panda and Sahoo, 1990). The porous nature and high surface area to volume ratio of PVA electrospun nanofibers provided a large loading capacity for the sensing material (copper salt) and an increased functionalized surface area (increase in the availability of the detection sites), for glyphosate molecule binding. In addition, a high surface area to volume ratio allowed for the rapid mass transfer rate of glyphosate molecules to the copper ions situated within the nanofiber mat (Matlock-Coangelo and Baeumner, 2014).

Colorimetric spectrophotometric studies on glyphosate detection by Jan *et al.* (2009) reported a LOD of 1.1. µg/ml over a glyphosate concentration range of 1.0-70 µg/ml. More recently, similar studies by Sharma *et al.* (2012) and Waiman *et al.* (2012) reported a Sandell sensitivity of 0.091 ug.cm$^3$ (equivalent to 0.091 µg/ml, over a glyphosate concentration range of approximately 0-40 µg/ml and the lowest quantifiable glyphosate concentration at 0.084 µg/ml (over a glyphosate concentration range of 0.084-21.8 µg/ml), respectively. The practical LOD obtained for pure glyphosate using cd-PVA sensor system was within the range of reported values in literature. Although good results were reported for LOD values using spectrophotometric detection methods, it must be taken into consideration that these methods utilized much larger sample volumes in comparison to the current study. Compared to standard methods used for glyphosate detection (e.g. HPLC and GC) (summarized in Chapter 1, Table 1.5), the current method demonstrated a lower sensitivity. However, standard methods for glyphosate detection are often limited due to cost and complexity and the present method is extremely advantageous, due to its simplicity, potential for on-site application and immediate response time.

Interestingly, the cd-PVA sensor system displayed a greater sensitivity (19.5 fold increase) towards pure glyphosate when compared to glyphosate in formulation (Wo and Ro) (Table 6.4); this observation was similar to the findings reported for the scale-down method (refer to Chapter 4, section 4.5.2). This result suggests that the cd-PVA sensor system may also be susceptible to the adjuvants present in formulation, which may have caused an overall reduction in the system sensitivity at lower glyphosate concentrations. The colorimetric chemical sensor for glyphosate detection in literature demonstrated an LOD value of 7.28 µg/ml (Da Silva *et al.*, 2011). In comparison, the current method proposed in our study demonstrated a higher sensitivity for both pure glyphosate and glyphosate in formulation.

The MRL set for glyphosate in drinking water/water varies greatly between different countries and agencies. The health based value for glyphosate in drinking water, set by the WHO, is 0.9 µg/ml (WHO, 2004) and the USEPA has set the MRL for glyphosate in drinking water at 0.7 µg/ml (Coutinho *et al.,* 2008; Miro *et al.,* 2012). In South Africa no water quality guidelines are implemented currently for glyphosate. However as previously mentioned (refer to Chapter 1, section 1.2.5), studies by Mensah *et al.* (2013) resulted in the derivation of short-term (0.25 µg/ml) and long-term (0.002 µg/ml) water standards for glyphosate in the formulation

Roundup®. With the exception of the long-term standards derived by Mensah *et al.* (2013), the cd-PVA sensor system demonstrated sufficient sensitivity for the detection of pure glyphosate in water; however, based on the MRL's, this system demonstrated limited sensitivity with regards to glyphosate detection in the formulations Wo and Ro.

A review by Wang *et al.* (2013) has highlighted the recent rapid advancement of research towards the production of ultrasensitive sensors using the electrospinning/netting (ESN) process for the development of 3-D nanostructures. ESN combines the electrospinning process and the electro-netting process for the production of nano-fiber/nets, which are in essence nano-nets which are supported by the conventional nanofiber network structure (Wang *et al.,* 2013). Amongst several attractive characteristics, these structures display extremely small diameters (less than 20 nm), which would result in significantly high surface areas, which would, in turn, improve sensor sensitivity (Wang *et al.,* 2013). This technique has been successfully demonstrated in the development of ultrasensitive sensors for the detection of formaldehyde and copper. Ding *et al.* (2011b) developed a highly sensitive and selective colorimetric sensor strip, based on polyaniline/polyamide-6 NFN, for the detection of $Cu^{2+}$ in aqueous solutions, with a reported practical LOD (naked eye assessment) of 0.0001 μg/ml. More recently, Wang *et al.* (2012) developed an ultrasensitive colorimetric gas sensor, based on methyl yellow impregnated nylon-6 NFN for the detection of formaldehyde, with a reported practical LOD (naked eye assessment) of 0.04 μg/ml. Based on the findings in the current study we propose that the sensitivity of the cd-PVA sensor system for the detection glyphosate, more specifically glyphosate in formulation could be vastly improved by further optimizing the surface chemistry of the PVA nanofiber (1-D structure) using the electrospinning/netting method.

### 6.5.5 Application of the cd-PVA sensor system to real environmental water samples (recovery studies)

The applicability of the cd-PVA sensor system was investigated by determining the recovery of glyphosate in environmental water samples. For the recovery study, no chemical analysis of environmental water samples was conducted, however the un-spiked (negative control: environmental water sample containing no glyphosate) control samples did not demonstrate cd-

PVA sensor responses (Figure 6.8). The sample matrices selected for this study were therefore compatible with the cd-PVA sensor assay i.e. none of the water samples contained detectable (if glyphosate was present in the water sample it would be at concentrations lower than the practical limit of detection observed for pure glyphosate, glyphosate in Ro and Wo using the cd-PVA sensor system) levels of glyphosate, which may have led to false positive results. The use of negative controls to determine the compatibility of sample matrices for a specific assay, in the absence of chemical analysis, has been reported in literature (Hossain and Brennan, 2011b).

As previously mentioned, recovery studies were conducted without employing any pre-treatment strategies (other than a simple filtration step to remove large particulate matter). The observed visual response (macroscopic images) to pure glyphosate and glyphosate in Ro and Wo demonstrated a good correlation with the quantitative data (Figure 6.9).

Environmental water samples were obtained from two different water systems that demonstrated varied characteristics and matrix complexities, namely the Swartkops Estuary and Grey Dam. Overall the recoveries observed in the two environmental water samples Figures 6.9A1, 69B1 and 6.9C1 ranged from 7.81 % to 118.02 % for pure glyphosate, 14.49 %to 169.2 % for glyphosate in Ro and 38.82 % to 229.73% for glyphosate in Wo, respectively. The wide range of recoveries observed strongly suggest that the sensing capacity of the cd-PVA sensor system is susceptible to matrix effects in environmental water systems, which are most likely governed by water matrix type and complexity (Lieberzeit and Dickert, 2007) and may therefore cause interfering effects when quantifying glyphosate.

The poorest recoveries for pure glyphosate (spiked concentrations: 60 and 200 µg/ml), and glyphosate in Ro (spiked concentrations: 65 and 250 mg/ml) and Wo (65 and 250 mg/ml) were observed in water samples obtained along varying points of the Swartkops Estuary, namely: sample A (Bridge N3), B (Brickfields) and C (Fishwater flats). More than one representative sample was selected from the Swartkops estuary due to the large temporal and spatial variability observed in this region (Binning and Bair, 2001), which would result in a varied distribution of different compounds/ions along the different sampling sites. The Swartkops Estuary samples were representative of a nutrient rich, aquatic region, characterized by moderate to high salinity (Gardner *et al.,* 1983), located in a highly industrialized and urbanized area, which would make it susceptible to various anthropogenic influences (Gyedu-Ababio *et al.*, 1999). The Swartkops

Estuary is considered a polluted water system with previous pollution studies indicating the presence of several pollutants including, varying high concentrations of heavy metals such as copper, zinc and manganese and hydrocarbons (Bate *et al.*, 2004; Binning and Baird, 2001; Hilmer and Bate, 1987). The poor recovery observed in the Swartkops Estuary may have been attributed to the presence of pollutants in the aquatic system, together with the high matrix complexity (nutrient rich and moderate to high salinity) presented by this water system, which may have interfered with the recovery of pure glyphosate and glyphosate in Ro and Wo. Although the Swartkops Estuary demonstrates high temporal and spatial variability, the recoveries obtained from the different sites (A, B and C) all demonstrated poor recoveries and definitive comparisons could not be made between the sites.

The best recovery (for environmental water systems) was observed in the Grey Dam samples spiked with pure glyphosate at both concentrations tested (60 µg/ml: 118.02 % ± 2.3, 200 µg/ml: 110.42 % ± 2.8). Interestingly, the recovery for glyphosate in Wo at lower concentrations (65 mg/ml: 229.7 % ± 13.06) demonstrated possible interfering effects and poor recovery results were also observed for glyphosate in Ro (65 mg/ml: 169.2 % ± 9.41, 250 mg/ml: 256 % ± 24.71). Grey Dam is an untreated water reservoir, which is located a few kilometers outside Grahamstown. Grey Dam water is used for recreational purposes (swimming activities) and provides a source of drinking water (once the water has been pumped through the water treatment plant) for the City (Tandlich *et al.*, 2010). Studies on Grey Dam are extremely limited however; a study by Tandlich *et al.*, 2010 described Grey Dam as a receiving site for human fecal contamination, based on the information available at the time of this study (Tandlich *et al.*, 2010). When compared to the Swartkops Estuary; the Grey Dam site represents a relatively unpolluted water system which may explain the overall improved recoveries observed for the Grey Dam water samples, more specifically for pure glyphosate. Although overall improved recoveries were observed for the Grey Dam water samples when compared to the Swartkops Estuary, results observed for glyphosate in the Wo and Ro formulations strongly suggested the presence of interfering compounds/ions in this water system. Pure glyphosate may demonstrate a higher tolerance to possible interfering species presented in this specific water system when compared to glyphosate in formulation. In addition, the differences observed between the Wo and Ro formulation also suggest the possible role of adjuvants present in formulation, which

together with compounds and ions present in the environmental water, may exert a combined or synergistic interfering effect on the determination of glyphosate.

Although the overall recoveries observed in this study were not ideal with respect to the direct application (no pre-treatment) of the cd-PVA system to the determination of glyphosate in environmental waters, the results obtained allowed insight into the possible susceptibility of the cd-PVA sensor system to matrix effects.

Very good recoveries for pure glyphosate and glyphosate in the formulations Ro and Wo were obtained for the control water sample E (distilled water, which represented pristine water samples) at all the concentrations tested (Figure 6.9). This result validated the capacity of the cd-PVA sensor system to successfully quantify glyphosate (pure and in formulation) in water provided matrix interferents are not present.

Recovery studies conducted by González-Martinez *et al.* (2005) for a glyphosate immunosensor supported the findings of the current study with respect to matrix interfering effects being observed in the absence of pre-treatment strategies. Recoveries higher than 150 % were reported in three different environmental water samples. This effect was attributed to the presence of the anion hydrogen carbonate in the water samples and the interfering mechanism proposed was based on the interaction between the nucleophilic nitrogen atom from glyphosate and the electrophilic carbon from hydrogen carbonate. Other studies in literature reporting on the recovery of glyphosate in water samples generally indicated higher recovery rates when compared to our study; however it must be noted that these studies conducted various pre-treatment and pre-concentration strategies before sample application and recovery analysis. Colorimetric spectrophotometric analysis by Jan *et al.,* (2009) indicated a glyphosate recovery above 85 % at 5, 10, 15 μg/ml glyphosate concentrations in environmental water samples. Colorimetric spectrophotometric studies by Sharma *et al.* (2012) revealed recovery rates in water between 94.2 and 97.9 % for pure glyphosate at concentrations between 33.8 and 84.5 μg. Similar recovery rates (between 92.4 and 96.5 %) were obtained for glyphosate in the formulation, Glyfos Daker, at the same concentrations, however the nature (environmental water sample or tap water) of the water samples used was not described in the study. The recovery values reported by Da Silva *et al.* (2011) for the glyphosate chemical sensor in river water samples was between 93.2 and 102.6 % for pure glyphosate (75-300 μg/ml) and between 91.3

and 102.9 % (75-300 μg/ml) for glyphosate in three different glyphosate commercial formulations. Based on the results of our study and the recovery rates reported after pre-treatment/pre-concentration strategies in literature, we can deduce that the pre-treatment/pre-concentration of water samples prior to glyphosate determination would significantly improve the recoveries observed.

### 6.5.6 The specificity and selectivity of the cd-PVA sensor system

The cross-reactivity of the cd-PVA sensor to AMPA and glycine, (the structural analogous to glyphosate) was investigated. The results shown in Figure 6.10B indicate that glycine and AMPA only produced 16 % of the sensor response observed for pure glyphosate and naked eye observations demonstrated no clear color alteration upon the application of the two compounds to the sensor strips (Figure 6.10A). The results observed are similar to the reported findings shown for the scale-method (refer to Chapter 4, Figure 4.6); however a slightly greater response was displayed by the cd-PVA sensor system. This could be attributed to the overall increased sensitivity of the cd-PVA sensor. Overall this result suggests that the cd-PVA sensor system demonstrates a high specificity for glyphosate. Similar to the scale-down method (refer to Chapter 4, section 4.5.2), the results observed may likely be explained by the poor reactivity of carbon disulfide with glycine and AMPA (primary amines) for the formation of the dithiocarbamate intermediate, in comparison to the reactivity of carbon disulfide with glyphosate (secondary amine).

The selectivity (via interference studies) of the cd-PVA sensor system was evaluated to determine the susceptibility of the sensor to compounds commonly found in environmental waters. Results in Figures 6.11 and 6.12 strongly suggest that different compounds and ions exhibited varied interfering effects on the cd-PVA sensor system.

The ability of glyphosate and dithiocarbamates to bind strongly and selectively to metals has been well established (Fuentes-Martinez *et al.,* 2009, Jian *et al.,* 1999, Zhou *et al.,* 2013). The selectivity of the cd-PVA sensor system (Figure 6.11) indicated interfering effects from all the metal ions tested with the exception of $Zn^{+}$ ions (alkali metal) for pure glyphosate. Glyphosate/ glyphosate dithiocarbamate demonstrated high selectivity for the alkaline earth metals at the

concentrations tested in this study ($Ca^{2+}$ and $Mg^{2+}$), as significant interfering effects were more pronounced in reactions containing these two metal ions, with $Ca^{2+}$ exhibiting the greatest interference overall (Figure 6.11F). The glyphosate dithiocarbamate ligand also showed an affinity for complex formation with the transition metals ($Fe^{2+}$, $Mn^{+}$ and $Zn^{2+}$). The results of this study are not surprising as the metal chelating properties of glyphosate and dithiocarbamates have been regularly exploited in literature for the determination of varying trace metals (Badr *et al.*, 1995; Batterham *et al.*, 1997; Ramesh *et al.*, 2002; Wai, 1995, Zhou *et al.*, 2013). Interfering effects were observed in the presence the compounds EDTA and citric acid for glyphosate in the formulations Ro and Wo, as well as the counterions, $SO_4^{2-}$ (for pure glyphosate and Wo) and $Cl^{-}$ (for glyphosate in the formulations Ro and Wo) (Figure 6.12) and, interestingly, the overall effect observed indicated significant ($P \leq 0.05$, $P \leq 0.01$) increases and decreases in the detection signal with the addition of these compounds and ions at varying concentrations.

Reports in literature present contrasting results, which strongly suggest that interfering effects are dependent of several factors, including the type of detection system used, the concentration of the analyte being detected and the interfering compounds of interest. Studies by Steenkamp and Coetzee (1993), investigating the determination of toxic heavy metals (e.g. nickel, cobalt, cadmium and lead) by reversed-phase high performance liquid chromatography using the chelating ligand, sodium diethyldithiocarbamate, showed that sulfate (10 mg/ml), chloride (10 mg/ml) and phosphate (5 mg/ml) anions inhibited metal complex formation. However, nitrate ion concentrations as high as 100 mg/ml caused no significant effects. Earlier findings by Bond and Wallace (1981) indicated no interfering effects from sulfate, chloride anions at excess concentrations (10 fold the concentration of added copper) on copper determination based on metal-dithiocarbamate complex formation and reversed-phase liquid chromatography coupled to electrochemical detection. The various effects of different anions and cations on the determination of lead and cadmium using pulse polarography, after the adsorption of the metal ions to morpholine-4-dithiocarbamte-CTMAB-napthalene or microcrystalline naphthalene absorbents, were investigated by Dubey and Puri (1994). The results of their study showed no interference effects from ions and compounds such as citrate, sulfate, zinc and manganese, however ferrous (III) ions and EDTA caused significant interference/s evidenced by the severe reduction in the detection of lead and cadmium.

EDTA and citric acid are known to form complexes with copper (Kimura *et al.,* 2007; Liu and Lin, 2013; Pitluck *et al.,* 1987; Van Kley and Clayrell, 1973). Van Staden and Botha (1999) evaluated the use of EDTA and citrate as masking agents for interfering ferrous ions in the spectrophotometric determination of copper (complexed to diethyldithiocarbamate). The results of the Van Staden and Botha (1999) study indicated that increasing concentrations of EDTA enhanced the complexation of copper to the dithiocarbamate and demonstrated no significant effects on the sensitivity of this system. However, increasing concentrations of citrate demonstrated an increase in sensitivity and percentage interference in the presence and absence of ferrous ions, which was characterized by increases in peak heights. Therefore, this study proposed that the observed effects were due to the ability of citrate to form complexes with copper and ferrous ions and contributed to the signal detected. This theory is likely to explain the increased interference signals observed in the present study.

The differential selectivity of the glyphosate/glyphosate dithiocarbamate for the various interfering metal ions, anions in its pure glyphosate form, and within formulation, suggests that adjuvants present in formulation were a contributing factor. Overall, the results indicate that the interference observed was dependent of the concentration of the interfering ion, together with the form in which glyphosate was detected.

The data observed in this study confirms the high susceptibility of the cd-PVA sensor system to compounds and ions commonly found in environmental water systems and would explain the poor recoveries observed in environmental water systems, in particular the recoveries observed for the Swartkops Estuary samples. It can be concluded that pre-treatment/pre-concentration methods would be a requirement for improvement of the applicability of the cd-PVA sensor system for the detection of glyphosate in environmental water systems. Studies by Da Silva *et al.* (2011), based on the colorimetric chemical sensor for the detection of glyphosate support, some of the findings of the current study, with regards to the interference from metal ions, more specifically copper and ferrous ions on the detection of glyphosate. This study successfully employed the use of a clean-up solid-phase extraction procedure of environmental water samples. Future studies could investigate the use of this procedure towards improving the applicability of the cd-PVA sensor system.

## 6.6 Conclusions

- Although the cd-PVA sensor system demonstrated an optimal color development time of 50 minutes and a color stability of up to 4 hours, reagent mobility was observed over time, which subsequently lead to color non-uniformity. A color development time of 5 minutes proved suitable for the study and was therefore selected for future analysis.
- The cd-PVA sensor showed good short-term stability (~ 2.5 weeks) under ambient storage (23 ºC) conditions, however findings strongly suggested the susceptibility of this system to moderate to high humidity conditions, which was shown by the poor storage stability at 4 ºC.
- The cd-PVA sensor system demonstrated good internal precision (RSD values below 20 %, RSR: 39.4 ± 3.16), however this system was limited with regards to reproducibility (RSD values above 20 %). This was attributed to the heterogeneous nature of the nanofiber mats produced during electrospinning.
- The calibration studies indicated practical LOD values of 0.1 μg/ml and 1.95 μg/ml for pure glyphosate and glyphosate in the formulations Ro and Wo, respectively. Based on the calibration curve characteristics the cd-PVA system would be suitable for semi-qualitative/qualitative detection for glyphosate at lower concentrations and quantification could be achieved at higher concentrations.
- The cd-PVA sensor demonstrated very good specificity towards the glyphosate structural analogs AMPA and glycine.
- The cd-PVA sensor system was susceptible to matrix effects from environmental water systems and the susceptibility of the system to interfering species commonly found in environmental water systems was confirmed. Therefore, the pre-treatment/ pre-concentration of environmental water samples would be a requirement when using this assay.
- Very good recoveries (between 94.9 % ± 5.8 and 112.2 ± 18.6) were observed in the pristine water sample (distilled water), which validated the capacity of the cd-PVA sensor to successfully quantify glyphosate in the absence of matrix effects.

# CHAPTER 7- GENERAL CONCLUSIONS AND FUTURE RECOMMENDATIONS

The current study involved the investigation of the acute toxicity effects (*in vitro* studies) of glyphosate and glyphosate formulations (Ro and Wo) in humans at low to moderate dose exposure and the development and characterization (analytical performance) of a novel nanofiber-based colorimetric sensor (cd-PVA sensor) for glyphosate determination in water.

Glyphosate toxicity studies were undertaken to validate the need for the development of a rapid, simple and cost-effective detection method, for glyphosate determination in water. Overall, the main aims of the present study were important, particularly for countries such as South Africa, where a large majority of the country´s population (primarily rural communities) remain highly dependent on natural water systems (Nkwonta and Ochieng, 2009). The extensive use of glyphosate based herbicides in South Africa, together with the lack of knowledge (mainly due to financial limitations and the availability of analytical techniques) and the absence of regulatory limits with regards to the levels of glyphosate present in environmental water systems (Dabrowski *et al.*, 2005; Dalvie *et al.*, 2009; Dalvie *et al.*, 2006; Mensah, 2013) further highlighted the importance of this study.

Glyphosate has been classified as a category III (relatively low acute toxicity) and E herbicide (no evidence of reproductive toxicity and carcinogenicity) which suggests that this herbicide displays a low toxicological potential in humans (USEPA, 1993; WHO, 2004). Although some studies assessing the toxicological capacity of glyphosate at sub-lethal concentrations are in support of the classification criteria recognized for glyphosate (Mladinic *et al.*, 2009; Pieniążek *et al.*, 2009), the theory that glyphosate is relatively non-toxic to humans contradicts studies, which have demonstrated the capacity of glyphosate/glyphosate based formulations to cause several deleterious effects in human (including endocrine disruption, genotoxicity and cytotoxicity), at environmentally relevant concentrations and concentrations likely to be encountered by humans (refer to Table 1.4, section 1.2.4).

Toxicological studies conducted in human white blood cells, human whole blood cells and the HEC1A human endometrial cancer cell line, confirmed the cytotoxic potential of pure glyphosate and glyphosate in the formulations Ro and Wo at low (environmentally relevant exposure levels) to moderate (occupational and residential exposure levels) exposure.

The human whole blood model demonstrated greater sensitivity when compared to the human white blood cell model and was therefore considered a more suitable model for toxicity assessments in this study. Interestingly, the results of cytotoxicity studies in human whole blood demonstrated two different dose-response profiles, namely monotonic (exposure to Wo) and non-monotonic (exposure to pure glyphosate and Ro) dose response profiles. The non-monotonic dose-response relationship observed in this study has been reported in literature primarily in toxicological studies investigating the effects low dose exposures for various compounds (Vandenberg *et al.,* 2012). Although not conclusively determined, our study proposed that this toxicological profile may be linked to overcompensations by the cell system, which is caused due to the disruption of homeostasis (Calabrese and Baldwin, 2001). This finding provided the scope for future work in this specific area.

Results observed in human whole blood and the HEC1A cell line also indicated the role of adjuvants in glyphosate toxicity, made evident by the varying toxicities displayed by the two different formulations (Ro and Wo).

The HEC1A cell line proved a suitable and sensitive model for this study, as the most significant cytotoxicity results were observed in this cell line after exposure to pure glyphosate (cell reduction) and the formulation Wo (cell proliferation), when compared to results obtained for the MCF-7 and the MDA-MB-231 breast cancer cell lines. This finding strongly suggests that the toxicity displayed by glyphosate varies depending on cell type and, to the best of our knowledge, no reports have demonstrated the toxic effects of glyphosate in the HEC1A cancer cell line.

Some authors have reported on the endocrine disruptive capacity of glyphosate (Gasnier *et al.,* 2009; Kojima *et al.,* 2004), however results from genotoxic studies indicated the carcinogenetic potential of pure glyphosate and the glyphosate based formulations Ro and Wo in both the ER-positive HEC1A cancer cell line and the ER-negative MDA-MB-231 cancer cell. This

highlighted the possibility that glyphosate and its formulations may cause cell damage through estrogenic and non-estrogenic mechanisms.

Pro-inflammatory studies revealed preliminary evidence suggesting that pure glyphosate and glyphosate formulations (Ro and Wo) demonstrated the capacity to elicit an acute inflammatory response in human whole blood cells, however this result should be considered tentative as future work would be required before immunomodulation is considered a mechanism of toxicity for glyphosate.

Overall our data supports the theory that glyphosate and glyphosate based herbicides display acute toxic effects in humans at low to moderate dose exposure and subsequently validated the development of the nanofiber-based cd-PVA sensor for glyphosate detection in water. The scope of this study primarily investigated the acute toxic effects of low concentrations of glyphosate within the range permitted by regulatory authorities specifically for the validation of the cd-PVA sensor system. Environmental monitoring studies have however demonstrated the presence of glyphosate residues in surface and ground waters (Chapter 1, Table 1.3) at levels lower than the test concentrations assessed in the present study. Future toxicity studies should include assessments at glyphosate concentration levels observed in environmental water systems (The average concentration of glyphosate found in surface and ground waters in South Africa is still largely unknown) to provide greater insight on the toxic effects of this herbicide and its formulations under more representative conditions.

Several detection methods have been developed for the determination of glyphosate in water (refer to Chapter 1, section 1.2.6). Although these methods demonstrate high sensitivity and are able to detect glyphosate a very low concentrations, these methods are often limited by cost, time and the use of complicated instruments that require skilled technicians. The potential impact of glyphosate on human health, together with the extremely limited monitoring of glyphosate concentrations in South African environmental waters, has highlighted the need for the development of a cost-effective, rapid and reliable detection method for glyphosate.

Our study demonstrated the development of a novel first generation nanofiber-based colorimetric sensor (cd-PVA sensor) for the detection of glyphosate and glyphosate in formulation in water. To the best of our knowledge, only one chemical sensor (filter paper-based sensor) has been

reported for glyphosate (Da Silva *et al.*, 2011) to date and there have been no reports for nanofiber-based chemical sensors for glyphosate. The detection method selected for the current study was based on the principle reaction reported by Jan *et al.* (2009), which involved the reaction of glyphosate with carbon disulfide for the formation of a glyphosate dithiocarbamate intermediate, followed by a reaction with copper (in the form of copper nitrate) for the formation of a yellow colored complex, which could be detected spectrophotometrically at 435 nm. The principle assay reported by Jan *et al.* (2009) required the use of large sample volumes, therefore towards improving the applicability of this assay for sensor development, this study demonstrated the successful scale-down of the principal assay method to a total assay volume of 1 ml. The scale-down method was successfully applied to the detection of pure glyphosate and glyphosate in formulation (Ro and Wo). Analytical performance parameters, including specificity and sensitivity, were determined for the purposes of comparative analysis with the cd-PVA sensor system. The scale-down method was optimized with respect to reagent concentration, pH and reaction time, which would serve as the foundation in proof of concept experiments for cd-PVA sensor system.

The scale-down method was subsequently followed by the successful production of collectable, bead-free cd-PVA nanofibers mats, using the electrospinning process. SEM analysis of the nanofiber mats indicated a heterogeneous nanofiber mat structure, therefore future studies were conducted using one mat per experiment to reduce experimental variation. The resultant cd-PVA nanofiber mats were cut into 10 mm × 10 mm squares and served as colorimetric chemical sensors for glyphosate detection in water.

The proof of concept study involved the application of a small volume (30 µl sample volume, which sufficiently covered the entire sensing area) of a glyphosate dithiocarbamate intermediate sample (1000 µg/ml) onto the cd-PVA nanofiber sensor strips, which resulted in an immediate (approximately 3 seconds) color change from blue to yellow in the presence of glyphosate. The proof of concept for the cd-PVA system was validated and the cd-PVA sensor system developed in this study successfully detected glyphosate at a volume 4-fold lower than was required for the scale-down method. The cd-PVA sensor system was optimized with respect to pH (pH 12) and carbon disulfide concentration (6 %). During the proof of concept study the cd-PVA sensor system was characterized by its simplicity (simple assay method and quantification procedure)

and a rapid/immediate sensor response (naked eye detection) in the presence of glyphosate, which would provide an advantage over previous glyphosate detection methods.

Following the development of the cd-PVA sensor system for glyphosate detection, the final objective of the current study was to investigate various analytical parameters (i.e. color development and stability, storage stability, cd-PVA system precision, cd-PVA system reproducibility, sensitivity, selectivity and specificity), to determine the practical applicability of the cd-PVA sensor system.

The cd-PVA sensor system was characterized by the ability to detect glyphosate in formulation (Ro and Wo), good specificity with regards to the glyphosate structural analogs (AMPA and glycine) (16 % sensor response), a satisfactory system precision (RSD values below 20 %) and good short-term storage stability (~ 2.5 weeks) under ambient storage conditions. The cd-PVA sensor system also demonstrated good sensitivity, more specifically in the detection of pure glyphosate (practical LOD value of 0.1 μg/ml). The detection limit for pure glyphosate was comparable and within the range of the detection limits reported for spectrophotometric glyphosate detection methods (Jan *et al.*, 2009; Sharma *et al.*, 2012; Waiman *et al.*, 2012). More importantly, based on the MRL guidelines set by the USEPA (0.7 μg/ml) and WHO (0.9 μg/ml) for glyphosate in drinking water and the proposed short term standards (0.25 μg/ml) proposed by Mensah *et al.* (2013) for the glyphosate formulation, Roundup® in South African environmental waters, the cd-PVA sensor system demonstrated satisfactory sensitivity for the detection of pure glyphosate. Although the cd-PVA sensor showed poorer sensitivity with respect to the detection of glyphosate in Ro and Wo (when compared to water guidelines), which may limit applicability, the practical LOD values (1.95 μg/ml) obtained for glyphosate (in both formulations) overall demonstrated greater sensitivity when compared to the reported chemical sensor for glyphosate (reported LOD, 7.28 μg/ml) (Da Silva *et al.*, 2011). Some studies (Chapter 1, Table 1.3) have indicated the presence of glyphosate residues, in environmental water systems at lower levels than the LOD reported for the cd-PVA sensor. Future studies should involve enhancing the sensitivity of the cd-PVA sensor system, to improve its applicability over a wider range of glyphosate concentrations.

Although recovery and interference studies confirmed the susceptibility of the cd-PVA sensor system to compounds and ions commonly found in environmental water systems, good

recoveries were observed in distilled water samples representative of pristine waters, which validated the ability of the cd-PVA sensor to quantify glyphosate and glyphosate in formulation (Ro and Wo) in water, in the absence of interfering matrix effects. Based on these findings it was concluded that pre-treatment/pre-concentration, strategies such as solid-phase extraction, would be a requirement when using this assay in future studies.

The cd-PVA sensor demonstrated various advantageous characteristics; however this sensor also presented some limitations with regards to its practical applicability. These included color non-uniformity across the sensor area over time (attributed to the mobility of matrix components within the nanofiber network), poor system reproducibility (attributed to the heterogeneous nanofiber mat structure) and a limited long-term stability (attributed to the low mechanical integrity of PVA and potential susceptibility of the system to high humidity conditions). The limitations encountered in the cd-PVA sensor system appear to be directly linked to nanofiber structural design, which suggests that this would be a key factor to investigate for future studies. Focus should be placed on further optimization of processes which would control the structural composition and integrity of the cd-PVA nanofibers, ultimately with the aim to enhance the analytical performance of the system and subsequently improve its practical applicability.

Several methods have been proposed throughout the current study as possible future strategies for improving the analytical performance of the cd-PVA sensor (refer to Chapter 6) examples include:

1. Further optimization of the electrospinning process under environmentally controlled conditions, for the production of homogenous nanofiber mats, with smaller nanofiber diameters and pore sizes, which would improve the reproducibility and structural integrity (improve long-term storage and reduce reagent migration) of the sensor system.

2. The use of cross-linking methods/blending methods/the incorporation of structural reinforcing compounds such as hydrotalcite for the improvement PVA nanofiber structural integrity (improve long-term storage) and the potential for the reduction in reagent migration due to stabilization effects (Kubo and Kadla, 2003; Scothford *et al.,* 1998; Zhou *et al.,* 2011a).

3. The incorporation of cellulose nanocrystals into the PVA nanofiber matrix, to improve the rigidity and resistance of the cd-PVA sensor system to humidity effects (improve long-term stability) (Ago *et al.*, 2012).

4. The optimization of the surface chemistry of the cd-PVA sensor system, by converting the 1-D nanostructure of PVA nanofibers to a 3-D nanostructure using the electrospinning/netting method, which would potentially significantly improve the sensitivity of the cd-PVA sensor system, particularly for the detection of glyphosate in formulation (Wang *et al.*, 2013).

5. In the current study, the derivatization of glyphosate was based on the principle reaction reported by Jan *et al.* (2009) and therefore involved the use of carbon disulfide. When using this assay careful handling and the appropriate disposal of this chemical would be required. Future studies could explore the use green chemistry protocols for the derivatization of glyphosate.

Although the cd-PVA sensor system would require further work to improve its practical applicability, the knowledge gained from this current study has provided the foundation for future developments in nanofiber-based colorimetric chemical sensors for the detection of glyphosate.

# Chapter 8- REFERENCES

Abbaspour A. Khajehzadeh A. Noori A. 2008. A simple and selective sensor for the determination of absorbic acid in vitamin C tablets based on paptode. *Analytical Sciences* 24: 721-725.

Abbaspour A. Mirahmadi E. Khajehzadeh A. 2010. Disposable sensor for quantitative determination of hydrazine in water and biological sample. *Analytical Methods* 2: 349-353.

Abe K. Suzuki K. Citterio D. 2008. Inkjet-printed microfluidic multianalyte chemical sensing paper. *Analytical Chemistry* 80: 6928-6934.

Abu-Saied M.A. Khalil K.A. Al-Deyab S.S. 2012. Short communications: preparation and characterization of poly vinyl acetate nanofiber doping copper metal. *International Journal of Electrochemical Science* 7: 2019-2027.

Achiorno C.L. De Villalobos C. Ferrari L. 2008. Toxicity of the herbicide glyphosate to *Chordodes nobilii* (Gordiida, Nematomorpha). *Chemosphere* 71: 1816-1822.

Acuri H.A. Canduri F. Pereira J.H. da Silveira N.J.F. Camera Jr J.C. de Oliveira J.S. Basso l.A. Palma M.S. Santos D.S. Azevedo Jr W.F. 2004. Molecular models for shikimate pathway enzymes of *Xylella fastidiosa* . *Biochemical and Biophysical Research Communications* 320: 979-991.

Adams B.D. Furneaux H. White B.A. 2007. The micro-ribonucleic acid (miRNA) miR-206 targets the human estrogen receptor-α (ER-α) and represses ERα messenger RNA and protein expression in breast cancer cell lines. *Molecular Endocrinology* 21: 1132-1147.

Adhikari B. and Majumdar S. 2004. Polymer in sensor applications. *Progress in Polymer Science* 29: 699-766.

Afkami A. Sarlak N. Zarei A.R. 2006. Spectrophotometric determination of salicylamide and paracetamol in biological samples and pharmaceutical formulations by a differential kinetic method. *Acta Chimica Slovencia* 53: 357-362.

African Centre for Biosafety. 2008. Agrofuels in South Africa: projects, players and poverty. An information document (http://www.biosafetyafrica.net) accessed December 2013.

African Centre for Biosafety. 2012. Genetically modified crops in South Africa 2008-2012. An information document (http://www.biosafetyafrica.net) accessed December 2013.

African Centre for Biosafety. 2013. GM maize lessons for Africa: cartels, collusions and control of South Africa´s staple food. An information document (http://www.biosafetyafrica.net) accessed January 2014.

Ago M. Okajima K. Jakes J.E. Park S. Rojas O.J. 2012. Lignin-based electrospun nanofibers reinforced with cellulose nanocrystals. *Biomacromolecules* 13: 918-926.

## Chapter 8: References


Ahn H.J. Yoon H.J. Lee B.I. Suh S.W. 2004. Crystal structure of chorismate synthase: A novel FMN-binding protein fold and functional insights. *Journal of Molecular Biology* 336: 903-915.

Akamatsu K. Ikedo S. Nawafune H. Yanagimoto H. 2004. Direct patterning of copper on polyimide using ion exchangeable surface templates generated by site-selective surface modification. *Journal of the Americam Chemical Society* 126: 10822-10823.

Aksakal O. Erturk F.A. Sunar S. Bozari S. Agar G. 2013. Assessment of genotoxic effects of 2,4-dichlorophenoxyacetic acid on maize by RAPD analysis. *Industrial Crops and Products* 42: 552-557.

Albers C.N. Banta G.T. Hansen P.E. Jacobsen O.S. 2009. The influence of organic matter on sorption and fate of glyphosate in soil-comparing different soils and humic substances. *Environmental Pollution* 157: 2865-2870.

Albert K.J. Lewis N.S. Schauer C.L. Sotzing G.A. Stitzel S.E. Vaid T.P. Walt D.R. 2000. Cross-reactive chemical sensor arrays. *Chemical Reviews* 100: 2595-2626.

Alferness P.L. and Iwata Y. 1994. Determination of glyphosate and (aminomethyl)phosphonic acid in soil, plant and animal matrices, and water by capillary gas chromatography with mass-selective detection. *Journal of Agriculture and Food Chemistry* 42: 2751-2759.

Ali M.M.N. Kaliannan P. Venuvanalingam P. 2005. Conformation and function of *N*-hydroxy-glyphosate and *N*-amino-glyphosate: A comparative study using ab initio MO theory. *Journal of Molecular Structure: THEOCHEM* 714: 99-108.

Aliferis K.A. and Jabaji S. 2011. Review: Metabolomics-a robust bioanalytical approach for the discovery of the modes of action of pesticides. *Pesticide Biochemistry and Physiology* 100: 105-117.

Al-Rajab A.J. and Schiavon M. 2010. Degradation of $^{14}$C-glyphosate and aminomethylphosphonic acid (AMPA) in three agricultural soils. *Journal of Environmental Sciences* 22: 1374-1380.

Anadón A. Martínez-Larrañaga M.R. Martínez M.A. Castellano V.J. Martíinez M. Martin M.T. Nozal M.J. Bernal J.L. 2009. Toxicokinetics of glyphosate and its metabolite aminomethyl phosphonic acid in rats. *Toxicology Letters* 190: 91-95.

Anderson D. Yu T.W. McGregor D.B. 1998. Review: Comet assay responses as indicators of carcinogen exposure. *Mutagenesis* 13: 539-555.

Anderson O. 1999. Principles and recent developments in chelation treatment of metal intoxication. *Chemistry Reviews* 99: 2683-2710.

Andreu V. and Picó Y. 2004. Determination of pesticides and their degradation products in soil: critical review and comparison of methods. *Trends in Analytical Chemistry* 23: 10-11.

Ansara-Ross T.M. Wepener V. Van Den Brink P.J. Ross M.U. 2012. Pesticides in South Africa fresh waters. *African Journal of Aquatic Science* 37: 1-16.

## Chapter 8: References


Antachopoulos C. Meletiadis J. Sein T. Roilides E. Walsh T.J. 2007. Concentration dependent effects of caspofungin on the metabolic activity of *Aspergillus* species. *Antimicrobial agents and chemotherapy* 51: 881-887

Anthony R.G. and Hussey P.J. 1999. Review: Dinitroaniline herbicide resistance and the microtubule cytoskeleton. *Trends in Plant Science* 4: 112-116.

Antón F.A. Cuadra L.M. Gutierrez P. Laborda E. Laborda P. 1993. Degradational behavior of the pesticides glyphosate and diflubenzuron in water. *Environmental Contamination and Toxicology* 51: 881-888.

Anwar W.A. 1997. Biomarkers of human exposure to pesticides. *Environmental Health Perspectives* 105: 801-805.

Aparicio V.C. De Gerónimo E. Marino D. Primost J. Carriquiriborde P. Costa J.L. 2013. Environmental fate of glyphosate and aminomethylphosphonic acid in surface waters and soil of agriculture basins. *Chemosphere* 93: 1866-1873.

Araújo A.S.F. Monteiro R.T.R. Abarkeli R.B. 2003. Effect of glyphosate on the microbial activity of two Brazilian soils. *Chemosphere* 52: 799-804.

Araujo P. 2009. Key aspects of analytical method validation and linearity evaluation. *Journal of Chromatography B* 877: 2224-2234.

Argese E. Bettiol C. Marchetto D. De Vettori S. Zambon A. Miana P. Ghetti P.F. 2005. Study on the toxicity of phenolic and phenoxy herbicides using submitrochondrial particle assay. *Toxicology in Vitro* 19: 1035-1043.

Arregui M.C. Lenardón A. Sanchez D. Maitre M.I. Scotta R. Enrique S. 2003. Monitoring glyphosate residues in transgenic glyphosate-resistant soybean. *Pest Management Science* 60: 163-166.

Arshak K. Moore E. Lyons G.M. Harris J. Clifford S. 2004. A review of gas sensors employed in electronic nose applications. *Sensor Review* 24: 181-198.

Arya S.K. Krishnan S. Silva H. Jean S. Bhansali S. 2012. Advances in materials for room temperature hydrogen sensors. *Analyst* 137: 2743-2756.

Aryanpour N. Mansouri-Torshizi H. Nakhajavan M. Shirazi F.H. 2012. Cytotoxicity of diimine palladium (II) complexes of alkyldithiocarbmate derivatives on human lung, ovary, and liver cells. *Iranian Journal of Pharmaceutical Research* 11: 689-695.

Astiz M. De Alaniz J.T. Marra C.A. 2009. Effect of pesticides on cell survival in liver and brain rat tissues. *Ecotoxicology and Environmental Safety* 72: 2025-2032.

## Chapter 8: References


Astiz M. Diz-Chaves Y. Garcia-Segura L.M. 2013. Sub-chronic exposure to the insecticide dimethoate induces a proinflammatory status and enhances the neuroinflammatory response to bacterial lipopolysaccharide in the hippocampus and stiratum of male mice. *Toxicology and Applied Pharmacology* 272: 263-271.

Badr I.H.A. Meyerhoff M.E. Hassan S.S.M. 1995. Novel response mechanism and application of sulfite sensitive polymeric membrane electrode based on dithiocarbamate complexes of mercury (II). *Analytica Chimica Acta* 310: 211-221.

Bagestani M.A. Zand E. Soufizadeh S. Bagherani N. Deihimfard R. 2007. Weed control and wheat (*Triticum aestivum L.*) yield under application of 2,4-D plus carfentrazone-ethyl and florasulam plus flumetsulam: evalustion of the efficacy. *Crop Protection* 26: 1759-1764.

Bajguz A. and Tretyn A. 2003. Review: The chemical characteristic and distribution of brassinosteroids. *Phytochemistry* 62: 1027-1046.

Bakand S. and Hayes A. 2010. Troubleshooting methods for toxicity of airborne chemicals *in vitro. Journal of Pharmacological and Toxicological Methods* 61: 76-85.

Balaji T. Sasidharan M. Matsunaga H. 2005. Optical sensor for the visual detection of mercury using mesoporous silica anchoring porphyrin moiety. *The Analyst* 130: 1162- 1167.

Balaji T. Sherif A. Matsunaga H. Hanaoka T. Mizukami F. 2006. Optical sensors based on the nanostructured cage materials for the detection of toxic metal ions. *Angewandte Chemie* 118: 7960-7966.

Barbosa E.R. 2001. Parkinsonism after glycine-derivative exposure. *Movement Disorders* 16: 565-568.

Bargagli R. 1999. Herbicides, defoliants. *Encyclopedia of Environmental Science* 20: 316.

Barja B.C. and Dos Santos Alfonso M. 2005. Aminomethylphosphonic acid and glyphosate adsorption onto goethite: a comparative study. *Environmental Science and Technology* 39: 585-592.

Basabe-Desmonts L. Reinhoudt D.N. Crego-Calama M. 2007. Design of fluorescente materials for chemical sensing. *Chemical Society Reviews* 36: 993-1017.

Basi S. Noga G. Hunsche M. 2013. Relevance of the deposit structure for the upatke and bio-efficacy of diquat, as monitored by the spatially resolved chlorophyll fluorescence. *Pesticide Biochemistry and Physiology* 107: 218-225.

Bate G. Smailes P. Adams J. 2004. A water quality index for use with diatoms in the assessment of rivers. *Water SA* 30: 493-498.

Battaglin W.A. Kolpin D.W. Scribner E.A. Kuivila K.M. Sandstrom M.W. 2005. Glyphosate, other herbicides and transformation products in Midwestern streams, 2002. *Journal of the American Water Resources Association* 323-332.

Batterham G.J. Munksgaard N.C. Parry D.L. 1997. Determination of trace metals in sea water by inductively coupled plasma mass spectrometry after off line dithiocarbamate solvent extraction. *Journal of Analytical Spectrometry* 12: 1277-1280.

## Chapter 8: References


Belbachir O. Matringe M. Chevallier D. Tissut M. 1980. Physiological actions of dinoterb, a phenol derivative. 2. Effects on isolated plant mitochondria and chloroplasts. *Pesticide Biochemistry and Physiology* 14: 309-313.

Benachour N. and Seralini G.E. 2009. Glyphosate formulation induce apoptosis and necrosis in human umbilical, embryonic and placental cells. *Chemical Research in Toxicology* 22: 97-105.

Benachour N. Sipahutar H. Moslemi S. Gasnier C. Travert C. Seralini G.E. 2007 Time and dose dependent effects of Roundup on human embryonic and placental cells. *Archives of Environmental Contamination and Toxicology* 53: 126-133.

Benedetti A.L. De Lourdes Vituri C. Trentin A.G. Domingues M.A.C. Silva M.A. 2004. The effects of sub-chronic exposure of Wistar rats to the herbicide Glyphosate-Biocarb®. *Toxicological Letters* 153: 227-232.

Benedini V.D. Antunes P.A. Catalheiro E.T.G. Chierice G.O. 2006. Thermoanalytical and solution stability studies of hexamethylenedithiocarbamates. *Journal of Brazilian Chemistry Society* 17: 680-688.

Bergshoef M.M. and Vancso G.J. 1999. Transparent nanocomposites with ultrathin electrospun nylon-4,6 fiber reinforcement. *Advanced Materials* 11: 1362-1365.

Bermúdez-Couso A. Fernández-Calviño D. Alvarez-Enjo M.A. Simal-Gándara J. Nóvoa-Muñoz J.C. Arias-Estévez M. 2013. Pollution of surfasse waters by metalaxyl and nitrate from non-point sources. *Science of the Total Environment* 461-462: 282-289.

Berryman D. Houde F. DeBlois C. O´Shea M. 2004. Nonylphenolic compounds in drinking and surface waters downstream of treated textile and pulp and paper effluents: a survey and preliminary assessment of their potential effects on public health and aquatic life. *Chemosphere* 56: 247-255.

Beuret C.J. Zirulnik F. Giménez M.S. 2005. Effect of the herbicide glyphosate on liver lipoperoxidation in pregnant rats and their fetuses. *Reproductive Toxicology* 19: 501-504.

Bhaskara B.L. and Nagaraja P. 2006. Direct sensitive spectrophotometric determination of glyphosate by using ninhydrin as a chromogenic reagent in formulations and environmental water samples. *Helvetica Chimica Acta* 89: 2686-2693.

Bhattarai N. Edmondson D. Veiseh O. Matsen F.A. Zhang M. 2005. Electrospun chitosan-based nanofibers and their cellular compatibility. *Biomaterials* 26: 6176-6184.

Biagini R.E. Smith J.P. Sammons D.L. MacKenzie B.A. Striley C.A.F. Robertson S.K. Snawder J.E. 2004. Development of a sensitivity enhanced multiplex fluorescence covalent microbead immunosorbent assay (FCMIA) for the measurement of glyphosate, atrazine and metachlor mercapture in water and urine. *Analytical and Bioanalytical Chemistry* 379: 368-374.

Binimelis R. Pengue W. Monterroso I. 2009. "Transgenic treadmill": Responses to the emergence and spread of glyphosate-resistant johnsongrass in Argentina. *Geoforum* 40: 623-633.

## Chapter 8: References


Binning K. and Baird D. 2001. Survey of heavy metals in the sediments of the Swartkops River Estuary, Port Elizabeth South Africa. *Water SA* 7: 461-466.

Binns J.A. Illigner P.M. Nel E.L. 2001. Water shortage, deforestation and development: South Africa´s working for water programme. *Land Degradation and Development* 12: 341-355.

Birch N.C. and Stickle D.F. 2003. Example of use of a desktop scanner for data acquisition in a colorimetric assay. *Clinica Chimica Acta* 333: 95-96.

Birnbaum L.S. and Fenton S.E. 2003. Review: Cancer development exposure to endocrine disruptors. *Environmental Health Perspectives* 111: 389-394.

Biziuk M. Przyjazny A. Czerwinski J. Wiergowski M. 1996. Review: Occurrence and determination of pesticides in natural and treated waters. *Journal of Chromatography A* 754: 103-123.

Blair A.C. and Wolfe L.M. 2004. The evolution of an invasive plant: an experimental study with *Silene latifolia. Ecology* 85: 3035-3042.

Bogaard A. Hodgson J.G. Wilson P.J. Band S.R. 1998. An index of weed size for assessing the soil productivity of ancient crop fields. *Vegetation History and Archaeobotany* 7: 17-22.

Bollmohr S. Day J.A. Schulz R. 2007. Temporal variability in particle-associated pesticide exposure in a temporarily open estuary, Western Cape, South Africa. *Chemosphere* 68: 479-488.

Bolognesi C. 2003. Review: Genotoxicity of pesticides: a review of human biomonitoring studies. *Mutation Research* 543: 251-272.

Bolognesi C. Bonatti S. Degan P. Gallerani E. Peluso M. Rabboni R. Roggieri P. Abbondandolo A. 1997. Genotoxic activity of glyphosate and its technical formulation Roundup. *Journal of Agricultural Food Chemistry* 45: 1957-1962.

Bolto B. Tran T. Hoang M. Xie Z. 2009. Crosslinked poly(vinyl alcohol) membranes. *Progress in Polymer Science* 34: 969-981.

Bond A.M. and Wallace G.G. 1981. Determination of copper as a dithiocarbamate complex by reversed-phase liquid chromatography with electrochemical detection. *Analytical Chemistry* 53: 1209-1213.

Bond A.M. and Wallace G.G. 1984. Preparation of metal dithiocarbamate complexes for chromatographic separation and multi-element determinations. *Analytica Chimica Acta* 164: 223-232.

Boocock M.R. and Coggins J.R. 1983. Kinetics of 5-enolpyruvylshikimate-3-phosphate synthase inhibition by glyphosate. *Federation of European Biochemical Societies Letters* 154: 127-133.

Borggaard O.K. and Gimsing A.L. 2008. Fate of glyphosate in soils and the possibility of leaching to ground and surface waters: a review. *Pest Management Science* 64: 441-456.

Bosque-Sendra J.M. Almansa-Lopez E. Garcia-Campana A.M. Cuadros-Rodriguez L. 2003. Data analysis in the determination of stoichiometries and stability constants of complexes. *Analytical Sciences* 19: 1431-1439.

## Chapter 8: References


Botero-Coy A.M. Ibáñez M. Sancho J.V. Hernández F. 2013. Direct liquid chromatography-tandem mass spectrometry determination of underivatized glyphosate in rice, maize and soybean. *Journal of Chromatography A* 1313: 157-165.

Botta F. Fauchin N. Blanchoud H. Chevreuil M. Guery B. 2012. Phyt'Eaux Cités: Applications and validations of a programme to reduce surface water contamination with urban pesticides. *Chemosphere* 86: 166-176.

Bowes J. Crofts A.R. Arntzen C.J. 1980. Redox reactions on the reducing side of photosystem II in chloroplasts with altered herbicide binding properties. *Archives of Biochemistry and Biophysics* 200: 303-306.

Boyd-Boland A.A. Chai M. Luo Y.Z. Zhang Z. Yang M.J. Pawliszyn J.B. 1994. New solvent-free sample preparation techniques based on fiber and polymer technologies. *Environmental Science & Technology* 28: 569-574.

Bradshaw L.D. Padgette S.R. Kimball S.L. Wells B.H. 1997. Perspectives on glyphosate resistance. *Weed Technology* 11: 189-198.

Brake D.G. and Evenson D.P. 2004. A generational study of glyphosate-tolerant soybeans on mouse fetal, postnatal, pubertal and adult testicular development. *Food and Chemical Toxicology* 42: 29-36.

Bromilow R.H. and Chamberlain K. 2000. The herbicide glyphosate and related molecules: physiochemical and structural factors determining their mobility in phloem. *Pest Management Science* 56: 368-373.

Bromilow R.H. Chamberlain K. Evans A.A. 1990. Physiochemical aspects of phloem translocation of herbicides. *Weed Science* 38: 305-314.

Broser M. Gloeckner C. Gabdulkhakov A. Guskov A. Buchta J. Kern J. Mueh F. Dau H. Saenger W. Zouni A. 2011. Structural basis of cyanobacterial photosystem II inhibition by the herbicide terbutryn. *The Journal of Biological Chemistry* 286: 1-16.

Budde W.L. 2004. Review: analytical mass spectrometry of herbicides. *Mass Spectrometry Reviews* 23: 1-24.

Buell S. Van Vliet K.J. Rutledge G.C. 2009. Mechanical properties of glassy polyethylene nanofibers via molecular dynamics simulations. *Macromolecules* 42: 4887-4895.

Buman R.A. Gealy D.R. Fuerst E.P. 1992. Relationship between temperature and triazinone herbicide activity II. Herbicide absorption by protoplasts and herbicide inhibition of photosynthetic. *Pesticide Biochemistry and Physiology* 43: 29-36.

Bussan A.J. and Dyer W.E. 1999. Herbicides and rangeland. Sheley R.L. and J.K. Petroff edition. *Biology of Noxious Rangeland Weeds.* Corvallis, Oregan State University Press 116-132.

## Chapter 8: References


Buteau-Lozano H. Velasco G. Cristofari M. Balaguer P. Perrot-Applanat M. 2008. Xenoestrogens modulate vascular endothelial growth factor secretion in breast cancer cells through an estrogen receptor-dependent mechanism. *Endocrinology Journals* 196: 399-412.

Butler T.M. MacCraith B.D. McDonagh C. 1998. Leaching in sol-gel derived films for optical pH sensing. *Journal of Non-Crystalline Solids* 224: 249-258.

Buttner W.J. Post M.B. Burgess R. Rivkin C. 2011. An overview of hydrogen safety sensors and requirements. *International Journal of Hydrogen Energy* 36: 2462-2470.

Byer J.DD. Struger J. Klawunn P. Todd A. Sverko E. 2008. Low cost monitoring of glyphosate in surface waters using ELISA method: an evaluation. *Environmental Science and Technology* 42: 6052-6057.

Caetano M.S. Freitas M.P. Da Cunha E.F.F. Ramalho T.C. 2013. Construction and assessment of reaction models of Clas I EPSP synthase. Part II: Investigation of the EPSP ketal. *Journal of Biomolecular Structure and Dynamics* 31: 393-402.

Cakmak I. Yazici A. Tutus Y. Ozturk L. 2009. Glyphosate reduced seed and leaf concentrations of calcium, manganese, magnesium, and iron in non-glyphosate resistant soybean. *European Journal of Agronomy* 31: 114-119.

Calabrese E.J. and Baldwin L.A. 2001. Hormesis: U-shaped dose responses and their centrality in toxicology. *Trends in Pharmacological Sciences* 22: 285-291.

Camposeo A. Greenfeld I. Tantussi F. Pagliara S. Moffa M. Fuso F. Allegrini M. Zussman E. Pisignano D. 2013. Local mechanical properties of electrospun fibers correlate to their internal nanostructure. *Nano Letters* 13: 5056-5062.

Candela L. Alvarez-Benedi J. De Melo M.T.C. Rao P.S.C. 2007. Laboratory studies on glyphosate transport in soils of Maresme area near Barcelona, Spain: transport model parameter estimation. *Geoderma* 140: 8-16.

Candela L. Caballero J. Ronen D. 2010. Glyphosate transport through weathered granite soils under irrigated and non-irrigated conditions – Barcelona, Spain. *Science of the Total Environment* 408: 2509-2516.

Cantrell K. Erenas M.M. De Orbe-Paya I. Capitan-Vallvey L.F. 2010. Use of the hue parameter of the hue, saturation, value color space as a quantitative analytical parameter for bitonal optical sensors. *Analytical Chemistry* 82: 531-542.

Cao R. Pérez L.G. Moya R. Díaz A. 2000. Interaction of copper(II) dithiocarbamates with hydrogen peroxide. *Journal of Mexican Chemical Society* 44: 158-162.

Carlisle S.M. and Trevors J.T. 1988. Review: Glyphosate in the environment. *Water, Air and Soil Pollution* 39: 409-420.

Carter A. 2000. How pesticides get into water-and proposed reduction measures. *Water* doi: 10.1039/b006243j.

Cartigny B. Azaroual N. Imbenotte M. Mathieu D. Vermeersch G. Goullé J.P. Lhermitte M. 2004. Determinaiton of glyphosate in biological fluids by $^{1}H$ and $^{31}P$ NMR spectroscopy. *Forensic Science International* 143: 141-145.

Casper C.L. Stephens J.S. Tassi N.G. Chase B. and Rabolt J.F. 2004. Controlling surface morphology of electrospun polystyrene fibers: effect of humidity and molecular weight in the electrospinning process. *Macromolecules* 37: 573-578.

Cassatella M.A. Meda L. Bonora S. Ceska M. Constantin G. 1993. Brief definitive report: Interleukin 10 (IL-10) inhibits cytokines from human polymorphonuclear leukocytes. Evidence for an autocrine role of tumor necrosis factor and IL-1β in mediating the production of IL-8 triggered by lipopolysaccharide. *The Journal of Experimental Medicine* 178: 2207-2211.

Castro J.V. Peralba M.C.R. Ayub M.A.Z. 2007. Biodegradation of the herbicide glyphosate by filamentous fungi in platform shaker and batch reactor. *Journal of Environmental Science and Health Part B* 42: 883-886.

Castro-Rivera E. and Safe S. 1998. Estrogen and anti-estrogen responsiveness of HEC1A endometrial adenocarcinoma cells in culture. *Journal of Steroid Biochemistry and Molecular Biology* 64: 287-295.

Cate D.M. Nanthasurasak P. Riwkulkajorn P. L`Orange C. Henry C.S. Volckens J. 2014. Rapid detection of transition metals in welding fumes using paper-based analytical devices. *The Annals of Occupational Hygiene* 58: 413-423.

Cedergreen N. and Olesen C.F. 2010. Can glyphosate stimulate photosynthesis? *Pesticide Biochemistry and Physiology* 96: 140-148.

Chahal GG.S. Jordan D.L. Shew B.B. Bradenburg R.L. York A.C. Burton J.D. Danehower D. 2012. Interactions of agrochemicals applied to peanut, part 1: Effects on herbicides. *Crop Protection* 41: 134-142.

Chamel A. and Gambonnet B. 1997. Sorption and diffusion of an ethoxylated stearic alcohol and an ethoxylated stearic amine into and through isolated plant cuticles. *Chemosphere* 34: 1777-1786.

Chan Y.C. Chang S.C. Hsuan S.L. Chien M.S. Lee W.C. Kang J.J. Wang S.C. Liao J.W. 2007. Cardiovascular effects of herbicides and formulated adjuvants on isolated rat aorta and heart. *Toxicology in Vitro* 21: 595-603.

Chang S.Y. and Liao C.H. 2002. Analysis of glyphosate, glufosinate and aminomethylphosphonic acid by capillary electrophoresis with indirect fluorescence detection. *Journal of Chromatography A* 959: 309-315.

Charudattan R. 2001. Biological control of weeds by means of plant pathogens: significance for integrated weed management in modern agro-ecology. *BioControl* 46: 229-260.

Checchetto V. Teardo E. Carraretto L. Formentin E. Bergantino E. Giacometti G.M. Szabo I. 2013. Review: Regulation of photosynthesis by ion channels in cyanobacteria and higher plants. *Biophysical Chemistry* 182: 51-57.

## Chapter 8: References


Cheng Q. Wang S. Rials T.G. 2009. Poly (vinyl) alcohol nanocomposites reinforced with cellulose fibrils isolated by high intensity ultrasonication. *Composites Part A: Applied Science and Manufacturing* 40: 218-224.

Chen M.X. Cao Z.Y. Jiang Y. Zhu Z.W. 2013a. Direct determination of glyphosate and its major metabolite, aminomethylphosphonic acid, in fruits and vegetables by mixed-mode hydrophilic interaction/weak anion-exchange liquid chromatography coupled with electrospray tandem mass spectrometry. *Journal of Chromatography A* 1272: 90-99.

Chen S. Hong Y. Liu Y. Liu J. Leung C.W.T. Li M. Kwok R.T.K. Zhao E. Lam J.W.Y. Yu Y. Tang B.Z. 2013b. Full-range intracellular pH sensing by an aggregation-induced emission active two-channel ratiometric fluorogen. *Journal of the American Chemical Society* 135: 4926-4929.

Chew S.Y. Hufnagel T.C. Lim C.T. Leong K.W. 2006. Mechanical properties of single electrospun drug-encapsulated nanofibres. *Nanotechnology* 17: 3880-3891.

Chigome S. and Torto N. 2011. Review: A review of opportunities for electrospun nanofibers in analytical chemistry. *Analytica Chimica Acta* 706: 25-36.

Chiu H.Y. Lin Z.Y. Tu H.L. Whang C.W. 2008. Short communication: Analysis of glyphosate and aminomethylphosphonic acid by capillary electrophoresis with electrochemiluminescence detection. *Journal of Chromatography A* 1177: 195-198.

Cho E.J. Ryu B.J. Lee Y.J. Nam K.C. 2005. Visible colorimetric fluoride ion sensors. *Organic Letters* 7: 2607-2609.

Choi J. Choi D. Lee S. Ryu C.M. Hwang I. 2011. Cytokinins and plant immunity: old foes or new friends. *Trends in Plant Science* 16: 388-394.

Chronakis I.S. 2005. A review: Novel nanocomposites and nanoceramics based on polymer nanofibers using electrospinning process. *Journal of Material Processing Technology* 167: 283-293.

Chronakis I.S. Grapeson S. Jakob A. 2006. Conductive polypyrrole nanofibers via electrospinning: electrical and morphological properties. *Polymer* 47: 1597-1603.

Cikalo M.G. Goodall D.M. Matthews W. 1996. Analysis of glyphosate using capillary electrophoresis with indirect detection. *Journal of Chromatography A* 745: 189-200.

Clair E. Mesnage R. Travert C. Sérallini G.E. 2012. A glyphosate-based herbicide induces necrosis and apoptosis in mature ray testiculae cell *in vitro*, and testosterone decrease at lower levels. *Toxicology in Vitro* 26: 269-279.

Clegg E.S. Stephenson G.R. Hall J.C. 1999. Development of an enzyme-linked immunosorbent assay for the detection of glyphosate. *Journal of Agriculture and Food Chemistry* 47: 5031-5037.

Clements D.R. Di Tommaso A. Jordan N. Booth B.D. Cardina J. Doohan D. Mohler C.L. Murphy S.D. Swanton C.J. 2004. Review: Adaptability of plants invading North American cropland. *Agriculture, Ecosystems and Environment* 104: 379-398.

## Chapter 8: References


Coates J. 2000. Interpretation of infrared spectra, a practical approach. R.A. Meyers (Ed.). John Wiley & Sons Ltd, Chichester. *Encyclopedia of Analytical Chemistry* 10815-10837.

Cobianco S. Lezzi A. Scotti R. 2000. A spectroscopic study of Cu(II)-complexes of chelating resins containing nitrogen and sulfur atoms in the chelating groups. *Reactive & Functional Polymers* 43: 7-16.

Coleman J.O.D. Frova C. Schröder P. Tissut M. 2002. Exploiting plant metabolism for the phytoremediation of persistent herbicides. *Environmental Science and Pollution* 9: 18-28.

Comes R.D. Bruns V.F. Kelley A.D. 1976. Residues and Persistence of glyphosate in irrigation water. *Weed Science* 24: 47-50.

Conolly R.B. and Lutz W.K. 2004. Nonmonotonic dose-relationships: mechanistic basis, kinetic modeling, and implications for risk assessment. *Toxicological Sciences* 77: 151-157.

Corbera M. Hidalgo M. Salvado V. Wieczorek P.P. 2005. Determination of glyphosate and aminomethylphosphonic acid in natural water using the capillary electrophoresis combined with enrichment step. *Analytica Chimica Acta* 540: 3-7.

Corsini E. Sokooti M. Galli C.L. Moretto A. Colosio C. 2013. Pesticide induced immunotoxicity in humans: A comprehensive review of the existing evidence. *Toxicology* 307: 123-135.

Coutinho C.F.B. Coutinho L.F.M. Mazo L.H. Nixdorf S.L. Camara C.A.P. Lanças F.M. 2007. Direct determination of glyphosate using hydrophilic interaction chromatography with coulometric detection at copper microelectrode. *Analytica Chimica Acta* 592:30-35.

Coutinho C.F.B. Coutinho L.F.M. Mazo L.H. Nixdorf S.L. Camara C.A.P. 2008. Short communication: Rapid and direct determination of glyphosate and aminomethylphosphonic acid in water using anion-exchange chromatography with coulometric detection. *Journal of Chromatography A* 208: 246-249.

Cox C. and Surgan M. 2006. Unidentified inert ingredients in pesticides: implications for human and environmental health. *Environmental Health Perspectives* 114: 1803-1806.

Crespo-Corral E- Santos-Delgado M.J. Polo-Diez L.M. Soria A.C. 2008. Determination of carbamate, phenylurea and phenoxy acid herbicide residues by gas chromatography after pottasium *tert*-butoxide/dimethyl sulphoxide/ethyliodide derivatization reaction. *Journal of Chromatography A* 1209: 22-28.

Crnogorac G. and Schwack W. 2009. Residue analysis of dithiocarbamate fungicides. *Trends in Analytical Chemistry* 28: 40-50.

Da Silva A. Fernandes F.C.B. Tognolli J.O. Pezza L. Pezza H.R. 2011. A simple and green analytical method for determination of glyphosate in commercial formulations and water by diffuse reflectance spectroscopy. *Spectrochimica Acta Part A: Molecular and Biomolecular Spectroscopy* 1881-1885.

Dabrowski J.M. and Balderacchi M. 2013. Development and field validation of an indicator to assess the relative mobility and risk of pesticides in the Lourens River catchment, South africa. *Chemosphere* 93: 2433-2443.

## Chapter 8: References


Dabrowski J.M. Bollen A. Bennett E.R. Schulz R. 2005. Pesticide interception by emergent aquatic macrophytes: potential to mitigate spray-drift input in agriculture streams. *Agriculture, Ecosystems and Environment* 111: 340-348.

Dabrowski J.M. Peall S.K.C. Van Niekerk A. Reinecke A.J. Day J.A. Schulz R. 2002. Predicting runoff-induced pesticide input in agricultural sub-catchment surface waters: linking catchment variables and contamination. *Water Research* 36: 4975-4984.

Dabrowski J.M. Shadung J.M. Wepener V. 2014. Prioritizing agricultural pesticides used in South Africa based on their environmental mobility and potential human health effects. *Environmental International* 62: 31-40.

Dakashev A. Pavlov S. Stancheva K. 2013. Application of digital camera and digital image processing technique for molecular absorption analysis in the visible spectrum. *Universal Journal of Chemistry* 1: 129-134.

Dalkvist T. Topping C.J. Forbes V.E. 2009. Population-level impacts of pesticide-induced chronic effects on individuals depend more on ecology than toxicology. *Ecotoxicology and Environmental Safety* 72: 1663-1672.

Dalvie M.A. Africa A. London L. 2006. Disposal of unwanted pesticides in Stellenbosch, South Africa. *Science of the Total Environment* 361: 8-17.

Dalvie M.A. Africa A. London L. 2009. Change in the quantity and acute toxicity of pesticides sold in South Africa cop sectors 1994-1999. *Environmental International* 35: 683-687.

Dalvie M.A. Naik I. Channa K. London L. 2011. Urinary dialkyl phosphate levels before and after firat season chlorpyrifos spraying amongst farm workers in the Western Cape, South Africa. *Journal of Environmental Science and Health Part B: Pesticides, food contaminants, and agricultural wastes* 46: 163-172.

Damonte M. Torres Sánchez R.M. Dos Santos Afonso M. 2007. Some aspects of the glyphosate adsorption on montmorillonite and its calcined form. *Applied Clay Science* 36: 86-94.

Datta A. and Knezevic S.Z. 2013. A review: Chapter six-flaming as an alternative weed control method for conventional and organic agronomic crop production systems. *Advances in Agronomy* 118: 399-428.

Datta S. Christena L.R. Rajaram Y.R.S. 2013. Enzyme immobilization: An overview on techniques and support materials. *3 Biotech* 3: 1-9.

Dayan F.E. and Watson S.B. 2011. Plant cell membrane as a marker for light-dependent and light-independent herbicide mechanisms of action. *Pesticide Biology and Physiology* 101: 182-190.

Dayan F.E. De Zaccaro M.M.L. 2012. Chlorophyll fluorescence as a marker for herbicide mechanisms of action. *Pesticide Biochemistry and Physiology* 102: 189-197.

## Chapter 8: References


De Armond P.D. DiGoregorio A.L. 2013. Rapid liquid chromatography-tandem mass spectrometry-based method for the analysis of alcohol ethoxylates and alkylphenol ethoxylates in environmental samples. *Journal of Chromatography A* 1305: 154-163.

De Lima G.M. Menezes D.C. Cavalcanti C.A. Dos Santos A.F. Ferreira I.P. Paniago E.B. Wardall J.L. Wardell S.M.S.V. Krambrock K. Mendes I.C. Beraldo H. 2011. Synthesis characterization and biological aspects of copper (II) dithiocarbamate complexes, $[Cu\{S_2CNR(CH_2CH_2OH)\}_2]$, (R=Me, Et, Pr and $CH_2CH_2OH$). *Journal of Molecular Structure* 988: 1-8.

De Liz Oliveira Cavalli V.L. Cattani D. Rieg C.E.H. Pierozan P. Zanatta L. Parisotto E.B. Filho D.W. Silva F.R.M.B. Pureur R.P. Zamoner A. 2013. Roundup disrupts male reproductive functions by triggering calcium-mediated cell death in rat testis and Sertoli cells. *Free Radical Biology and Medicine B* 65: 335-346.

De Llasera M.P.G. Almaraz G.L. Avila L.E.V. Alvarez P. 2005. Matrix solid-phase dispersion extraction and determination by high performance liquid chromatography with fluorescence detection of residues of glyphosate and aminomethylphosphonic acid in tamato fruit. *Journal of Chromatography A* 1093: 139-146.

De Miranda Colombo S. and Masini J.C. 2011. Developing a fluorimetric sequence injection methodology to study adsorption/desorption of glyphosate on soil and sediment samples. *Microchemical Journal* 98: 260-266.

De Santana H. Toni L.R.M. Benetoli L.O.B. Zaia C.T.B.V. Rosa M. Zaia D.A.M. 2006. Effect in glyphosate adsorption on clays and soils heated and characterization by FT-IR spectroscopy. *Geoderma* 136: 738-750.

Deitzel J.M. Kleinmeyer J. Harris D. Tan N.C.B. 2001. The effect of processing variables on the morphology of electrospun nanofibers and textiles. *Polymer* 42: 261-272.

Deitzel J.M. Kleinmeyer J. Harris D. Tan N.C.B. 2001. The effects of processing variables on the morphology of electrospun nanofibers and textiles. *Polymer* 42: 261-272.

Deng C. Zhao Q. Shukla R. 2000. Detecting hormesis using non-parametric rank test. *Human & Experimental Toxicology* 19: 703-708.

Denizot F. and Lang R. 1986. Rapid colorimetric assay for cell growth and survival: modification to the terazolium dye procedure giving improved sensitivity and reliability. *Journal of Immunological Methods* 89: 271-277.

Department of Water Affairs and Forestry (DWAF). 1996. South African water quality guidelines. Volume 7: aquatic ecosystems. Pretoria, South Africa.



Department of Water Affairs and Forestry (DWAF). 1996. South African water quality guidelines. Volume 7: aquatic ecosystems. Pretoria, South Africa.

Department of Water and Environmental Affairs (DWA). September 2004. 1st edition. National water resource strategy: Chapter2: South Africa´s water situation and strategies to balance supply and demand.

Deshpande S. and Hall J.C. 2000. Auxin herbicide resistance may be modulated at the auxin-binding site in wild mustard (*Sinapis arvensis L.*): A light scattering study. *Pesticide Biochemistry and Physiology* 66: 41-48.

Devine M.D. and Shukla A. 2000. Altered target sites as a mechanism of herbicide resistance. *Crop Protection* 19: 881-889.

Dewey S.A. and Appleby A.P. 1983. A comparison between glyphosate and assimilate translocation patterns in tall morningglory ( *Ipomoea purpurea*). *Weed Science* 31: 308-314.

Dick R.E. and Quinn J.P. 1995. Glyphosate-degrading isolates from environmental samples: occurrence and pathways of degradation. *Applied Microbiology and Biotechnology* 43: 545-550.

Dimitrakopoulos I.K. Thornaidis N.S. Megoulas N.C. Koupparis M.A. 2010. Effect of suppressor current intensity on the determination of glyphosate and aminomethylphosphonic acid by suppressed conductivity ion chromatography. *Journal of Chromatography A* 1217: 3619-3627.

Dinehart S.K. Smith L.M. McMurry S.T. Anderson T.A. Smith P.N. Haukos D.A. 2009. Toxicity of a glufosinate and several glyphosate based herbicides to juvenile amphibians from the Southern High Plains, USA. *Science of the Total Environment* 407: 1065-1071.

Dinelli G. Marotti I. Bonetti A. Minelli M. Catizone P. Barnes J. 2006. Physiological and molecular insight on the mechanisms of resistance to glyphosate in *Conyza canadensis* (L.) Cronq. biotypes. *Pesticide Biochemistry and Physiology* 86: 30-41.

Dinelli G. Vicari A. Catizone P. 1996. Review: Monitoring of herbicide pollution in water by capillary electrophoresis. *Journal of Chromatography A* 733: 337-347.

Ding B. Kim H.Y. Lee S.C. Lee D.R. Choi K.J. 2002. Preparation and characterization of nanoscaled poly(vinyl alcohol) fibers via electrospinning. *Fibers and Polymers* 3: 73-79

Ding B. Si Y. Wang X. Yu J. Feng L. Sun G. 2011b. Label-free ultrasensitive colorimetric detection of copper (II) ions untilizing polyanilline/polyamide-6 nano-fiber/net sensor strips. *Journals of Materials Chemistry* 21: 13345-13353.

Ding W. Reddy K.N. Zablotowicz R.M. Bellaloui N. Bruns H.A. 2011a. Physiological responses of glyphosate-resistant and glyphosate-sensitive soybean to aminomethylphosphonic acid, a metabolite of glyphosate. *Chemosphere* 83: 593-598.

Dion H.M. Harsh J.B. Hill Jr H.H. 2001. Competitive sorption between glyphosate and inorganic phosphate on clay minerals and low organic matter soils. *Journal of Radioanalytical and Nuclear Chemistry* 249: 385-390.

Dominguez E. Cuartero J. Heredia A. 2011. Review: An overview on plant cuticle biomechanics. *Plant Science* 181: 77-84.

## Chapter 8: References


Domonkos I. Kis M. Gombos Z. Ughy B. 2013. Carotenoids, versatile components of oxygenic photosynthesis. *Progress in Lipid Research* 52: 539-561.

Donmez I. Kayaci F. Ozgit-Akgun C. Uyar T. Biyikli N. 2013. Fabrication of hafnia hollow nanofibers by atomic layer deposition using electrospun nanofiber templates. *Journal of Alloys and Compounds* 559: 146-151.

Dos Santos D.M. Rosa M. De Marchi R. Godoi A.F.L. Turra A. Montone R.C. 2013. Matrix effect on butyltin analysis of sediments and fish tissues by GC-PFPD. *Journal of the Brazialian Chemical Society* 24: 998-1005.

Dost F.N. 2003. Toxicology and potential health risk of chemicals that may be encountered by workers using forest vegetation management options. Part IV: Risk to workers using glyphosate formulations. Forest Practices Branch BC Ministry of Forests. ISBN 0-7726-4985-5.

Dotti F. Varesano A. Montarsolo A. Aluigi A. Tonin C. Mazzuchetti G. 2007. Electrospun porous mats for high efficiency filtration. *Journal of Industrial Textiles* 37: 151-162.

Droppa M. Horváth G. Vass I. Demeter S. 1981. Mode of action of photosytem II herbicides studied by thermoluminescence. *Biochemica et Biophysica Acta* 638: 210-216.

Du J. Wang S. You H. Zhao X. 2013. Understanding the toxicity of carbon nanotubes in the environment is crucial to the control of nanomaterials in producing and processing and the assessment of health risk for human: A review. *Environmental Toxicology and Pharmacology* 36: 451-462.

Dubey R.K. and Puri B.K. 1994. Simultaneous determination of lead and cadmium in various environmental and biological samples by differential pulse polarography after adsorption of their morpholine-4-carbodithioates onto microcrystalline naphthalene or morpholine-4-dithiocarbamate-CTMAB-napthalene adsorbent. *Talanta* 42: 65-72.

Ducruet J.M. and Ort D.R. 1988. Enhanced susceptibility of photosynthesis to high leaf temperature in triazine-resistant *Solanum Nigrum L.* evidence for photosystem II $D_1$ protein site of action. *Plant Science* 56: 39-48.

Duez P. Dehon G. Kumps A. Dubois J. 2003. Statistics of the Comet assay: a key to discriminate between genotoxic effects. *Mutagenesis* 18: 159-166.

Duke S.O. 1990. Overview of herbicide mechanisms of action. *Environmental Health Perspectives* 87: 263-271.

Duke S.O. 2003. Weeding with transgenes. *Trends in Biotechnology* 21: 192-194.

Duke S.O. Baerson S.R. and Rimando A.M. 2003. Glyphosate. *Encyclopedia of Agrochemicals*.

Dunkelberg H. Fuchs J. Hengstler J.G. Klein E. Oesch F. Strüder K. 1994. Genotoxic effects of the herbicides alachlor, atrazine, pendimethaline, and simazine in mammalian cells. *Bulletin of Environmental Contamination and Toxicology* 52: 498-504.

## Chapter 8: References


Duramad P. Tager I.B. Leikauf J. Eskenazi B. Holland N.T. 2006. Expression of Th1/Th2 cytokines in human blood after *in vitro* treatment with chlorpyrifos, and its metabolites in combination with endotoxin LPS and allergen *Der p1*. *Journal of Applied Toxicology* 26: 458-465.

Dzygiel P. and Wieczorek P. 2000. Extraction of glyphosate by supported liquid membrane technique. *Journal of Chromatography A* 889: 93-98.

Eash D.T. and Bushway R.J. 2000. Review: Herbicide and plant growth regulator analysis by capillary electrophoresis. *Journal of Chromatography A* 880: 281-294.

Eason J.R. Johnston J.W. de Vré L. 2000. Short communication: Reversal of glyphosate inhibition of *Sandersonia aurantiaca* flower senescence with aromatic amino acids. *Postharvest Biology and Technology* 18: 81-84.

Eberbach P.L and Douglas L.A. 1991. Method for the determination of glyphosate and (aminomethyl)phosphonic acid in sopil using electron capture gas chromatography. *Journal of Agriculture and Food Chemistry* 39: 1776-1780.

Ecobichon D.J. 2001. Pesticide use in developing countries. *Toxicology* 160: 27-33.

Eiswerth M:E. Donaldson S.G. Johnson W.S. 2000. Potential environmental impacts and economic damages of Eurasian watermilfoil (*Myriophyllum spicatum*) in Western Nevada and Northeastern California. *Weed Technology* 14: 511-518.

Elandalloussi L.M. Rodrigues P.M. Afonso R. Leite R.B. Nunes P.A. Cancela M.L. 2005. Shikimate and folate pathways in the protozoan parasite *Perkinsus olseni*. *Molecular and Biochemical Parasitology* 142: 106-109.

El-demerdash F.M. Yousef M.I. Elagamy E.I. 2001. Influence of paraquat, glyphosate and cadmium on the activity of some serum enzymes and protein electrphoretic behavior (*In vitro*). *Journal of Environmental Science and Health Part B: Pesticides, Food Contaminants and Agricultural Wastes* 36: 29-42.

Elder J.F. Perry S.K. Brady F.P. 1975. Application of energy-dispersive X-ray fluorescence to trace metal analysis of natural waters. *Environmental Science & Technology* 9: 1038-1042.

Ellerbee A.K. Phillips S.T. Siegel A.C. Mirica K.A. Martinez A.W. Striehl P. Jain N. Prentiss M. Whitesides G.M. 2009. Quantifying colorimetric assays in paper-based microfluidic devices by measuring the transmission of light through paper. *Analytical Chemistry* 8447-8452.

El-Safty S.A. and Shenashen M.A. 2012. Mercury-ion optical sensors. *Trends in Analytical Chemistry* 38: 98-115.

El-Shenawy N.S. 2009. Oxidative stress responses of rats exposed to Roundup and its active ingredient glyphosate. *Environmental Toxicology and Pharmacology* 28: 370-38.

Emteborg H. Baxter D.C. Sharp M. Frech W. 1995. Evaluation, mechanism and application of solid-phase extraction using a dithiocarbamate resin for the sampling and determination of mercury species in humic-rich natural waters. *Analyst* 120: 69-77.

Ertas Y. and Uyar T. 2014. Main-chain polybenzoxazine nanofibers via electrospinning. *Polymer* 55: 556-564.

Ertel W. Kramer J.P. Kenney J. Steckholzer U. Jarrar D. Trentz O. Schildberg W. 1995. Downregulation of proinflammatory cytokines release in whole blood from septic patients. *Blood* 85: 1341-1347.

Eurpean Commission review report. 2002. Directorate E: Food safety, plant health, animal health and welfare, International questions: Glyphosate. Report no. 6511/VI/99.

Evelyne C. Andre C. Georges T. Michel T. 1992. Quantitative relationships between structure and penetration of phenylurea herbicides through isolated plant cuticles. *Chemosphere* 24: 189-200.

Fagerström A. Kocherbitov V. Westbye P. Bergström Mamontova V. Engblom J. 2013. Characterization of a plant leaf cuticle model wax, phase behaviour of model wax-water systems. *Thermochimica Acta* 571 42-52.

Fairbairn D.W. Olive P.L. O´Neill K.L. 1995. The Comet assay: a comprehensive review. *Mutation Research* 339: 37-59.

Farré M.J. Brosillon S. Doménech X. Peral J. 2007. Evaluation of the intermediates generated during the degradation of Diuron and Linuron herbicides by the photo-fenton reaction. *Journal of Photochemistry and Photobiology A: Chemistry* 189: 364-373.

Faust F. Kassi F. Knasmüller S. Boedecker R.H. Mann M. Mersch-Sundermann V. 2004. The use of the alkaline Comet assay with lymphocytes in human biomonitoring studies. *Mutation Research* 566: 209-229.

Feghali C.A. and Wright T.M. 1997. Cytokines in acute and chronic inflammation. *Frontiers in Bioscience* 2: 12-26.

Feng C. Khulbe K.C. Matsuura T. Tabe S. Ismail A.F. 2013. Review: Preparation and characterization of electro-spun nanofiber membranes and their possible applications in water treatment. *Separation and Purification Technology* 102: 118-135.

Feng P.C.C. and Chiu T. 2005. Distribution of [$^{14}$C] glyphosate in mature glyphosate-resistant cotton from application to a single leaf or over the top spray. *Pesticide Biochemistry and Physiology* 82: 36-45.

Feng P.C.C. Pratley J.E. Bohn J.A. 2009. Resistance of glyphosate in *Lolium rigidum* II. Uptake, translocation and metabolism. *Weed Science* 47: 412-415.

Fenoll J. Sabater P. Navarro G. Vela N. Pérez-Lucas G. Navarro S. 2013. Abatement kinetics of 30 sulfonylurea herbicide residues in water by photocatalytic treatment with semiconductor materials. *Journal of Environmental Management* 130: 361-368.

Fernandes T.C.C. Mazzeo D.E.C. Marin-Morales M.A. 2009. Origin of nuclear and chromosomal alterations derived from the action of an aneugenic agent-trifluralin herbicide. *Ecotoxciology and Environmental Safety* 72: 1680-1686.

Fields S.C. 1999. Synthesis of natural products containing a C-P bond. *Tetrahedron* 55: 12237-12273.

Finet C. and Jaillais Y. 2012. Review: Auxology: When auxin meets plant evo-devo. *Developmental Biology* 369: 19-31.

Fogalia T.A. Gregory L.M. Maerker G.G. Osman S.F. 1971. Reaction of 2,3-dialkylaziridines with carbon disulfide. *Journal of Organic Chemistry* 56: 1068-1072.

Folmer L.C. Sanders H.O. Julin A.M. 1979. Toxicity of the herbicide pure glyphosate and several of its formulations to fish and aquatic invertebrates. *Archives of Environmental Contamination and Toxicology* 8: 269-278.

Fong H. Chun I. Reneker D.H. 1999. Beaded nanofibers formed during electrospinning. *Polymer* 40: 4585-4592.

Forlani G. Mangiagalli A. Nielsen E. Suardi C.M. 1999. Degradation of the phosphonate herbicide glyphosate in soil: Evidence for a possible involvement of unculturable microorganisms. *Soil Biology and Biochemistry* 31: 991-997.

Foy C.L. Forney D.R. Cooley W.E. 1964. Chapter 4: History of weed introductions. *Exotic Plant Pests and North American Agriculture* : 65-92.

Fragiorge E.J. Azenha A. de Rezende A. Graf U. Spanó M.A. 2008. Comparative genotoxicity evaluation of imidazolinone herbicides in somatic cells of *Drosophila melanogaster*. *Food and Chemical Toxicology* 46: 393-401.

Frank R. Braun H.E. Ripley B.D. Clegg B.S. 1990. Contamination of rural ponds with pesticide, 1971-85, Ontario, Canada. *Bulletin of Environmental Contamination and Toxicology* 44: 401-409.

Frei E. Kuchenmeister F. Gliniorz R. Breuer A. Schmezer P. 2001. *N*-nitrososdimethylamine is activated in microsomes from hepatocytes to reactive metabolites which damage DNA of non-parenchymal cell in rat liver. *Toxicological Letters* 123: 227-234.

Frenot A. and Chronakis I.S. 2003. Polymer nanofibers assembled by electrospinning. *Current Opinion in Colloid and Interface Science* 8: 64-75.

Freuze I. Jadas-Hecart A. Poyer A. Pierre-Yves C. 2007. Influence of complexation phenomena with multivalent cations on the analysis of glyphosate and aminomethyl phosphonic acid in water. *Journal of Chromatography A* 1175: 197-206.

Frey M.W. and Li L. 2007. Electrospinning and porosity measurements of nylon-6/poly(ethylene oxide) blended nonwovens. *Journal of Engineered Fibers and Fabrics* 2: 31-37.

Friends of the Earth International. 2008. Agriculture and Food: who benefits from gm crops?: the rise pesticide use. Executive summary (http://www.foei.org) accessed January 2014.

## Chapter 8: References


Fritz J.S. and Sutton S.A. 1956. Titration of mecury with Bis(2-hydroxyethyl)dithiocarbamate. *Analytical Chemistry* 28: 1300-1303.

Frone A.N. Panaitescu D.M. Donescu D. Spataru C.I. Radovici C. Trusca R. Somoghi R. 2011. Preparation and characterization of PVA composites with cellulose nanofibers obtained by ultrasonication. *Bioresources* 6: 487-512.

Fuentes-Martinez J.P. Toledo-Martinez I. Roman-Bravo P. y Garcia G.P. Godoy-Alcantar C. Lopez-Cardoso M. Morales-Rojas H. 2009. Diorganotin(IV) dithiocarbamate complexes as chromogenic sensors of anion binding. *Polyhedron* 28: 3953-3966.

Gardner B.D. Connell A.D. Eagle G.A. Moldan A.G.S. Oliff W.D. Orren M.J. Watling R.J. 1983. South African pollution survey 1976-1979. South African National Scientific Programmes Report No 73: 1-113. Marine pollution committee of the South African National Committee for Oceanographic Research (SANCOR).

Garg K. and Bowlin G.L. 2011. Electrospinning jets and nanofibrous structures. *Biomicrofluidics* 5: 1-19.

Garrido J. Cagide F. Franco M.M. Borges F. Garrido E.M. 2014. Microencapsulation of herbicide MCPA with native β-cyclodextrin and its methyl and hydroxylpropyl derivative: An experimental and theoretical investigation. *Molecular Structure* doi: http://dx.doi.org/10.1016/j.molstruc.2013.12.067.

Gasnier C. Benachour N. Clair E. Travert C. Langlois F. Laurant C. Decroix-Laporte C. Seralini G.E. 2010. Dig 1 protects against cell death provoked by glyphosate-based herbicides in human liver cell lines. *Journal of Occupational Medicine and Toxicology* 5: 1-13.

Gasnier C. Dumont C. Benachour N. Clair E. Chagnon M. Séralini G. 2009. Glyphosate-based herbicides are toxic and endocrine disruptors in human cell lines. *Toxicology* 262: 184-191.

Gauch R. Leuenberger U. Müller U. 1989. The determination of the herbicide glyphosate and its chief metabolite aminomethylphosphonic acid (AMPA) in drinking water with the aid of HPLC. *Zeitshcrift für Lebensmittel Unterschung und Forschung* 188: 36-38.

Ge X. D´Avignon D.A. Ackerman J.J.H. Sammons R.D. 2012. Observation and identification of 2-C-methyl-$_D$-erythritol-2,4-cyclopyrophosphate in horseweed and ryegrass treated with glyphosate. *Pesticide Biochemistry and Physiology* 104: 187-191.

Gehin A. Guillaume Y.C. Millet J. Guyon C. Nicod L. 2005. Vitamins C and E reverse of herbicide – induced toxicity on human epidermal cells HaCaT: a biochemometric approach. *International Journal of Pharmaceutics* 288: 219-226.

Geiger D.R. and Bestman H.D. 1990. Self-limitation of herbicide mobility by phytotoxic action. *Weed Science* 38: 324-329.

Geiger D.R. Kapitan S.W. Tucci M.A. 1986. Glyphosate inhibits photosynthesis and allocation of carbon to starch in sugar beet leaves. *Plant Physiology* 82: 468-472.

Geiger D.R. Shieh W. Fuchs M.A. 1999. Cause of self-limited translocation of glyphosate in *Beta vulgaris* plants. *Pesticide Biochemistry and Physiology* 64: 124-133.

George J and Shukla Y. 2011. Review: Pesticides and cancer: insights into toxicoproteomic-based findings. *Journal of Proteomics* 74: 2713-2722.

George J. Prasad S. Mahmood Z. Shukla Y. 2010. Studies on glyphosate-induced carcinogenicity in mouse skin: A proteomic approach. *Journal of Proteomics* 73: 951-964.

Gerecke A.C. Schärer M. Singer H.P. Müller S.R. Schwarzenbach R.P. Sägesser M. Ochsenbein U. Popow G. 2002. Sources of pesticides in surface waters in Switzerland: pesticide load through waste water treatment plants-current situation and reduction potential. *Chemosphere* 48: 307-315.

Gevao B. Semple K.T. Jones K.C. 2000. Bound pesticide residue in soils: A review. *Environmental Pollution* 108: 3-14.

Ghanem A. Bados P. Kerhoas L. Dubroca J. Einhom J. 2007. Glyphosate and AMPA analysis in sewage sludge by LC-ESI-MS/MS after FMOC derivatization on strong anion exchange resin as solid support. *Analytical Chemistry* 79: 3794-3801.

Gimenes M.J. Zhu H. Raetano C.G. Oliveira R.B. 2013. Dispersion and evaporation of droplets amended with adjuvants on soybeans. *Crop Protection* 44: 84-90.

Gimseng A.L. Borggaard O.K. Bang M. 2004. Influence of soil composition on adsorption of glyphosate and phosphate by contrasting Danish surface soils. *European Journal of Soil Science* 55: 183-191.

Gimsing A.L. and Borggaard O.K. 2002a. Competitive adsorption and desorption of glyphosate and phosphate on clay silicates and oxides. *Clay Minerals* 37: 509-515.

Gimsing A.L. and Borggaard O.K. 2002b. Effect of phosphate on the adsorption of glyphosate on soils, clay minerals and oxides. *International Journal of Environmental Analytical Chemistry* 82: 545-552.

Gimsing A.L. Szilas C. Borggaard O.K. 2007. Sorption of glyphosate and phosphate by variable-charge tropical soils from Tanzania. *Geoderma* 138: 127-132.

Glass R.L. 1981. Colorimetric determination of glyphosate in water after oxidation to orthophosphate. *Analytical Chemistry* 53: 921-923.

Glass R.L. 1987. Adsorption of glyphosate by soils and clay minerals. *Journal of Agriculture and Food Science* 35: 497-500.

Glover J.F. Irwin J.T. Darbre P.D. 1988. Interaction of phenol red with estrogenic and antiestrogenic action on growth of human breast cancer cells ZR-75-1 and T-47-D. *Cancer Research* 48: 3693-3697.

González A.G. and Herrador M.A. 2007. A practical guide to analytical method validation, including measurement uncertainty and accuracy profiles. *Trends in Analytical Chemistry* 26: 227-238.

González N.V. Soloneski S. Larramendy M.L. 2009. Dicamba-induced genotoxicity in Chinese hamster ovary (CHO) cells is prevented by vitamin D. *Journal of Hazardous Materials* 163: 337-343.

González-Martinez M.A. Brun E.M. Puchades R. Maquieira A. Ramsey K. Rubio F. 2005. Glyphosate immunosensor: Application for water and soil analysis. *Analytical Chemistry* 77: 4219-4227.

González-Torralva F. Gil-Humanes J. Barro F. Brants F. De Prado R. 2012a. Target site mutation and reduced translocation are present in a glyphosate resistant *Lolium multiflorum Lam.* Biotype from Spain. *Plany Physiology and Biochemistry* 58: 16-22.

González-Torralva F. Rojano-Delgado A.M. Luque De Castro M.D. Mülleder N. De Prado R. 2012b. Two non-target mechanisms are involved in glyphosate-resistant horseweed (*Conyza canadensis* L. Cronq.) biotypes. *Journal of Plant Physiology* 169: 1673-1679.

Gout E. Bligny R. Genix P. Tissut M. Douce R. 1992. Effect of glyphosate on plant cell metabolism. $^{31}P$ and $^{13}C$ NMR studies. *Biochimie* 74: 875-882.

Govaert L.E. and Peijs T. 1995. Influence of applied stress and temperatures on the deformation behavior of high-strength poly(vinyl alcohol) fibres. *Polymer* 36: 3589-3592.

Grainger R.S. and Innocenti P. 2007. New applications of dithiocarbamates in organic synthesis. *Heteroatom Chemistry* 18: 568-571.

Grand A.F. and Tamres M. 1968. Titration of some metal diethyldithiiocarbamates by iodine in chloroform. *Analytical Chemistry* 23: 1902-1904.

Green J.M. and Beestman G.B. 2007. Recently patented and commercialized formulation and adjuvant technology. *Crop Protection* 26: 320-327.

Green M.J. 1996. Report: A practical guide to analytical method validation. *Analytical Chemistry News & Features* 305-309.

Gregoire C. Elsaesser D. Huguenot D. Lange J. Lebeau T. Merli A. Mose R. Passeport E. Payraudeau S. Schütz T. Schulz R. Tapia-Padilla G. Tournebize J. Trevisan M. Wanko A. 2009. Mitigation of agricultural nonpoint-source pesticide pollution in artificial wetland ecosystems. *Environmental and Chemical Letters* 7: 205-231.

Gressel J. 1999. Tandem constructs: preventing the rise of superweeeds. *TIBTECH* 17: 361-366.

Grossmann K. and Scheltrup F. 1997. Selective induction of 1-aminocyclopropane-1-carboxylic acid (ACC) synthase activity is involved in the selectivity of the auxin herbicide quinclorac between barnyard grass and rice. *Pesticide Biochemistry and Physiology* 58: 145-153.

Grossmann K. Scheltrup F. Kwiatkowski J. Caspar G. 1996. Induction of abscisic acid is a common effect of auxin herbicides in susceptible plants. *Journal of Plant Physiology* 149: 475-478.

Grunewald K. Schmidt W. Unger C. Hanschmann G. 2001. Behavior of glyphosate and aminomethylphosphonic acid (AMPA) in soils and water of reservoir Radeburg II catchment (Saxony/Germany). *Journal of Plant Nutrition and Soil Sciences* 164: 65-70.

Gui Y.X. Fan X.N. Wang H.M. Wang G. Chen S.D. 2012. Glyphosate induced cell death through apoptotic and autophagic mechanisms. *Neurotoxicology and Tetratology* 34: 344-349.

## Chapter 8: References


Güngördü A. 2013. Comparative toxicity of methidathion and glyphosate on early life stages of three amphibian species: *Pelophylax ridibundus, Pseudepidalea viridis* and *Xenopus laevis*. *Aquatic Toxicology* 140-141: 220-228.

Gunn J. and Zhang M. 2010. Review: polyblend nanofibers for biomedical applications: perspectives and challenges. *Trends in Biotechnology* 28: 189-197.

Guo Z.Q. Chen W.Q. Duan X.M. 2010. Highly selective visual detection of Cu (II) utilizing intramolecular hydrogen bond-stabilized merocyanine in aqueous buffer solution. *Organic Letters* 12: 2202-2205.

Guo Z.X. Cai Q. Yang Z. 2005. Determination of glyphosate and phosphate in water by ion chromatography-inductively coupled plasma mass spectrometry detection. *Journal of Chromatography A* 1100: 160-167.

Gupta P. and Wilkes G.L. 2003. Some investigations on the fiber formation by utilizing a side-by-side bicomponent electrospinning approach. *Polymer* 44: 6353-6359.

Gupta P. Elkins C. Long T.E. Wilkes G.L. 2005. Electrospinning of linear homopolymers of poly(methyl methacrylate): exploring relationships between fiber formation, viscosity, molecular weight and concentration in a good solvent. *Polymer* 46: 4799-4810.

Gyedu-Ababio T.K. Furstenberg J.P. Baird D. Vanreusel A. 1999. Nematodes as indicators of pollution: a case study from the Swartkops River system, South Africa. *Hydrobiologia* 397: 155-169.

Hagner M. Penttinen O. Tiilikkala K. Setälä H. 2013. The effect of biochar, wood vinegar and plants on glyphosate leaching and degradation. *European Journal of Soil Biology* 58: 1-7.

Halls D.J. 1969. Review: the properties of dithiocarbamates. *Mikrochimica Acta* 62-77.

Halls D.J. Townshend A. Zuman P. 1968. The polarographic determination of some dithiocarbamates and their heavy metal complexes. *Analyst* 93: 219-223.

Hamzah H.H. Yusof N.A. Salleh A.B. Bakar F.A. 2011. An optical test strip for the detection of benzoic acid in food. *Sensors* 11: 7302-7313.

Hanke I. Singer H. Hollender J. 2008. Ultratrace-level determination of glyphosate, aminomethylphosphonic acid and glufosinate in natural waters by soild-phase extraction followed by liquid chromatography-tandem mass spectrometry: performance tuning of derivatization, enrichment and detection. *Analytical Bioanalytical Chemistry* 391: 2265-2276.

Hanke I. Wittmer I. Bischofberger S. Stamm C. Singer H. 2010. Relevance of urban glyphosate use for surface water quality. *Chemosphere* 81: 422-429.

Hao C. Morse D. Morra F. Zhao X. Yang P. Nunn B. 2011. Direct aqueous determination of glyphosate and related compounds by liquid chromatography/tandem mass spectrometry using reversed-phase and weak anion-exchange mixed-mode column. *Journal of Chromatography A* 1218: 5638-5643.

Hartmann A. Agurell E. Beevers C. Brendler-Schwaab S. Burlinson B. Clay P. Collins A. Smith A. Speit G. Thybaud V. Tice R.R. 2003. Recommendations for conducting the *In vivo* alkaline Comet assay. *Mutagenesis* 18: 45-51.

Hartmann A. and Speit G. 1997. The contribution of cytotoxicity to DNA-effects in the single cell gel test (Comet assay). *Toxicology Letters* 90: 183-188.

Hartung T. 2011. Review: From alternative methods to a new toxicology. *European Journal of Pharmaceutics and Biopharmaceutics* 77: 338-349.

Hassan C.M. and Peppas N.A. 2000. Structure and applications of poly(vinyl alcohol) hydrogels produced by conventional crosslinking or by freezing/thawing methods. *Advances in Polymer Science* 153: 37-65.

Hassan M.A. Yeom B.Y. Wilkie A. Pourdeyhimi B. Khan S.A. 2013. Fabrication of nanofiber meltblown membranes and their filtration properties. *Journal of Membrane Science* 427: 336-344.

Hayashi K. Sasaki Y. Tagashira S. Hirata K. 1987. Short communication: spectrophototmetric determination of copper (II) with carbon disulphide, a secondary amine and triton X-100. *Analytica Chimica Acta* 198: 271-275.

Hazen J.L. 2000. Adjuvants-terminology, classification and chemistry. *Weed Technology* 14: 773-784.

Hearn C.H. and Joens J.A. 1991. The near UV absorption spectrum of $CS_2$ and $SO_2$ at 300K. *Journal of Quantitative Spectroscopy and Radiative Transfer* 45: 69-75.

Hedberg D. and Wallin M. 2010. Effects of Roundup and glyphosate formulations on intracellular transport, microtubules and actin filaments in *Xenopus laevis* melanophores. *Toxicology in Vitro* 24: 975-802.

Helander M. Saloniemi I. Saikkonen K. 2012. Glyphosate in northern ecosystems. *Trends in Plant Science* 17: 569-574.

Hellmann C.H. Berlardi J. Dersch R. Greiner A. Wendorff J.H. Bahnmueller S. 2009. High precision deposition electrospinning of nanofibers and nanofiber nonwovens. *Polymer* 50: 1197-1205.

Hennion M.C. 1999. Review: Solid-phase extraction method development, sorbents and coupling with liquid chromatography. *Journal of Chromatography A* 856: 3-54.

Hernández A.F. Parrón T. Tsatsakis A.M. Requena M. Alarcón R. López-Guarnido O. 2013. Toxic effects of pesticide mixtures at a molecular level: Their relevance to human health. *Toxicology* 307: 136-145.

Hernández F. Serrano R. Miralles M.C. Font N. 1996. Gas and liquid chromatography and enzyme linked immuno sorbent assay in pesticide monitoring of surface water from the western Mediterranean (Comunidad Valenciana, Spain). *Chromatographia* 42: 151-158.

Heu C. Elie-Caille C. Mougey V. Launay S. Nicod L. 2012. A step further toward glyphosate-induced epidermal cell death: Involvement of mitochondrial and oxidative mechanisms. *Environmental Toxicology and Pharmacology* 34: 144-153.

Hilmer T. and Bate G.C. 1987. Technical note: Hydrocarbon levels in the Swartkops estuary: A preliminary study. *Water SA* 13: 181-184.

Hirai K. Sugimoto H. Ishiba T. 1997. Reaction of 1,3-dithiolium cation with xanthate and diothiocarbamate anions. *Journal of Organic Chemistry* 42: 1543-1548.

Hirayama E. Sugiyama T. Hisamoto H. Suzuki K. 2000. Visual and colorimetric lithium ion sensing based on digital color analysis. *Analytical Chemistry* 72: 465-474.

Hogendoorn E.A. Ossendrijver F.M. Dijkman E. Baumann R.A. 1999. Short communication: Rapid determination of glyphosate in cereal samples by means of pre-column derivatization with 9-fluorenylmethyl chloroformate and coupled-column liquid chromatography with fluorescence detection. *Journal of Chromatography A* 833: 67-73.

Hokanson R. Fudge R. Chowdhary R. Busbee D. 2007. Alteration of estrogen-regulated gene expression in human cells induced by the agricultural and horticultural herbicide glyphosate. *Human and Experimental Toxicology* 26: 747-752.

Holt J.S. 1994. Impact of weed control on weeds: New problems and research needs. *Weed Science Society of America* 8: 400-402.

Holt J.S. 2013. Herbicides. *Encyclopedia of Biodiversity* 4: 87-95.

Holvoet K.M.A. Seuntjens P. Vanrolleghem P.A. 2007. Monitoring and modeling pesticide fate in surface waters at the catchment scale. *Ecological Modelling* 209: 53-64.

Holzner W. 1982. Concepts, catergories and characteristics of weeds. *Geobotany* 2: 3-20.

Hossain S.M.Z. and Brennan J.D. 2011b. *ß*-galactosidase-based colorimetric paper sensor for determination of heavy metals. *Analytical Chemistry* 83: 8772-8778.

Hovhannisyan G.G. 2010. Review: Fluorescence in situ hybridization in combination with the Comet assay and micronucleus test in genetic toxicology. *Molecular Cytogenetics* 17: 3-11.

Hsiang Y.H. Hertzberg R. Hecht S. Liu L.F. 1985. Camptothecin induces protein-linked DNA breaks via mammalian DNA topoisomerase I. *The Journal of Biological Chemistry* 280: 14873-14878.

Hsu C.C. and Whang C.W. 2009. Microscale phase extraction of glyphosate and aminomethylphosphonic acid in water and guave fruit extract using alumina-coated iron oxide nanoparticles followed by capillary electrophoresis and electrochemiluminescence detection. *Journal of Chromatography A* 1216: 8575-8580.

Hu J.Y. Chen C.L. Li J.Z. 2008. A simple method for the determination of glyphosate residues in soil by capillary gas chromatography with nitrogen phosphorous. *Journal of Analytical Chemistry* 63: 371-375.

Hu Y.S. Zhao Y.Q. Sorohan B. 2011. Removal of glyphosate from aqueous environment by adsorption using water industrial residuel. *Desalination* 271: 150-156.

Hua K.Y. Deng C.M. He C. Shi L.Q. Zhu D.F. He Q.G. Cheng J.G. 2013. Organic semiconductors-coated polyacrylonitrile (PAN) electrospun nanofibrous mats for highly sensitive chemosensors via evanescent-wave guiding effect. *Chinese Chemical Letters* 24: 643-646.

Huang *J.* Silva E.N. Shen Z. Jiang B. Lu H. 2012. Effects of glyphosate on photosynthesis, chlorophyll fluorescence and physiochemical properties of cogongrass (*Imperata cylindrical L.*). *Plant Omics Journal* 5: 177-183.

Huang J. Virji S. Weiller B.H. Kaner R. 2002. Polyaniline nanofibers: Facile synthesis and chemical sensors. *Journal of American Chemical Society* 125: 314-315.

Huang K.J. Hsiao Y.S. Whang W.T. 2011. Low temperature formation of self-assembled 1,5-diaminoanthraquinone nanofibers: substrate effects and field emission characteristics. *Organic Electronics* 12: 686-693.

Huang L. Nagapudi K. Apkarian R.P. Chaikof E.L. 2001. Engineered collagen-PEO nanofibers and fabrics. *Journal of Biomaterials Science* 12: 979-993.

Huang W. Beach E.D. Fernandez-Cornejo J. Uri N.D. 1994. An assessment of the potential risk of groundwater and surface water contamination by agricultural chemicals used in vegetable production. *The Science of the Total Environment* 153: 151-167.

Huang X.J. and Choi Y.K. 2007. Review: Chemical sensors based on nanostructured materials. *Sensors and Actuators B* 122: 659-671.

Huang Z.M. Zhang Y.Z. Kotaki M. Ramakrishna S. 2003. A review on polymer nanofibers by electrospinning and their applications in nanocomposites. *Composite Science and Technology* 63: 2223-2253.

Huber A. Bach M. Frede H.G. 2000. Pollution of surface waters with pesticides in Germany: Modeling non-point source inputs. *Agriculture, Ecosystems and Environment* 80: 191-204.

Huguenot D. Bois P. Jezequel K. Cornu J.Y. Lebeau T. 2010. Selection of low cost materials for the sorption of copper and herbicides as single or mixed compounds in increasing complexity matrices. *Journal of Hazardous Materials* 182: 18-26.

Hui J.K.H. and MacLachlan M.J. 2010. Fibrous aggregates from dinuclear zinc (II) salphen complexes. *Dalton Transactions* 39: 7310-7319.

Hui-Min Q. Jin-Ju G. Chao H. Hong-Qiang R. 2013. Determination of phosphite, phosphate, glyphosate and aminomethylphosphonic acid by two dimensional ion chromatography system coupled with capillary ion chromatography. *Chinese Journal of Analytical Chemistry* 41: 1910-1914. Y

Hultberg M. 2007. Cysteine turnover in human cell lines is influenced by glyphosate. *Environmental Toxicology and Pharmacology* 24: 19-22.

Humphries M.S. 2013. DDT residue contamination in sediments from Lake Sibaya in northern Kwazulu-Natal, South Africa: Implications for conservation in a a world heritage site. *Chemosphere* 93: 1494-1499.

Huston P.L. and Pignatello J.J. 1999. Degradation of selected pesticide active ingredients and commercial formulations in water by the photo-assisted fenton reaction. *Water Research* 33: 1238-1246.

Ibáñez M. Pozo O.J. Sancho J.V. López F.J. Hernández F. 2006. Re-evaluation of glyphosate determination in water by liquid chromatography coupled to electrospray tandem mass spectrometry. *Journal of Chromatography A* 1134: 51-55.

Iqbal N. Trivellini A. Masood A. Ferrante A. Khan N.A. 2013. Review: Current understanding on ethylene signaling in plants: The influence of nutrient availability. *Plant Physiology and Biochemistry* 73: 128-138.

Jacobsen P.R. Axelstad M. Boberg J. Isling L.K. Christiansen S. Mandrup K.R. Berthelsen L.O. Vinggaard A.M. Hass U. 2012. Persistant developmental toxicity in rat offspring after low dose exposure to a mixture of endocrine disrupting pesticides. *Reproductive Toxicology* 34: 237-250.

Jagger M.P. Huo Z. Riches P.G. 2002. Inflammatory cytokine (interleukin 6 and tumour necrosis alpha) release in a human whole blood system in response to *Streptococcus pneumoniae* serotype 14 and its capsular polysaccharide. *Clinical and Experimental Immunology* 130: 467-474.

Jan M.R. Shah J. Muhammad M. Ara B. 2009. Glyphosate herbicide residue determination in samples of environmental importance using a spectrophotometric method. *Journal of Hazardous Materials* 169: 742-745.

Javaid A. Shafique S. Shafique S. 2009. Invasion of noxious alien weed *Perthenium hysterophorus L.* grazing lands of Lahore, Pakistan. *The Journal of Animal and Plant Sciences* 19: 149-153.

Jayawardane B.M. Coo L.D. Cattrall R.W. Kolev S.D. 2013. The use of a polymer inclusion membrane in a paper-based sensor for the selective determination of Cu (II). *Analytica Chimica Acta* 803: 106-112.

Jeliazkova B.G. Doicheva M.A. Tosheva L.B. 1996. EPR study on the chemistry and photochemistry of copper (II) dithiocarbamate mixed-ligand complexes. *Applied Magnetic Resonance* 10: 151-157.

Jenkins A.L. Yin R. Jensen J.L. 2001. Molecularly imprinted polymer sensors for pesticide and insecticide detection in water. *Analyst* 126: 798-802.

Jian F. HaiTao N. Tong L. XunGai W. 2008. Review: Applications of nanofibers. *Chinese Science Bulletin* 53: 2265-2286.

Jian F. Wang Z. Bai Z. You X. Fun H.K. Chinnakali K. Razak I.A. 1999. The crystal structure, equilibrium and spectroscopic studies of bis(dialkyldithiocarbamate) copper (II) complexes $[Cu_2(R_2dtc)_4]$ (dtc= dithiocarbamate). *Polyhedron* 18: 3401-3406.

Jiang J. and Lucy C.A. 2007. Determination of glyphosate using off-line ion exchange preconcentration and capillary electrophoresis-laser induced fluorescence detection. *Talanta* 72: 113-118.

Jiang L.X. Jin L.G. Guo Y. Tao B. Qiu L.J. 2013. Glyphosate effects on the gene expression of the apical bud in soybean (*Glycine max*). *Biochemical and Biophysical Research Communications* 437: 544-549.

Jofré E. Mori G. Castro S. Fabra A. Rivarola V. Balegno H. 1996. 2,4-Ddichlorophenoxyacetic acid affects the attachement of *Azospirillum brasilense* Cd to maize roots. *Toxicology* 107: 9-15.

Johnson K. Aarden L. Choi Y. De Groot E. Creasey A. 1996. The proinflammatory cytokine response to coagulation and endotoxin in whole blood. *Blood* 87: 5051-5060.

Johnson W.G. Davis V.M. Kruger G.R. Weller S.C. 2009. Review: Influence of glyphosate-resistant cropping systems on weed species shifts and glyphosate-resistant weed populations. *European Journal of Agronomy* 31: 162-172.

Jones R. 2005. Review: The ecotoxicological effects of Photosytem II herbicides on corals. *Marine Pollution Bulletin* 51: 495-506.

Jordan N. 1993. Prospects for weed control through crop interference. *Ecological Society of America* 3: 84-91.

Jursinic P.A. McCarthy S.A. Bricker T.M. Stemler A. 1991. Characteristics of two atrazine binding sites that specifically inhibit photosytem II function. *Biochemica et Biophysica Acta* 1059: 312-322.

Kadajji V.G. and Betageri G.V. 2011. Review: water soluble polymers for pharmaceutical applications. *Polymers* 3: 1972-2009.

Kaliannan P. Ali M.M.N. Seethalakshmi T. Venuvanalingam P. 2002. Electronic structure and conformation of glyphosate: an ab initio MO study. *Journal of Molecular Structure (Theochem)*. 618: 117-125.

Kan K.R. Johnson E.A. Fath D.M. Tompkins C.P. Hamilton T.A. Fruchey H.H. 2007. Temproal expression of neuroinflammatory markers and brain injury following acute soman poisoning. *In Defence against the Effects of Chemical Hazards: Toxicology, Diagnosis and Medical Countermeasures* 149: 1-14.

Kataoka H. Ryu S. Sakiyama N. Makita M. 1996. Short communication: Simple and rapid determination of the herbicide glyphosate and glufosinate in river water, soil and carrot samples by gas chromatography with flame photometric detection. *Journal of Chromatography A* 726:253-258.

Katepalli H. Bikshapathi M. Sharma C.S. Verma N. Sharma A. 2011. Synthesis of hierarchical fabrics by electrospinning of PAN nanofibers on activated carbon microfibers for environmental remediation applications. *Chemical Engineering Journal* 171: 1194-1200.

Kauppinen T. Kogevinas M. Johnson E. Becher H. Bertazzi P.A. de Mesquita H.B.B. Coggon D. Green L. Littorin M. Lynge E. Mathews J. Neuberger M. Osman J. Pannett B. Pearce N. Winkelmann R. Saracci R. 1993. Chemical exposure in manufacture of phenoxy herbicides and chlorophenols and in spraying of phenoxy herbicides. *American Journal of Industrial Medicine* 23: 903-920.

Kawahigashi H. Hirose S. Ohkawa H. Ohkawa Y. 2007. Research review paper: Herbicide resistance of transgenic rice plants expressing human CYP1A1. *Biotechnology Advances* 25: 75-84.

Kawai S. and Uno B. 1991. Short communication: determination of glyphosate and its major metabolite aminomethylphosphonic acid by high-performance liquid chromatography after derivatization with *p*-toluenesulphonyl chloride. *Journal of Chromatography* 540: 411-415.

Kawasaki T. Ogata M. Kawasaki C. Ogata J.I. Inoue Y. Shigematsu A. 1999. Ketamine suppresses proinflammatory cytokine production in human whole blood *in vitro. Critical Care and Trauma* 89: 665-669.

Kelley K.B. and Riechers D.E. 2007. Recent development in auxin biology and new opportunities for auxinic herbicide research. *Pesticide biochemistry and Physiology* 89: 1-11.

Kenawy E.R. Abdel-Hay F.I. El-Newehy M.H. Wnek G.E. 2007. Controlled release of ketoprofen from electrospun poly(vinyl)alcohol nanofibers. *Materials Science and Engineering A* 459: 390-396.

Kennedy K. Schroeder T. Shaw M. Haynes D. Lewis S. Bentley C. Paxman C. Carter S. Brando V.E. Bartkow M. Heam L. Mueller J.F. 2012. Long term monitoring of photosystem II herbicides –correlation with remotely sensed freshwater extent to monitor changes in the quality of water entering the Great barrier Reef, Australia. *Marine Pollution Bulletin* 65: 292-305.

Keyvanfard M. and Karamian M. 2009. Spectrophotometric reaction rate method for the determination of trace amounts of Ruthenium (III) by its catalytical effect on the oxidation of spadns by metaperiodate in miceel medium. *Asian Journal of Chemistry* 21: 942-948.

Khan M.H. Hassan G. Khan N. Khan M.A. 2003. Efficacy of different herbicides for controlling broadleaf weeds in wheat. *Asian Journal of Plant Sciences* 2: 254-256.

Khenifi A. Derriche Z. Mousty C. Prévot V. Forano C. 2010. Adsorption of glyphosate and glufosinate by $Ni_2AlNO_3$ layered double hydroxide. *Applied Clay Science* 47: 362-371.

Khoury G.A. Gehris T.C. Tribe L. Sánchez R.M.T dos Santos Afonso M. 2010. Glyphosate adsorption on montmorillonite: Na experimental and theoretical study of surface complexes. *Applied Clay Science* 50: 167-175.

Khrolenko M.V. and Wieczorek P.P. 2005. Determination of glyphosate and its metabolite aminomethylphosphonic acid in fruit juices using supported-liquid membrane preconcentration method with high-performance liquid chromatography and UV detection after derivatization with *p*-tuluenesulphonyl chloride. *Journal of Chromatography A* 1093: 111-117.

Ki C.S. Back D.H. Gang K.D. Lee K.H. Um I.C. Park Y.H. 2005. Characterization of gelatin nanofiber prepared from gelatin-formic acid solution. *Polymer* 46: 5094-5102.

Kielak E. Sempruch C. Mioduszewska H. Klocek J. Leszczyński B. 2011. Phytotoxicity of Roundup Ultra 260 SL in aquatic ecosystems: Biochemical evaluations with duckweed (*Lemna minor L.*) as a model plant. *Pesticide Biochemistry and Physiology*. 99: 237-243.

Kilinc Ő. Grasset R. Reynaud S. 2011. The herbicide aclonifen: The complex theoretical bases of sunflower tolerance. *Pesticide Biochemistry and Physiology* 100: 193-198.

Kim H.N. Guo Z. Zhu W. Yoon J. Tian H. 2011. Recent progress on polymer-based fluorescent and colorimetric chemosensors. *Chemical Society Reviews* 40: 79-93.

Kim I.D. Rothschild A. Lee H.B. Kim D.Y. Jo S.M. Tuller H.L. 2006. Ultrasensitive chemiresistors based on electrospun $TiO_2$ nanofibers. *Nano Letters* 6: 2009-2013.

Kim J. Yun B. Choi J.S. Kim T. Kwak S. Cho K. 2004. Death mechanisms caused by carotenoid biosynthesis inhibitors in green and in undeveloped plant tissues. *Pesticide Biochemistry and Physiology* 78: 127-139.

Kim J.H. Kim J.Y. Lee Y.M. Kim K.Y. 1992. Properties and swelling characteristics of cross-linked poly (vinyl alcohol)/chitosan blend membrane. *Journal of Applied Polymer Science* 45: 1711-1717

Kim J.O. Park J.K. Kim J.H. Jin S.G. Yong C.S. Li D.X. Choi Y. Woo J.S. Yoo B.K. Lyoo W.S. Kim J.A. Choi H.G. 2008. Development of polyvinyl alcohol-sodium aliginate gel-matrix-based wound dressing system containing nitrofurazone. *International Journal of Pharmaceutics* 359: 79-86.

Kim J.S. and Reneker D.H. 1999. Polybenzimidazole nanofiber produced by electrospinning. *Polymer Engineering and Science* 39: 849-854.

Kim Y. Johnson R.C. Hupp J.T. 2001. Gold nanoparticle-based sensing of spectroscopically silent heavy metal ions. *Nano Letters* 1: 165-167.

Kim Y.H. Hong J.R. Gil H.W. Song H.Y. Hong S.Y. 2013. Mixtures of glyphosate and surfactant TN20 accelerate cell death via mitochondrial damage induced apoptosis and necrosis. *Toxicology in vitro* 27: 191-197.

Kimura T. Takase K.I. Tanaka S. 2007. Concentration of copper and copper-EDTA complex at the pH junction formed in soil by an electrokinetic remediation process. *Journal of Hazardous Material* 143: 668-672.

Kishore G.M. and Jacob G.S. 1987. Degradation of glyphosate by *Pseudomonas sp.* PG2982 via a sarcosine intermediate. *The Journal of Biological Chemistry* 202: 12164-12168.

Kjaer J. Ernstsen V. Jacobsen O.H. Hansen N. De Jonge L.W. Olsen P. 2011. Transport modes and pathways of the strongly sorbing pesticide glyphosate and pendimethalin through structure drained soils. *Chemosphere* 84: 471-479.

Klinger M.H.F. and Jelkmann W. 2002. Role of blood platelets in infection and inflammation. *Journal of Interferon and Cytokine Research* 22: 913-922.

Knoche M. 1994. Review: Effect of droplet size and carrier volume on performance of foliage-applied herbicides. *Crop Protection* 13: 163-178.

Knoche M. and Bukovac M.J. 1993. Interaction of surfactant and leaf surface in glyphosate absorption. *Weed Science* 41: 87-93.

Knowles W.S. Anderson K.S. Andrew S.S. Phillion D.P. Ream J.E. Johnson K.A. Sikorski J.A. 1993. Synthesis and characterization of *N*-amino-glyphosate as a potent analog inhibitor of *E.coli* EPSP synthase. *Bioorganic and Medicinal Chemistry Letters* 3: 2863-2868.

Kojima H. Takeuchi S. Niiyama K. Kobayashi K. 2004. Screening for estrogen and androgen receptor activities in 200 pesticides by *In vitro* reporter gene assays using Chinese hamster ovary cells. *Environmental Health Perspectives* 112: 524-531.

Koller V.J. Furhacker m. Nersesyan A. Misik M. Eisenbauer M. Knasmueller S. 2012. Cytotoxic and DNA-damaging properties of glyphosate and Roundup in human-derived buccal epithelial cells. *Archives of Toxicology* doi 10.1007/00204-012-0804-8.

Komoβa D. Gennity I. Sandermann H. 1992. Plant metabolism of herbicides with C-P bonds: Glyphosate. *Pesticide Biochemistry and Physiology* 43: 85-94.

Konar S.K. and Roy D.N. 1990. Short communication: Method for the determination of residues of the herbicide glyphosate and its principal metabolite, aminomethylphosphonic acid in plant materials by nitrogen-selective gas chromatography. *Analytica Chimica Acta* 229: 277-280.

Kools S.A.E. Van Roovert M. Van Gestel C.A.M. van Straalen N.M. 2005. Glyphosate degradation as a soil health indicator for heavy metal polluted soils. *Soil Biology and Biochemistry* 37: 1303-1307.

Koren K. Borisov S.M. Klimant I. 2012. Stable optical oxygen sensing materials based on click-coupling of fluorinated platinum (II) and palladium (II) porphyrins-A convenient way to eliminate dye migration and leaching. *Sensors and Actuators B* 169: 173-181.

Koski A. Yim K. Shivkumar S. 2004. Effect of molecular weight on fibrous PVA produced by electrospinning. *Materials Letters* 58: 493-497.

Krakauer T. 2002. Stimulant-dependent modulation of cytokines and chemokines by airway epithelial cells: cross talk between pulmonary epithelial and peripheral blood mononuclear cells. *Clinical and Diagnostic Laboratory Immunology* 9: 126-131.

Krauβ N. 2003. Mechanisms for photosystem I and II. *Current Opinion in Chemical Biology* 7: 540-550.

Kreno L.E. Leong K. Farha O.K. Allendorf M. Van Duyne R.P. Hupp J.T. 2011. Metal-organic framework materials as chemical sensors. *Chemical Reviews* 112: 1106-1125.

Krogh K.A. Halling-Sorensen B. Mogensen B.B. Vejrup K.V. 2003. Environmental properties and effects of nonionic surface adjuvants in pesticides : a review. *Chemosphere* 50: 871-901.

Krogh K.A. Vejrup K.V. Mogensen B.B. Halling-Sørensen B. 2002. Liquid chromatography-mass spectrometry method to determine alcohol ethoxylates and alkylamine ethoxylates on soil interstitial water, ground water and surface water samples. *Journal of Chromatography A* 957: 45-57.

Krzyśko-Lupicka T. and Orlik A. 1997. The use of glyphosate as the sole source of phosphorus or carbon for the selection of soil-borne fungal strains capable to degrade this herbicide. *Chemosphere* 34: 2601-2605.

Kubo S. and Kadla J.F. 2003. The formation of strong intermolecular interactions in immiscible blends of poly(vinyl alcohol) (PVA) and lignin. *Biomacromolecules* 4: 561-567

Kumaravel T.S. and Jha A.N. 2006. Reliable Comet assay measurements for detecting DNA damage induced by ionizing radiation and chemicals. *Mutation Research* 605: 7-16.

Kylin H. 2013. Time-integrated sampling of glyphosate in natural waters. *Chemosphere* 90: 1821-1828.

La Catoni R. and Gratani L. 2014. Variations in leaf respiration and photosynthesis ratio in response to air temperature and water availability among Meditteranean evergreen species. *Journal of Arid Environments* 102: 82-88.

Laganà A. Fago G. Marino A. Penazzi V.M. 2000. Liquid chromatography mass spectrometry tandem for multiresidue determination of selected post-emergence herbicides after soil column extraction. *Analytica Chimica Acta* 415: 41-56.

Laintz K.E. Yu J.J. Wai C.M. 1992. Seperation of metal ions with sodiumbis(trifluoroethyl)dithiocarbamate chelation and supercritical fluid chromatography. *Analytical Chemistry* 64: 311-315.

Laisk A. Oja V. Eichelmann H. Dall´Osto L. 2014. Action spectra of photosystems II and I and quantum yield of photosynthesis in leaves in State 1. *Biochemica et Biophysicca Acta* 1837: 315-325.

Laitinen P. Rämö S. Nikunen U. Jauhiainen L. Siimes K. Turtola E. 2009. Glyphosate and phosphorus leaching and residues in boreal sandy soil. *Plant Soil* 323: 267-283.

Lambropoulou D.A. and Albanis T.A. 2007. Review: Liquid-phase micro-extraction techniques in pesticide residue analysis. *Journal of Biochemical and Biophysical Methods* 70: 195-228.

Landry D. Dousset S. Fournier J.C. Andreux F. 2005. Leaching of glyphosate and AMPA under two soil management practices in Burgundy vineyards (Vosne-Romanée, 21-France). *Environmental Pollution* 138: 191-200.

Lane M. Lorenz N. Saxena J. Ramsier C. Dick R.P. 2012. Microbial activity, community structure and potassium dynamics in rhizosphere soil of soybean plants treated with glyphosate. *Pedobiologia – International Journal of Soil Biology* 55: 153-159.

Lange U. Roznyatovskaya N.V. Mirsky V.M. 2008. Review: Conducting polymers in chemical sensors and arrays. *Analytica Chimica Acta* 614: 1-26.

Langiano V.C. and Martinez C.B.R. 2008. Toxicity and effects of a glyphosate-based herbicide on the Neotropical fish *Prochilodus lineatus. Comparative Biochemistry and Physiology Part C* 147: 222-231.

Lanza F. and Sellergreen B. 2001. The application of molecular imprinting technology to solid-phase extraction. *Chromotographia* 53: 599-611.

Larsen K. Najle R. Lifschitz A. Virkel G. 2012. Effects of sub-lethal exposure of rats to the herbicide glyphosate in drinking water: glutathione transferase enzyme activities, levels of reduced glutathione and lipid peroxidation in liver, kidneys and small intestine. *Environmental Toxicology and Pharamcology* 34: 811-818.

Lee A.W.M. Chan W.H. Chiu C.M.L. Tang K.T. 1989. Short communication: ultraviolet spectrophotometric determination of primary and secondary aliphatic amines by formation of dithiocarbamates. *Analytica Chimica Acta* 218: 157-160.

Lee E.A. Zimmerman L.R. Bhullar B.S. Thurman E.M. 2002. Linker-assisted immunoassay and liquid chromatography/mass spectrometry for the analysis of glyphosate. *Analytical Chemistry* 74: 4937-4943.

Lee G. Kim J. Lee J.H. 2008. Development of magnetically separable polyaniline nanofibers for enzyme immobilization and recovery. *Enzyme and Microbial Technology* 42: 466-472.

Lee H.U. Jung D.U. Lee J.H. Song Y.S. Park C. Kim S.W. 2013. Detection of glyphosate by quantitative analysis of fluorescence and single DNA using DNA-labeled fluorescent magnetic core-shell nanoparticles. *Sensors and Actuators B* : *Chemical* 177: 879-896.

Lee J.S. Choi K.H. Ghim H.D. Kim S.S. Chun D.H. Kim H.Y. Lyoo W.S. 2004. Role of molecular weight of atatic poly(vinyl alcohol) (PVA) in the structure and properties of PVA nanofabric prepared by electrospinning. *Journal of Applied Polymer Science* 93: 1638-1646.

Lee K.H. Kim H.Y. Bang H.J. Jung Y.H. Lee S.G. 2003. The change of bead morphology formed on electrospun polystyrene fibers. *Polymer* 44: 4029-4034.

Lee S.K. and Okura I. 1997. Optical sensor for oxygen using a porphyrin-doped sol-gel glass. *Analyst* 122: 81-84.

Lehnen L.P. and Vaughn K.C. 1992. The herbicide sindone B disrupts spindle microtubule organizing centers. *Pesticide Biochemistry and Physiology* 44: 50-59.

Lemaire G. Mnif W. Mauvais P. Balaguer P. Rahmani R. 2006. Activation of α and β-estrogen receptors by persistant pescticides in reporter cell lines. *Life Sciences* 79: 1160-1169.

Lerbs W. Stock M. Parthier B. 1990. Physiological aspects of glyphosate degradation in *Alcaligenes spec.* strain GL. *Archives of Microbiology* 153: 146-150.

Lev O. Tsionsky M. Rabinovich L. Glezer V. Sampath S. Pankratov I. Gun J. 1995. Organically modified sol-gel sensors. *Analytical Chemistry* 67: 22-30.

Leyden D.E. and Cuttrell G.H. 1975. Preconcentration of trace metals using chelating groups immobilized via silylation. *Analytical Chemistry* 47: 1812-1817.

Li D. and Xia Y. 2004. Review: Electrospinning of nanofibers: reinventing the wheel?. *Advanced Materials* 16: 1151-1170.

Li H.H. Hao R.L. Wu S.S. Guo P.C. Chen C.J. Pan L.P. Ni H. 2011. Commentary: Occurance, function and potential medicinal applications of the phytohormone abscisic acid in animals and humans. *Biochemical Pharmacology* 82: 701-712.

Li J. Suo J. Wang S. 2009. The effect of copper (II) on the thermal and mechanical properties of poly(vinyl alcohol)/silica hybrid. *Polymer Engineering and Science* DOI 10.1002/pen.

Li Z. Zhang H. Zheng W. Wang W. Huang H. Wang C. MacDiarmid A.G. Wei Y. 2008. Highly sensitive and stbale humidity nanosensors based on LiCl doped $TiO_2$ electrospun nanofibers. *Journal of American Chemical Society* 190: 5036-5037.

Liao Y. Zhang C. Zhang Y. Strong V. Tang J. Li X.G. Kalantar-zadeh K. Hoek E.M.V. Wang K.L. Kaner R.B. 2011. Carbon nanotube/polyaniline composite nanofibers: facile synthesis and chemosensors. *Nano Letters* 11: 954-959.

Lieberzeit P.A. and Dickert F.L. 2007. Review: Sensor technology and its application in environmental analysis. *Analytical and Bioanalytical Chemistry* 387: 237-247.

Likhar P.R. Arundhathi R. Ghosh S. Kantam M.L. 2009. Polyaniline nanofiber supported $FeCl_3$: An efficient and reusable heterogeneous catalyst for the acylation of alcohols and amines with acetic acid. *Journal of Molecular Catalysis A: Chemical* 302: 142-149.

Lin N. and Garry V.F: 2000. *In vitro* studies of cellular and molecular developmental toxicity of adjuvants, herbicides, and fungicides commonly used in Red River Valley, Minnesota. *Journal of Toxicology and Environmental Health* 60: 423-439.

Lin S.L. Yan L.Y. Liang X.W. Wang Z.B. Wang Z.Y. Qiao J. Schatten H. Sun Q.Y. 2009. A novel variant of ER-alpha, ER-alpha36 mediates testosterone stimulated ERK and Akt activation in endometrial cancer Hec1A cells. *Reproductive Biology and Endocrinology* 7: 1-8.

Lin T. Wang H. Wang H. Wang X. 2004. The charge effect of cationic surfacatants on the elimination of fibre beads in the electrospinning of polystyrene. *Nanotechnology* 15: 1375-

Linden H. Sandmann G. Chamovitz D. Hirschberg J. Böger P. 1990. Biochemical characterization of *Synechococcus* mutants selected against the bleaching herbicide norflurazon. *Pesticide Biochemistry and Physiology* 36: 46-51.

Lindner E. Cosofret V.V. Kusy R.P. Buck R.P. 1993. Responses of $H^+$ selective solvent polymeric membrane electrodes fabricated from modified PVC membranes. *Talanta* 40: 957-967.

Linz G.M. and Homan H.J. 2011. Use of glyphosate for managing invasive cattail (*Typha* spp.) to disperse blackbird (Icteridae) roosts. *Crop Protection* 30: 98-104.

Lioi M.B. Scarfi M.R. Santoro A. Barbieri R. Zeni O. Salvemini F. Berardino D.D. Ursini M.V. 1998. Cytogenetic damage and induction of pro-oxidant state in human lymphocytes exposed *In Vitro* to gliphosate, vinclozolin, atrazine and DPX-E9636. *Environmental and Molecular Mutagenesis* 32: 39-46.

Litz N.T. Weigert A. Krause B. Heise S. Grützmacher G. 2011. Comparative studies on the retardation and reduction of glyphosate during subsurface passage. *Water Research* 45: 3047-3054.

Liu C.C. and Lin Y.C. 2013. Reclamation of copper-contaminated soil using EDTA or citric acid coupled with dissolved organic matter solution extracted from distillery sludge. *Environmental Pollution* 178: 97-101.

Liu C.M. McLean P.A. Sookdeo C.C. Cannon F.C. 1991. Degradation of the herbicide glyphosate by members of the family *Rhizobiaceae*. *Applied and Environmental Microbiology* 57: 1799-1804.

Liu Z. 2004. Effects of surfactants on foliar uptake of herbicides-a complex scenario. *Colloids and Surfaces B* 35: 149-153.

Liu Z.Q. Gaskin R.E. Zabkiwicz J.A. 2004. Visualization of the effect of a surfactant on the uptake of xenobiotics into plant foliage by confocal laser scanning microscopy. *Weed Research* 44: 237-243.

Lobnik A. Oehme I. Murkovic I. Wolfbeis O.S. 1998. pH optical sensors based on sol-gels: chemical doping versus covalent immobilization. *Analytica Chimica Acta* 367: 159-165.

Lodovichi M.V. Blanco A.M. Chantre G.R. Bandoni J.A. Sabbatini M.R. Vigna M. López R. Gigón R. 2013. Operational planning of herbicide-based weed management. *Agricultural Systems* 121: 117-129.

London L. Dalvie M.A. Nowicki A. Cairncross E. 2005. Approaches for regulating water in South Africa for the presence of pesticides. *Water SA* 31: 53-60.

Long Y. Chen H. Yang Y. Wang H. Yang Y. Kean N.L. Pei J. Liu F. 2009. Electrospun nanofibrous film doped with a conjugated polymer for DNT fluorescence sensor. *Macromolecules* 42: 6501-6509.

Lorraine-Colwill D.F. Powles S.B. Hamkes T.R. Hollinshead P.H. Warner S.A.J. Preston C. 2003. Investigations into the mechanisms of glyphosate resistance in *Lolium rigidum*. *Pesticide Biochemistry and Physiology* 74: 62-72.

Lukás D. Sarkar L. Martinová K. Vodsed A.D. Lubasová J. Chaloupek J. Pokorný P. Mikeš P. Chvojka J. Komárek M. 2009. Physical principles of electrospinning (electrospinning as a nano-scale technology of the twenty-first century). *Textile Progress* 41: 59-140.

Lv Y.Y. Xu W. Lin F.W. Wu J. Xu Z.K. 2013. Electrospun nanofibers of porphyrinated polyimide for the ultra-detection of trace TNT. *Sensors and Actuators B: Chemical* 184: 205-211.

Ma Z. Kotaki M. Yong T. He W. Ramakrishna S. 2005. Surface engineering of electrospun polyethylene terephthalate (PET) nanofibers towards development of a new material for blood vessel engineering. *Biomaterials* 26: 2527-2536.

Macherel D. Ravanel P. Tissut M. 1982. Effects of herbicidal carbamates on mitochondria and chloroplasts. *Pesticide Biochemistry and Physiology* 18: 280-288.

Maharaj S. 2005. Modelling the behavior and fate of priority pesticides in South Africa. Thesis: Master of Science in environmental and water science. Department of Earth Sciences, University of the Western Cape, South Africa.

Maitra A. Abbas A.K. Kumar V. Fausto N. 2008. The endocrine system. *Pathologic Basis of Disease* 1155-1226.

Mäkelä P. Peltonen-Sainio P. Jokinen K. Pehu E. Setälä H. Hinkkanen R. Somersalo S. 1996. Uptake and translocation of foliar-applied glycinebetaine in crop plants. *Plant Science* 121: 221-230.

Makled M.H. Sheha E. Shanap T.S. El-Mansy M.K. 2013. Electrical conduction and dielectric relaxation in *p*-type PVA/CuI polymer composite. *Journal of Advanced Research* 4: 531-538.

Malaguerra F. AlbrechtsenH.J. Binning P.J. 2013. Assessment of the contamination of drinking water supply wells by pesticides from surface water resources using finite element reactive transport model and global sensitivity analysis technique. *Journal of Hydrology* 476: 321-331.

Malakondaiah N. and Fang S.C. 1978. Influence of monuron on photosystem II and light-dependent $^{14}CO_2$ fixation in isolated $C_3$ and $C_4$ plants. *Pesticide Biochemistry and Physiology* 9: 33-38.

Malašauskiene J.and Milašius R. 2010. Mathematical analysis of diameter distribution of electrospun nanofibers. *Fibers and Textiles in Eastern Europe* 18: 45-48

Mallat E. and Barceló D. 1998. Analysis and degradation study of glyphosate and of aminomethylphosphonic acid in natural waters by means of polymeric and ion-exchange solid-phase extraction columns followed by ion-chromatography-post-column derivatization with fluorescence detection. *Journal of Chromatography A* 823: 129-136.

Mamy L. and Barriuso E. 2005. Glyphosate adsorption in soils compared to herbicides replaced with the introduction of glyphosate resistant crops. *Chemosphere* 61: 844-855.

Mamy L. Barriuso E. Gabrielle B. 2005. Environmental fate of herbicides trifluralin, metazachlor, metamitron and sulcotrione compared with that of glyphosate, a substitute broad spectrum herbicide for different glyphosate-resistant crops. *Pest Management Science* 61: 905-916.

Mañas F. Peralta L. Raviolo J. Ovando H.G. Weyers A. Ugnia L. Cid M.G. Larripa I. Gorla N. 2009a. Genotoxicity of glyphosate assessed by the Comet assay and cytogenetic tests. *Environmental Toxicology and Pharmacology* 28: 37-41.

Mañas F. Peralta L. Raviolo J. Ovando H.G. Weyers A. Ugnia L. Gonzalez Cid M. Larripa I. Gorla N. 2009b. Genotoxicity of AMPA, the environment metabolite of glyphosate assessed by the Comet assay and cytogenetic tests. *Ecotoxicology and Environmental Safety* 72: 834-837.

Mann R.M. and Bidwell J.R. 1999. The toxicity of glyphosate and several glyphosate formulations to four species of SouthWestern Australian frogs. *Archives of Environmental Contamination and Toxicology* 36: 193-199.

Mann R.M. Hyne R.V. Choung C.B. Wilson S.P. 2009. Review: Amphibians and agricultural chemicals: review of the risks in a complex environment. *Environmental Pollution* 157: 2903-2927.

Maqueda C. Morillo E. Undabeytia T. Martin F. 1998. Sorption of glyphosate and Cu(II) on a natural fulvic acid complex: mutual influence. *Chemosphere* 37:1063-1072

Marc J. Mulner-Lorillon O. Bellé R. 2004. Glyphosate-based pesticides affect cell cycle regulation. *Biology of the Cell* 96: 245-249.

Markaverich B. Mani S. Alejandro M.A. Mitchell A. Markaverich D. Brown T. Velez-Trippe C. Murchison C. O´Malley B. Faith R. 2002. A novel endocrine-disrupting agent in corn with mitogenic activity in human breast and prostatic cancer cells. *Environmental Health Perspectives* 110: 169-177.

Martenies S.E. and Perry M.J. 2013. Environmental and occupational pesticide exposure and human sperm parameters: A systematic review. *Toxicology* 307: 66-73.

Martinez A. Reyes I. Reyes N. 2007. Cytotoxicity of the herbicide glyphosate in human peripheral blood mononuclear cells. *Biomedica* 27: 594-604.

Martini C.N. Gabrielli M. Vila M.C. 2012. A comercial formulation of glyphosate inhibits proliferation and differentiation to adipocytes and induces apoptosis in 3T3-L1 fribroblasts. *Toxicology in Vitro* 26: 1007-1013.

Masifunde Education and Development Project Trust. 2010. Threats to the food security and food sovereignty in the Eastern Cape. Impacts of the Massive Food Production Programme (MFPP), GMOs, and cash crops in four villages in the Amathole District Municipality. An Information document (http://www.biosafety-info.net) accessed December 2013.

Masojidek J. Souček P. Máchova J. Frolik J. Klem K. Malý. 2011. Detection of photosynthetic herbicides: algal growth inhibition test vs. electrochemical photosystem II biosensor. *Ecotoxicology and Environemental Safety* 74: 117-122.

Mateos-Naranjo E. Redondo-Gómez S. Cox L. Cornejo J. Figueroa M.E. 2009. Effectiveness of glyphosate and imazamox on the control of the invasive cordgrass *Spartina densiflora*. *Ecotoxicology and Environmental Safety* 72: 1694-1700.

Matlock-Colangelo L. and Baeumner A.J. 2014. Biologically inspired nanofibers for use in translational bioanalytical systems. *Annual Review of Analytical Chemistry* 7: 23-42.

Matsuo Y. Hatase K. Sugle Y. 1998. Preparation and characterization of poly (vinyl alcohol)-and $Cu(OH)_2$-poly(vinyl alcohol)-intercalated graphite oxides. *Chemistry of Materials* 10: 2266-2269.

Matthews J.A. Wnek G.E. Simpson D.G. Bowlin G.L. 2002. Electrospinning of collagen nanofibers. *Biomacromolecules* 3: 232-238.

Mbanaso F.U. Coupe S.J. Charlesworth S.M. Nnadi E.O. 2013. Laboratory-based experiments to investigate the impact of glyphosate containing herbicide on pollution attenuation and biodegradation in a model pervious paving system. *Chemosphere* 90: 737-746.

McAuliffe K.S. Hallas L.E. Kulpa C.F. 1990. Glyphosate degradation by *Agrobacterium radiobacter* isolated from activated sludge. *Journal of Industrial Microbiology* 6: 219-221.

McCann J.T. Chen J.I.L. Dan L. Ye Z.G. Xia Y. 2006. Electrospinning of polycrystalline barium titanate nanofibers with controllable morphology and alignment. *Chemical Physics Letters* 424:: 162-166.

McCann J.T. Li D. Xia Y. 2004. Electrospinning of nanofibers with core-sheath, hollow, or porous structure. *Journal of Materials Chemistry* 15: 735-738.

McClain A. and Hseih Y.L. 2004. Synthesis of polystyrene-supported dithiocarbamates and their complexation with metal ions. *Journal of Applied Polymer Science* 92: 218-225.

McConnell J.S. and Hossner L.R. 1985. pH-Dependent adsorption isotherms of glyphosate. *Journal of Agriculture and Food Science* 33: 1075-1078.

McGuinness M. and Dowling D. 2009. Review: Plant-associated bacterial degradation of toxic organis compounds in soil. *International Journal of Environmental Research and Public health* 6: 2226-2247.

Meakins N.C. Bubb J.M. Lester J.N. 1994. The behavior of the *s*-triazine herbicides, atrazine and simazine, during primary and secondary biological waste water treatment. *Chemosphere* 28: 1611-1622.

Mecer G.N. 2007. A simple diffusion model of the effect of droplet size and spread area on foliar uptake of hydrophilic compounds. *Pesticide Biochemistry and Physiology* 88: 128-133.

Meinhardt H.R. 2009. Evaluation of predictive models for pesticide behavior in South African soils. Thesis: Doctor of Philosophy in Zoology. School of Environmental Sciences and Development, North-West University, Pochefstroom, South Africa.

Melander B. And Rasmussen G. 2001. Effects of cultural methods and physical weed control on intrarow weed numbers, manual weeding and marketable yield in direct-sown leek and bulb onion. *Weed Research* 41: 491-508.

Melander B. Holst N. Rasmussen I.A. Hansen P.K. 2012. Direct control of perennial weeds between crops-implications for organic farming. *Crop Protection* 40: 36-42.

Mengistu A. Reddy K.N. Bellaloui N. Walker E.R. 2013. Effect of glyphosate on *Macrophomina phaseolina in vitro* and its effect on disease severity of soybean in the field. *Crop Protection* 54: 23-28.

Mensah P.K. Palmer C.G. Muller W.J. 2013. Derivation of South African water quality guidelines for Roundup® using species sensitivity distribution. *Ecotoxicology and Environmental Safety* 96: 24-31.

Mesnage R. Bernay B. Séralini G.E. 2013. Ethoxylated adjuvants of glyphosate-based herbicides are active principles of human toxicity. *Toxicology* 313: 122-128.

Mesri M. and Altieri D.C. 1999. Leukocyte microparticles stimulate endothelial cell cytokine release and tissue factor induction in JNK1 signaling pathway. *The Journal of Biological Chemistry* 274: 23111-23118.

Metcalf-Wallach J. 2007. Demand-side approaches to water scarcity: South Africa and the National Water act. *International Development Environment and Sustainability* 1-5.

Miller J.J. Hill B.D. Chang C. Lindwall C.W. 1995. Residue detection in soil and shallow groundwater after long-term herbicide applications in southern Alberta. *Canadian Journal of Soil Science* 349-356.

Millie D.F. Greene D.A. Johnsen P.B. 1990. Effects of the carotenoid-inhibiting herbicide, fluridone, on *Oscillatoria agardhii* Gomont (cyanobacteria). *Aquatic Toxicology* 16: 41-52.

Min M. Wang X. Chen Y. Wang L. Huang H. Shi J. 2013. Highly sensitive and selective $Cu^{2+}$ sensor based on electrospun rhodamine dye doped poly(ether sulfones) nanofibers. *Sensors and Actuators B: Chemical* 188: 360-366.

Miransari M. and Smith D.L. 2014. Review: Plant hormones and seed germination. *Environmental and Experimental Botany* 99:110-121.

Miro N.L. Ferreira F.W. Breijo G. E. Ibáñez C.J. Sánchez L.G. Baixauli J.G. 2012. Glyphosate detection by voltammetric techniques. A comparison between statistical methods and an artificial neural network.

Mithila J. and Hall J.C. 2007. Production of an auxinic herbicide-resistant microspore –derived doubled haploid wild mustard (*Sinapsis arvensis L.*) plant. *Crop Protection* 26: 357-362.

Mitsis T. Efthimiadou A. Bilalis D.J. Danalatos N.G. Efthimiadis P. Konstantas A. 2011. Short communication: Maximizing oilseed rape´s yield by glyphosate under Mediterranean condtions. *Industrial Crops and Protection* 33: 544-548.

Mladinic M. Berend S. Vrdoljak A.L. Kopjar N. Radic B. Zeljezic D. 2009. Evaluation of genome damage and its relation to oxidative stress induced by glyphosate in human lymphocytes *in vitro*. *Environmental and molecular mutagenesis* 50: 800-807.

Moller P. Knudsen L.E. Loft S. 2000. The Comet assay as a rapid test in biomonitoring occupational exposure to DNA-damaging agents and confounding factors. *Cancer Epidemiology Biomarkers and Prevention* 9: 1005-1015.

Momba M.N.B. and Mnqumevu B.V. 2000. Detection of fecal coliform bacteria and heterotrophic plate count bacteria attached to houshold containers during the storage of drinking groundwater in a rural community. WISA 2000 Biennial Conference Sun City, South Africa.

Momba MNB. Tyafa Z. Makala N. Brouckaert B.M. Obi C.L. 2006. Safe drinking water still a dream in rural areas of South Africa. Case study: The Eastern Cape Province. Paper presented at the Water Institute of South Africa (WISA) biennial conference. May 21-25 2006. Durban, South Africa.

Mona M.H. Gaafar R.M. Helal I.B. Omran N.E. Salama W.M. 2013. Evaluation of cytotoxic effects of atrazine and glyphosate herbicides on *Biomphalaria glabrata* snails. *The Journal of Basic & Applied Zoology* 66: 68-75.

Moreland D.E. and Huber S.C. 1979. Inhibition of photosynthesis and respiration by substituted 2,6-dinitroaniline herbicides III. Effects of electron transport and membrane properties of isolated mung bean mitochondria. *Pesticide Biochemistry and Phyisology* 11: 247-257.

Moreland D.E. Farmer F.S. Hussey G.G. 1972a. Inhibition of photosynthesis and respiration by substituted 2,6-dinitoaniline herbicides. I. Effects on chloroplast and mitochondrial activities. *Pesticide Biochemistry and Physiology* 2: 342-353.

Moreland D.E. Farmer F.S. Hussey G.G. 1972b. Inhibition of photosynthesis and respiration by substituted 2,6-dinitoaniline herbicides. II Effects on responses in excised plant tissues and treated seedlings. *Pesticide Biochemistry and Physiology* 2: 354-363.

Moreno N.C. Sofia S.H. Martinez C.B.R. 2014. Genotoxic effects of the herbicide Roundup Transorb® and its active ingredient glyphosate on the fish *Prochilodus lineatus* . *Environmental Toxicology and Pharamcology* 37: 448-454.

Morillo E. Undabeytia T. Maqueda C. 1997. Adsorption of glyphosate on the clay mineral montmorillonite: effect of Cu (II) in solution and adsorbed on the mineral. *Environmental Sciences and Technology* 31: 3588-3592.

Morillo E. Undabeytia T. Maqueda C. Ramos A. 2000. Glyphosate adsorption on soils of different characteristics influence of copper addition. *Chemosphere* 40: 103-107.

Mörtl M. Németh G. Juracsek J. Darvis B. Kamp L. Rubio F. Székács A. 2013. Determination of glyphosate residues in Hungarian water samples by immunoassay. *Microchemical Journal* 107: 143-151.

Mothes-Wagner U. Reitze H.K. Seitz K.A. 1990. Environmental actions of agrochemicals 2. Histological effects of the herbicide/insecticide dinoseb-acetate (2-*sec*-*butyl*-4,6-dinitrophenyl acetate) on the spider mite *Tetranychus urticae* (Acari: Teranychidae) reared on herbicide treated *Phaseolus vulgaris*. *Experimental & Applied Acarology* 9: 289-310.

Motojyuku M. Saito T. Akieda K. Otsuka H. Yamamoto I. Inokuchi S. 2008. Determination of glyphosate, glyphosate metabolites, and glufosinate in human serum by gas chromatography-mass spectrometry. *Journal of Chromatography B* 875: 509-514.

Motulsky H. and Christopoulos A. 2003. Fitting models to biological data using linear and nonlinear regression: A practical guide to curve fitting. Graphpad Software Inc, San Diego CA, www.graphpad.com

Mtero F. 2012. Commercialization, de-agrarianisation and the accumulation/reproduction dynamic: massive maize production schemes in the Eastern Cape, South Africa. Paper presented at the international conference on global land grabbing. October 17-19 2012. Department of Development Sociology, Cornell University, Ithaca, New York, USA.

Mudigoudra B.S. Masti S.P. Chougale R.B. 2012. Short communication: thermal behavior of poly(vinyl alcohol)/poly(vinyl pyrolidone)/chitosan ternary polymer blend films. *Research Journal of Recent Sciences* 1: 83-86.

Mueller B.J. and Lovett R.J. 1987. Salt-induced phase separation of the determination of metals as their diethyldithiocarbamate complexes by high-performance liquid chromatography. *Analytical Chemistry* 59: 1405-1409.

Mueller T.C. Main C.L. Thompson M.A. Steekel L.E. 2006. Comparison of glyphosate salts (isopropylamine, diammonium and potassium) and calcium and magnesium concentrations on the control of various weeds. *Weed Technology* 20: 164-171.

Müller G.F.J Stürzel M. Mülhaupt R. 2014. Silica nanotubes and hollow silica nanofibers: Gas phase mineralization, polymerization catalysis and *in-situ* polyethylene nanocomposites. *Polymer* 55: 465-470.

Mulugeta M. and Megersa N. 2004. Carrier-mediated extraction of bipyridilium herbicides across the hydrophobic liquid membrane. *Talanta* 64: 101-108.

Muoghalu J.I. 2008. Growth, reproduction and resource allocation of *Tithonia diversifolia* and *Tithonia rotundifolia. Weed Research* 48: 157-162.

Muradov M.B. Abdinov A.S.H. Hajimamedov R.H. Eyivazova G.M. 2009. Dielectric properties of nanocomposites on the basis of copper sulfide nanoparticles and a polymer matrix. *Engineering and Applied Electrochemistry* 45: 167-170.

Murthy R.S.S. and Ryan D.E. 1982. Preconcentration of copper, cadmium, mercury and lead from sea and tap water samples on a dithiocarbamatecellulose derivative. *Analytica Chimica Acta* 140: 163-169.

Murugan R. and Ramakrishna S. 2007. Review: design strategies to tissue engineering scaffolds with controlled fiber orientation. *Tissue Engineering* 13: 1845-1866.

Naebe M. Lin T. Staiger M.P. Dai L. Wang X. 2008. Electrospun single-walled carbon anotube/polyvinyl alcohol composite nanofibers: structure-property relationships. *Nanotechnology* 19 305702 doi: 10.1088/0957-4484/19/30/305702

Nakashima K. Yoshimura T. Mori H. Kawaguchi M. Adachi S. Nakao T. Yamazaki F. 2002. Effects of pesticides on cytokines production by human peripheral blood mononuclear cells-fenitrothion and glyphosate. *Chudoku Kenkyu* 15: 159-165.

Nath N. and Chilkoti A. 2002. A colorimetric gold nanoparticles sensor to interrogate biomolecular interactions in real time on a surface. *Analytical Chemistry* 74: 504-509.

Neumann M. Liess M. Schulz R. 2003. A qualitative sampling method for monitoring water quality in temporary channels or point source and its applications to pesticide contamination. *Chemosphere* 51: 509-513.

Newton J.W. and Tyler D.D. 1989. Liberation of ammonia by soybean leaf pieces induced with herbicides which inhibit photosystem II. *Plant Science* 60: 61-66.

Nieuwenhuizen P.J. Ehlers A.W. Haasnoot J.G. Janse S.R. Reedijk J. Baerends E.J. 1999. The mechanism of zinc(II)-dithiocarbamate-accelerated vulcanization uncovered, theoretical and experimental evidence. *Journal of American Chemistry Society* 121: 163-168.

Niu Y. Matos A.L. Abrantes L.M. Viana A.S. Jin G. 2012. Antibody oriented immobilization on gold using the reaction between carbon disulfide and amine groups and its application in immunosensing. *Langmuir* 28: 17718-17725.

Nkwonta O.I. and Ochieng G.M. 2009. Water pollution in Soshanguve environs of South Africa. *World Academy of Science, Engineering and Technology* 56: 2009.

Noguchi K. and Yoshida K. 2008. Interaction between photosynthesis and respiration in illuminated leaves. *Mitochondria* 8: 87-99.

Nowak I. and Shaw L.M. 1995. Mycophenolic acid binding to human serum: characterization and relation to pharmacodynamics. *Clinical Chemistry* 41: 1011-1017.

Nurse R.E. Swanton C.J. Tardif F. Sikkema P.H. 2006. Weed control and yield are improved when glyphosate is preceded by residual herbicide in glyphosate-tolerant maize (*Zhea mays*). *Crop Protection* 25: 1174-1179.

O´Riordan T.C. Voraberger H. Kerry J.P. Papkovsky D.B. 2005. Study of migration of active components of phosphorescent oxygen sensors for food packaging applications. *Analytica Chimica Acta* 530: 135-141.

Ohkawa H. Tsujii H. Ohkawa Y. 1999. Review: The use of cytochrome P450 genes to introduce herbicide tolerance in crops. *Pesticide Science* 55: 867-874.

Oliveira J.E. Scagion V.P. Grassi V. Correa D.S. Mattoso L.H.C. 2012. Modification of electrospun nylon nanofibers using layer-by-layer films for application in flow injection electronic tongue: detection of paraoxon pesticide in corn crop. *Sensors and Actuators B* 171-172: 249-255.

Oliver K. White A.J.P. Hogarth G. Wilton-Ely J.D.E.T. 2011. Multimetallic complexes of group 10 and 11 metals based on polydentate dithiocarbamate ligands. *Dalton Transactions* 40: 5852-5864.

Olorunsogo O.O. Bababunmi E.A. Bassir O. 1979. Effect of glyphosate on rat liver mitochondria *in vivo*. *Bulletin of Environmental Contamination and Toxicology* 22: 357-364.

Olson H. Betton G. Robinson D. Thomas K. Monro A. Kolaja G. Lilly P. Sanders J. Sipes G. Bracken W. Dorato M. Van Deun K. Smith P. Berger B. Heller A. 2000. Concordance of the toxicity of pharmaceuticals in humans and in animals. *Regulatory Toxicology and Pharmacology* 32: 56-67.

Ostrowski M. and Jakubowska A. 2013. *GH3* expression and IAA-amide synthetase activity in pea (*Pisum sativum L.*) seedlings are regulated by light, plant hormones and auxinic herbicides. *Journal of Plant Physiology* 170: 361-368.

Panda P.K. and Sahoo B. 1990. A review: Synthesis and applications of electrospun. *Nanotechnology* 1: 399-417.

Parashar V. Parashar R. Sharma B. Pandey A.C. 2009. Parthenium leaf extract mediated synthesisof silver nanoparticles: A novel approach towards weed utilization. *Digest Journal of Nanomaterials and Biostructures* 4: 45-50.

Park H. Song T. Han H. Paik U. 2013. Short communication: Electrospun $Li_4Ti_5O_{12}$ nanofibers sheathed with conductive $TiN/TiO_xN_y$ layer as an anode material for high power Li-ion batteries. *Journal of Power Sources* 244: 726-730.

Parrón T. Requena M. Hernández A.F. Alarcón. 2013. *Toxicology Letters* http://cbc.doi.org/10.10.16/j.toxlet.2013.11.009.

Paterson S. Mackay D. Tam D. Shiu W.Y. 1990. Uptake of organic chemicals by plants: A review of processes, correlations and models. *Chemosphere* 21: 297-331.

Patsias J. Papadopoulou A. Papadopoulou-Mourkidou E. 2001. Automated trace level determination of glyphosate and aminomethyl phosphonic acid in water by on-line anoin-exchange solid-phase extraction followed by cation-exchange liquid chromatography and post-column derivatization. *Journal of Chromatography A* 932: 83-90.

Paul M.J and Meyer J.L. 2001. Streams in the urban landscape. *Annual Review of Ecology and Systematics* 32: 333-365.

Paull R.E. 1999. Effect of temperature and relative humidity on fresh commodity quality. *Postharvest Biology and Technology* 15: 263-277.

Pedersen B.P. Neve P. Andreasen C. Powles S.B. 2007. Ecological fitness of a glyphosate-resistant *Lolium rigidum* population: Growth and seed production along a competition gradient. *Basic and Applied Ecology* 8: 258-268.

Peijs T. Van Vught R.J.M. Govaert L.E. 1995. Mechanical properties of poly(vinyl alcohol) fibers and composites. *Composites* 26: 83-90.

Peixoto F. 2005. Comparative effects of the Roundup and glyphosate on mitochondrial oxidative phosphorylation. *Chemosphere* 61: 1115-1122.

Pereiro I.R. Irimia G. Cano E.R. Torrijos R.C. 2004. Optimisation of a gas chromatographic-mass spectrometric method for the determination of phenoxy acid herbicides in water samples as silyl derivatives. *Analytica Chimica Acta* 524: 249-256.

Peresin M.D. Vesterinen A:H. Habibi Y. Johansson L.S. Pawlak J.J. Nevzorov A.A. Rojas O.J. 2014. Crosslinked PVA nanofibers reinforced with cellulose nanocrystals: water interactions and thermomechanical properties. *Journal of Applied Polymer Science DOI: 10.1002/app.40334*

Peresin M.S. Habibi Y. Vesterinen A.H. Rojas O.J. Pawlak J.J. Seppälä. 2010. Effect of moisture on electrospun nanofiber composites of poly(vinyl alcohol) and cellulose nanocrystals. *Biomacromolecules* 11: 2471-2477.

Peresin M.S. Habibi Y. Zoppe J.O. Pawlak J.J. Rojas O.J. 2010b. Nanofiber composites of polyvinyl alcohol and cellulose nanocrystals: Manufacture and characterization. *Biomacromolecules* 11: 674-681.

Perez-Carreon J.I. Dargent C. Merhi M. Fattel-Fazenda S. Arce-Popoca E. Villa-Treviño S. Rouimi P. 2009. Tumor promoting and co-carcinogenic effects in medium-term rat hepatocarcinogenesis are not modified by co-administration of 12 pesticides in mixture at acceptable daily intake. *Food and Chemical Toxicology* 47: 540-546.

Perkins M.C. Bell G. Briggs D. Davies M.C. Friedman A. Hart C.A. Roberts C.J. Rutten F.J.M. 2008. The application of ToF-SIMS to the analysis of herbicide formulation penetration into and through leaf cuticles. *Colloids and Surfaces B: Biointerfaces* 67:1-13.

Peruzzo P.J. Porta A.A. Ronco A.E. 2008. Levels of glyphosate in surface waters, sediments and soils associated with direct sowing soybean cultivation in north pampasic region of Argentina. *Environmental Pollution* 156: 61-66.

Pessagno R.C. Sánchez R.M.T. Dos Santos Afonso M. 2008. Glyphosate behavior at soil and mineral-water interfaces. *Environmental Pollution* 153: 53-59.

Peterson S.M. and Batley G.E. 1993. The fate of endosulfan in aquatic ecosystems. *Environmental Pollution* 82: 143-152.

Petit V. Cabridenc R. Swannell R.P.J. Sokhi R.S. 1995. Review of strategies for modelling the environmental fate of pesticides discharged into riverine systems. *Environment International* 21: 167-176.

Pham Q.P. Sharma U. Mikos A.G. 2006. A review: electrospinning of polymeric nanofibers for tissue engineering applications. *Tissue Engineering* 12: 1197-1210.

Pieniążek D. Bukowska B. Duda W. 2004. Comparison of the effect of Roundup ULTRA 360 SL pesticide and its active compound glyphosate on human erythrocytes. *Pesticide Biochemistry and Physiology* 79: 58-63.

Piola L. Fuchs J. Oneto M.L. Basack S. Kesten E. Casabé N. 2013. Comparative toxicity of two glyphosate-based formulations to *Eisenia andrei* under laboratory conditions. *Chemosphere* 91: 545-551.

Pipke R. and Amrhein N. 1988. Degradation of the phosphonate herbicide glyphosate by *Arthrobacter atrocyaneus* ATCC 13752. *Applied and Environmental Microbiology*. 54: 1293-1296.

Pirrung M.C. Cao J. Chen J. 1998. Ethylene biosynthesis: processing of a substrate analog supports a radical mechanism for the ethylene-forming enzyme. *Chemistry and Biology* 5: 49-57.

Pitluck M.R. Pollard B.D. Haworth D.T. 1987. Short communication: determination of stability constants of a copper/citric acid complex by ion-exchamge chromatography and atomic absorption spectrometry. *Analytica Chimica Acta* 197: 339-342.

Pitt R. Clark S. Field R. 1999. Groundwater contamination potential from stormwater infiltration practices. *Urban Waters* 1: 217-236.

Poletta G.L. Larriera A. Kleinsorge E. Mudry M.D. 2009. Genotoxicity of the herbicide formulation Roundup® (glyphosate) in broad-snouted caiman (*Caiman latirostris*) evidence by the Comet assay and the Micronucleus test. *Mutation Research/Genetic Toxicology and Environmental Mutagenesis* 672: 95-102.

Popp M. Hann S. Mentler A. Fuerhacker M. Stingeder G. Koellensperger G. 2008. Determination of glyphosate and AMPA in surface and waste water using high-performance ion chromatography coupled to inductively coupled plasma dynamic reaction cell mass spectrometry (HPIC-ICP-DRC-MS). *Analytical and Bioanalytical Chemistry* 391: 695-699.

Powles S.B. and Preston C. 2006. Evolved glyphosate resistance in plants: biochemical and genetic basis of resistance. *Weed Technology* 20: 282-289.

Prati D and Bossdorf O. 2004. Brief communication: Allelopathic inhibition of germination by *Alliaria petiolata* (Brassicaceae). *American Journal of Botany* 91: 285-288.

Price C.E. and Anderson N.H. 1985. Uptake of chemicals from the foliar deposits: effects of plants species and molecular structure. *Pesticide Science* 16: 369-377.

Qian K. Tang T. Shi T. Wang F. Li J. Cao Y. 2009. Residue determination of glyphosate in environmental water samples with high-performance liquid chromatography and UV detection after derivatization with 4-chloro-3,5-dinitrobenzotrifluoride. *Analytica Chimica Acta* 635: 222-226.

Qureshi R. and Bhatti G.R. 2001. Determination of weed communities in wheat (*Triticum aestivum L.*) fields of district Sukkur. *Pakistan Journal of Botany* 1: 109-115.

Raghavendra A.S. Padmasree K. Saradadevi K. 1994. Review: Interdependence of photosynthesis and respiration in plant cells: interactions between chloroplasts and mitochondria. *Plant Science* 97: 1-14.

Rajabzedah S. Liang C. Ohmukai Y. Maruyama T. Matsuyama H. 2012. Effect of additives on the morphology and properties of poly(vinylidenefluoride) blend hollow fiber membrane prepared by thermally induced phase separation method. *Journal of Membrane Science* 423-424: 189-194.

Raju C. Rao J.L. Reddy B.C.V. Brahmam K.V. 2007. Thermal and IR studies on copper doped polyvinyl alcohol. *Materials Science* 30: 215-218.

Ramakrishna S. Fujhara K. Teo W.E. Yong T. Ma Z. Ramaseshan R. 2006. Electrospun nanofibers: solving global issues. *Materials Today* 9: 40-50.

Ramesh A. Mohan K.R. Seshaiah K. 2002. Preconcentration of trace metals on Amberlite XAD-4 resin coated with dithiocarbamates and determination by inductively coupled plasma-atomic emission spectrometry in saline matrices. *Talanta* 57: 243-252.

Ramsey R.J.L. Stephenson G.R. Hall J.C. 2005. A review of the effects of humidity, humecants, and surfactant composition on the absorption and efficacy of high water-soluble herbicides. *Pesticide Biochemistry and Physiology* 82: 162-175.

Rao J. Jiang X. Wang Y. Chen B. 2011. Mini review: Advances in the understanding of the structure and function of ER-α36, a novel variant of human estrogen receptor-alpha. *Journal of Steroid Biochemistry and Molecular Biology* 127: 231-237.

Rask A.M. and Kristoffersen P. 2007. A review of non-chemical weed control on hard surfaces. *Weed Research* 47: 370-380.

Rasmussen J.J. Baattrup-Pedersen A. Larsen P.W. McKnight U.S. Kronvang B. 2011. Buffer strip width and agricultural pesticide contamination in Danish lowland streams: implications for stream and riparian management. *Ecological Engineering* 37: 1990-1997.

Ravanel P. Liegeois M.H. Chevallier D. Tissut M. 1999. Soil thin-layer chromatography and pesticide mobility through soil microstructures. New technical approach. *Journal of Chromatography A* 864 145-154.

Raveendran S. Dhandayuthapani B. Nagaoka Y. Yoshida Y. Maekawa T. Kumar D.S. 2013. Biocompatible nanofibers based on extermophilic bacterial polysaccharide Muran from *Halomonas Maura*. *Carbohydrate Polymers* 92: 1225-1233.

Rebeiz C.A. Montazer-Zouhoor A. Hopen H.J. Wu S.M. 1984. Review: photodynamic herbicides: 1. Concept and phenomenology. *Enzyme Microbiology and Technology* 6: 390-401.

Reddy K.N. Rimando A.M. Duke O.S. 2004. Aminomethylphosphonic acid, a metabolite of glyphosate, causes injury in glyphosate-treated, glyphosate resistant soybean. *Journal of Agricultural and Food Chemistry* 52: 5139-5143.

Reddy K.N. Rimando A.M. Duke S.O. Nandula V.K. 2008. Aminomethylphosphonic acid accumulation in plant species treated with glyphosate. *Journal of Agricultural and Food Chemistry* 56: 2125-2130.

Regner G. 2012. Mechanism of light induced water splitting in photosystem II of oxygen evolving organisms. *Biochemica et Biophysica Acta* 1817: 1164-1178.

Reneker D.H. and Chun I. 1996. Nanometre diameter fibers of polymer, produced by electrospinning. *Nanotechnology* 7: 216-223.

Revitt D.M. Ellis J.B. Llewellyn N.R. 2002. Seasonal removal of herbicides in urban runoff. *Urban Water* 4: 13-19.

Richard E.P. Goss J.R. Arntzen C.J. 1979. Glyphosate does not inhibit photosynthetic electron transport and phosphorylation in pea (*Pisum sativum*) chloroplast. *Weed Science* 27: 684-688.

Richard S. Moslemi S. Sipahutar H. Benachour N. Seralini G. 2005. Differential effects of glyphosate and Roundup on human placental cells and aromatase. *Environmental Health Perspective* 113: 716-720.

Richardson R.P. Rhyne C.D. Fong Y. Hesse D.G. Tracey K.J. Marano M.A. Lowry S.F. Antinacci A.C. Calvano S.E. 1989. Periphiral blood leukocyte kinetics following *in vivo* lipopolysaccharide (LPS) administration to normal human subjects. *Analytical Surgery* 210: 239-245.

Ridlen J.S. Klopf G.J. Nieman T.A. 1997. Determination of glyphosate and related compounds with tris(2,2′-bipyridyl)ruthenium(II) electrogenerated chemiluminescence detection. *Analytica Chimica Acta* 341: 195-204.

Rios C. Salvado V. Hidalgo M. 2004. Preconcentration of the herbicide glyphosate and its metabolite AMPA by immobilized metal ion affinity chromatography (IMAC). *Journal of Separation Science* 27: 602-606.

Ritter L. Solomon K. Sibley P. Hall K. Keen P. Mattu G. Linton B. 2002. Sources, pathways, and relative risks of contaminants in surface water and groundwater: A perspective prepared for the Walkerton inquiry. *Journal of Toxicology and Environmental Health, Part A* 65:1-142.

Rodrigues J.V. Worsham A.D. Corbin F.T. 1982. Exudation of glyphosate from wheat (*Triticum aestivum*) plants and its effects on interplanted corn (*Zea mays* ) and soybeans (*Glycine Max*). *Weed Science* 30: 316-320.

Rogachev I. Gusis V. Gusis A. Cortina J.L. Gressel J. Warchawsky A. 1999. Spectrophotometric determination of copper complexation properties of new amphiphilic dithiocarbamates. *Reactive & Functional Polymers* 42: 243-254.

Rojano-Delgado A.M. Hipolito De Prado R. de Castro M.D.L. Franco A.R. 2012. Limited uptake, translocation and enhanced metabolic degradation contribute to glyphosate tolerance in *Mucuna var. utilis* plants. *Phytochemistry* 73: 34-41.

Rošic R. Pelipenko J. Kocbek P. Baumgartner S. Bešter-Rogač M. Kristl J. 2012. The role of rheology of polymer solutions in predicting nanofiber formation by electrospnning. *European Polymer Journal* 48: 1374-1384.

Rother H.A. Hall R. London L. 2008. Pesticides among emerging farmers in South Africa: contributing factors and stakeholder perspectives. *Development Southern Africa* 25: 399-424.

Roux S.J. and Steinebrunner I. 2007. Extracellular ATP: an unexpected role as a signaler in plants. *Trends in Plant Science* 12: 522-527.

Roy D.N. Konar S.K. Banerjee S. Charles D.A. Thompson D.G. Prasad R. 1989. Persistence, movement and degradation of glyphosate in selected Canadian Boreal Forest soils. *Journal of Agriculture and Food Chemistry* 37: 437-440.

Royer A. Beguin S. Tablet J.C. Hulot S. Reding M.A. Communal P.Y. 2000. Determination of glyphosate and aminomethylphosphonic acid residues in water by gas chromatography with tandem mass spectrometry after exchange ion resin purification and derivatization. Application on vegetable matrices. *Analytical Chemistry* 72: 3826-3832.

Royston P. 1992. Approximating the Shapiro-Wilk W test for non-normality. *Statistics and Computing* 2: 112-119.

Rubio F. Veldhuis L.J. Clegg B.S. Fleeker J.R. Hall J.C. 2003. Comparison of a Direct ELISA and an HPLC method for glyphosate determinations in water. *Journal of Agriculture and Food Chemistry* 51: 691-696.

Rueppel M.L. Brightwell B.B. Schaefer J. Marvel J.T. 1977. Metabolism and degradation of glyphosate in soil and water. *Journal of Agriculture and Food Chemistry* 25: 517-527.

Ruizzo M.A. Bertekap R. Mishkind M.L. 1992. Consequences of herbicide-induced pigment deficiencies on thylakoid membrane proteins of *Chlamydomonas reinhardtii*. *Plant Science* 81: 13-20.

Rutherford A.W. Zimmermann J.L. Mathis P. 1984. The effect of herbicides on components of the PS II reaction centre measured by EPR. *Federation of European Biochemical Societies* 165: 156-162.

Sadi B.B.M Vonderheide A.P. Caruso J.A. 2004. Analysis of phosphorous herbicides by ion-pairing reversed-phase liquid chromatography coupled to inductively coupled plasma mass spectrometry with octapole reaction cell. *Journal of Chromatography A* 1050: 92-101.

Saenger W. Jordan P. Krauβ N. 2012. The assembly of protein subunits and cofactors in photosystem I. *Current Opinion in Structural Biology* 12: 244-254.

Safarpour H. and Asiaie R. 2005. Determination of glyphosate as cross-contaminant in a commercial herbicide by capillary electrophoresis-electrospray ionization-mass-spectrometry. *Electropphoresis* 26: 1562-1566.

Safi S. Morshed M. Ravandi S.A.H. Ghiaci M. 2007. Study of electrospinning of sodium alginate, blended solutions of sodium alginate/poly(vinyl alcohol) and sodium alginate/poly(ethylene oxide). *Journal of Applied Polymer Science* 104: 3245-3255.

Sagatys D.S. Dahlgren C. Smith G. Bott R.C. White J.M. 2000. The complex chemistry of *N*-(phosphonomethyl)glycine (glyphosate): Preparation and characterisation of the ammonium, lithium, sodium (4 polymorphs) and silver(I) complexes. *Journal of the Chemical Society Dalton Transactions*. DOI: 10.1039/b002748k.

Saitúa H. Giannini F. Padilla A.P. 2012. Drinking water obtaining by nanofiltration from waters contaminated with glyphosate formulations: Process evaluation by means of toxicity tests and studies on operating parameters. *Journal of Hazardous Materials* 227-228: 204-210.

Sajeev U.S. Anand K.A. Menon D. Nair S. 2008. Control of nanostructures in PVA, PVA/chitosan blends and PCL through electrospinning. *Bulletin of Materials Science* 31: 343-351

Sánchez G. Serrano J.L. Garcia J. Lòpez G. Pérez J. Molins E. 1999. Reactivity towards some weak protic electrophiles of the di-μ-hydroxo complex $[\{Pd(\mu\text{-}OH)(tmeda)\}_2]$ $[BPh_4]_2$: crystal structure of $[\{Pd(\mu\text{-}OH)(tmeda)\}_2(\mu\text{-}OH)(\mu\text{-}HNC_6H_4Cl\text{-}p)]$ $[BPh_4]_2$. *Inorganica Chimica Acta* 287: 37-46.

Sánchez-Bayo F. Hyne R.V. Desseille K.L. 2010. An amperometric method for the detection of amitrole, glyphosate and its aminomethyl-phosphonic acid metabolite in environmental waters using passive samplers. *Analytica Chimica Acta* 675: 125-131.

Sandberg C.L. Meggitt W.F. Penner D. 1980. Absorption, translocation and metabolism of $^{14}C$-glyphosate in several weed species. *Weed Research* 20: 195-200.

Sandmann G. Bramley P.M. Böger P. 1980. The inhibitory mode of action of the pyridazinone herbicide norflurazon on a cell-free carotenogenic enzyme system. *Pesticide Biochemistry and Physiology* 14: 185-191.

Santier S. and Chamel A. 1998. Reassessment of the role of cuticular waxes in the transfer of organic molecules through plant cuticles. *Plant Physiology and Biochemistry* 36: 225-231.

Sato K. Jin J.Y. Takeuchi T. Miwa T. Suenami K. Takekoshi Y. Kanno S. 2001. Intergrated pulsed amperometric detection of glufosinate, bialaphos and glyphosate at gold electrodes in anion-exchange chromatography. *Journal of Chromatography A* 919: 313-320.

Scheltrup F. and Grossmann K. 1995. Abscisic acid is a causative factor in the mode of action of the auxinix herbicide quinmerac in cleaser (*Galium aparine L.*). *Journal of Plant Physiology* 147: 118-126.

Schmid J. and Amrhein N. 1994. Review: Molecular organization of the shikimate pathway in higher plants. *Phytochemistry* 39: 737-749.

Scholz S. Sela E. Blaha L. Braunbeck T. Galay-Burgos M. Carcía-Franco M. Guinea J. Klüver N. Schirmer K. Tannenberger K. Tobor-Kaplon M. Witters H. Belanger S. Benfenati E. Creton S. Cronin M.T.D. Eggen R.I.L. Embry M. Ekman D. Gourmelon A. Halder M. Hardy B. Hartung T. Hubesch B. Jungmann D. Lampi M.A. Lee L. Léonard M. Küster E. Lillicrap A. Luckbach T. Murk A.J. Navas J.M. Peijnenburg W. Repetto G. Salinas E. Schüürmann G. Spielmann H. Tollefsen K.E. Walter-Rohde S. Whale G. Wheeler J.R. Winter M.J. 2013. A European perspective on alternatives to animal testing for environmental hazard identification and risk assessment. *Regulatory Toxicology and Pharmacology* 67: 506-530.

Schönherr J. 2002. A mechanistic analysis of penetration of glyphosate salts across astomatous suticular membranes. *Pest Management Science* 58: 343-351.

Schramm L.L. 2000. Surfactants: Fundamentals and Applications in the Petroleum Industry. Cambridge University Press. Cambridge, United Kingdom.

Schreuder R.H. Martijn A. Poppe H. Kraak J.C. 1986. Determination of the composition of ethozylated alkylamines in pesticide formulations by high-performance liquid chromatography using ion-pair extraction detection. *Journal of Chromatography* 368: 339-350.

Schulz R. 2001. Rainfall all induced sediment and pesticide input from orchards into the Lourens river, Western Cape, South Africa: importance of a single event. *Water Research* 35: 1869-1876.

Schwarzenbach R.P. Escher B.I. Fenner K. Hofstetter T.B. Johnson C.A. Von Gunten U. Wehrli B. 2006. Review: The challenge of micropollutants in aquatic systems. *Science* 313: 1072-1077.

Schwenger-Erger C. and Barz W. 2000. Decreased rate of degradation of the D1 protein in Metribuzin-resistant photoautotrophic *Chenopodium rubrum* cell cultures. *Journal of Plant Physiology* 156: 458-461.

Scothford C.A.Cascone M.G. Downes S. Giusti P. 1998. Osteoblast responses to collagen-PVA bioartificial polymers in vitro: the effects of cross-linking method and collagen content. *Biomaterials* 19: 1-11

See H.H. Hauser P.C. Sanagi M.M. Ibrahim W.A.W. 2010. Dynamic supported liquid membrane tip extraction of glyphosate and aminomethylphosphonic acid followed by capillary electrophoresis with contactless conductivity detection. *Journal of Chromatography A* 1217: 5832-5838.

Sell S.A. McClure M.J. Garg K. Wolfe P.S. Bowlin G.L. 2009. Electrospinning of collagen/biopolymers for regenerative medicine and cardiovascular tissue engineering. *Advanced Drug Delivery Reviews* 61: 1007-1019.

Shapiro S.S. and Wilk M.B. 1965. An analysis of variance test for normality (complete samples). *Biometrika* 52: 591-611.

## Chapter 8: References


Shar G.A. and Banger M.I. 2002. Spectrophotometric determination of copper (II) with diethyldithiocarbamate in polyoxyethylenedodecylether (Brij-35) media. *Journal of Chemical Society of Pakistan* 24: 185-189.

Sharma D.K. Gupta A. Kashyap R. Kumar N. 2012. Spectrophotometric method for the determination of glyphosate in relation to its environmental and toxicological analysis. *Archives of Environmental Science* 6: 42-49.

Sharma R.D and Amalthe S. 2012b. Quantitative determination and removal of zinc using disposable colorimetric sensors: an appropriate alternative to optodes. *Journal of Chemical and Pharmaceutical Research* 4: 1097-1105.

Sharma R.D. and Amalthe S. 2012a. Cadmium ion sensing paptode based on digital RGB color analysis. *Journal of Pharmacy and Biological Sciences* 3: 41-48.

Sheals J. Sjoberg S. Persson P. 2002. Adsorption of glyphosate on goethite: molecular characterization of surface complexes. *Environmental Science and Technology* 36:3090-3095.

Shen J. Huang J. Liu L. Ye W. Lin J. Van der Bruggen B. 2013. The use of BMED for glyphosate recovery from glyphosate neutralization liquor in view of zero discharge. *Journal of Hazardous Materials* 260: 660-667.

Shenoy S.L. Bates W.D. Frisch H.L. Wnek G.E. 2005. Role of chain entanglements of fiber formation during electrospinning of polymer solutions: good solvent, non-specific polymer-polymer interaction limit. *Polymer* 46: 3372-3384.

Sherr C.J. 1996. Cancer cell cycles. *American Association for the Advancement of Science* 274: 1672-1677.

Shi Y. and Seliskar C.J. 1997. Optically transparent polyelectrolyte-silica composite materials: preparation, characterization, and application in optical chemical sensing. *Chemistry of Materials* 9: 821-820.

Shikanai T. 2014. Central role of cyclic electron transport around photosystem I in the regulation of photosynthesis. *Curren Opinion in Biotechnology* 28: 25-30.

Shrivastava G. and Gupta V.B. 2011. Methods for determination of limit of detection and limit of quantitation of the analytical methods. *Chronicles of Young Scientists* 2: 21-25.

Singh B.K. and Walker A. 2006. Microbial degradation of organophosphorus compounds. *FEMS Microbiological Review* 30: 428-471.

Skark C. Zullei-seibert N. Schöttler U Schlett C. 1998. The occurrence of glyphosate in surface water. *International Journal of Environmental Analytical Chemistry* 70: 93-104.

Sloan M.E. and Camper N.D. 1981. Trifluralin effects on carrot callus tissue. *Pesticide Biochemistry and Physiology* 15: 201-208.

Snipes C.E. and Mueller T.C. 1992. Cotton (*Gossypium hirsutum*) yield response to mechanical and chemical weed control systems. *Weed Science* 40: 249.254.

Solomon G.M. and Schettler T. 2000. Review: Environment and health: endocrine disruption and potential human health implications. *Canadian Medical Association Journal* 163: 1471-1476.

Sprankle P. Meggit W.F. Penner D. 1975a. Rapid inactivation of glyphosate in the soil. *Weed Science* 23: 224-228.

Sprankle P. Meggitt W.F. Penner D. 1975b. Adsorption, mobility and microbial degradation of glyphosate in the soil. *Weed Science* 23: 229-234.

Sprankle P. Sandberg C.L. Meggitt W.F. Penner D. 1978. Separation of glyphosate and possible metabolites by thin-layer chromatography. *Weed Science* 26: 673-674.

Spycher S. Nendza M. Gasteiger J. 2004. Comparison of different classification mehods applied to a mode of toxic action data set. *QSAR & Combinatorial Science* 23: 779-791.

Stachewicz U. Bailey R.J. Wang W. Barber A.H. 2012. Size dependent mechanical properties of electrospun polymer fibers from composite structure. *Polymer* 53: 5132-5137.

Stalikas C.D. and Konidari C.N. 2001. Review: Analytical methods to determine phosphonic and amino acid group-containing pesticides. *Journal of Chromatography A* 907: 1-19.

Statistics South Africa (StatsSA) 2012. Census 2011: census in brief. Published by Statistics South Africa, Private Bag X44, Pretoria 0001. Report no. 03-01-41.

Steenkamp P.A. and Coetzee P.P. 1993. Simultaneous determination of toxic heavy metals in metformin hydrochloride using reversed-phase high performance liquid chromatography. *Fresenius Journal of Analytical Chemistry* 346: 1017-1021.

Steinmann H.H. Dickeduisbergb M. Theuvsen L. 2012. Use and benefits of glyphosate in German arable farming. *Crop Protection* 42: 164-169.

Stenrød M. Charnay M. Benoit P. Eklo O.M. 2006. Spatial variability of glyphosate mineralization and soil microbial characteristics in two Norwegian sandy loam soils as affected by surface topographical features. *Soil Biology & Biochemistry* 38: 962-971.

Stevens P.J.G. Baker E.A. Anderson N.H. 1988. Factors affecting the foliar absorption and redistribution of pesticides. 2. Physiochemical properties of the active ingredient and the role of surfactant. *Pesticide Science* 24: 31-53.

Stewart M. Olsen G. Hickey C.W. Ferreira B. Jelić A. Petrović M. Barcelo D. 2014. A survey of emerging contaminants in the estuarine receiving environment around Auckland, New Zealand. *Science of the Total Environment* 468-469: 202-210.

Stoddard M.B. Pinto V. Keiser P.B. Zollinger W. 2010. Evaluation of whole blood cytokine release assay for use in measuring endotoxin activity of group b *Neisseria meningitides* vaccines made from lipid A acylation mutants. *Clinical and Vaccine Immunology* 17: 98-107.

Stoner M. Wormke M. Saville B. Samudio I. Qin C. Abdelrahim M. Safe S. 2004. Estrogen regulation of vascular endothelial growth factor gene expression in ZR-75 breast cancer cells through interaction of estrogen receptor α and SP proteins. *Oncogene* 23: 1052-1063.

Struger J. Thompson D. Staznik B. Martin P. McDaniel T. Marvin C. 2008. Occurrence of glyphosate in surface waters of southern Ontario. *Bulletin of Environmental Contamination and Toxicology* 80: 378-384.

Su P. Wang C. Yang X. Chen X. Gao C. Feng X.X. Chen J.Y. Gou Z. 2011. Electrospinning of chitosan nanofibers: the favorable effect of metal ions. *Carbohydrate Polymers* 84: 239-246.

Subbiah T. Bhat G.S. Tock R.W. Parameswaran S. Ramkumar S.S. 2005. Electrospinning of nanofibers. *Journal of Applied Polymer Science* 96: 557-569.

Sunohara Y. and Matsumoto H. 2008. Quinclorac-induced cell death is accompanied by generation of reactive oxygen species in maize root tissue. *Phytochemistry* 69: 2312-2319.

Sunohara Y. Shirai S. Wongkantrakorn N. Matsumoto H. 2010. Sensitivity and physiological responses of *Eleusine indica* and *Digitaria adscendens* to herbicide quinclorac and 2,4-D. *Environmental and Experimental Botany* 68: 157-164.

Suslick K.S. 2004. An optoelectronic nose: `Seeing` smells by means of colorimetric sensor arrays. *MRS Bulletin* 720-725.

Suzuki Y. Endo M. Jin J. iwase K. Iwatsuki M. 2006. Tristimulus colorimetry using a digital still camera and its application to determination of iron and residual chlorine in water samples. *Analytical Sciences* 22: 411-414.

Swain S.M. and Singh D.P. 2005. Tall tales from sly dwarves: novel functions of gibberellins in plant development. *Trends in Plant Science* 10: 123-129.

Swanton C.J. and Weise S.F. 1991. Integrated weed management: the rationale and approach. *Weed Technology* 5: 657-663.

Tan S.H. Inai R. Kotaki M. Ramakrishna S. 2005. Systematic parameter study for ultra-fine fiber fabrication electrospinning process. *Polymer* 46: 6128-6134.

Tandlich R. Luyt C.D. Muller W.J.N. 2010. Project progress report prepared for the Water Research Commission. Project No. K8/806: 1-52.

Tandon S.K. Singh S. Jain V.K. Prasad S. 1996. Chelation in metal intoxication XXXVIII: effect of structurally different chelating agents in treatment of nickel intoxication in rat. *Fundemental and Applied Toxicology* 31: 141-148.

Tao J. and Shivkumar S. 2007. Molecular weight dependent structural regimes during electrospinning of PVA. *Materials Letters* 61: 2325-2328.

Tatum V.L. 2004. Toxicity, transport, and fate of forest herbicides. *Wildlife Society Bulletin* 32: 1042-1048.

Taverniers I. De Loose M. Bockstaele E.V. 2004. Trends in quality in the analytical laboratory II. Analytical method validation and quality assurance. *Trends in Analytical Chemistry* 23: 535-552.

Tegeder M. 2012. Transporters for amino acids in plant cells: some functions and many unknowns. *Current opinion in Plant Biology* 15: 315-321.

Tekel J. Tahotná S. Vaverková. 1998. Gas chromatographic method for the determination of uracil herbicide in roots of *Echinacea angustifolia* Moench (Asteraceae). *Journal of Pharmaceutical and Biomedical Analysis* 16: 753-758.

Ternan N.G. Mc Grath J.W. Mc Mullan G. Quinn J.P. 1998. Review: Organophosphonates: occurrence, synthesis and biodegradation by microorganisms. *World Journal of Microbiology and Biotechnology* 14: 635-647.

Thiere G. and Schulz R. 2004. Runoff-related agricultural impact in relation to macroinvertebrate communities of the Lourens river, South Africa. *Water Research* 38: 3092-3102.

Thompson C.J. Chase G.G. Yarin A.L. Reneker D.H. 2007. Effects of parameters on nanofiber diameter determined from electrospinning model. *Polymer* 48: 6913-6922.

Thongprakaisang S. Thiantanawat A. Rangkadilok N. Suriyo T. Satayavivad J. 2013. Glyphosate induces human breast cancer cells growth via estrogen receptors. *Food and Chemical Toxicology* 59: 129-136.

Tice R.R. Agurell E. Anderson D. Burlison B. Hartmann A. Kobayashi H. Miyamae Y. Rojas E. Ryu E. Sasaki Y.F. 2000. Single cell gel/Comet assay: guidelines for *In Vitro* and *In Vivo* genetic toxicology testing. *Environmental and Molecular Mutagenesis* 35: 206-221.

Tilman. D. 1999. Global environmental impact of agricultural expansion: The need for sustainable and efficient practices. *Proceedings of the National Academy of Sciences USA* 96: 5995-6000.

Tiwari S.K. and Venkatraman S.S. 2012. Importance of viscosity parameters in electrospinning: of monolithic and core-shell fibers. *Materials Science and Engineering C* 32: 1037-1042.

Tomita H. 1996. Solution spinning of high-$T_c$ oxide superconductor: 5. The influence of yttrium and barium ions on the poly (vinyl alcohol)-copper (II) complex. *Polymer* 37: 1071-1077.

Torstensson N.T.L.and Aamisepp A. 1977. Detoxication of glyphosate in soil. *Weed Research* 17: 209-212.

Toskas G. Cherif C. Hund R.D. Laourine E. Mahltig B. Fahmi A. Heinemann C. Hanke T. 2013. Chitosan (PEO)/silica hybrid nanofibers as a potential biomaterial for bone regeneration. *Carbohydrate Polymers* 94: 713-722.

Toumi M. Raouafi N. Boujlel K. Tapsoba I. Picard J.P. Bordeau M. 2008. Electrogenerated base-promoted synthesis of dithiocarbamate acid esters and 3-(*N*-substituted-amino)-2-cyanodithiocrotonates from primary and secondary amines and carbon disulfide. *Phosphorous, Sulfur and Silicon* 182: 2477-2490.

Tracey K.J. 2002. Review: The inflammatory reflex. *Nature* 420: 853-859.

Tsui M.T.K. and Chu L.M. 2003. Aquatic toxicity of glyphosate-based formulations: comparison between different organisms and the effects of environmental factors. *Chemosphere* 52: 1189-1197.

Tsunoda N. 1993. Simultaneous determination of the herbicides glyphosate, gluforinate and bialaphos and their metabolites by capillary gas chromatography-ion-trap-mass spectrometry. *Journal of Chromatography* 637: 167-173.

Tuschl H. and Schwab C. 2003. Cytotoxic effects of the herbicide 2,4-dichlorophenoxyacetic acid in HepG2 cells. *Food and Chemical Toxicology* 41: 385-393.

Tush D. Loftin K.A. Meyer M.T. 2013. Characterization of polyoxyethylene tallow amine surfactants in technical mixtures and glyphosate formulations using ultr-high performance liquid chromatography and triple quadrupole mass spectrometry. *Journal of Chromatography A* 1319: 80-87.

Ündeğer Ü. And Başaran N. 2005. Effects of pesticides on human peripheral lymphocytes *in vitro* : induction of DNA damage. *Archives of Toxicology* 79: 169-176.

United States Environmental Protection Agency (USEPA). 1993. Prevention, pesticides and toxic substances: Glyphosate. Report no. EPA-738-F-93-011.

Upstone S.L. 2000. Ultraviolet/visible light absorption spectrophotometry in clinical chemistry. *Encyclopedia of Analytical Chemistry.* R.A. Meyers (Ed.). John Wiley & Sons Ltd, Chichester, England. 1699-1714.

Uyar T. and Besenbacher F. 2008. Electrospinning of uniform polystyrene fibers: the effect of solvent conductivity. *Polymer* 49: 5336-5343.

Van Dongen J.T. Gupta K.J. Ramirez-Aguilar S.J. Araujo W.L. Nunes-Nesi A. Fernie A.R. 2011. Review: Regulation of respiration in plants: a role for alternative metabolic pathways. *Journal of Plant Physiology* 168: 1434-1443.

Van Ginkel C.G. Stroo C.A. Kroon A.G.M. 1993. Biodegradability of ethoxylated fatty amiones: detoxification through a central fission of these surfactants. *The Science of the Total Environment, Supplement* 689-697.

Van Kley H. and Claywell C.S. 1973. Evaluation of EDTA as the chelator in the biuret reagent. *Clinical Chemistry* 19: 621-623.

Van Staden J.F. and Botha A. 1999. Spectrophotometric determination of Cu(II) with sequential injection analysis. *Talanta* 49: 1099-1108.

Van Stempvoort D.R. Roy J.W. Brown S.J. Bickerton G. 2014. Residues of the herbicide glyphosate in riparian groundwater in urban catchments. *Chemosphere* 95: 455-463.

Van Toor R.F. Hayes A.L. Cooke B.K. Holloway P.J. 1994. Relationships between the herbicidal activity and foliar uptake of surfactant containing solutions of glyphosate applied to foliage of oats and field beans. *Crop Protection* 13: 260-270.

Vandenberg L.N. Colborn T. Hayes T.B. Heindel J.J. Jacobs D.R. Lee D.H. Shioda T. Soto A.M. Vom Saal F.S. Welshons W.V. Zoeller R.T. Myers J.P. 2012. Review: Hormones and endocrine-disrupting chemicals: Low dose effects and nonmonotonic dose responses. *Endocrine Reviews* 33: 378-455.

Vaughn K.C. 2006. The abnormal cell plates formed after microtubule disrupter herbicide treatment are enriched in callose. *Pesticide Biochemistry and Physiology* 84: 63-71.

Veiga F. Zapata J.M. Fernandez Marcos M.L. Alvarez E. 2001. Dynamics of glyphosate and aminomethylphosphonic acid in a forest in Galicia, north-west Spain. *The Science of the Total Environment* 271: 135-144.

Ventura C. Nunez M. Miret N. Lamas D.M. Randi A. Venturino A. Rivera E. Cocca C. 2012. Differential mechanisms of action are involved in chlorpyrifos effects in estrogen-dependent or –independent breast cancer cells exposed to low or high concentrations of the pesticide. *Toxicology Letters* 213: 184-193.

Vereecken H. 2005. Review: Mobility and leaching of glyphosate. *Pest Management Science* 61: 1139-1151.

Verma B.C. Chauhan S. Sharma N. Sharma U. Sharma D.K. Sood A. 1986. Analytical application of the amine-carbon disulphide reaction in acetonitrile. *Talanta* 33: 703-704.

Vigfusson N.V. and Vyse E.R. 1980. The effect of the pesticides, Dexon, Captan and Roundup, on sister chromatid exchanges in human lymphocytes *in vitro*. *Mutation Research* 79: 53-57.

Viriji S. Huang J. Kaner R.B. Weiler B.H. 2004. Polyaniline nanofiber gas sensors: examination of response mechanisms. *NanoLetters* 4: 491-496.

Vock E.H. Lutz W.K. Hormes P. Hoffmann H.D. Vamvakasa S. 1998. Discrimination between genotoxicity and cytotoxicity in the induction of DNA-double strand breaks is cells treated with etoposide, melphalan, cisplatin, potassium cyanide, Triton X 100, and γ-radiation. *Mutation Research* 413: 83-94.

Vogelgesang J. and Hädrich J. 1998. Limits of detection, identification and determination: statistical approach for practitioners. *Accreditation and Quality Assurance* 3: 242-255.

Vom Saal F.S. and Welshons. 2006. Large effects from small exposures II. The importance of positive controls in low-dose research on bisphenol A. *Environmental Research* 100: 50-76.

Vreeken R.J. Speksnijder P. Pastrova B. Noij T.H.M. 1998. Selective analysis of the herbicides glyphosate and aminomethylphosphonic acid in water by on-line solid-phase extraction-high-performance liquid chromatography –electrospray ionization mass spectrometry. *Journal of Chromatography A* 794: 187-199.

Wai C.M. 1995. Supercritical fluid extraction of trace metals from solid and liquid materials for analytical applications. *Analytical Sciences* 11: 165-167.

Waiman C.V. Avena M.J. Garrido A. Band B:F. Zanini G.P. 2012. A simple and rapid spectrophotometric method to quantify the herbicide glyphosate in aqueous media. Application to adsorption isotherms on soils and goethite. *Geoderma* 170: 154-158.

Walker R.H. and Buchanan G.A. 1982. Crop manipulation in integrated weed management systems. *Weed Science* 30: 17-24.

Walum E. 1998. Acute Oral Toxicity. *Environmental Health Perspectives* 106: 497-503.

Wan Y.Q. He J.H. Yu J.Y. Wu Y. 2006. Electrospinning of high-molecule PEO solution. *Journal of Polymer Science* 103: 3840-3843.

Wang C.J. and Liu Z.Q. 2007. Foliar uptake of pesticides-present status and future challenge. *Pesticide Biochemistry and Physiology* 87:1-8.

Wang G. Ji Y. Huang X. Yang X. Gouma P.I. Dudley M. 2006. Fabrication and characterization of polycrystalline $WO_3$ nanofibers and their applications for ammonia sensing. *Journal of Physical Chemistry* 110: 23777-23782.

Wang L. Chen W. Ma W. Liu L. Ma W. Zhao Y. Zhu V. Xu L. Kuang H. Xu C. 2011. Fluorescent strip sensor for rapid determination of toxins. *Chemical Communications* 47: 1574-1576.

Wang S. and Arnold W.A. 2003. Abiotic reduction of dinitroaniline herbicides. *Water Research* 37: 4190-4200.

Wang X. and Kilgore M.W. 2002. Signal cross-talk between estrogen receptor alpha and beta and the peroxisome proliferator-activated receptor gamma 1 in MDA-MB-231and MCF-7 breast cancer cells. *Molecular and Cellular Endocrinology* 194: 123-133.

Wang X. Ding B. Sun G. Wang M. Yu J. 2013. Electro-spinning/netting: A strategy for the fabrication of three-dimensional polymer nano-fiber/nets. *Progress in Materials Science* 58: 1173-1243.

Wang X. Si Y. Wang J. Ding B. Yu J. Al-Deyab S.S. 2012. A facile and highly sensitive colorimetric sensor for the detection of formaldehyde based on electro-spinning/netting nano-fiber/nets. *Sensors and Actuators B: Chemical* 163: 186-193.

Wang Y. Li D. Ren W. Liu Z. Dong S. Wang E. 2008. Ultrasensitive colorimetric detection of protein by aptamer-Au nanoparticles conjugates based on a dot-blot assay. *Chemical Communications* 1: 2520-2522.

Warnemuende E.A. Patterson J.P. Smith D.R. Huang C. 2007. Effects of tilling no-till soil on losses of atrazine and glyphosate to runoff water under variable intensity simulated rainfall. *Soil & Tillage Research* 95: 19-26.

Watkins L.R. Maier S.F. Goehler L.E. 1995. Review article: Immune activation: the role of pro-inflammatory cytokines in inflammation, illness responses and pathological pain states. *Pain* 63: 289-302.

Watkins L.R. Hutchinson M.R. Milligan E.D. Maier S.F. 2007. Review article: "Listening" and "talking" to neurons: Implications of immune activation for pain control and increasing the efficacy of opioids. *Brain Research Reviews* 56: 148-169.

Wei M. Lee J.Kang B. Mead J. 2005. Preparation of core-sheath nanofibers from conducting polymer blends. *Macromolecular Rapid Communications* 26: 1127-1132.

Werner T. Klimant I. Wolfbeis O.S. 1995. Ammonia-sensitive polymer matrux employing immobilized indicator ion pairs. *Analyst* 120: 1627-1631.

Williams G.M. Kroes R. Munro I.C. 2000. Safety evaluation and risk assessment of the herbicide Roundup and its active ingredient, glyphosate, for humans. *Regulatory Toxicology and Pharmacology* 31: 117-165.

Willis A.J. Memmott J. Forrester R.L. 2000. Report: Is there evidence for post-invasion evolution of increased size among invasive plant species?. *Ecology Letters* 3: 275-283.

Wilmesmeier S. and Wiermann R. 1995. Influence of EPTC (S-ethyl-dipropyl-thiocarbamate) on the composition of surface waxes and sporopollenin structure in *Zea Mays* . *Journal of Plant Physiology* 146: 22-28.

Wilski S. Johanningmeier U. Hertel S. Oettmeier W. 2006. Herbicide binding in various mutants of the photosystem II D1 protein of *Chlamydomonas reinhardtii*. *Pesticide Biochemistry and Physiology* 84: 157-164.

Wong P.K. 2000. Effects of 2,4-D, glyphosate and paraquat on growth, photosynthesis and chlorophyll-a synthesis of *Scenedesmus quadricauda* Berb 614. *Chemosphere* 41: 177-182.

Woodburn A.T. 2000. Glyphosate: production, pricing and use worldwide. *Pest Management Science* 56: 309-312.

World Health Organization (WHO). 1994. Glyphosate: Environmental health criteria No 159. Geneva.

World Health Organization (WHO). 2004. 3rd edition. Summary statement: Glyphosate and AMPA in drinking water. WHO guidelines for drinking water quality.

Wu L. Yuan X. Sheng J. 2005. Immobilization of cellulase in nanofibrous PVA membranes by electrospinning. *Journal of Membrane Science* 25: 167-173.

Wuilloud R.G. Shah M. Kannamkumarath S.S. Altamirano J.C. 2005. The potential of inductively coupled plasma-mass spectrometric detection for capillary electrophoretic analysis of pesticides. *Electrophoresis* 26: 1598-1605.

Wutor V.C. Togo C.A. Pletschke B.I. 2007. The effect of physio-chemical compounds on the activity of β-$_D$-galactosidase (B-GAL), a marker for enzyme indicator of microorganisms in water. *Chemosphere* 68: 622-627.

Wycherley D. Rose M.E. Giles K. Hutton T.M. Rimmer D.A. 1996. Capillary electrophoresis with detection by inverse UV spectroscopy and electrospray mass spectrometry for the examination of quartenary ammonium herbicides. *Journal of Chromatography A* 734: 339-349.

Xiao-Ling A. Jia-Jun W. Hong-Jun Z. Sheng Q. 2011. Occurance of glyphosate-resistant horseweed (*Conyza Canadensis*) population in China. *Agricultural Sciences in China* 10: 1049-1055.

Xing Z. Gauldie J. Cox G. Baumann H. Jordana M. Lei X.F. Achong K. 1998. IL-6 is an anti-inflammatory cytokine required for controlling local or systematic acute inflammatory responses. *Journal of Clinical Investigations* 101: 311-320.

Yadav G.D. and Jadhav Y.B. 2002. Synthesis of 2,4-dichlorophenoxyacetic acid: novelties of kinetics of inverse phase transfer catalysis. *Journal of Molecular Catalysis* 184: 151-160.

Yanase D. and Andoh A. 1992. Translocation of photosynthesis-inhibiting herbicides in wheat leaves measured by phytofluorography, the chlorophyll fluorescence imaging. *Pesticide Biochemistry and Physiology* 44: 60-67.

Yang Y.K. and Tae J. 2006. Acridinium salt based fluorescent and colorimetric chemosensor for the detection of cyanide in water. *Organic Letters* 8: 5721-5723.

Yao D.C.I. Brune D.C. Vermaas W.F.J. 2012. Lifetimes of photosytem I and II in the cyanobacterium sp. PCC 6803. *Federation of European Biochemical Sciences Letters* 586: 169-173.

Yao J. Bastiaansen C.W.M. Peijs T. 2014. Review: High strength and high modulus electrospun nanofibers. *Fibers* 2: 158-187.

Yao L. Haas T.W. Guiseppi-Elie A. Bowlin G.L. Simpson D.G. Wnek G.E. 2003. Electrospinning and stabilization of fully hydrolyzed poly(vinyl alcohol) fibers. *Chemical Materials* 15: 1860-1864.

Yao Y. Tian D. Li H. 2010. Cooperative binding of bifunctionalized and click-synthesized silver nanoparticles for colorimetric $Co^{2+}$ sensing. *Applied Materials* 2: 684-690.

Yared E. McMillan T.J. Martin F.L. 2002. Genotoxic effects of oestrogens in breast cells detected by the micronucleus assay and the Comet assay. *Mutagenesis* 17: 345-352.

Yebra-Buirrun M.C. Bermejo-Barrera A. Bermejo-Barrera P. 1991. Application of a poly(dithiocarbamate) resin with macroreticular support to the determination of trace amounts of cadmium and lead in non-saline waters. *Analyst* 116: 1033-1035.

Yokoi H. Kawata S. Iwaizumi M. 1986. Interaction modes between heavy metal ions and water-soluble polymers. Spectroscopic and magnetic reexamination of the aqueous solutions of cupric ions and poly (vinyl alcohol). *Journal of American Chemical Society* 108: 3358-3361.

Yoshioka N. Asano M. Kuse A. Mitsuhashi T. Nagasaki Y. Ueno Y. 2011. Rapid determination of glyphosate, glufosinate, bialaphos, and their major metabolites in serum by liquid chromatography-tandem mass spectrometry using hydrophilic interaction chromatography. *Journal of Chromatography A* 1218: 3675-3680.

You J. and Koropchak J.A. 2003. Condensation nucleation light scattering detection with ion chromatography for direct determination of glyphosate and its metabolite in water. *Journal of Chromatography A* 989: 231-238.

You J. Kaljurand M. Koropchak J.A. 2003. Direct determination of glyphosate in environmental waters using capillary electrophoresis with electrospray condensation nucleation light scattering detection. *International Journal of Environmental Analytical Chemistry* 83: 797-806.

Young J.C. Khan S.U. Marriage P.B. 1977. Fluorescence detection and determination of glyphosate via its *N*-nitroso derivative by thin layer chromatography. *Journal of Agriculture and Food Chemistry* 25: 918-922.

Yu J.H. Fridrikh S.V. Rutlegde G.C. 2004. Production of submicrometer diameter fibers by two-fluid electrospinning. *Advanced Materials* 16: 1562-1566.

Yu W. Ma Q. Li X. Dong X. Wang J. Liu G. 2014. One-pot coaxial electrospinning fabrication and properties of magnetic-luminescent bifunctional flexible hollow nanofibers. *Materials Letters* 120: 126-129.

Yu W. Zhang R. Li R. Guo S. 2007. Isolation and characterization of glyphosate regulated genes in soybean seedlings. *Plant Science* 172: 497-504.

Yu Y. and Zhou Q.X. 2005. Adsorption characteristics of pesticides methamidophos and glyphosate by two soils. *Chemosphere* 58: 811-816.

Yuan X. Guo P. Qi X. Ning N. Wang H. Wang H. Wang X. Yang Y. 2013. Safety of herbicide Sigma Broad on Radix Isatidis ( *Isatis indigotica Fort*.) seedlings and their photosynthetic responses. *Pesticide Biochemistry and Physiology* 106: 45-50.

Yuan Z.Y. and Su B.L. 2004. Titanium oxide nanotubes, nanofibers and nanowires. *Colloids and Surfaces A: Physiochemical Engineering Aspects* 241: 173-183.

Yue Y. Zhang Y. Zhou L. Qin J. Chen X. 2008. *In vitro* study on the binding of herbicide glyphosate to human serum albumin by optical spectroscopy and molecular modeling. *Journal of photochemistry and Photobiology B: Biology* 90: 26-32.

Zabaloy M.C. Gómez E. Garland J.L. Gómez M.A. 2012. Assessment of microbial community function and structure in soil microcosms exposed to glyphosate. *Applied Soil Ecology* 61: 333-339.

Zandstra B.H. and Nishimoto R.K. 1977. Movement and activity of glyphosate in purple nutsedge. *Weed Science* 25: 268-274.

Zelaya I.A. Anderson J.A.H. Owen M.D.K. Landes R.D. 2011. Evaluation of spectrophotometric and HPLC methods for shikimic acid determination in plants: models in glyphosate-resistant and susceptible crops. *Journal of Agriculture and Food Chemistry* 59: 2202-2212.

Zhang C. and Suslick K.S. 2005. A colorimetric sensor array for organic in water. *Journal of American Chemistry Society* 127: 11548-11549.

Zhang D. Zhang M. Liu Z. Yu M. Li F. Yi T. Huang C. 2006. Highly selective colorimetric sensor for cysteine and homocysteine based on azo derivatives. *TTetrahedron Letters* 47: 7093-7096.

Zhang H. Li B. Lei B. Li B. Li W. Lu S. 2007. Preparation and oxygen sensing properties of sol-gel derived thin film based on a covalently grafted ruthenium (II) complex. *Sensors and Actuators B* 123: 508-515.

Zhang J. Hoogmartens J. Van Schepdael A. 2008. Review: Advances in CE-mediated microanalysis: An update. *Electrophoresis* 29: 56-65.

Zhao B. Zhang J. Gong J. Zhang H. Zhang C. 2009. Glyphosate mobility in soils by phosphate application: Laboratory column experiment. *Geoderma* 149: 290-297.

Zhao P. Yan M. Zhang C. Peng R. Ma D. Yu J. 2011b. Determination of glyphosate in foodstuff by one novel chemiluminescence-molecular imprinting sensor. *Spectrochimica Acta Part A: Molecular and Biomolecular spectroscopy* 78: 1482-1486.

Zhao W. Ali M.M. Aguirre S.D. Brook M.A. Li Y. 2008. Paper-based bioassays using gold nanoparticle colorimetric probes. *Analytical Chemistry* 80: 8431-8437.

Zhao X. Pan B. Zhang W. Zhang S. Zhang Q. 2011a. Review: Polymer-supported nanocomposites for environmental application. *Chemical Engineering Journal* 170: 381-394.

Zhou C.F. Wang Y.J. Cheng-Cheng L. Sun R.J. Yu Y.C. 2013. Subacute toxicity of copper and glyphosate and their interaction to earthworm (*Eisena fetida*). *Environmental Pollution* 180: 71-77.

Zhou Q. Xu G. Wang J. Qin C. Dai L. 2011. Poly(vinyl alcohol)/hydrotalcite composite nanofibre: Preparation and characterization. *Iranian Polymer Journal* 20: 357-365.

Zhu D. Zhang R. Ma C. Yin H. 2002. Synthesis of N,N-dialkyl dithiocarbamate triphenyltin(IV) and crystal structures of $Ph_3SnS_2CN(C_2H_5)_2$ and $Ph_3SNS_2CN(C_5H_{10})$. *Indian Journal of Chemistry* 41: 1634-1638.

Zhu H. Coleman D.M. Dehen C.J. Geisler I.M. Zemlyanov D. Chmielewski J. Simpson G.J. Wei A. 2008. Assembly of dithiocarbamate-anchored monolayers on gold surfaces in aqueous solutions. *Langmuir* 24: 8660-8666.

Zhu Y. He X. Luo Y. Zou S. Zhou X. Huang K. Xu W. 2013. A 90-day feeding study of glyphosate-tolerant maize with the *G2-aroA* gene in Sprague-Dawley rats. *Food and Chemical Toxicology* 51: 280-287.

Zhu Y. Zhang F. Tong C. Liu W. 1999. Short communication: Determination of glyphosate by ion chromatography. *Journal of Chromatography A* 850: 297-301.

Zimdahl R.L. 2007. Fundementals of weed science. 3rd edition. Academic Press (Elsevier), London WCIX8RR, United Kindgom.

Zimmerman H.G. and Neser S. 1999. Trends and Prospects for biological control of weeds in South Africa. *African Entomology Memoir* 1: 165-173.

Zong X. Kim K. Fang D. Ran S. Hsiao B.S. Chu B. 2002. Structure and process relationship of electrospun bioabsorbable nanofiber membranes. *Polymer* 43: 4403-4412.

Zuo W. Zhu M. Yang W. Yu H. Chen Y. Zhang Y. 2005. Experimental study relationship between jet instability and formation of beaded fibers during electrospinning. *Polymer Engineering & Science* 45: 704-709.

## Appendix I: Reagent List

**Table I.I:** Reagents list and chemical suppliers

| Reagent | Chemical supplier (catalog number) |
|---|---|
| 3-(4,5-Dimethythiazol-2-YI)-2,5-diphenyltetrazolium bromide (MTT) | Duchefa Biochemie (298-93-1) |
| Aminomethylphosphonic acid (AMPA) | Sigma-Aldrich (657611-59) |
| Ammonia solution (32 %) | Merck (112 20 40 LC) |
| Ammonium chloride | Associated Chemical Enterprises (12125-02-9) |
| Boric acid | Merck (1.100165.0500) |
| Calcium chloride | Merck (1524900 EM) |
| Camptothecin | Cell biolabs, Inc |
| Carbon disulfide | Sigma-Aldrich (335266-1L) |
| Chloroform | Merck (1.02447.0500) |
| Citric acid | Merck (1.00244.0500) |
| Copper (II) nitrate hydrate | Sigma-Aldrich (13778-31-9) |
| Copper (II) sulfate | Sigma-Aldrich (C3036-250G) |
| Dimethyl sulphoxide (DMSO) | Merck (SAAR1865000LP) |
| Dulbecco´s Modified Eagle´s Medium (DMEM,+ 4.5 g/L glucose, + L-glutamine, containing phenol red) | Lonza (BE12-604F) |
| ELISA kit (IL-1β) | eBioscience (88-7010-22) |

| | |
|---|---|
| ELISA kit (IL-6) | eBioscience (88-7066-22) |
| ELISA kit (TNF-α) | eBioscience (88-7346-22) |
| Ethylenediamine tetracetic acid disodium salt (EDTA) | Merck (223-60-20EM) |
| Ferrous sulfate | Merck (234-60-00EM) |
| Fetal bovine serum (FBS) | Thermoscientific (SV30143.02) |
| Glycine | Merck (SAAR2676600EM) |
| Glyphosate (purity: 99.5 %) | Sigma-Aldrich (4221) |
| Lipopolysaccharide (LPS, from *Escherichia coli* 0111) | Sigma-Aldrich (L4391) |
| Magnesium chloride | Sigma-Aldrich (M8266) |
| Manganese (II) sulfate | Sigma-Aldrich (M7634) |
| OxiSelect™ Comet Assay Kit | Cell biolabs, Inc (STA-351) |
| Penicillin-streptomycin | Gibco Invitrogen Corporation (15140-122) |
| Poly (vinyl) alcohol (99 % hydrolyzed, $M_w$: 146,000-186,000) | Sigma-Aldrich (363065) |
| Pottasium chloride | Merck (504-20-20EM) |
| Pottasium hydrogen carbonate | Merck (4854-0500) |
| Rosewell Park Memorial Institute Medium (RPMI, (+ 25mM HEPES, +L-glutamine) 1640 | Thermoscientific (SH30255.01) |
| Roundup® (Efekto, 360 g/L glyphosate potassium salt) | Local store (Eastern Cape, South Africa) |

| | |
|---|---|
| Sodium chloride | Merck (1.06404.0500) |
| Sodium hydroxide | Sigma-Aldrich (221465) |
| Sodium sulfate | Merck (5825200EM) |
| Tris(hydroxymethyl) aminomethane | Merck (1.08382.1000) |
| Triton® X-100 | Merck (1.08603.1000) |
| Tryphan blue | Sigma-Aldrich (T8154) |
| Trypsin (10 %) | Thermoscientific (SV30037.01) |
| Wipeout® (Kombat, 500 g/L glyphosate potassium salt) | Local store (Eastern Cape, South Africa) |
| Zinc sulfate | Merck (758.2860EM) |

## Appendix II: Standard curves for the determination of TNF-α, IL-1β, IL-6 in human whole blood and isolated white blood cells.

ELISA standard curves for TNF-α (4-500 pg/ml), IL-1β (4-500 pg/ml) and IL-6 (2-200 pg/ml) were generated using commercial ELISA kits, according to manufacturer's instructions (eBioscience). Absorbance values were determined spectrophotometrically at 450 nm (reference wavelength: 570 nm) using a Biotek Powerwave XS microplate reader. Standard curves constructed for the human whole blood and human white blood cell model are shown in Figures II.I and II.II, respectively.

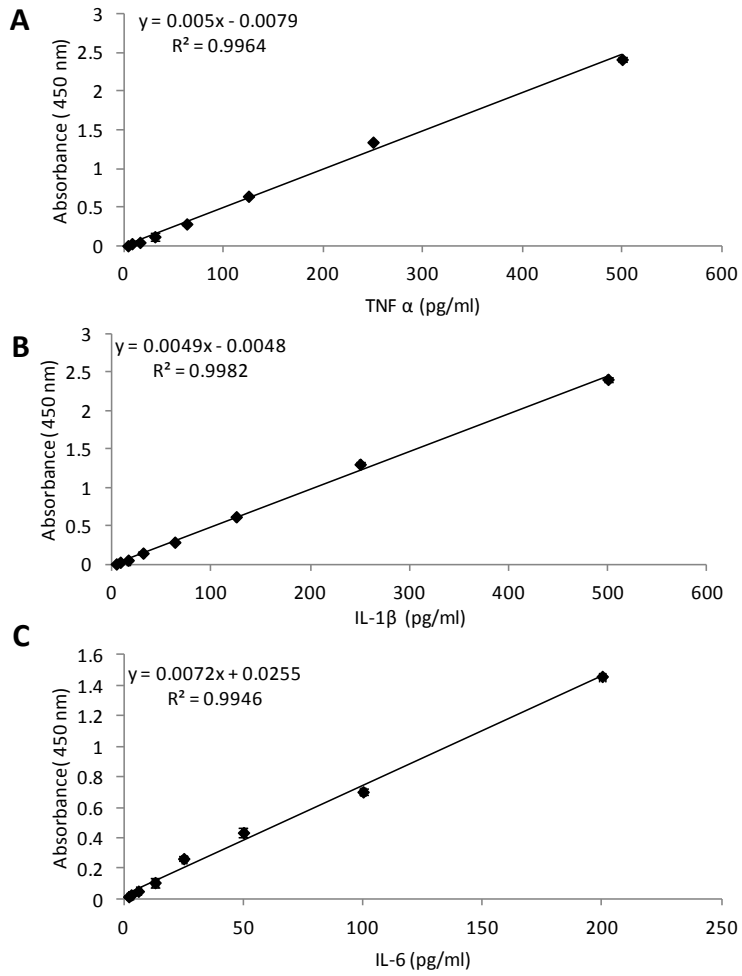


**Figure II.I:** ELISA standard curves (whole blood). **A:** TNF-α **B:** IL-1β **C:** IL-6.

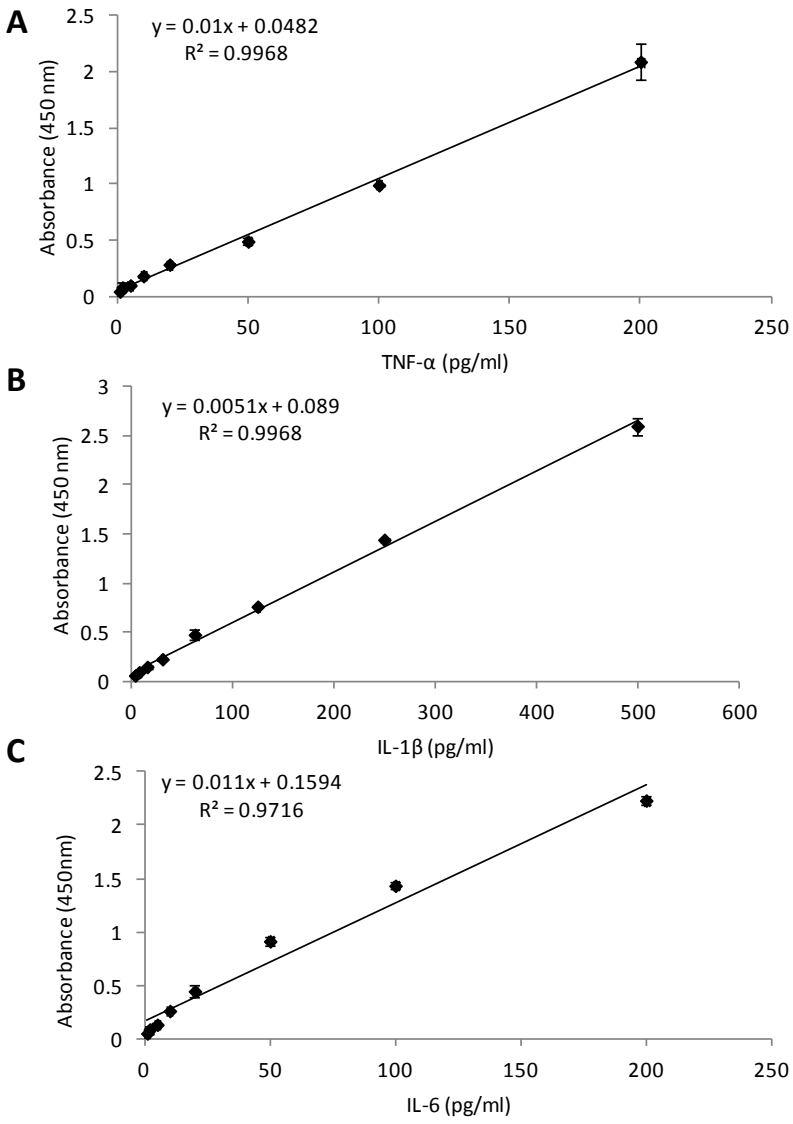


**Figure II.II:** ELISA standard curves (white blood cells). **A:** TNF-α **B:** IL-1β **C:** IL-6.

## Appendix III: Comet assay %TDNA results and the correlation study between TL (µm) and OTM

The % TDNA shown in Figure III.I was obtained using Image J (Comet assay plugin) analysis and demonstrates DNA damage in the HEC1A, MCF-7 and MDA-MB-231 cancer cell lines following a 4 hour exposure period to pure glyphosate (500 and 1000 µg/ml) and glyphosate in the formulation Ro and Wo (500 and 800 µg/ml). Camptothecin (35 µg/ml) was used as a positive control in this study.

The correlation studies comparing the data obtained using the TL and OTM measurements (mean values as percentages against the untreated control) are shown in Figure III.II.

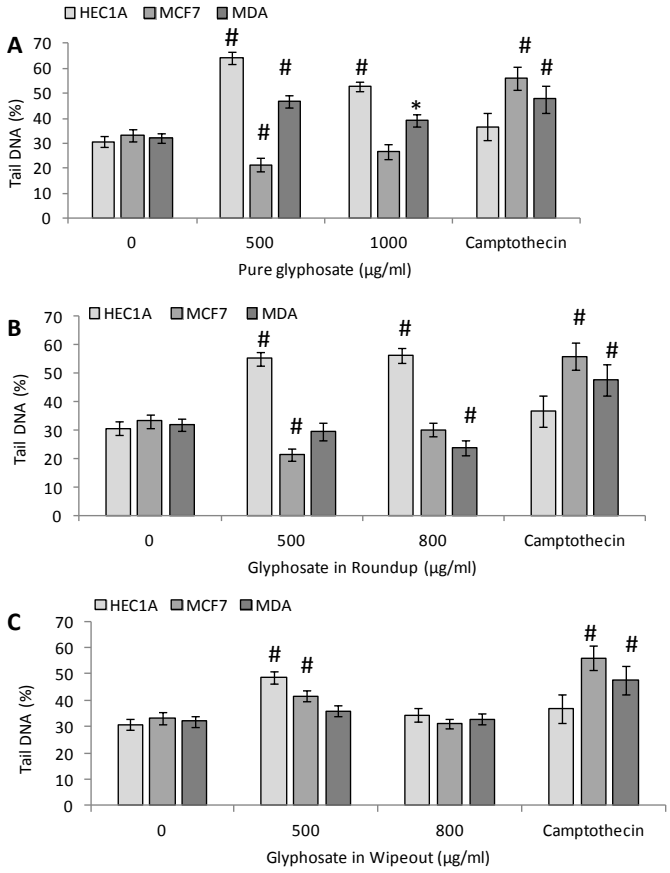


**Figure III.I:** DNA damage in HEC1A, MCF-7 and MDA cell lines assessed by tailDNA (%). Cells were exposed at 37 °C over a 4 hour period to different concentrations (untreated, test concentration and reference concentration) of **A:** pure glyphosate **B:** Ro and **C:** Wo. Camptothecin (35 µg/ml) was used as a positive control in this study. Values are presented as mean values ± SEM (n=50). ANOVA single factor analysis was used to determine significant differences from the untreated control $^{*}P \leq 0.05$, $^{\#}P \leq 0.01$.

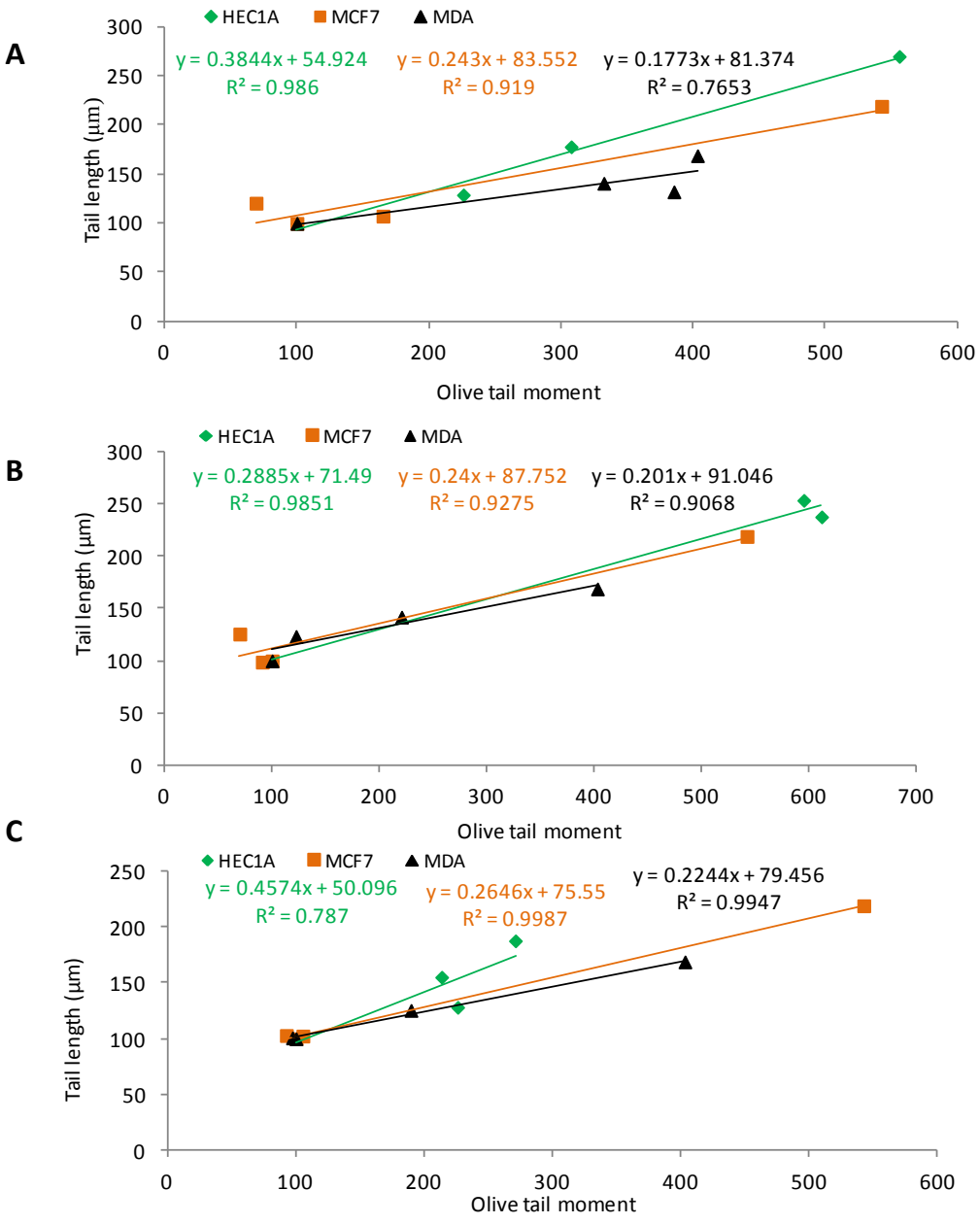


**Figure III.II:** Correlation curves comparing tail length (TL) and Olive tail moment (OTM) measurements described as percentages (obtained from mean values) against the untreated control at different glyphosate doses (0, 500, 800 or 1000 µg/ml). The results of the positive control (Camptothecin, 35 µg/ml) were included in this study are indicated by the last data point on each curve. Untreated control= 100%. **A:** Pure glyphosate **B:** Ro **C:** Wo.

## Appendix IV: Estimated fiber diameters calculated for pure PVA and copper-doped PVA nanofibers based on the frequency table.

Table IV.I and Table IV.II show the frequency table and mean fiber diameters for pure PVA and copper-doped PVA.

**Table IV.I:** Frequency table for pure PVA nanofibers and the calculated mean fiber diameter (μm)

| **Class interval** | **Frequency ($F_i$)** | **Midpoint value ($M_i$)** | **($F_i$)($M_i$)** |
|---|---|---|---|
| 0.1-0.2 | 13 | 0.15 | 1.95 |
| 0.2-0.3 | 30 | 0.25 | 7.5 |
| 0.3-0.4 | 5 | 0.35 | 1.75 |
| 0.6-0.7 | 8 | 0.65 | 5.2 |
| 0.7-0.8 | 3 | 0.75 | 2.25 |
| 0.8-0.9 | 3 | 0.85 | 2.55 |
| 0.9-1 | 2 | 0.95 | 1.9 |
| 1-1.1 | 1 | 1.05 | 1.05 |
| 1.1-1.2 | 2 | 1.15 | 2.3 |
| 1.2-1.3 | 3 | 1.25 | 3.75 |
| ∑ | **70** | | **30.2** |
| **Mean fiber diameter (μm): ($F_i$)($M_i$)/($F_i$)** | | **0.43 ± 0.22** | |

**Table IV.II:** Frequency table for copper-doped PVA nanofibers and the calculated mean fiber diameter (μm)

| **Class interval** | **Frequency ($F_i$)** | **Midpoint value ($M_i$)** | **($F_i$)($M_i$)** |
|---|---|---|---|
| 0.1-0.2 | 6 | 0.15 | 0.9 |
| 0.2-0.3 | 25 | 0.25 | 6.25 |
| 0.3-0.4 | 10 | 0.35 | 3.5 |
| 0.4-0.5 | 11 | 0.45 | 4.95 |
| 0.5-0.6 | 8 | 0.55 | 4.4 |
| 0.6-0.7 | 8 | 0.65 | 5.2 |
| 0.9-1 | 2 | 0.95 | 1.9 |
| ∑ | **70** | | **27.1** |
| **Mean fiber diameter (μm): ($F_i$)($M_i$)/($F_i$)** | | **0.39 ± 0.09** | |